Design, development and evaluation of a novel percutaneous Ascending Thoracic Aortic Graft (ATAG)

Thesis submitted for

MD (Res)

Queen Mary, University of London

July 2012

Dr Thomas Roger Keeble

Department of Cardiology, The London Chest Hospital

William Harvey Research Institute

Word count: 53,323 excluding Appendix and References

Proverbs 1:2

"To learn wisdom and moral instruction, and to discern wise counsel"

To Leigh, Rory, Marcus, Mum and Dad – I love you – thank you.

Abstract

There is a huge unmet clinical need for a new, safe and effective minimally invasive treatment for Acute Ascending Aortic Dissection (AAAD) (1). In 2012 AAAD has a mortality rate of 1-2% per hour within the first 24 hours, and even with contemporary surgical techniques, advanced intensive and post operative care, the mortality from AAAD following surgery in most series remains in the unacceptable range of 10-30% at 30 days (2;3). 28% of patients presenting with AAAD are denied life saving surgery often because of age or co-morbidity - medical therapy alone associated with an in hospital mortality rate in excess of 50% (2;4-6).

Currently available endovascular stent grafts used in the descending thoracic and abdominal aorta are not adequately designed to be utilised within the ascending aorta. They have a large stowed diameter 22-25 French (F), with a rigid covering of either Dacron or ePTFE, and a stiff inflexible delivery system unlikely to traverse the aortic arch without complication.

While the contemporary results of elective surgery for ascending thoracic aortic aneurysm (ATAA) are good, with an elective mortality of <5%, surgical results for AAAD have improved little over the last 20 years, with a 30 day mortality rate between 10-30% (3;7). With the emerging role of endovascular stent grafts in the treatment of thoracic aneurysm and dissection, with shorter hospital stays and improved outcomes I believe now is the time for the development of a percutaneous solution for AAAD.

Potential ascending thoracic aortic graft (ATAG) designs must take into account the very close proximity of intimal tear to both the coronary arteries and aortic valve, allowing a

good proximal graft seal without compromising coronary flow or aortic valve competence. ATAG should have a low profile, with a thin non porous covering and a flexible delivery sheath with accurate and precise deployment characteristics.

Following a literature review and novel anatomical data collection from computerised tomography (CT) and magnetic resonance imaging (MRI) scans of AAAD and ATAA patient cohorts, it seems that 3 embodiments of ATAG should be designed and developed, all sharing advanced core technologies including a laser-cut nitinol stent frame, thin polyurethane (PU) material covering and accurate and precise deployment mechanisms:

1) The “supra-coronary tubular ATAG”, for treating AAAD with an intimal tear in the ascending aorta, no coronary or aortic valve involvement and adequate landing zones above the coronary arteries and before the right brachiocephalic trunk (RBCT). It is likely that this graft will be capable of treating at least a third of all patients with AAAD (8).

2) The “inverted t-shirt ATAG” to proactively protect coronary artery flow and achieve proximal seal within the sinuses in patients with an intimal tear in close association or involving the coronary arteries.

3) The “valved ATAG” to treat patients who have significant aortic regurgitation (AR), to achieve a proximal seal at the annulus when anatomy suggests it would be difficult to achieve with embodiment 1) or 2), and in those patients who have a hugely dilated aortic root, so that the ATAG can seal proximally at a relatively normal annulus size, and seal distally at a normal ascending aorta diameter

proximal to the RBCT. This could be the treatment option for the 25-35% of AAAD patients who currently require aortic valve repair or replacement (9).

The most complex of the 3 devices above is embodiment 2), the “inverted t-shirt ATAG”, as it must ensure proximal aortic seal within an often dilated sinus, without compromise to aortic valve and proactively protect both coronary arteries with 2 coronary sleeves. Basic proof of concept (PoC) of this embodiment has been demonstrated *in vitro* within a normal sized aortic glass model, with some important study limitations, nevertheless it does demonstrate that tracking an ATAG branched graft with 2 coronary sleeves is possible over 3 guidewires and deploying accurately within the aortic root under both direct vision and fluoroscopy.

Following successful PoC deployment I then specified and had manufactured a 2nd Generation ATAG (2G ATAG), with a laser-cut nitinol frame, longitudinal tie bars, and a novel thin PU graft covering material. The 2G ATAG has been shown to have adequate radial strength when compared to competitor devices, and can be stowed to 28 F for deployment.

During ATAG development 2 patents have been filed, and I wrote with Professor Rothman a successful NIHR I4I grant for £743,000 to take ATAG from the current 28 F 2G device, towards the goal of an 18 F device with bench testing, *in vitro* flow rig and deployment analysis, and in collaboration with the Royal Veterinary College (RVC) into an animal model over the next 3 years (beyond the scope of this thesis). I hope that within this next development cycle ATAG can be iterated into a device that might be ready to embark on a first in man (FIM) trial to offer the AAAD population an effective and less invasive treatment strategy.

Acknowledgements and Contributions

Professor Martin Rothman – The inventor of the ATAG, the supervisor and funder of this MD thesis – the man who always has a plan.

Andrew Pacey (Advotek Medical Devices) – Medical device engineer who I collaborated with for the design and build of the first PoC model graft and delivery system.

Stephanie Parnell (Queen Mary University London, QMUL) – final year medical student whom I supervised. She assisted me with the platelet activation work, CT aorta measurement, and cadaveric animal aortic dimensions.

Professor Stephen Greenwald (QMUL) – Invaluable knowledge and assistance with basic flow rig set up, pressure and flow measurement.

Professor Tim Warner (QMUL) – for supervising the platelet activation studies on stent graft material at William Harvey institute and allowing use of his facilities and laboratory support.

Professor Dan Brockman (RVC Professor of small animal surgery), Dr David Connelly (RVC Cardiologist) - collaborating with me from the RVC, aiding the development of *in vivo* animal trial work for the I4I grant application.

Dr Francesco Alpendurada and Dr Raad Mohiaddin, Research Fellow and Cardiac Magnetic Resonance (CMR) Consultant at the Royal Brompton CMR unit for allowing me access to and training me in the measurement of aortic diameters in their Marfan's syndrome patient cohort.

Professor Yen Ho – Professor of Cardiac Morphology at the Royal Brompton Hospital, who demonstrated human coronary and aortic valve anatomy with her cadaveric collection, enabling me to better understand the morphology of the aortic root in health and in disease.

Professor Salah Qanadli – Professor of Interventional Radiology at the Centre Hospitalier Universitaire Vaudois (CHUV hospital), Lausanne, Switzerland. He allowed me access and mentored me in the CT measurement of aortic diameters in a AAAD cohort.

Torsten Struntz and Andrew McCulloch were part of this project from the very outset following NHS Innovations London (NHSIL), PoC funding. Torsten was project manager and helped with the commercial introductions, and Andrew advised upon all issues relating to intellectual property (IP).

Thomas Nissl and the team at Qualimed, Hamburg, Germany – our prototype development engineering partner, for allowing me to visit their facility and perform all of the 2G ATAG stent graft testing.

Duncan Keeble – Chief design engineer at Lombard Medical Technologies an abdominal stent graft company based in Oxfordshire. He allowed me access to Lombard's *in vitro* arterial training rig and provided me with some materials so that I could manufacture the first PoC delivery system.

Dr Ayesha Qureshi – for helping with thesis format and proof reading.

Roy Hammans (Art2Science) – Professional artist for re-drawing all of my Figures.

Contents

Table of Tables

Table of Figures

Abbreviations and acronyms

1G	First Generation
2G	Second generation
3G	Third generation
AIIRB	Angiotensin II Receptor Blocker
AAA	Abdominal aortic aneurysm
AAD	Acute aortic dissection
AAAD	Acute Ascending Aortic Dissection
ACE	Angiotensin Converting Enzyme Inhibitor
ADP	Adenosine Di-phosphate
AIT	Adventitial inversion technique
AMI	Acute myocardial infarction
AP	Antero-posterior
AR	Aortic regurgitation
AS	Aortic Stenosis
ATAA	Ascending Thoracic Aortic Aneurysm
ATAG	Ascending Thoracic Aortic Graft
AV Flow	Arterio-venous Flow
AV	Aortic valve
BAV	Bicuspid aortic valve

BSA	Bovine serum albumin
CE	CE Mark Conformité Européenne, meaning "European Conformity"
CHD	Coronary heart disease
CHUV	Centre Hospitalier Universitaire Vaudois
CMR	Cardiac Magnetic Resonance
CPB	Cardio-pulmonary bypass
CT	Computerised Tomography
CVA	Cerebro-vascular accident
CX	Circumflex coronary artery
EARS	External Aortic Root Support
ePTFE	Expanded Polytetrafluoroethylene
F	French size (standard diameter sizing system)
FDA	Food and drug administration
FEA	Finite element analysis
FIM	First in man
GA	General anaesthetic
GRF	Gelatin-resorcin-formaldehyde-glutaraldehyde bio-glue
I4I	Invention for Innovation funding stream
ID	Internal diameter
IFU	Instructions for use
IP	Intellectual property

IRAD	International registry of aortic dissection
IZ	Implantation zone
LAD	Left anterior descending coronary artery
LCA	Left coronary artery
LMCA	Left main coronary artery
LSCA	Left subclavian artery
LVOT	Left ventricular outflow tract
MRA	Magnetic Resonance Angiography
MRI	Magnetic Resonance Imaging
OMT	Optical medical therapy
PPM	Permanent pacemaker
POC	Proof of Concept
PTFE	Polytetrafluoroethylene
PU	Polyurethane
PVT	Percutaneous Valve Technologies
QMUL	Queen Marys University, London
RBCT	Right brachio-cephalic trunk
RCA	Right coronary artery
RCCA	Right common carotid artery
RCT	Randomised controlled trial
RSCA	Right sub-clavian artery

RRA	Right radial artery
RVC	Royal Veterinary College, London
SD	Standard Deviation
STJ	Sino-tubular junction
STS	Society of Thoracic Surgeons (USA)
TAVI	Trans-catheter aortic valve implantation
TEVAR	Thoracic Endovascular Aortic Repair
TOE	Trans-oesophageal echocardiography
TRR	Total aortic root replacement
TTE	Trans-thoracic echocardiography
VSRR	Valve sparing aortic root replacement

Published patent pending

MewburnEllis
LLP
PATENTS • TRADE MARKS • DESIGNS • COPYRIGHT

Specification for Patent Application

COUNTRY	WO
APPLICATION No.	PCT/GB2009/000485
DATE FILED	23/02/2009
EARLIEST PRIORITY	22/02/2008

YOUR REF: NHSIL1000.2(PCT)
OUR REF: SC/LP8614317

APPLICANT: BARTS AND THE LONDON NHS TRUST
ICT Building
56-76 Ashfield Street
The Royal London Hospital
Whitechapel
London E1 1BB

TITLE: BLOOD VESSEL PROSTHESIS AND DELIVERY APPARATUS

INVENTOR: KEEBLE, Thomas
ROTHMAN, Martin

PRIORITY APPLICATION: GB 0803302.9 filed 22 February 2008

LONDON
33 Gutter Lane
London
EC2V 8AS
Tel +44 (0)20 7776 5300
Fax +44 (0)20 7776 5399

BRISTOL
22-24 Queen Square
Bristol
BS1 4ND
Tel 0117 945 1234
Fax 0117 926 5692

CAMBRIDGE
Newnham House
Cambridge Business Park
Cambridge CB4 0WZ
Tel 01223 420383
Fax 01223 423792

MANCHESTER
Bridgewater House
Whitworth Street
Manchester M1 6LT
Tel 0161 247 7722
Fax 0161 247 7766

An overview of my thesis

Descending thoracic aortic dissection and aneurysm are now commonly treated using endovascular stent grafts, inserted through a small calibre (approximately 6-8 mm) access sheath placed into the iliac or femoral artery. Stent grafts consist of an expandable stent scaffold, covered in a material which lines the inside of the dissection or aneurysm excluding flow into the false lumen, or preventing outward pressure on the aneurysmal segment. Endovascular treatment of the descending thoracic aorta when compared to an open surgical approach results in reduced mortality and morbidity as well as reducing hospital stay (5;6;10). Figure 1 below shows a schematic of a endovascular stent graft:

Figure 1: Schematic of a thoracic stent graft within the descending aorta

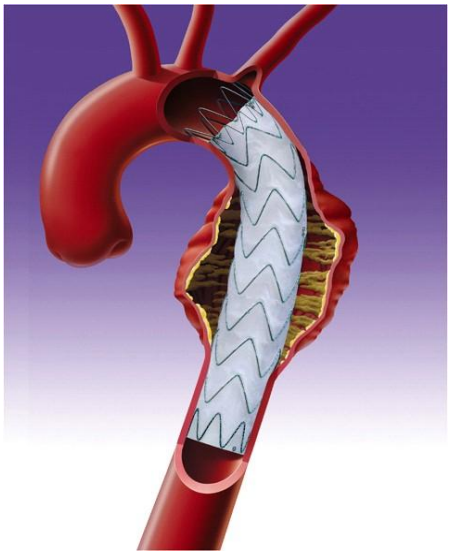

Covered descending thoracic endovascular stent graft, deployed percutaneously from a peripheral arterial sheath. The stent graft has a proximal seal within a normal diameter descending aorta, the graft material then excludes the aneurysmal segment with a distal landing zone within normal sized aorta.

In 2012 no commercially available endovascular stent graft yet exists to treat Acute Ascending Aortic Dissection (AAAD) or Ascending Thoracic Aortic Aneurysm (ATAA). Contemporary treatment remains open surgical, involving sternotomy, cardio-pulmonary bypass (CPB), and reconstructing the aorta with a graft material. To maintain coronary perfusion, coronary arteries are often re-implanted, and the aortic valve may be replaced or repaired to ensure aortic valve competence (9).

In 2007 Professor Rothman's concept of an Ascending Thoracic Aortic Graft (ATAG) was to design, develop and test a percutaneously deliverable stent graft with covering that would enable endovascular treatment of AAAD and potentially ATAA. In addition to excluding an ascending thoracic dissection flap or aneurysm, ATAG should have design features allowing preservation of coronary flow and aortic valve integrity - a vital feature given the close proximity of the ascending aorta to the aortic valve and coronary artery ostia.

There exists currently a huge unmet clinical need as 28% of patients presenting in the Western world with AAAD are turned down for conventional surgery, with an in hospital mortality rate of >50% (2). Not only that but despite improvements in AAAD diagnosis, surgical techniques and intensive care provision there has been very little improvement in AAAD surgical outcomes over the last 3 decades, despite falling mortality and morbidity associated with elective ATAA surgery (2). Newer, less invasive treatments must be sought for both AAAD and ATAA.

The aim of this thesis is to understand why there is currently no device capable of percutaneously treating AAAD and ATAA, and to then take the reader on a journey from the conception of ATAG in 2007, and document its development up to a 2G device ready

for advanced *in vitro* and *in vivo* testing. I hope this thesis will show the methodical, and meticulous iterative process necessary for a successful outcome as one must navigate through technical, scientific, clinical, commercial, financial, and regulatory challenges all of which must be overcome to achieve the ultimate aim of delivering a novel and effective minimally invasive solution to treat patients with ascending thoracic aortic disease - many of whom are currently turned down for conventional surgery with appalling clinical outcomes (2).

After original ATAG concept discussions with Professor Rothman I felt that because of the close proximity of both aortic valve and coronary arteries to the diseased aortic segment, the aortic root anatomy must be very well understood. The AAAD and ATAA disease processes must be well characterised and I wanted to understand the current gold standard surgical treatments available for these aortic syndromes, as any proposed endovascular solution must be capable of replicating the surgical end-result with regard to dissection exclusion, preservation of coronary flow, and retained integrity of aortic valve function.

In my search for understanding of the normal and diseased aortic root anatomy I collaborated with Professor Ho, Cardiac Morphologist at the Royal Brompton Hospital who demonstrated the aortic root and coronary anatomy to me with her cadaveric samples. She is well published in this area, but after discussions and literature searches in 2007 when this project began there appeared to be a paucity of anatomical data on the aortic root dimensions and coronary angulation in AAAD and ATAA; information that I felt was vital to allow me to proceed to design specification of the ATAG.

To acquire this novel aortic root and coronary anatomical data on AAAD and ATAA I collaborated with Professor Salah Qanadli, a Consultant interventional radiologist at the Centre Hospitalier Universitaire Vaudois (CHUV), Lausanne, Switzerland and Dr Raad Mohiaddin, Consultant Cardiologist in CMR at the Royal Brompton Hospital, London. Both are well published in the arena of aortic root measurement, and have appropriate cohorts of AAAD and ATAA patients from which I could perform my desired retrospective CT and MRI measurements (11).

Having gained a thorough understanding of the disease processes (AAAD and ATAA), current surgical treatments and an in depth anatomical assessment of the aortic root and coronary anatomy, I proceeded to describe a design input specification for the ATAG.

As an interventional cardiologist in training I was somewhat apprehensive about the transition from device design specification to the PoC prototype build, as I have limited understanding of materials science, and prototype manufacture. Throughout this process I collaborated with medical engineers who built the stent graft prototypes. During the PoC build I was supported by Andrew Pacey an engineer working for Advotek Medical devices (AMD), Hitchin, UK, and Leena Jatinen a PhD student from Imperial College, working with AMD. All subsequent medical engineering support (2G ATAG onwards) was provided by Qualimed GmbH, Hamburg, Germany.

My thesis describes in detail the design specification formulation and testing of the PoC ATAG and the 2G ATAG. This includes sections on the design and testing of the stent frame, the covering material (PU), and the delivery system. Lessons learned from testing enabled me to formulate a potential design specification for a 3G ATAG device ready for

sophisticated pulsatile flow *in vitro* analysis and potential *in vivo* animal model implantation.

At the time of my research fellow appointment Professor Rothman had already secured PoC funding and a small amount of follow on funding to proceed towards a 2G ATAG. During my research period I wrote as co-applicant, with Professor Rothman and was awarded a NIHR I4I grant for £743,000 (grant application detailed within Appendix) to develop a 3G ATAG with delivery system and test this within an *in vitro* flow rig, and within an *in* vivo animal model. To prepare for this next stage of work (to be performed by my successor) I collaborated with Professor Steve Greenwald (Professor of cardiovascular mechanics, QMUL, London) to set up a basic flow rig for *in vitro* testing, and with Professor Dan Brockman (Professor of small animal surgery, RVC, London) to investigate an appropriate animal model.

There are also short sections within this thesis on intellectual property (IP) and an overview of health economic data for the current costs of treating patients with AAAD.

The journey of this thesis from idea conceptualisation, literature review, anatomical data acquisition, design specification, through graft and delivery system build and testing, to setting up *in vitro* and *in vivo* testing protocols has been fascinating and I now have a more complete understanding of the steps involved in translating a new medical device from initial concept towards clinical reality.

Chapter One

Introduction

Chapter One: Introduction

1.1 Medical device innovation – the process

Many health care professionals will have in the course of their career what they believe to be a “novel” or “innovative” treatment solution, whether it be a simple change in design to an existing technology (an iterative design improvement), or a potentially “disruptive” technology which can completely change the treatment landscape for a particular clinical problem, for example balloon expandable stents in percutaneous coronary intervention (12). For a variety of reasons only a tiny proportion of all ideas will manage to make it to clinical utility, manufacture and widespread use.

Within the innovation department at Barts Health NHS Trust Professor Rothman set up an innovation development process which helps to “de-risk” and streamline the process from the outset and optimise the chances of an idea becoming a clinical reality. For the purposes of explanation this process is outlined below. While at first glance this may look like a linear progression from idea to manufacture, in the real world all factors are considered from the outset, as it would be pointless to design and develop a device that fulfilled all developmental criteria but could not then be mass produced cost effectively.

1 – IDEATION / EVALUATION OF FACTS

The first process after idea creation is a rigorous and critical evaluation of facts. This will encompass a review of the literature for clinical need, potential market size and value, device competition and early intellectual property searches establishing the likelihood of freedom to operate (FTO).

2 - FEASIBILITY (PoC)

Once an idea has been identified as fulfilling an important clinical need, and having an adequate market size, preliminary searches are undertaken to ensure that there is no obvious competitor device on the market and that there is freedom to operate. The next important step is to prove feasibility or PoC. This is often done relatively cheaply utilising off the shelf materials which are modified to fit the new purpose and prove the concept. PoC devices are then often used to raise early stage funding for the next development stage.

Feasibility studies also allow the inventor to crudely estimate the possible build costs, and compare that to the cost of the current standard of care.

3 - INTELLECTUAL PROPERTY (IP)

For a medical device to be successful in the market place the unique novelty points must be intellectually protected, usually through a family of patents. Throughout a development project like ATAG intellectual property is constantly collected and patents adjusted / drafted in collaboration with intellectual property lawyers from specialised medical device IP law firms. Also important, but often not patentable is the development of manufacturing “know-how”.

4 - REGULATORY ASSESSMENT

It is important early on in the process to engage and collect data for the relevant regulatory bodies. Many development companies have in-house regulatory personnel to

evaluate and collect the necessary device, material and processes information to minimise regulatory risk. Regulatory approval is vital in both Europe (to obtain CE Mark Conformité Européenne, meaning "European Conformity") and the USA (to obtain Food and Drug Administration - FDA approval) to enable companies to sell their device for a specified indication within these countries.

5 – RISK ANALYSIS

Risk to the success of the project is continually assessed. In general these are divided up into device specific failure modes, and more generic device and regulatory risks. Failure Mode Effect Analysis (FMEA) allows risk from the worst case scenario, to the more trivial ones to be fully appreciated and evaluated.

6 – DESIGN INPUT SPECIFICATION

With lessons learned from the PoC model and key user needs specification a “wish list” of design input characteristics are formulated.

7 – DESIGN OUTPUT SPECIFICATION

An assessment of what has been produced by the manufacturer and how it compares to what was specified in the design input specification.

8 – BENCH TESTING REQUIREMENTS

Bench testing is an essential element to ensure that the user need specifications are met in the design input and output specifications. The chosen bench tests must accurately

assess whether the design meets the user needs requirements. Throughout this process information about the design, manufacture and testing must be documented meticulously for the regulatory bodies so that the appropriate approval can be sought as expediently as possible.

9 – PROTOTYPES

Prototyping and bench testing is an iterative process gradually working towards a device that fulfils the user specification.

10 – ANIMAL TESTING

Most implantable devices will go through *in vivo* testing in an appropriate animal model. This phase of the development further validates the device and technique and there are inevitable new design inputs which are validated by the design outputs and results. Throughout all *in vitro* and *in vivo testing* there will be collection of data concerning material biocompatibility, toxicity, and thrombogenicity. Materials that are already in clinical use within the vascular arena will already have a regulatory dossier and this can in some cases streamline the regulatory process.

11 – CLINICAL TESTING & REGULATORY APPROVAL

Although beyond the scope of this thesis a device like ATAG will only achieve clinical utility and market acceptance after clinical testing in the form of a clinical trial and the achievement of regulatory approval (CE mark in Europe, FDA approval in USA).

12–MANUFACTURING

A manufacturer must be sourced which has the technical, regulatory and manufacturing skill and capacity to produce the device for market to the correct standards and quality, in adequate numbers in an appropriate time scale for an agreed cost. One must also consider manufacturer location, materials supply chain, and consideration of second suppliers. QualiMed GmbH, Hamburg, Germany - our partner for the 2G ATAG development has established a manufacturing skill set recognised by its ISO 13485:2003 and ISO 9001:2008 standards.

1.2 Anatomy of the ascending aorta, and its relationship to coronary arteries, aortic valve and great vessels in health

In 2007 I met with Professor Rothman to discuss an idea he had for a novel endovascular treatment modality for AAAD and potentially ATAA. His sketches showed a stent graft (length and diameter undetermined) with 2 coronary arms broadly looking like an "inverted t shirt".

To enable me to design a PoC ATAG device I wanted to understand the anatomy and dimensions of the aortic root and ascending aorta in health, and elucidate how much information existed about this region in aortic disease. Only with a high degree of anatomical understanding would I be able to commence on a design specification for the ATAG. This first section details the available normal aortic anatomical information, much of which was published from 2009 onwards in part due to the increased interest and number of Trans-catheter Aortic Valve Implantation (TAVI) procedures performed worldwide.

1.2.1 The Normal Aorta

The aorta is the main arterial route for carrying oxygenated blood from the heart to all of the body's tissues. For descriptive purposes it is divided into regions as documented in Figure 2 below:

Figure 2 Anatomy of the aorta

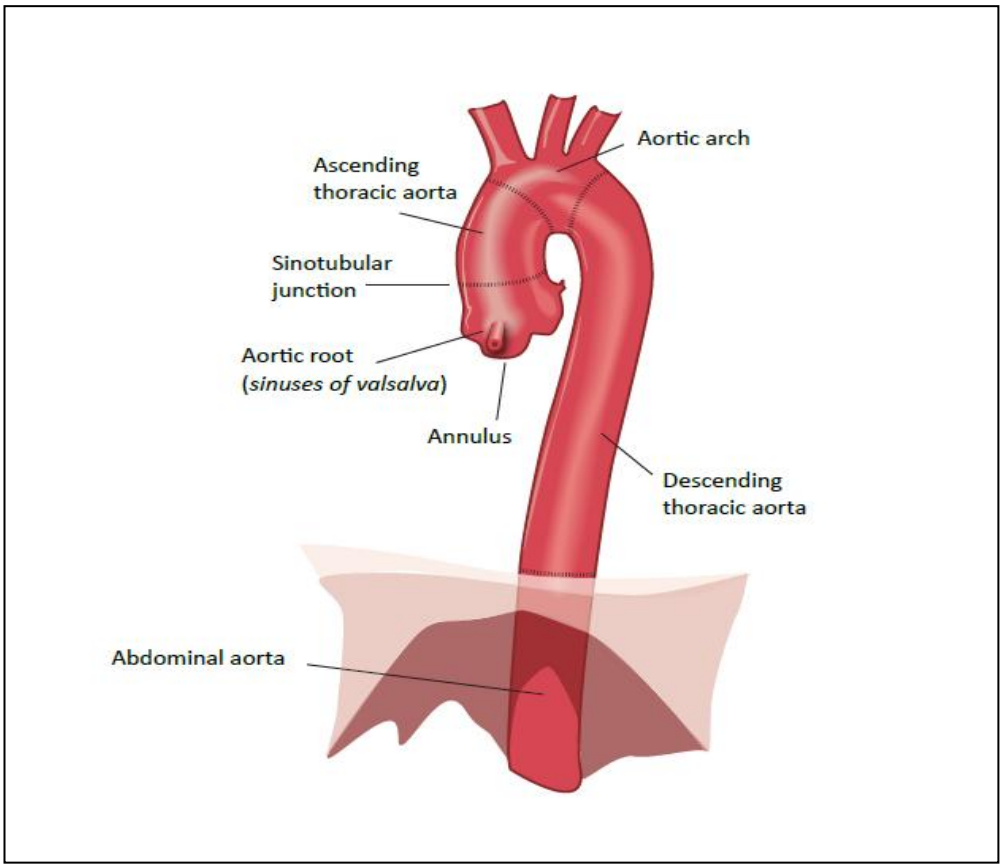

Blood is ejected from the left ventricular cavity out through the Left Ventricular Outflow Tract (LVOT) and aortic valve. There are then 3 sinuses of Valsalva - the right and left of which usually contain the ostia of the coronary arteries. The sinotubular junction (STJ) is where the aortic root becomes the ascending aorta. The ascending aorta becomes the arch at the right brachiocephalic trunk (RBCT) and then the descending aorta after the left subclavian artery (LSCA). Once the aorta has moved through the diaphragm it becomes the abdominal aorta (AA).

In order for me to develop a novel endovascular stent graft for the ascending aorta I felt it was vital to focus attention to understanding the anatomy of the portion of aorta from the left ventricular outflow tract (LVOT) up to the RBCT. This region includes the aortic valve whose integrity must be ensured, and the coronary arteries whose coronary flow must be preserved.

1.2.1.1 The LVOT to RBCT

It is universally accepted that for any patient undergoing endovascular intervention the specific vascular anatomy must be well understood. Work up for endovascular intervention including TAVI usually includes a high resolution heart and vascular CT scan. The information gathered allows the interventional team to plan the endovascular procedure, including device selection, accurate sizing, and access route planning. Normative thoracic aortic dimensions have previously been determined by CT angiography, however they were not electrocardiograph (ECG) gated and as such were subject to considerable axial and transverse motion during the cardiac cycle making the ascending aorta measurements less accurate and precise (13;14).

Professor Salah Qanadli an interventional radiologist working at the CHUV hospital in Lausanne, Switzerland and his cardiothoracic surgical colleagues have recently published data documenting normative size values for the ascending aorta, providing reference measurements in order to understand the ascending aortic anatomy better for the future development of novel endovascular procedures (11). Their results are interesting and provide “normal values” in patients without ascending aortic abnormality.

The CHUV group utilised a 64 slice ECG gated CT scanner and protocol giving high resolution (0.625 mm slice thickness). Acquisitions were obtained after injection of 100-120 ml of non-ionic contrast medium. ECG assistance for aortic studies allows the synchronisation of data acquisition to the heart cycle in order to obtain CT data during the diastolic phase when heart and aortic movement is minimal thus reducing the motion artefact. Dynamic data were also used for the pulsatility of the ascending aorta. The dynamic diameter change, and the torsional forces placed upon the ascending thoracic aorta with each and every systole and diastole add complexity both to how a the ATAG device might be appropriately sized, and also exerts mechanical challenges to the stent graft body, stent graft covering material, and the stent graft / vessel interface. If these torsional factors can be better understood and the ATAG device designed to accommodate these physiological stresses it is likely to have increased longevity.

Pulsatility was defined as the percentage difference of minimal and maximal antero-posterior (AP) and latero-medial (LM) diameters of the mid ascending aorta. Mean, median, maximum and minimum values were considered with standard deviations (SD).

The 77 patients in the Qanadli study consisted of 59 men and 18 women with an age range from 22 to 83 years. Mean age was 54.7 years (median 54).

Qanadli *et al.* measured 4 main diameters (D1-D4) and 4 lengths (L1-L4) as described in Figure 3 below:

Figure 3 CT aorta measurements according to Qanadli protocol

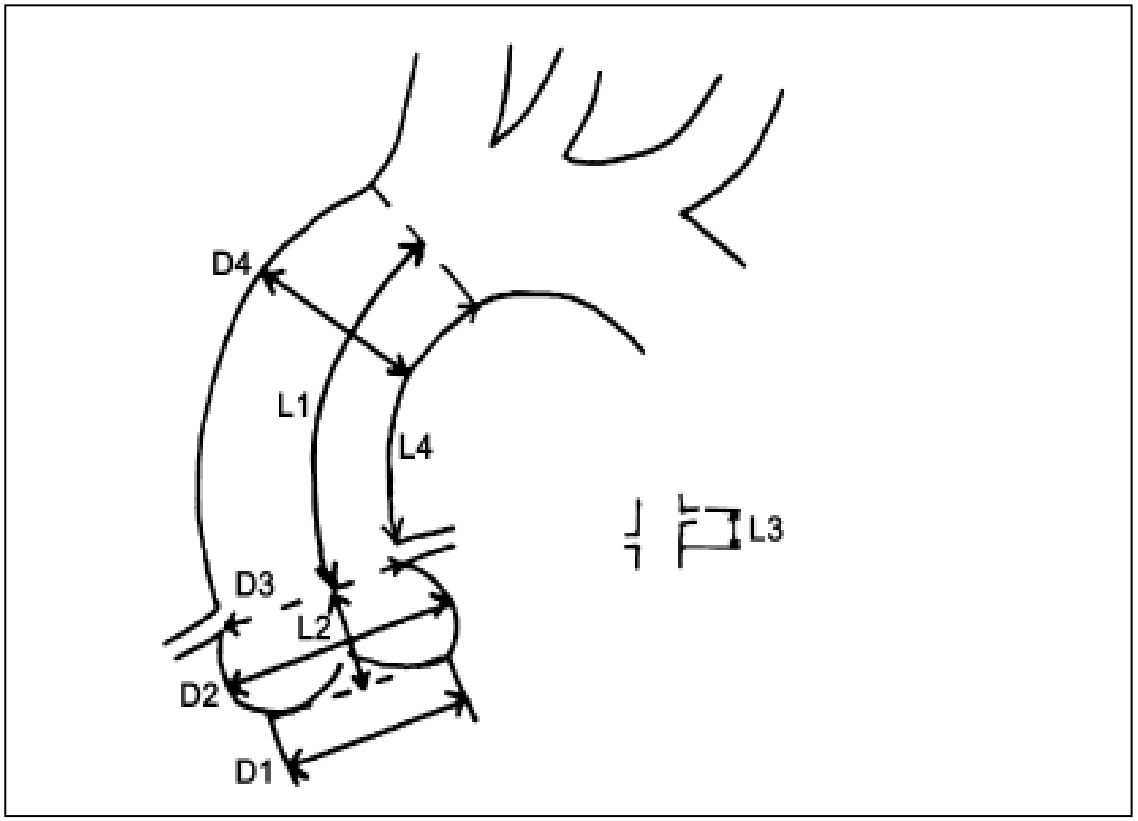

Figure adapted from Qanadli *et al. (11).* Qanadli protocol for aortic dimensions and lengths. Diameters measured included D1 - LVOT diameter, D2 coronary sinus diameter, D3 - STJ diameter, D4 - Mid ascending aorta diameter. Lengths measured included L1 - Length from coronary ostia to RBCA, L2- Length from annulus - coronary ostia, L3 - Distance between coronary ostia, L4 - Minimal arc from LMCA to RBCA.

The method by which Qanadli and colleagues manipulate the 3D CT dataset is also important. During post processing the group formulate a “centre line” to reflect the best possible “true” measurement of aortic diameters and distances i.e. truly perpendicular to the vessel, as shown in Figure 4 below:

Figure 4 Measurement at the level of the STJ in a 54 year old woman.

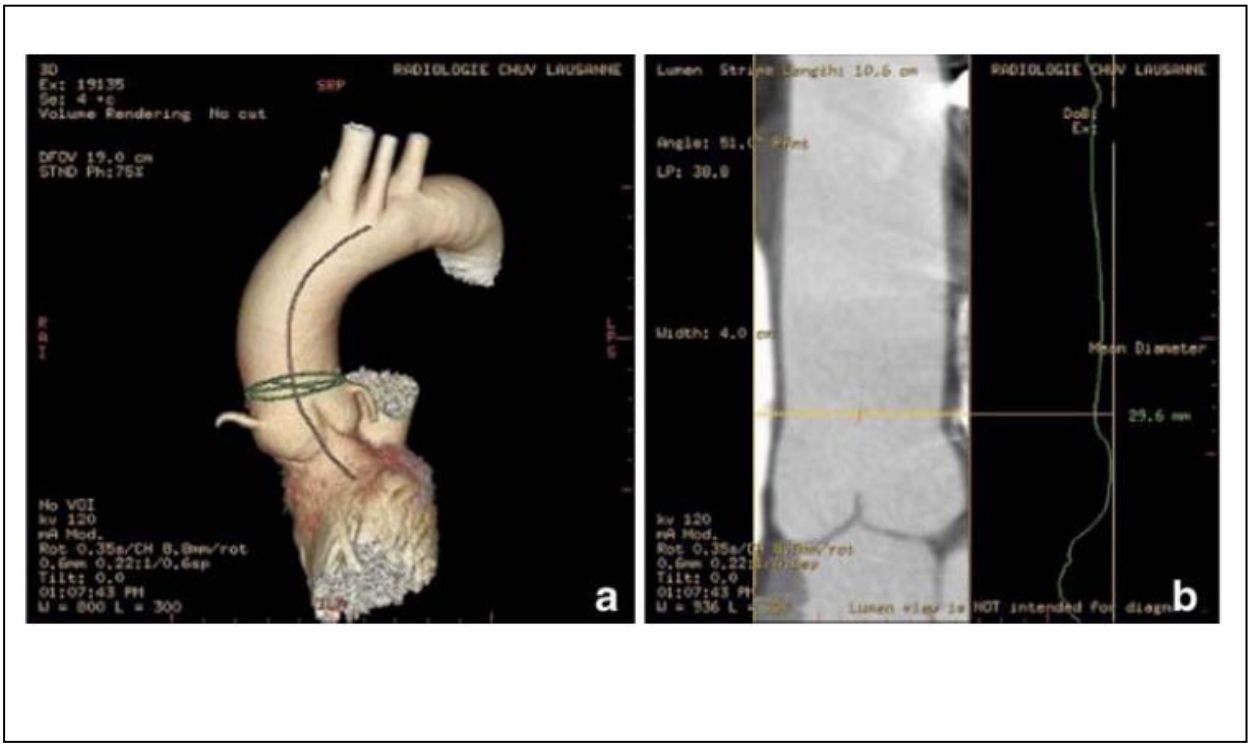

Reproduced with kind permission of Salah Qanadli (CHUV, CH) (11). a) Shows a volume rendered 3D reconstruction of the ascending aorta and the aortic arch with centre line super-imposed, and a circumferential measurement of the aortic diameter at the STJ. b) Lumen view of the ascending aorta, reconstructed from the centre line.

The Qanadli data of normative aortic measurements is summarised in Table 1 below:

Table 1 Normative mean aortic measurements by CT:

Measurement	**Mean diameter (mm +/- SD)**
D1 Outflow tract	20.3 +/- 3.4
D2 Coronary sinus	34.2 +/- 4.1
D3 STJ	29.7 +/- 3.4
D4 Mid ascending aorta	32.7 +/- 3.8
Measurement	**Mean distance (mm +/- SD)**
L1 Annulus to RBCT	92.6 +/- 11.8
L2 Annulus to coronary artery	12.1 +/- 3.7
L3 Distance between coronary ostia	7.2 +/- 3.1
L4 Minimal arc of ascending aorta from LMCA to RBCT	52.9 +/- 9.5

AP and transverse LM diameters of the mid ascending aorta during the cardiac cycle varied from a maximum of 34.2 mm to a minimum of 31.3 mm and from a maximum of 33.6 mm to a minimum of 31.2 mm. Computed cycle variations are therefore 8.4% and 7.3% respectively. This variation is lower than that described by Van Prehn *et al.* where using a similar CT protocol they described cycle diameter variation at 3 points as shown in Figure 5 below:

Figure 5 Points of aortic dimension variation with cardiac cycle

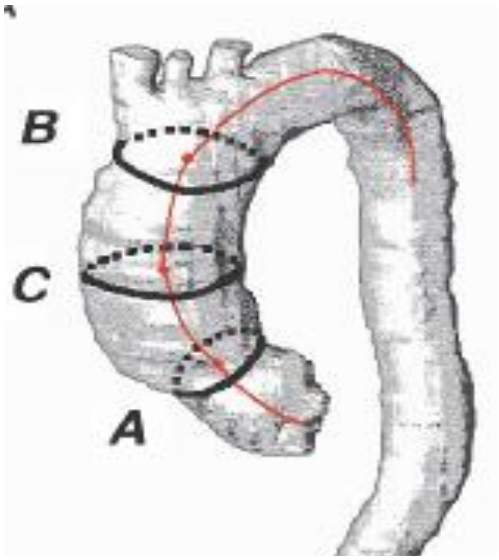

Adapted from Van Prehn *et al*.(15) Aortic dimension variation with cardiac cycle A) 5 mm above the coronary arteries 17.4% B) 5 mm below the RBCT 13.9% C) In the mid aorta 12.9%. All 3 levels showed significant maximum diameter change. Level A displayed significantly higher "pulsatility" compared to level B or C *(p=0.02)*. Level B and C did not differ significantly.

One possible explanation for the higher pulsatility compared to Qanadli's data could be related to the small cohort size (n=15) and that Van Prehn's cohort was made up of patients with diseased aortas – all had an abdominal aortic aneurysm (AAA mean diameter 6.5 cm) and a higher average age of 72.2 years (15). A recent study by De Heer *et al.* also support this dynamic aortic root sizing, with systolic diameters being significantly greater than those seen in diastole (16).

Conclusions relevant to ATAG:

The normal aorta measures around 20 mm at outflow tract, 34 mm at the sinus of Valsalva, 30 mm at the STJ and 33 mm at the ascending aorta (11).

The aortic annulus to the RBCT is less than 100 mm in length, the annulus to the RCA is 12 mm, and on average in this normal cohort the LMCA is 7 mm above the RCA. The inner curve from the LMCA to the point opposite the RBCT is approx 50 mm. Depending on the patient size, sex, curvature of the aorta, and the proximal and distal sealing zones the proposed ATAG device is likely to be between 50 and 100 mm in length (11).

In a normal cohort there is a systolic / diastolic pulsatility of 8%, which in diseased cohorts with AAA is described as up to 17% (11;15). ATAG must have an appropriate sizing protocol to enable the endograft to have a sufficient proximal and distal seal, preventing endoleak. The graft frame and the material must undergo rigorous fatigue testing as the aortic pressure and dynamic movement will place the graft materials under considerable mechanical stress.

1.2.1.2 Normal coronary artery anatomy and association with the aortic valve

The ascending aorta has remained a "no-go area" for routine endovascular therapy for numerous reasons including proximity to the aortic valve, difficulty in navigating devices into position around aortic arch, inadequate landing zone, size variation and difficulty in achieving accurate and precise deployment.

A further layer of complexity is then added when one considers the close proximity of the coronary arteries to the aortic valve.

This next section describes the size, angulation, take off and relationships between the coronary arteries and the aortic valve.

1.2.1.2.1 Coronary artery anatomy

The majority of the human population have 2 main coronary arteries a right coronary artery (RCA) and a left main coronary artery (LMCA) which splits into the circumflex (Cx) and left anterior descending artery (LAD) (17).

Approximately 1% of the population will have an anomalous coronary artery anatomy, which can be further sub-divided as follows:

30% - LAD and Cx coronary ostia originate separately from the left sinus of Valsalva rather than a LMCA that bifurcates.

28% have an anomalous origin of the Cx from the right sinus of Valsalva or RCA.

The RCA directly originating from the aorta in 11.2% of anomalous patients.

8% have an RCA originating from left sinus of Valsalva (17;18).

The location of the RCA as described by Qanadli *et al.* is 12 mm above the aortic annulus and more often than not within the sinus of Valsalva (11).

Christensen *et al.* measured the length of the LMCA using dual source CT images in a patient group with normal coronary arteries. The average LMCA length was 9.9 +/- 4.15 mm (mean +/- SD) (range 2-21). There was no significant difference in LMCA length between groups with right or left sided coronary dominance (19). These findings are also in reasonable agreement with a contemporary cadaveric study by Reig *et al.* in 2004 finding a mean LMCA length of 10.8 +/- 5.52 mm (mean +/- SD) (20).

1.2.1.2.2 Coronary artery anatomy in relation to the aortic valve

In 1997 Ho *et al.* published *"the location of the coronary arterial orifices in the normal heart*" in which they provided a very detailed analysis of relevant anatomy (21). The group examined 23 normal hearts collected at necropsy from male and female subjects who died from non cardiovascular causes. The age of death ranged from 29 to 79 years, with all hearts opened and dissected via an incision in the anterior longitudinal wall.

In all specimens the aortic valve possessed 3 leaflets, which were nearly equally spaced around the aorta – in only one case was there perfect symmetry. In each valve the mean height of the leaflets measured 13.4 +/- 1.43 mm (mean +/- SD) (range 10-15).

In all specimens the coronary arteries arose from the appropriate aortic sinuses. In 69% of specimens the LMCA arose below the level of the STJ. It arose at the level in 9%, and above the level in the remaining 22%. The highest position was 2 mm above the STJ, the lowest 2 mm below. The mean length of the LMCA was 10 +/- 2.3 mm (mean +/- SD).

The RCA arose below the STJ in 78% of specimens, at the level in 9% and above in 13%. The highest position was 2.5 mm above the junction. This is represented in Figure 6 below adapted from the Ho *et al.* paper (21).

Figure 6 Representation of location of coronary ostia

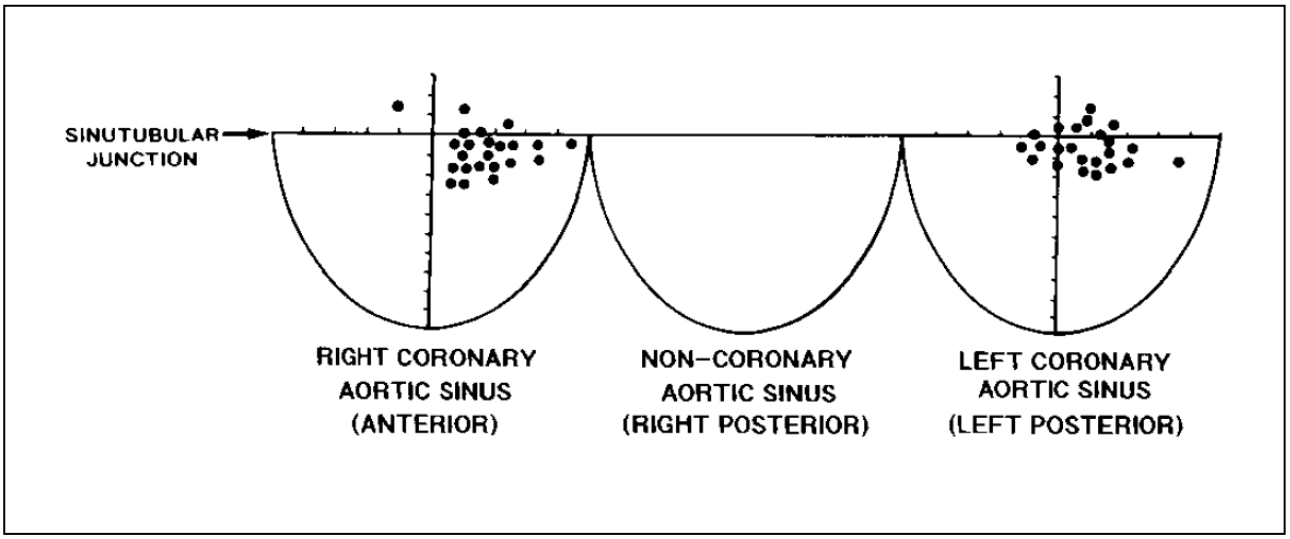

Adapted from Muriago *et al (21).* Figure shows the 3 aortic sinuses (anterio, right posterior and left posterior). RCA and LMCA orifices (dots) are not located in the centre of each aortic sinus, but instead there is a tendency for all orifices to be towards the zone of apposition of adjacent leaflets at the STJ.

These findings are consistent with McAlpine *et al.* who proposed that because the RCA is destined to pass around the tricuspid valve, it is appropriate for its orifice to be located

in the right half of the anterior aortic sinus therefore allowing the RCA to take a more direct path (22). Table 2 below shows the relationship between coronary ostia and STJ:

Table 2 Relationship between coronary ostia and STJ.

Both below	13
Both above	2
R above, L below	1
R below, L above	3
R at, L below	2
R below, L at	2

Adapted from Muriago et al. Right (R) and Left (L) coronary orifices above, below, or at the level of the STJ (21)

These data are important, as with such close proximity of the ostia of both the LMCA and RCA to the zone of apposition of the aortic valve leaflets (as seen in Figure 7 below) any endovascular device design which has a proximal sealing in this area must ensure that coronary artery flow is protected, without disrupting aortic valve function and integrity.

Figure 7 LMCA and RCA relative position to the STJ

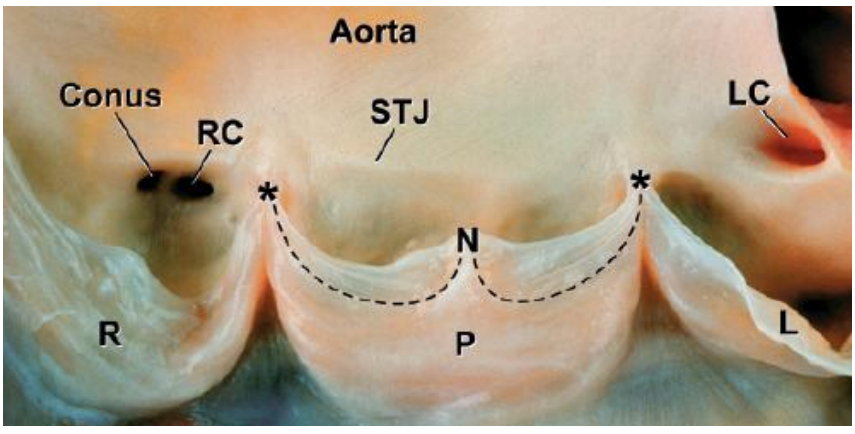

Conus branch, RCA and LMCA seen to originate within the sinuses of Valsalva below the STJ. RC – right coronary artery, R – right cusp, P - posterior cusp, STJ – sinotubular junction, L – left cusp, LC – left coronary artery.

If the ATAG is to be designed as an “inverted t-shirt” with coronary sleeves it is important to understand the diameters and length of both the LMCA and RCA, as well as the angulation and “take off” from within the respective aortic sinuses.

Dodge *et al.* in a cohort of 83 patients with normal coronary angiograms, report that the mean size of the LMCA was 4.5 +/- 0.5 mm (mean +/- SD), and the RCA varied between a mean of 3.9 +/- 0.6 mm (mean +/- SD) in right dominant circulations and 2.8 +/- 0.5 mm (mean +/- SD) in left dominant circulations. Women on average had smaller epicardial coronary arteries by -9% (*p<0.001)* even after correction for body surface area (BSA) (23). Dodge *et al.* in an earlier publication described the spatial location of the coronary arteries represented in Figure 8 and 9 below:

Figure 8 Spatial location of coronary arteries

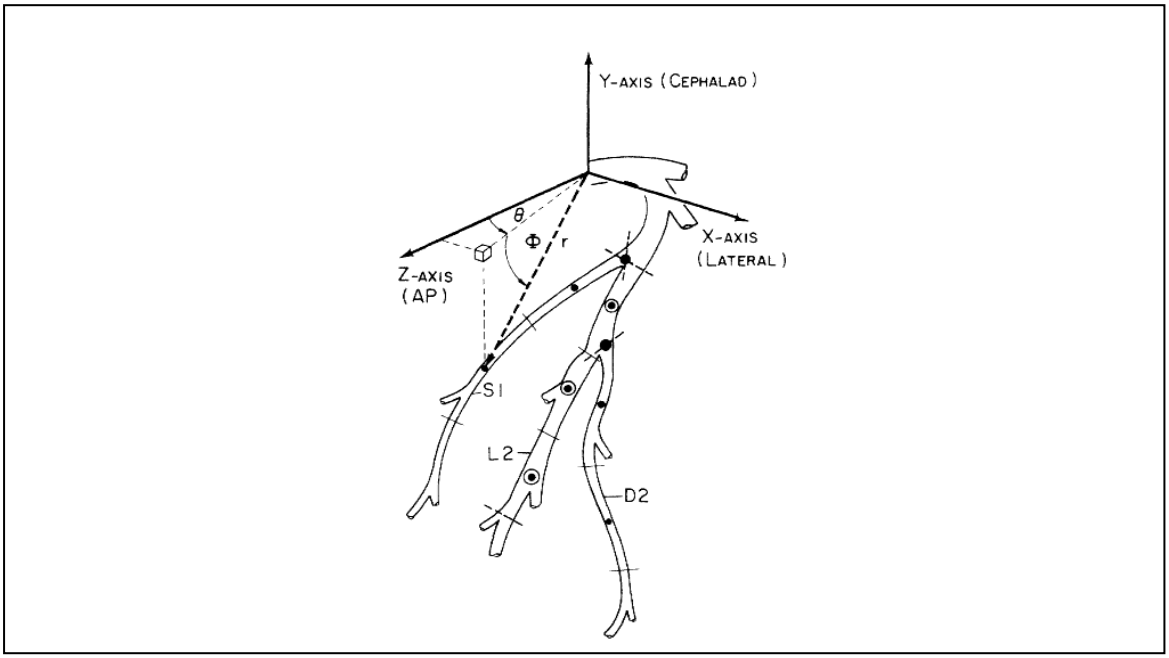

Figure adapted from Dodge *et al (24).* Spatial location of the coronary arteries in the Z-axis (antero-posterior), Y-axis (cephalad / caudal) and the X-axis lateral direction. S1 – 1st Septal, L2 – 2nd part of LAD, D2 – 2nd part of 1st diagonal.

Figure 9 Diagrammatic representation of normal coronary orientation

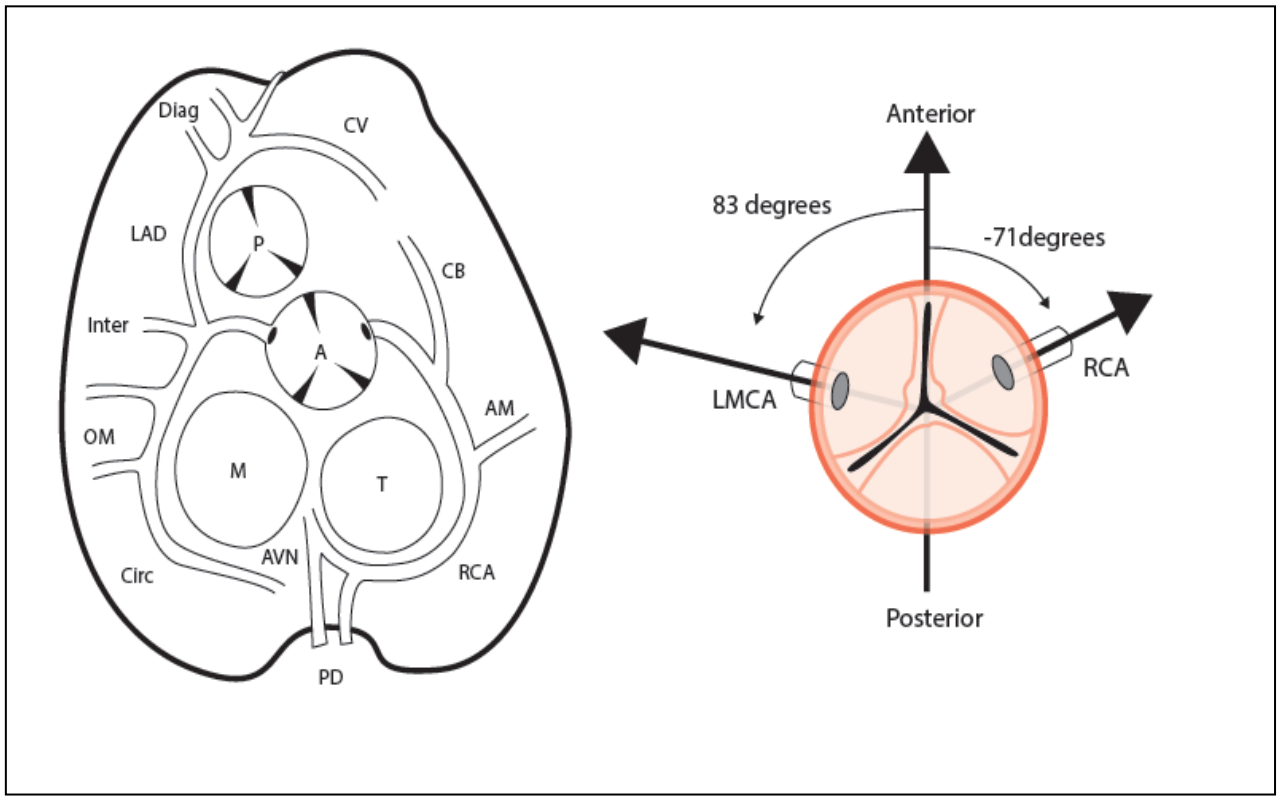

Adapted from Dodge *et al.(24).* Looking down on the heart from above, the LMCA and RCA are shown on the left with their branches detailed and labelled. The right hand figure shows a view of the aortic valve and coronary ostia from above, with the mean normal angle drawn between the LMCA and RCA. The LMCA has a take-off that is angulated 7 degrees cranial, and 83 degrees anti-clockwise from the AP plane (i.e. looking down on the aorta as a clockface originating at approximately the 9 o'clock position). In contrast the mean angulation of take-off of the RCA is 22 degrees caudal and -71 degrees in the clockwise direction from the AP plane (just after 2 o'clock on a clock face). CB – conus branch artery, AM – acute marginal artery, RCA – right coronary artery, T – tricuspid valve, PD – posterior descending artery, Circ – circumflex artery, M – mitral valve, OM – obtuse marginal artery, Inter – intermediate artery, A – aortic valve, LAD – left anterior descending artery, P – pulmonary valve, Diag – diagonal artery

Therefore in this cohort of normal individuals the mean angle between the LMCA and the RCA is (83 + 71) = 154 degrees.

Conclusions - Coronary artery and aortic valve anatomical association

The coronary arteries appear to have their origins about 12 mm above the aortic annulus, and the LMCA ostium is approximately 7 mm above the RCA ostium (11).

99% of the population have 2 main coronary arteries with >70% located within the respective sinus of Valsalva (i.e. below the STJ). Approximately 10% of coronary ostia originate at the level of the respective STJ, and approximately 15% originate above the STJ.

The LMCA is on average 4.5 mm in diameter and approximately 10 mm long (17;18). The LMCA ostium projects at a 7 degree angle slightly cranial, and 83 degrees anticlockwise from the AP plane, while the RCA is on average 3.9 mm in diameter (dominant circulation), with a 22 degree cephalad take off, 71 degrees clockwise from the AP direction, making an average angle between the 2 coronary ostia of 154 degrees (24).

Conclusions relevant to ATAG design specification:

The 2 coronary arteries are close to the aortic annulus (within 12 mm in this normal cohort). The ostia of the coronary arteries tend to sit within the respective sinus of the aortic valve - making the proximal fixation point / seal extremely important and potentially difficult to achieve without compromising the competence of the aortic valve. Achieving sufficient proximal seal, without endoleak, and preserving coronary flow without interruption of the aortic valve competence is going to be a real challenge.

The coronary arteries come off at an angle of 154 degrees to one another. To facilitate ATAG design specification it will be important to understand if this angle is maintained in AAAD and ATAA, as this will impact upon the degree of coronary sleeve angle variation required for the ATAG graft and what design features / materials / graft sizes and angulations will allow this to occur.

1.2.1.3 Aortic arch and peripheral vessels

For the ATAG to be delivered in a percutaneous fashion, from a distal access sheath, similar to that used with current TAVI devices, it is fundamental that the vascular tree diameters are well understood. In keeping with TAVI patient standardised work up, patients with AAAD and ATAA will also require a full vascular CT angiography or MR angiography (MRA). I will now review the available literature on normal artery diameter from aortic arch down to femoral artery.

I have condensed the maximal diameters of vessels from the aortic arch down to the femoral arteries into Table 3 below:

Table 3 Artery diameters from aortic arch to femoral artery

Artery	**Mean maximal diameter (+/-SD)**	**Author / Modality**
Aortic arch	27 +/- 3.6 mm	Dart *et al. (25)* / US
Descending aorta	24.6 +/- 3 mm	Wolak *et al.(26)* / CT

Table 3 cont.	**Mean maximal diameter (+/-SD)**	**Author / Modality**
Mean maximal common Iliac artery diameter	Male 13.3 +/- 2.0 mm Female 12.2 +/-1.3 mm	Paivansalo *et al. (27)* / US
Mean maximal common femoral artery diameter	Male 11+/-1.5 mm Female 9.7 +/-1 mm	Paivansalo *et al. (27)* / US

Mean maximal artery diameter and modality of measurement in large populations without CVD. US – Ultrasound , CT Computerised tomography.

While these are helpful data, the iliac and femoral diameters consist of a mean maximal diameter. In the setting of percutaneous therapies it is often more important to have the minimal diameter and the extent and position of calcification / stenoses to guide the location of the percutaneous puncture and ensure that the calibre of the vessel is sufficient and the tortuosity acceptable for insertion of a suitable introducer sheath.

In modern endovascular therapy work up all patients have a full vascular CT scan so that the access route and the type of sheath can be tailored to the patient. In poor quality small diameter femoral and iliac vessels, particularly in the elderly it is frequently necessary to place the introducer sheath into a surgically attached Dacron conduit often attached directly to the iliac artery – this is a potential access option for the ATAG device.

Over the last 5 years there have been considerable advances in the development of percutaneous TAVI technologies (28). As the devices and delivery systems have become of a smaller diameter, new access routes of insertion have evolved - including sub-clavian, direct aortic and left ventricular trans-apical (29). All access routes have

potential risks and benefits and access choice must be decided on a case by case basis, offering the patient the best possible outcome with the lowest possible risk.

1.2.1.4 Endovascular aortic nomenclature

Current aortic endovascular convention has divided the aorta into a number of “landing zones” allowing health care professionals to discuss aortic anatomies and interventions in a standardised manner. Figure 10 below shows this landing zone nomenclature (i.e. standardised description where an endovascular stent graft is positioned):

Figure 10 Endovascular aortic landing zone nomenclature

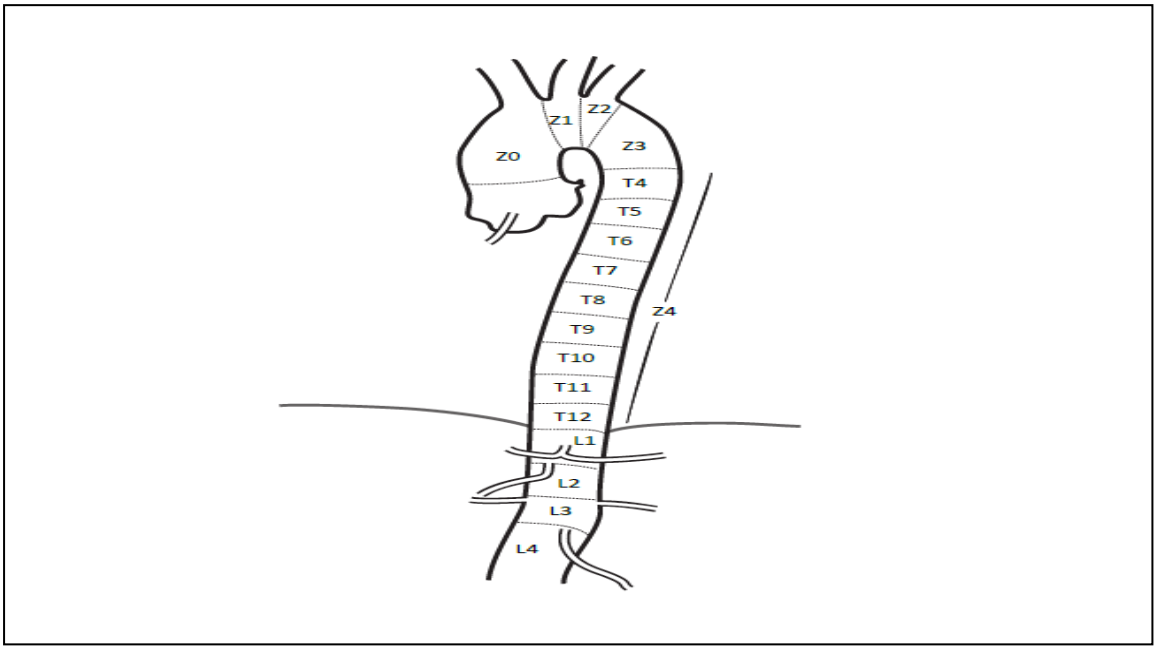

Adapted from Ishimaru (30). The positions of the proximal and distal ends of the endograft are indicated as zones (Z). The proximal end of the endograft should be indicated separately (i.e., as uncovered versus covered with graft material). As the nomenclature stands currently zone 0 encompasses the ascending aorta from the STJ up to and including the RBCT. Z1 – left common carotid, Z2 – LSCA, Z3 and Z4 which is sub-divided into T4-T12. The border between zones 3 and 4 is the end of the aortic arch curvature. The thoracic vertebral level (T4–T12) is aligned with the end of each vertebral body. Once the aorta has crossed the diaphragm it becomes L1-L4.

I think it is likely that as devices for ascending aortic intervention and TAVI evolve a further descriptive convention will be required to further sub-divide zone 0, and the aortic root below it. This would likely include the landing zone of the LVOT, the annulus, involvement and management of the coronary arteries as well as the sinus of Valsalva.

Conclusion - Aortic Arch to Femoral artery diameters

The aortic arch is on average 2.7 cm in diameter (although this is a diastolic measurement), leading down to a mean descending aortic diameter (at the level of the pulmonary bifurcation) of 24.6 mm. An average common iliac artery measures 12.2 mm in women, and 13.3 mm in men, values being significantly higher in both hypertensive males and females when compared to their normotensive controls (25-27).

The femoral artery diameter is on average 9.7 mm in women, and 11.0 mm in men, being significantly elevated in hypertensive females when compared to their normotensive controls (9.9 mm vs 9.6 mm in women $p<0.001$), but not significantly different in the male group 11.1 mm vs 10.9 mm $p=0.058$ (27).

We must accept that these are all findings and conclusions in a *relatively* "normal" population and that these values cannot be extrapolated to the severely dilated and dissected ascending aorta populations. In chapter 2, I will describe novel CT and CMR anatomical data collected from both a cohort of AAAD patients, and a group of patients with Marfan syndrome and ATAA.

1.3 The ascending aorta in diseased states

Although the major unmet clinical need for an endovascular device is in the treatment of AAAD, there is significant overlap in the pathophysiology and surgical management with patients presenting with ATAA. I wanted to understand the pathophysiology of ATAA, the current treatment modalities available and outcome data.

1.3.1 Ascending thoracic aortic aneurysm (ATAA)

ATAA is defined as a dilatation of the ascending aorta producing a cross sectional diameter of more than 1.5 times its normal value; values between 1.1 and 1.5 are considered dilated or ectatic ascending aorta (31). Normative values have already been discussed (Section 1.2.1.1) and there is generally good agreement between different imaging modalities including Echo, CT and MRI. Thoracic aortic aneurysms (TAA) involve the ascending aorta (ATAA) most commonly (50%), followed by descending (40%) and 10% affect the arch. 25% of patients with ATAA will have a concomitant abdominal aortic aneurysm (AAA) (32).

Aneurysmal disease of the aorta is clinically important because as the diameter of the aorta expands, linear wall stress increases which directly increases the risk of aortic rupture – an event with an extremely grave prognosis. Aneurysmal ascending aortas are also more likely to result in aortic dissection and other aortic syndromes often associated with a similarly poor outcome (33).

1.3.1.1 Incidence

The true incidence of ATAA is difficult to determine as many go undiagnosed. It has classically been quoted as being 2-5 cases per 100,000 / year, however in the Mayo Clinic sampling from 1980 – 1994 the incidence in Olmstead County, USA was of 10.4 cases per 100,000 / year (34). A possible explanation for this rising incidence is an aging population and increased utilisation of screening diagnostic imaging techniques (Echo, CT and MRI).

There are several significant differences between thoracic and abdominal aortic aneurysms. Age at onset for TAA is 10 years earlier (65 years versus 75 years); AAA are more predominant in men with a 6:1 male to female ratio, whereas TAAs occur only 1.7 times more frequently in men compared to women (35).

1.3.1.2 Pathogenesis

The ascending aorta has a greater concentration of elastic fibres and is more compliant than the descending aorta. The elastin to collagen ratio progressively decreases as the aorta traverses distally into the descending thoracic aorta. Elastin fibres and fibrillar collagens are the main determinants of the mechanical properties of the aorta and loss of elastin is one of the most consistent histo-pathological findings in patients with ATAA (35).

The pathophysiology of aneurysm formation is a complex and multi-factorial process involving interplay between genetic predisposition, haemodynamic stressors and concomitant aortic valve disease. Despite a diversity of genetic defects aortic diseases

develop through a common pathway of inflammation, proteolysis and disturbed survival of smooth muscle cells. A pronounced elevation in proteolytic matrix metalloproteinase enzymes and a notable decrease in inhibitory enzymes have been described in the wall of the aorta as mechanisms for the deleterious change in aneurysm disease (36). The medial degeneration results in a weakening of the aortic wall, which in turn leads to progressive aortic dilatation and eventually aneurysm formation (37).

1.3.1.3 Aetiology

Most ascending aneurysms have an unknown aetiology and are classified as idiopathic. Atherosclerosis is associated with aneurysms of the aortic arch and descending aorta, but spares the ascending aorta in which the pathogenesis appears more related to a genetic predisposition, haemodynamic stressors (hypertension) and bicuspid aortic valve (BAV) (32;38).

1.3.1.3.1 Degenerative aneurysms

Degenerative aneurysms comprise the majority of those seen in the ascending aorta. Cystic medial degeneration is known to occur to some extent with aging, but this process is accelerated by hypertension, with degradation of the extracellular matrix, loss of elastic fibres, and smooth muscle cell necrosis. As a consequence the aortic wall becomes stiff and progressively dilates (38).

1.3.1.3.2 Connective tissue disease

When cystic medial degeneration occurs at a younger age it is classically associated with recognised connective tissue disorders such as Marfan syndrome or less commonly, Ehlers Danlos syndrome (32).

In those with Marfan syndrome ATAA predominantly involves the aortic root in a pattern known as "*annulo-aortic ectasia"*. Penetrance is variable, and in some with Marfan syndrome the aortic root is significantly aneurysmal by teenage years while others have much slower progression of disease or no aortic dilatation (38). Marfan syndrome is an inherited connective tissue disorder which has an incidence of 1 in 5000, and about 25% of cases represent new mutations. While the syndrome affects many systems, the most prominent manifestations are skeletal, ocular and cardiovascular. 60-80% of all adults with Marfan syndrome have a dilatation of the sinus of Valsalva (32).

The Marfan gene mutation occurs in the portion of the genome encoding Fibrillin-1 on *Chromosome 15q21* a key component of the elastic scaffold. The Fibrillin-1 mutation results in fragmentation of the elastin network by matrix metalloproteinases, leading to inflammation, and cystic medial degeneration. There is also some data suggesting that the abnormal Fibrillin-1 has a low affinity for transforming growth factor Beta 1 (TGFβ1) leading to excessive production of TGF-β1 (39).

1.3.1.3.3 Bicuspid aortic valve

Bicuspid aortic valve (BAV) is a common congenital cardiac anomaly with an incidence of 1-2% of the general population (32). There has been considerable controversy as to

whether the aortic wall changes and the predisposition to aortic aneurysm are due to the abnormal haemodynamic stresses brought about by the BAV, or are caused by an associated inherited aortic wall abnormality (40).

Fedak *et al.* have shown that patients with BAV have an inherited defect in the genes that encode matrix elements resulting in Fibrillin-1 deficiency that might trigger matrix metalloproteinase production, which in a similar way to Marfan syndrome may accelerate cystic medial degeneration and increase aortic dilatation and aneurysm formation (41). More indirect evidence to support this hypothesis is the fact that once a stenotic BAV is replaced surgically it does not prevent progressive dilatation of the ascending aorta suggesting a more inherent structural defect (41).

1.3.1.3.4 Familial predisposition

Barbour *et al.* have demonstrated that development of aneurysmal disease can be linked to genetics in a non-syndromic way. Of patients with an aortic aneurysm, 15% had first degree relatives who were shown to have an aneurysm as well. This potential genetic pre-disposition suggests that screening of asymptomatic 1st degree relatives of patients with confirmed ATAA may be useful so that any early disease can be treated through surveillance, prophylactic optimal medical therapy (OMT) and early intervention if necessary (36).

Figure 11 below summarises the potential mechanism and interactions thought to be involved in ATAA formation:

Figure 11 Mechanisms of ATAA formation.

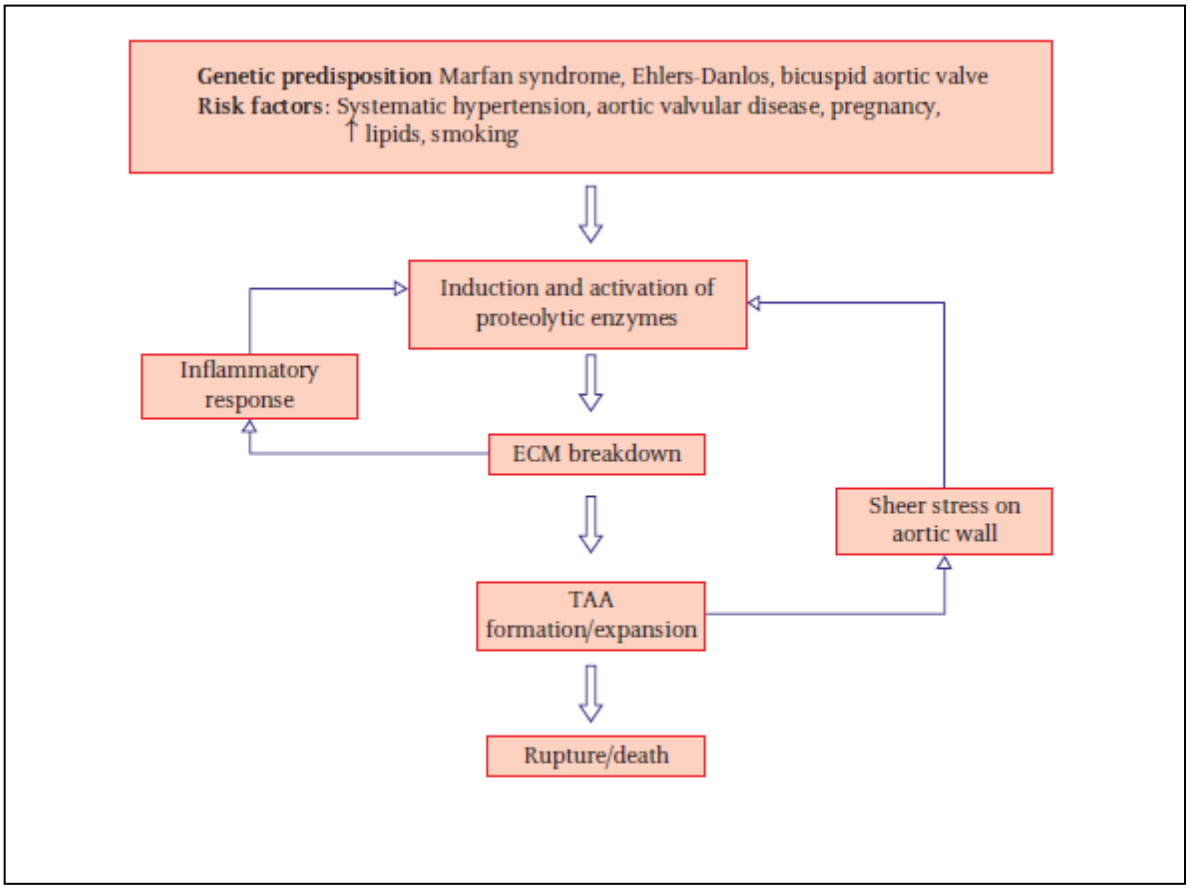

Mechanisms of ATAA adapted from Evangelista A.(32) TAA formation and expansion is an interplay between genetic predisposition, cardiovascular risk factors, and their effect upon the induction and activation of proteolytic enzymes. This can lead to extra cellular matrix (ECM) breakdown, bringing about an inflammatory response, aortic wall sheer stress and further aortic dilatation.

1.3.1.4 Clinical diagnosis

In the United Kingdom (UK) with increased screening (the use of cardiac echocardiography in heart failure) and the use of advanced imaging techniques (CT and MRI to investigate cardiac and lung abnormalities) many dilated or aneurysmal ascending aortas are an incidental finding.

1.3.1.4.1 Echocardiography

Trans-thoracic echocardiography (TTE) is an excellent imaging modality for both the diagnosis and follow up of the aortic root dimensions in the first 3-5 cm of the ascending aorta. Echo utilises ultrasound waves and is therefore safe, portable, rapid and relatively cheap. It does not require intravenous access and can be easily performed in outpatient clinics or in the community. In the majority of subjects it allows reproducible measurement of the aortic diameters and assessment of the degree of aortic valve involvement (either BAV, aortic stenosis or regurgitation). Figure 12 below shows a TTE image of a patient with an ascending aortic aneurysm:

Figure 12 TTE image of the annulus to ascending aorta

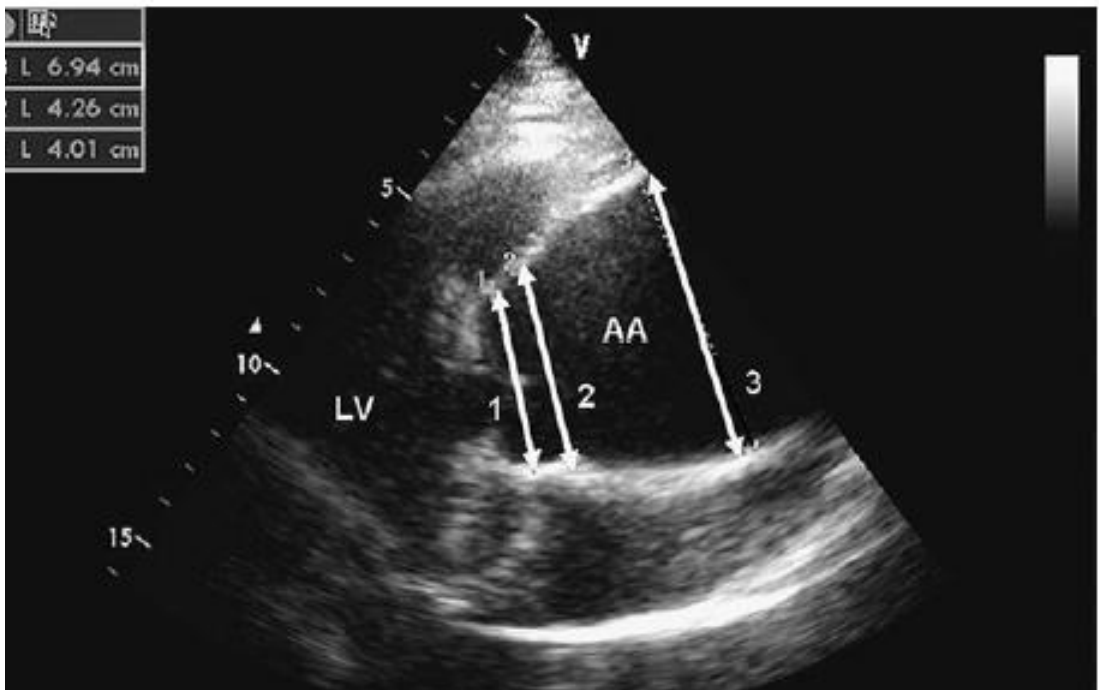

2D transthoracic echocardiogram, parasternal long axis view of the heart and aorta showing LV – left ventricle, 1) Sinus dimension (4.01 cm) 2) STJ dimension (4.26 cm) 3) Grossly dilated ascending aorta dimension (6.94 cm).

In patients with poor TTE windows then trans-oesophageal echocardiography (TOE) can be extremely useful giving similar information and visualising the ascending aorta with excellent resolution.

1.3.1.4.2 Tomographic imaging modalities

1.3.1.4.2.1 CT scanning

While TTE is a great screening and surveillance tool, vascular CT with its sub-millimetre spatial resolution is an extremely rapid and accurate modality to image the entire aorta (32). The only disadvantage is the need for intra-venous contrast agent which can cause contrast nephropathy, and that the technique utilises potentially harmful ionising radiation. This technique is described in more detail within Chapter 2.1 *"CT measurement of ascending aortic size in 9 patients with AAAD."*

1.3.1.4.2.2 Magnetic Resonance Imaging (MRI) scanning

MRI also offers excellent visualisation of the whole aortic anatomy. This technique is described in more detail in Chapter 2.2 "C*MR assessment of the aortic root, coronary arteries and ascending aorta of 62 patients with Marfan syndrome".* MRI does not utilise ionising radiation.

1.3.1.5 Natural history

In general aortic aneurysms develop slowly over many years, silently growing at an average rate in the ascending aorta of around 1 mm / year (32;42).

There is a very clearly defined “hinge point” in ascending aortic size after which complications are much more likely to occur. Figure 13 below demonstrates the “hinge point” of aortic size below:

Figure 13 Graph showing aneurysm size versus probability of complication

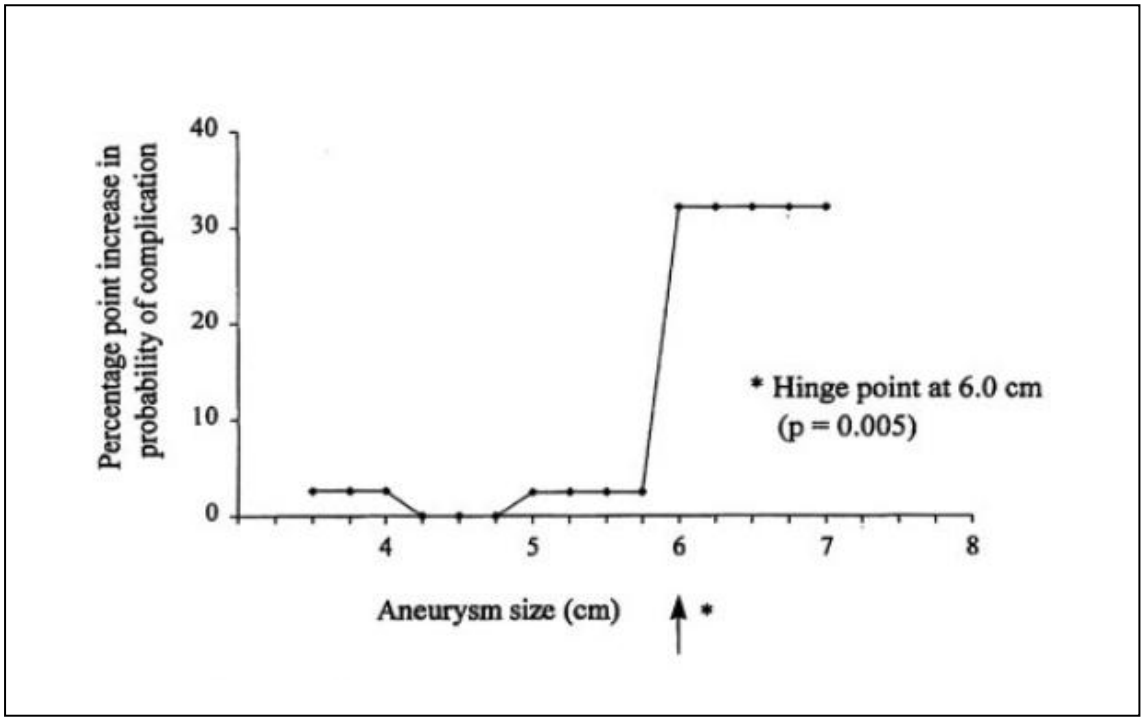

There is a very clear hinge point at 6 cm in size, where the risk of probability of complication increases dramatically. It is vital to recommend surgery before the ascending aortic dimension reaches this point. The recent AHA 2010 guidelines however go further and in patients with high risk of rupture surgery can be mandated with a smaller diameter. Adapted from Evangelista *et al. (32).*

The key with ATAA is firstly to make the diagnosis, and then surveillance and optimised medical therapy (OMT) until a point where the benefits of surgical management outweigh the risk of continued OMT.

1.3.1.6 Optimal medical treatment

OMT involves aggressive control of hypertension utilising most commonly beta-blockers and angiotensin converting enzyme (ACE) inhibitors or angiotensin II receptor blockers (AIIRB) as first line agents (43). It has been suggested that beta-blockers reduce aortic wall stress and are indicated for non-operative candidates with dilated aortas (>4 cm) in the absence of aortic regurgitation (AR), but like almost all of the AHA 2010 guidelines this recommendation is based on consensus opinion rather than clinical trials (44).

In patients with Marfan syndrome, beta-blockers have been the mainstay of pharmacotherapy based on a theoretical decrease in aortic wall stress. However, there are conflicting data regarding the effects of beta-blockers on elastic properties of the Marfan aorta.

A recent meta-analysis of six studies (one of which was a prospective randomised controlled trial (RCT) with >800 participants) showed no clinical benefit of beta-blockers in Marfan syndrome (45). In a study comparing the ACE inhibitor enalapril versus beta-blockade (propanolol or atenolol), the ACE inhibitor treated group had a significantly lower aortic stiffness index and a significantly lower rate of aortic root growth (46). The AIIRB Losartan has also been shown to reduce the rate of aortic dilatation in patients with Marfan syndrome (43). There is no evidence as to whether beta-blockers or ACE

inhibitors, alone or in combination, are preferable in the treatment of BAV or other ATAA aetiologies.

1.3.1.7 2010 AHA guidelines on the management of ATAA

A summary of the 2010 AHA guidelines on the management of ATAA is presented below (44):

The guidelines are divided into asymptomatic and symptomatic patients.

1.3.1.7.1 Recommendations for Asymptomatic Patients With ATAA

Class I

1. Asymptomatic patients with degenerative thoracic aneurysm, chronic aortic dissection, intramural hematoma, penetrating atherosclerotic ulcer, mycotic aneurysm, or pseudo aneurysm, who are otherwise suitable candidates and for whom the ascending aorta or aortic sinus diameter is 5.5 cm or greater, should be evaluated for surgical repair. (*Level of Evidence: C*)

2. Patients with Marfan syndrome or other genetically mediated disorders (vascular Ehlers-Danlos syndrome, Turner syndrome, BAV, or familial thoracic aortic aneurysm and dissection) should undergo elective operation at smaller diameters (4.0 to 5.0 cm depending on the condition) to avoid acute dissection or rupture. (*Level of Evidence: C*)

3. Patients with a growth rate of more than 0.5 cm / year in an aorta that is less than 5.5 cm in diameter should be considered for operation. (*Level of Evidence: C*)

4. Patients undergoing aortic valve repair or replacement and who have an ascending aorta or aortic root of greater than 4.5 cm should be considered for concomitant repair of the aortic root or replacement of the ascending aorta. (*Level of Evidence: C*)

Class IIa

1. Elective aortic replacement is reasonable for patients with Marfan syndrome, other genetic diseases, or BAV, when the ratio of maximal ascending or aortic root area (πr^2) in cm^2 divided by the patient's height in metres exceeds 10. (*Level of Evidence: C*)

2. It is reasonable for patients with Loeys-Dietz syndrome or a confirmed *TGFBR1* or *TGFBR2* mutation to undergo aortic repair when the aortic diameter reaches 4.2 cm or greater by TOE (internal diameter) or 4.4 to 4.6 cm or greater by CT imaging and / or MRI imaging (external diameter). (*Level of Evidence: C*)

This guidance assumes that the risk of operation is low (<5%), and that the risk of an adverse event (rupture, dissection, death) exceeds the risk of elective operation.

1.3.1.7.2 Recommendation for Symptomatic Patients With ATAA

Class I

1. Patients with symptoms suggestive of expansion of ATAA should be evaluated for prompt surgical intervention unless life expectancy from co-morbid conditions is limited or quality of life is substantially impaired. (*Level of Evidence: C*)

1.3.1.8 ATAA conventional surgical treatments

The type and timing of a curative surgical procedure is dependent on a number of genetic, anatomical, and physiological patient factors, as well as a number of surgeon and cardiothoracic centre factors.

1.3.1.8.1 Ascending aortic aneurysm

ATAA may cause dilatation of the STJ, which pulls the cusps apart preventing central co-aptation resulting in central AR as demonstrated in Figure 14 below:

Figure 14 Aortic dilatation preventing aortic valve co-aptation causing central AR

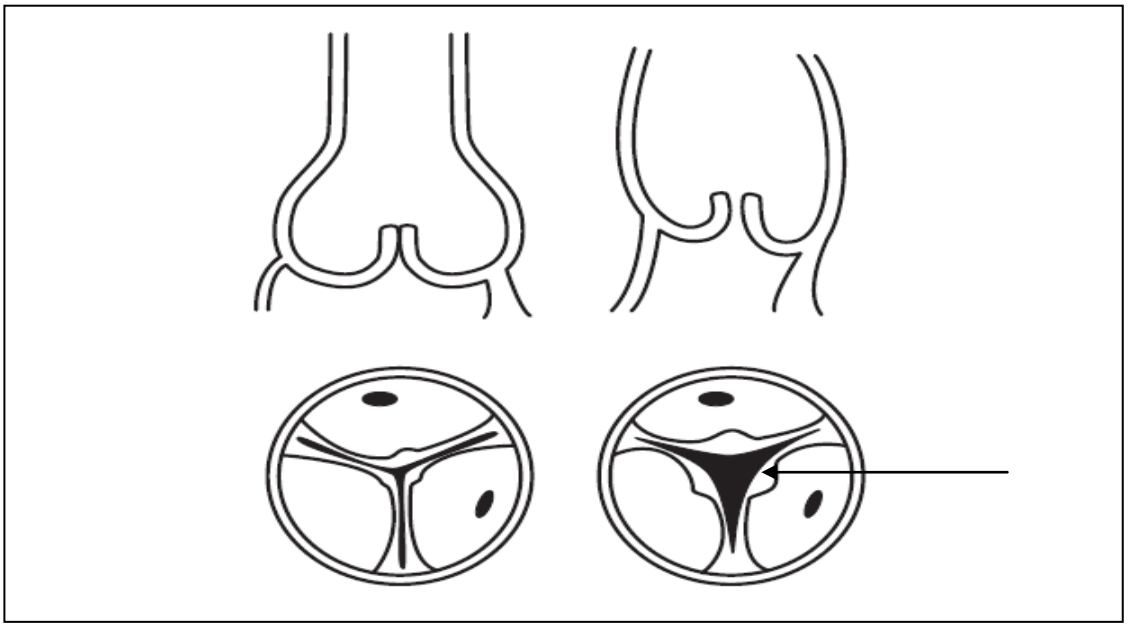

The diagram on the left shows a normal sized aortic root and sinuses with aortic valve cusps that are seen to co-apt in the midline preventing aortic incompetence. The diagram on the right side shows a dilated aortic root and ascending aorta which prevents leaflet co-aptation resulting in a degree of central AR (arrowed).

It is of paramount importance that the degree and mechanism of AR is carefully elucidated along with the dimensions of each component of the aortic root. Only with this information can a surgical procedure be properly planned.

Surgery for ATAA is performed using CPB. If the aortic valve is competent, “simple” replacement of the ascending aorta with a tubular Dacron graft is all that is needed with an “interposed graft”. Figure 15 shows this below:

Figure 15 An interposed ascending aortic graft

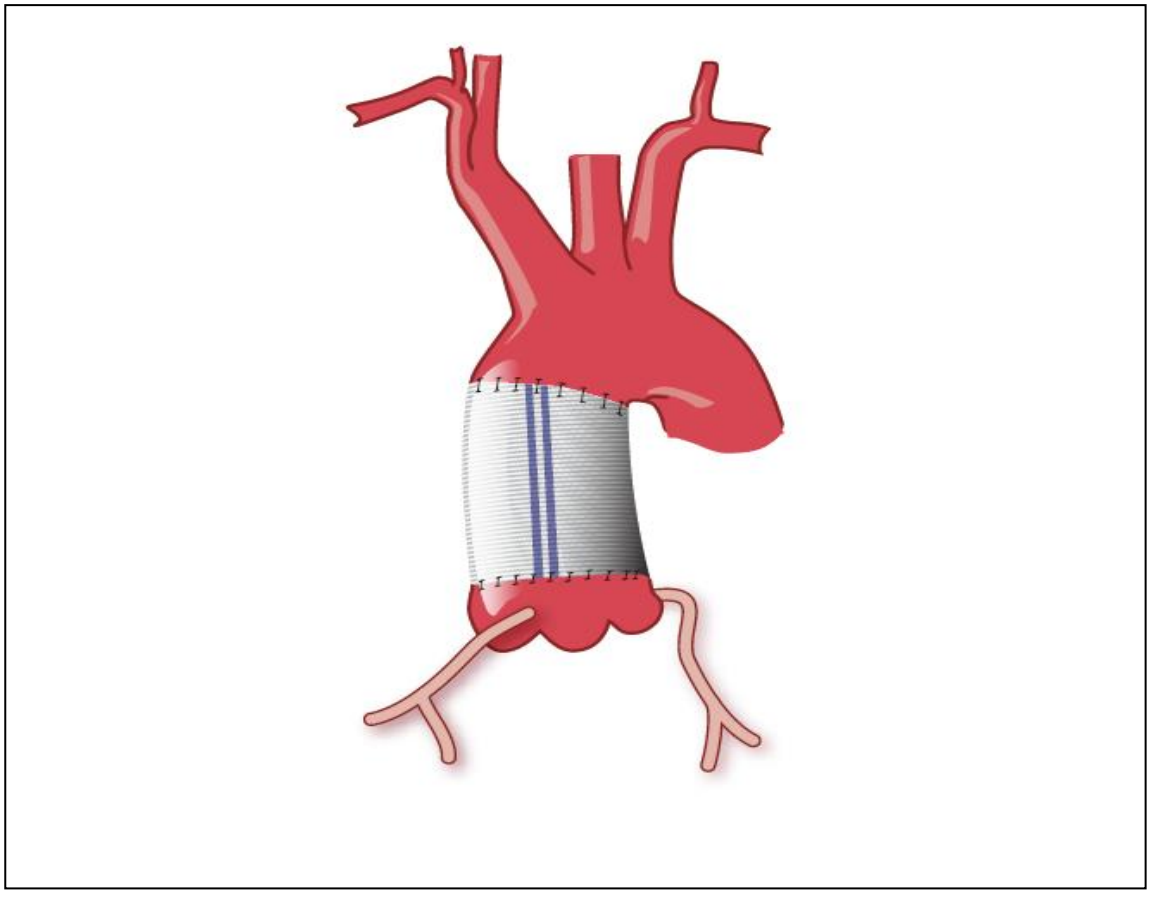

The interposed ascending aortic Dacron graft. The aortic root is of a normal diameter, and the Dacron graft (white with 2 blue strips) has an anastomosis just above the STJ, and just proximal to the RBCT. The aortic valve and the coronary arteries are not disturbed as both are functioning normally.

If the aortic valve is incompetent but the aortic cusps are normal and the mechanism is dilatation of the STJ, then the surgeon must re-establish valve competence by reducing the diameter of the STJ, as shown in Figure 16 below:

Figure 16 Valve competence is re-established by reducing the diameter of the STJ

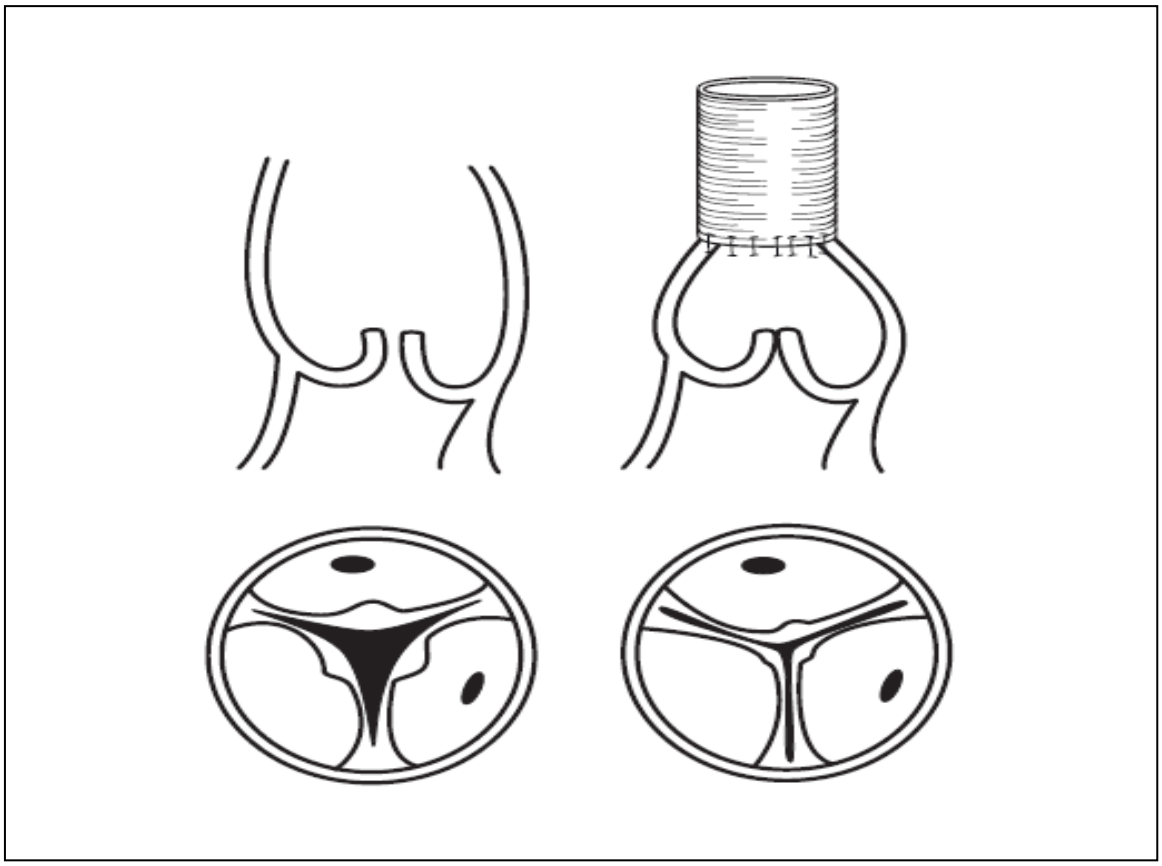

The aorta on the left hand side shows a dilated STJ resulting in poor aortic valve co-aptation and resultant significant AR. The diagram on the right shows a surgical technique that can be used to reduce STJ diameter and re-establish valve competence. The ascending aorta is cut 5 mm above the STJ, all 3 commissures are then pulled upwards and towards each other until the cusps co-apt centrally. At this smaller diameter a Dacron graft is then sutured to the ascending aorta at the level of the STJ, replacing the aneurysmal ascending aorta and at the same time re-establishing aortic valve competence.

If the non-coronary aortic sinus is aneurysmal it should be replaced along with the ascending aorta. This is accomplished by selecting a graft of an appropriate diameter

and then creating a neo-aortic sinus. This is then sutured directly to the remnant of the arterial wall and aortic annulus as shown in Figure 17 below:

Figure 17 Surgical neo-aortic sinus formation

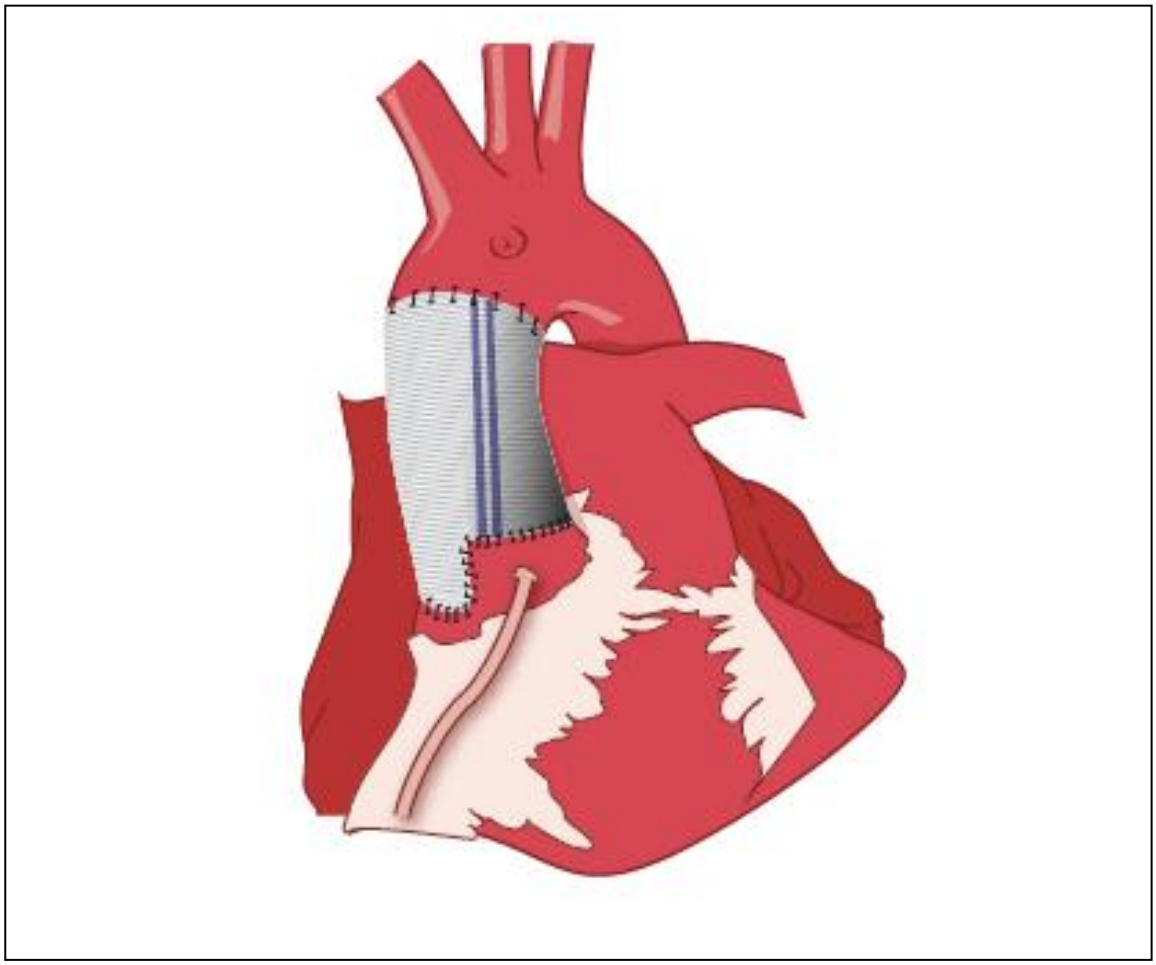

Non coronary neo-aortic sinus formation is accomplished surgically by selecting a Dacron graft (white material with 2 blue strips) of an appropriate diameter and then manually creating a neo-aortic sinus by cutting the Dacron in a bespoke manner. This is then sutured directly to the remnant of the arterial wall and aortic annulus.

Patients with ATAA and aortic valve disease not amenable to valve repair are treated by aortic valve replacement and supra-coronary replacement of the ascending aorta.

1.3.1.8.2 Aortic Root aneurysm

Aortic root aneurysm usually begins with dilatation of the aortic sinuses. Once this involves dilatation of the STJ and / or the aortic annulus, AR can become significant. The coronary artery orifices are often displaced cephalically. It is important to ascertain usually by TOE the precise mechanism of the AR – is it just dilatation with normal cusps, or are the cusps abnormal giving rise to greater than expected insufficiency. Larger aneurysms often give rise to overstretched aortic cusps which become thinned and develop large fenestrations in the commissural areas.

Replacement of the aortic root with a valved conduit has been the standard treatment for patients with aortic root aneurysms – the most commonly used conduit being a Dacron graft containing a mechanical valve (The Bentall procedure first described and performed in 1965) (47). Aortic valve homograft and bio-prosthetic valves can also be used, see Figure 18 below:

Figure 18 Bentall grafts with incorporated aortic valve

Image on the left shows the Dacron tubular graft with an integrated mechanical aortic valve. The image on the right hand side shows a similar Dacron graft with an integrated bioprosthetic aortic valve.

Replacement of the ascending aorta alone or in combination with aortic valve replacement can be performed with low operative mortality – Sioris *et al.* in 2004 reported elective operative mortality of less than 5% (7).

An alternative surgical option in patients with aortic root aneurysm and normal aortic cusps is aortic valve-sparing operations. These are more complex surgical procedures whereby the coronary arteries are detached from the root, and the aortic sinuses are excised and the aortic cusps are left attached to the aortic annulus and LVOT.

In essence there are 2 types of valve-sparing operation:

i) Remodelling of the aortic root and

ii) Re-implantation of the aortic valve.

1.3.1.8.3 Aortic root remodelling

In this operative procedure the aortic sinuses are excised and the coronary arteries detached as demonstrated in Figure 19 below:

Figure 19 Aortic root remodelling operation

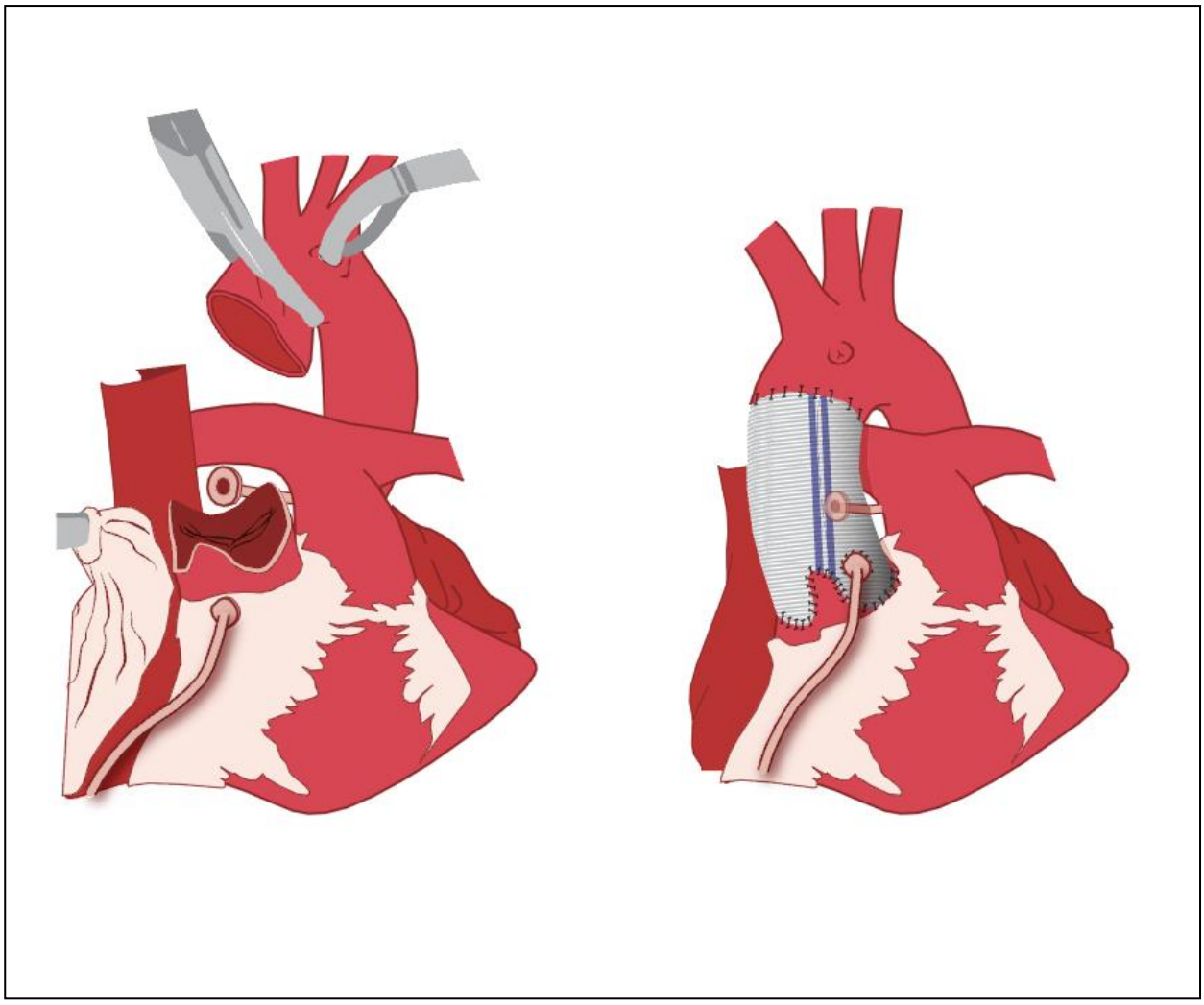

On CPB, the aortic sinuses are excised and the coronary arteries detached. Following which an appropriate sized piece of Dacron graft with "neo-aortic" sinuses (white material with blue stripes) is tailored and sutured to the remnants of the aortic sinuses and aortic annulus. The coronary arteries are the re-implanted into their respective neo-sinus.

1.3.1.8.4 Re-implantation of the aortic valve

This is an even more complicated procedure, see diagrammatic representation in Figure 20 below:

Figure 20 Surgical re-implantation of the aortic valve

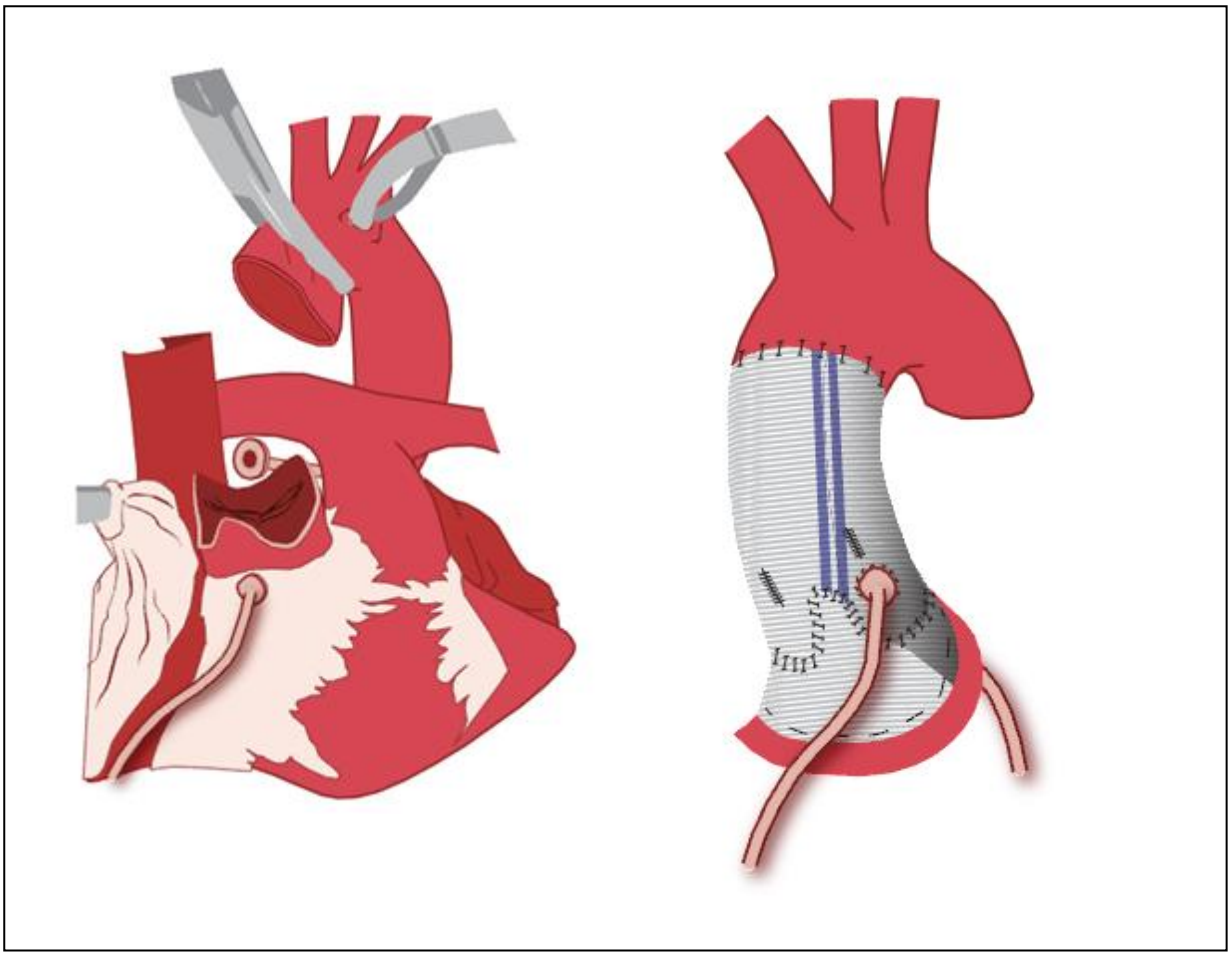

The coronary arteries are detached and the aortic sinuses excised as in Figure 19, but the aortic root is freed from the surrounding tissues to a level below the nadir of the aortic annulus. Following this a Dacron graft of appropriate size is sutured to the left ventricular outflow tract immediately below the aortic annulus. The remnants of the aortic sinus and aortic annulus are sutured inside the graft recreating the normal scalloped shape of the aortic annulus. The coronary arteries are then re-implanted.

Although there are only a few long term follow up studies, the results of aortic valve sparing operations are promising. In a recent review by David *et al.* of 103 Marfan patients prospectively followed for a mean of 7.3 years only 2 patients required re-operation for AR and 1 for infective endocarditis. Re-implantation of the aortic valve

appeared to show more stable valve function as compared to remodelling of the aortic root (48).

1.3.1.8.5 Elective aortic aneurysm surgery - outcomes

If dilatation of the aortic root is left untreated there is a high risk of death due to dissection or rupture of the aorta or heart failure resulting from severe AR (49). Since the first Bentall procedure in 1965, aortic root replacement has dramatically improved the survival of these patients (50). In 2012 there is still no agreement about the best method of dealing with malfunction of the aortic valve caused by dilatation of the Marfan aortic root.

Bentall and De Ba introduced total aortic root replacement (TRR) using a composite mechanical valve conduit and this was long considered the "gold standard", providing excellent early and late operative outcomes (47). However a proportion of patients receiving mechanical valves in this fashion do experience complications related to long term anti-coagulation.

Recently valve-sparing aortic root replacement (VSRR) operations have emerged as an alternative as already discussed. This technique preserves native valves and avoids the disadvantages of mechanical valve and long term anti-coagulation. However given the fact that Marfan patients carry a structural fibrillin-1 defect, controversy has risen about the durability of such a reconstruction (51). No RCT has ever addressed this problem. In 2011 Benedetto *et al.* published a systemic review and meta-analysis on the surgical management of aortic root disease in Marfan syndrome (52).

A total of 530 studies were identified, but after numerous exclusions to optimise quality eleven publications were included in the final analysis. Overall a total of 1385 patients were analysed (972 had TRR and 413 had VSRR). Mean follow up time was 8.0 years for TRR and 4.7 years for VSRR (*p=0.003*). The total number of patient years follow up was 935 and 344 respectively.

VSRR was associated with a fourfold increased rate of re-intervention on the aortic valve when compared to TRR (1.3% / year vs 0.3% / year *p=0.02*). When the VSRR was broken down further into re-implantation (0.7% / year re-intervention rate) and remodelling (2.4% / year re-intervention rate), re-implantation was superior to remodelling, but both were inferior as compared to TRR (*p=0.02*).

TRR was associated with an increased rate of thrombo-embolic events (0.7% / year vs 0.3% / year; *p=0.01*). There were no significant differences in endocarditis rates (0.3% vs 0.2% *p=0.32*). Overall the incidence of all valve related complications were comparable after TRR and VSRR (52).

1.3.1.8.6 Conclusions about elective ATAA surgery

In patients with ATAA, replacement of the ascending aorta alone or in combination with aortic valve replacement can be performed with low operative mortality – Sioris *et al.* in 2004 reported elective operative mortality of less than 5% (7).

VSRR has emerged over the last few years as an alternative to TRR in Marfan patients with little or no valve involvement. While anti-coagulation is not mandated with this approach in an often young group of patients this risk is exchanged for a greater re-

intervention rate, and concerns long term that the abnormal valve leaflets will not be durable. This data will only become available with time, and already there are ongoing prospective international registries comparing VSRR with TRR.

1.3.1.9 Alternatives to conventional aortic root surgery for ATAA

I felt it important to look beyond conventional aortic root surgery and investigate whether there are any minimally invasive or novel treatment modalities for the treatment of ATAA. External aortic root support (EARS) for Marfan Syndrome appears to be a novel and less invasive strategy to treat Marfan aortic dilatation and the technique with early data is described below:

In 1994 Robicsek *et al.* described an alternative to replacement of the ascending aorta, by externally wrapping the aorta at various aortic sites. This approach has however been largely abandoned because of several patterns of failure (53).

In 2004 Golesworthy an engineer suffering from Marfan syndrome described in collaboration with cardiothoracic surgeons Pepper and Treasure the development of a bespoke external aortic root support (EARS). The proposed EARS operation can be performed without CPB, without entering the circulation, and without interfering with the aortic valve in any way. If this external support can hold and support the whole of this aortic segment at a size where the risk of dissection is low, it may obviate or greatly postpone the need for more radical and ablative surgery (54).

The exact dimensions of the individual patient's aorta are taken from MRI images and processed using computer aided design to produce a 3D reconstruction of the patient's

aorta from the aorto-ventricular junction to beyond the RBCT (55). The X, Y and Z co-ordinates of the reconstructed aorta are then exported to a rapid prototyping machine and a model of the patient's aorta made in thermoplastic. This model then acts as a former upon which an external support is manufactured from medical grade polymer mesh. The finished support is then sterilised, packaged and sent to the surgeon with a vertical seam that can be opened by the surgeon to place the support around the aorta. Figure 21 below shows the EARS support.

Figure 21 Photograph of EARS

Bespoke made polymer mesh is sterilised, and the graft is brought onto the operating table, the longitudinal seam is opened and the support placed around the aorta, and then sutured to enclose the aorta.(56)

At operation through a median sternotomy the aorta is completely dissected from aorto-ventricular junction to the origin of the RBCT. The patient specific bespoke EARS graft is then brought onto the operating table, placed around the aorta, and then sutured to enclose the aorta preventing further aortic dilatation.

The first 20 patients (13 men and 7 women) underwent EARS from May 2004 to October 2009. There have been no operative deaths and the operation was completed exactly as planned in 19/20 patients while the 20th patient had partial release of the external support. In no patient was there a need to convert to root replacement or any other form of surgery. CPB was utilised for 20 minutes during the first patient only.

Only patient 20 had a complication - post operatively suffering a VF arrest. The circulation was restored after removing the anterior closing suture on the aortic root support. The patient made a normal recovery and was discharged home day 8. As a result the aorta in this patient is only partially supported and will be closely monitored.

The 20 patients involved in the EARS cohort had a median age of 33 years and had a median aortic diameter of 47 mm (range 40-54). The median operation time was 148 minutes compared to 374 minutes for conventional Marfan aortic root surgery. Patients had a shorter length of hospital stay when compared to their conventionally treated comparators (6 days vs 8 days in the conventional surgery cohort) (55). Table 4 below shows EARS demographic and follow up data (55):

Table 4 EARS demographic and follow up data (n=20)

Variable	Median	Inter-quartile range	Range
Age at operation (years)	33	26-39	16-58
Aortic diameter (mm)	47	43-48	40-54
Operation time (min)	148	136 – 163	125-415
Length of stay (days)	6	5-7	3-16
Follow up (months)	20	10-39	0-67
Change in aortic diameter (mm) (n=16)	-1	-2 - +1	-6 - +3

Meticulous follow up of these 20 patients has occurred and the dimensions of the ascending aorta at the level of the aortic valve cusps is presented in Figure 22 below:

Figure 22 Dimensions of the ascending aorta (mm) in the EARS cohort

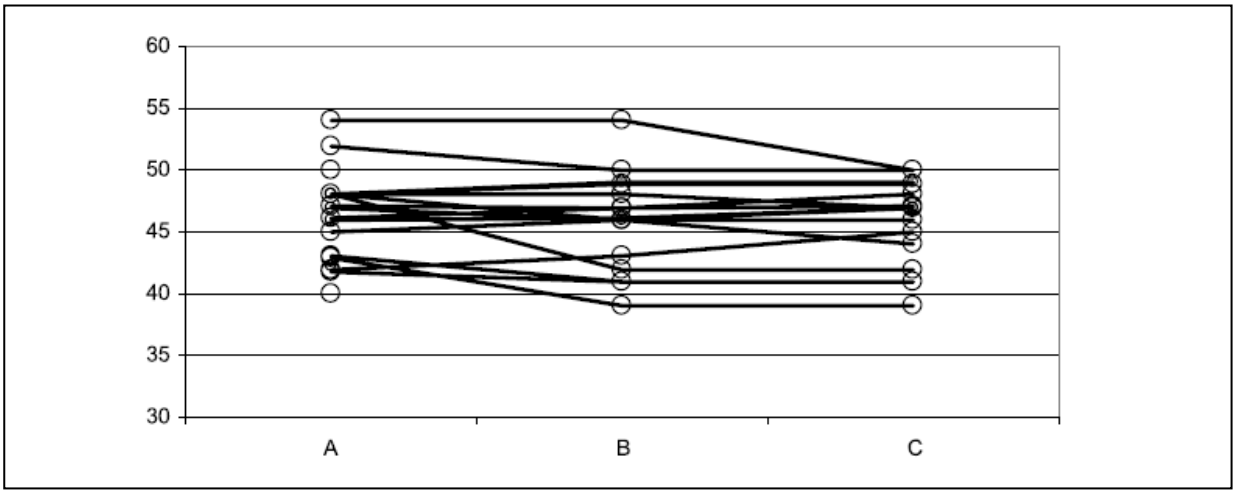

Dimensions of the ascending aorta (mm) (A) at the level of closure of the aortic valve cusps before operation, (B) at the first postoperative scan and (C) most recent MRI scan. There appears to be a tendency for EARS to reduce the diameter of the Marfan aorta which remains stable thereafter. The longest follow-up scan is five years after surgery (55).

1.3.1.9.1 Conclusions about the EARS procedure

The purpose of aortic root surgery in Marfan syndrome is to pre-empt the risk of dilatation thus saving the patient from AR and death due to aortic dissection. Successful placement of the external aortic support was achieved in 19 of the 20 patients, with only partial success in the 20th patient.

It would seem that the EARS procedure is safe, and that the magnitude of the surgery is greatly reduced when compared to conventional aortic root replacement. The hazards associated with CPB, myocardial ischaemia, deep circulatory arrest and the neurological risks associated are obviated. Operation times and hospitals stays are also shorter.

The follow up so far of this small cohort of patients would appear to suggest that the EARS procedure provides a robust and dependable result in preventing further ascending aortic dilatation. More patients will need to be treated in this manner, and their longer term outcomes published before EARS can be considered for RCT against conventional surgery, only then might it become an accepted treatment strategy for Marfan dilated aorta.

1.3.2 Ascending type A aortic dissection (AAAD)

Before considering the design specification of an endovascular solution to treat the unmet clinical need of AAAD it is mandatory to understand the disease process and the current treatment strategies and outcomes. Any endovascular solution must provide a similar technical result to that achieved by open surgery, including exclusion of the intimal tear, preservation of coronary artery flow, and maintenance of aortic valve competence.

AAAD is a challenging clinical emergency first described by Morgagni more than 200 years ago (57). In 1958, Hirst *et al* reviewed 505 patients with the condition, highlighting the high mortality rate and the infrequency of ante-mortem diagnosis (58).

One of the earliest and most famous documented deaths from AAAD was that of King George II:

On 25 October 1760 George II, then 76, rose at his normal hour of 6 am, called as usual for his chocolate, and retired to the closet-stool. The German valet de chambre heard a noise, memorably described as 'louder than the royal wind', and then a groan; he ran in and found the King lying on the floor, having cut his face in falling. Mr Andrews, surgeon of the household was called and bled his Majesty but in vain, as no sign of life was observed from the time of his fall. At necropsy the next day Dr Nicholls, physician to his late Majesty, found the pericardium distended with a pint of coagulated blood, probably from an orifice in the right ventricle, and a transverse fissure on the inner side of the ascending aorta 3.75 cm long, through which blood had recently passed in its external

coat to form a raised ecchymosis, this appearance being interpreted as an incipient aneurysm of the aorta" (59).

The typical AAAD process is characterised by rapid development of an intimal tear with a flap separating a true and a false lumen, as shown in Figure 23 below:

Figure 23 Aortic dissection showing intimal tear, true and false lumen

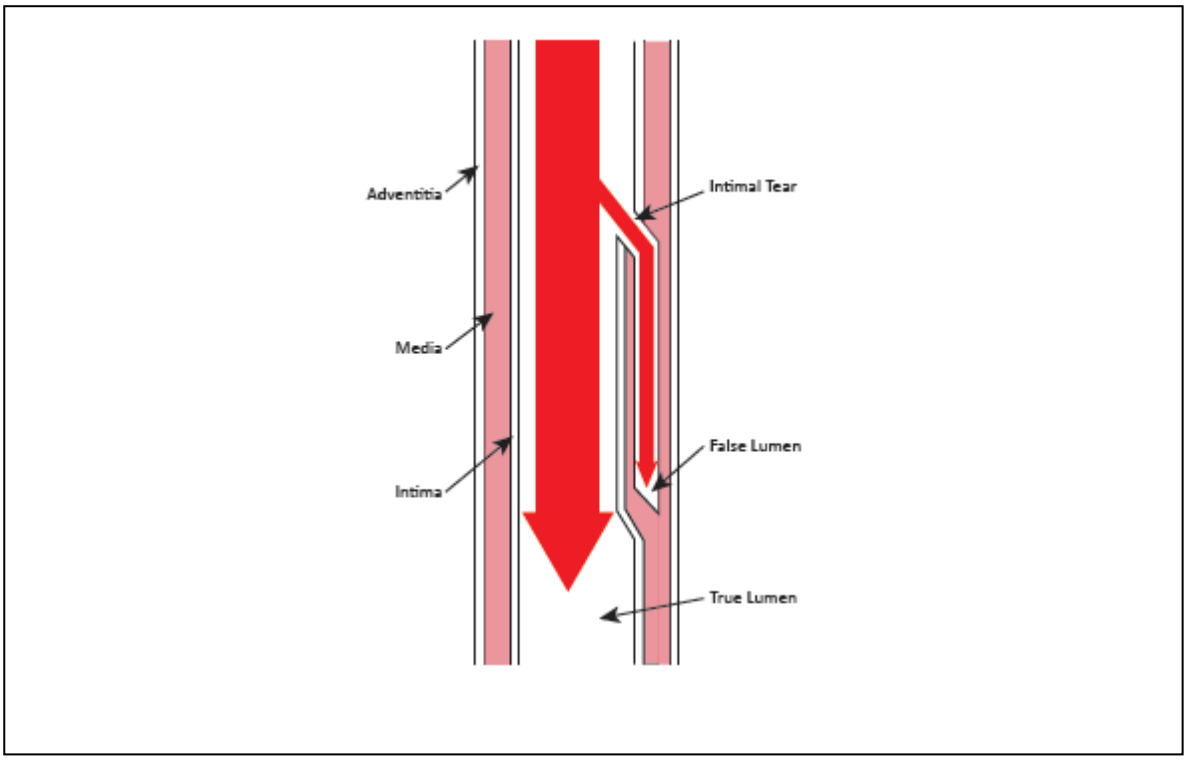

Figure shows a schematic of an arterial wall with three layers – the Adventitia, Media, and Intima. An Intimal tear is seen as a break within the Intima, allowing blood to track in both a true and false lumen.

In the majority of cases intimal tears are identified as sites of communication between true and false lumens. The dissection can spread from diseased segment of the aortic wall in either an antegrade or retrograde fashion, involving side branches and causing complications such as malperfusion syndrome by dynamic or static obstruction (from coronaries to femoral arteries), tamponade or AR (60).

1.3.2.1.1 Classification

The simplest classification described is that of Stanford and distinguishes between Type A and Type B (61). Type A means the dissection involves the ascending thoracic aorta; Type B dissection does not involve the ascending aorta. Most current consensus treatment guidelines are based on the Stanford nomenclature. Other classifications do exist including Debakey, and Penn and these are only briefly discussed within this thesis. Figure 24 below describes the Stanford aortic dissection classification:

Figure 24 Stanford classification of aortic aneurysm

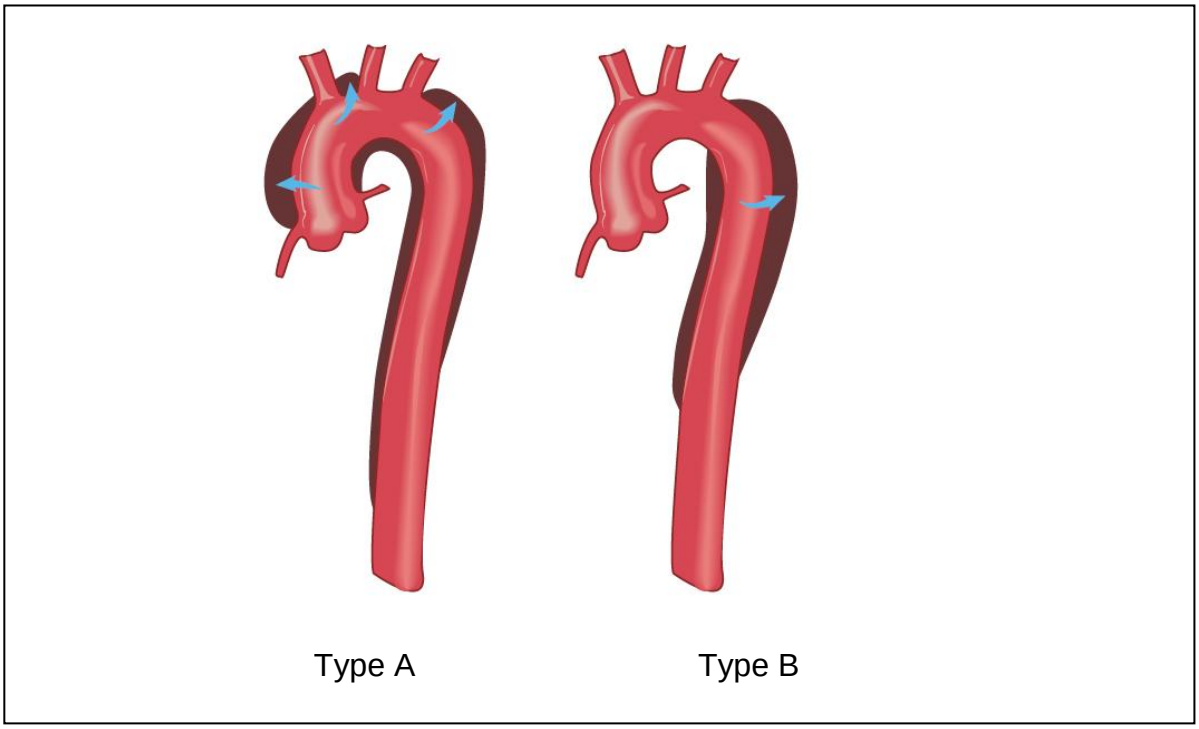

Type A aortic dissection affects the ascending aorta. The intimal tear is most commonly within the ascending aorta, but can be within the arch or descending with retrograde propagation of the false lumen. Type A dissections commonly propagate into the arch and descending aorta where there may be a re-entry tear. Type B dissections do not affect the ascending aorta.

1.3.2.1.2 Incidence

The true incidence of AAAD is difficult to determine as many cases go undiagnosed, but its documented incidence is approximately 3 per 100,000 per year, with at least 7,000 documented cases per year in the United States (62). A population based study in Sweden between 1987 and 2002 revealed 4425 cases of aortic dissection within a population of 8.7 million, equating to 3.4 cases per 100,000 people per year (63). During the 16 year study period the combined yearly incidence of aortic dissection and aneurysm increased by 50% in men and 30% in women. The reasons for this increase are unknown but might relate to improved identification of cases with enhanced imaging, or increasing age of the population or both. Overall about 20% of patients died before reaching hospital, 30% during hospital admission, and a further 20% over the next 10 years (63). AAAD continues to this day to be one of the most feared diagnoses with its early mortality rates remaining similar to that described by Hurst and Kime in their seminal article describing a mortality rate of 1-2% per hour for the first 24 hours after symptom onset from AAAD (58).

The peak incidence of aortic dissection is in the sixth and seventh decades of life, with a mean age of 62 years among more than a thousand subjects in the International Registry of Aortic Dissection (IRAD). Overall men are affected twice as often as women (68% vs 32%) and are affected at a younger age with male patients having a mean age of 60 years and women patients a mean age of 67 years (64).

1.3.2.1.3 Pathophysiology

A healthy aorta with an intact medial layer rarely dissects. Any disease process or condition that damages the elastic or muscular components of the media predisposes the aorta to dissection. The commonest associated factors for aortic dissection are a history of hypertension, old age, atherosclerosis, and previous cardiac surgery. Marfan syndrome is an important risk factor for aortic dissection especially in young patients (<40 years). Table 5 details the incidence of risk factors for AAAD in IRAD (65):

Table 5 Incidence of AAAD risk factor variables

Variable	**Incidence in IRAD (n=617)**
Age (mean in years at presentation)	61 years
Sex (male)	67%
Hypertension	67%
Atherosclerosis	28%
Previous cardiac surgery	16%
Known aortic aneurysm	7%
Marfans syndrome	6%
Bicuspid aortic valve	4%
Previous aortic dissection	3%

Like ATAA there seems to be a significant genetic basis for AAAD that is not associated with a recognised connective tissue deficiency syndrome. Up to 19% of patients who present with a thoracic aneurysm or dissection have a first degree relative with a similar history (66).

The increasing use of high resolution imaging to assess the aorta has led to the identification of a range of intimal and intramural pathological changes that have been related to dissection – including intramural haematoma, and atherosclerotic ulcers. Commentators have suggested that aortic dissection is the end process of an array of different pathological processes, many of which promote weakening of or increased stress on the aortic wall, or both. The sequence of events might begin with a tear in a damaged intima possibly evolved from an atherosclerotic ulcer. Alternatively disruption of the vasa vasorum might result in an intramural haematoma which later ruptures into the aortic lumen (66). Regardless of the sequence of events once a dissection path is started, blood can travel for a variable distance in an antegrade or retrograde manner, or both before commonly re-entering the arterial true lumen.

1.3.2.1.4 Complications of aortic dissection

In an established aortic dissection the principle complications are aortic rupture, AR, acute myocardial infarction (AMI), tamponade and end organ ischaemia (malperfusion syndrome) as shown in Figure 25 below:

Figure 25 Complications of aortic dissection

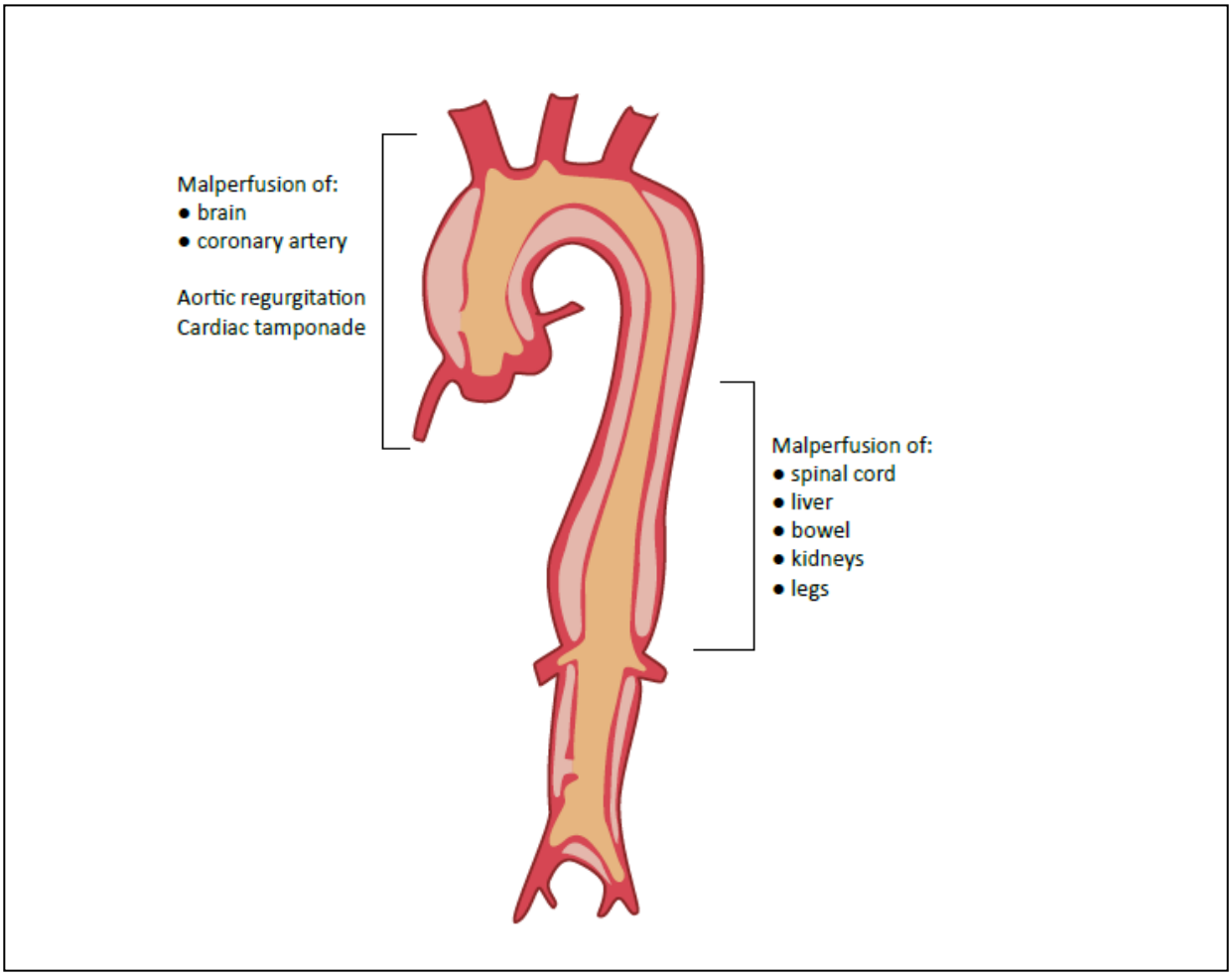

Malperfusion syndromes can compromise flow to the coronary arteries resulting in AMI, or cerebral arteries causing cerebro-vascular accident (CVA). The dissection can cause AR, and tamponade causing the patient to present with hypotension and shock. Depending on the path of the dissection, patients can present with malperfusion of spinal cord, liver, bowel, kidneys and legs.

Malperfusion to any organ can be static as a result of fixed obstructions at the arterial origin, or dynamically affected by pressure changes in the true and false lumens. High pressure within the false lumen can compress the true lumen inducing ischaemia to any end organs fed by that artery.

1.3.2.1.5 Clinical presentation and diagnosis

Most patients present with chest pain which is classically described as “tearing” or “ripping” through to the back. Hypotension or shock is seen in about a quarter of AAAD patients at presentation (usually as a result of tamponade, AR, or heart failure), whereas hypertension is a more common finding in those with Type B dissection (2). Table 6 below summarises the commonest AAAD presentations seen in the IRAD registry (65):

Table 6 Clinical characteristics of AAAD presentations

Symptom and signs	**IRAD Type A database (n=617)**
Chest / back pain	85%
Severe / worst pain ever	90%
Hypotension / shock	27%
Aortic regurgitation	44%
Pulse deficit	33%
Widened mediastinum on CXR	63%
Myocardial ischaemia or infarction (on ECG)	24%

Aortic dissection can be extremely difficult to diagnose as given the varying malperfusion syndromes it can mimic the *de novo* presentation of AMI, CVA, thrombo-embolic peripheral vascular disease, acute abdomen – the list is extensive. CT angiography or echocardiography is usually needed in patients in whom clinically acute aortic dissection

is suspected on the basis of presentation (67). A systemic review of the diagnostic accuracy of TOE, CT angiography, and MRI reported a mean sensitivity of more than 95% for all 3 investigations (68). MRI was slightly better than the other two at showing aortic dissection in a patient with high pre-test probability, whereas CT was better at correctly excluding an aortic dissection in a patient with a low pre-test probability.

In the UK the most commonly utilised diagnostic modality available in most hospitals 24 hours a day is the CT scan. High resolution CT scanning enables 3D reconstruction to be made, which in turn can help to plan appropriate management. Size of the true and false lumen can be measured, localisation of the intimal tear established, and involvement of aortic branches can be ascertained. The presence or absence of other complications including peri-aortic haematoma, AR, mediastinal haematoma and pericardial effusion and tamponade can also rapidly be elucidated. Current guidelines recommend the use of echocardiography or CT, or both in the initial imaging of patients with suspected AAAD. Ionising radiation is a distinct disadvantage of CT, and therefore in the non urgent, chronic dissection follow up magnetic resonance angiography (MRA) is favoured (69).

Figure 26 below shows CT, MRI, and TOE image diagnoses of AAAD:

Figure 26 Shows CT, MRI, TOE images obtained in the diagnosis of AAAD

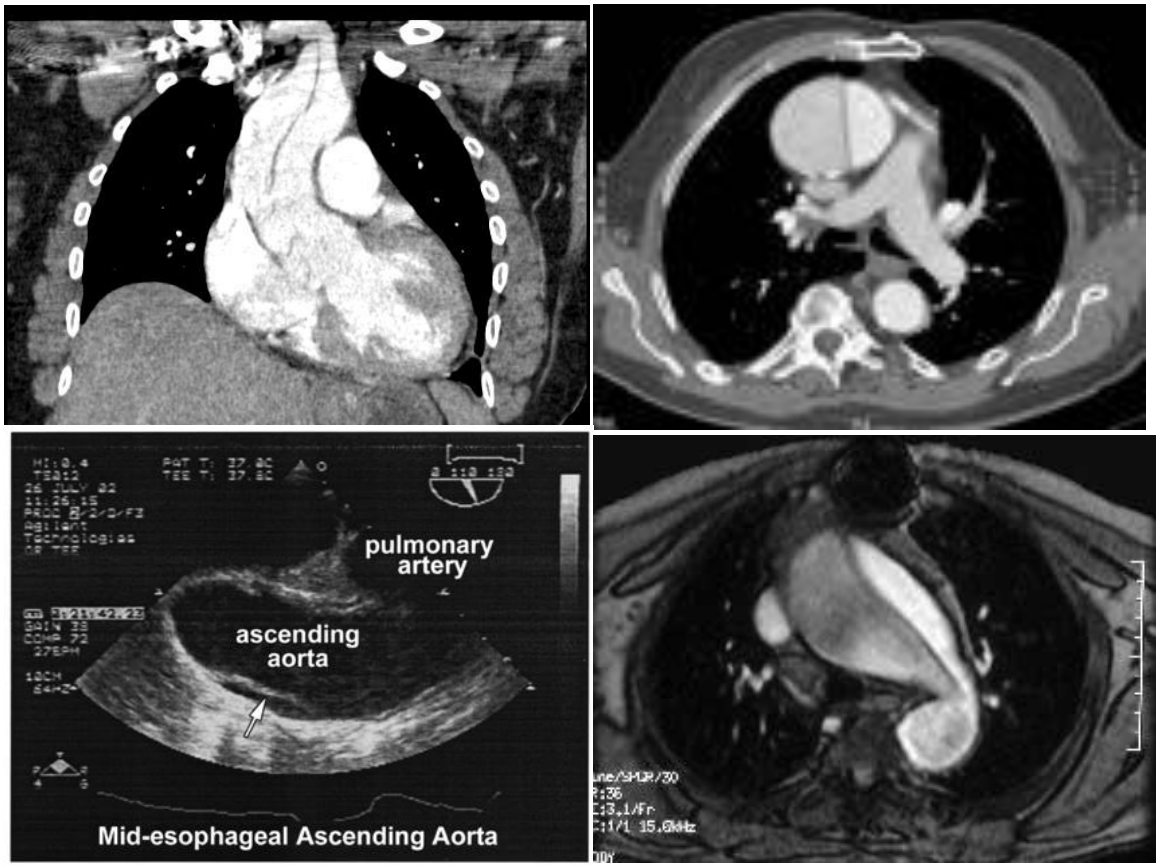

Images clockwise from top left show 1) CT imaging of AAAD, showing a almost central dissection line,2) and 3) MRI imaging of AAAD, showing smaller white "true lumen" and grey larger "false lumen", and finally 4) a TOE diagnosis of AAAD showing an intimal flap (arrowed).

1.3.2.1.6 Management and outcome

AAAD is highly lethal, with mortality ranging between 1-2% per hour early after symptom onset (2). AAAD is always a surgical emergency. Medical management alone is associated with a mortality of nearly 20% by 24 hours, 30% by 48 hours, 40% by day 7, and 50% by one month. Even with surgical repair, mortality rates are 10% by 24 hours,

13% by 7 days, and 20% at 30 days as recently documented in the largest registry of aortic dissection (2). Figure 27 below shows a graph of mortality from Type A and Type B aortic dissection when treated medically compared surgical treatment.

Figure 27 Graph of percentage cumulative mortality of Type A & B dissection

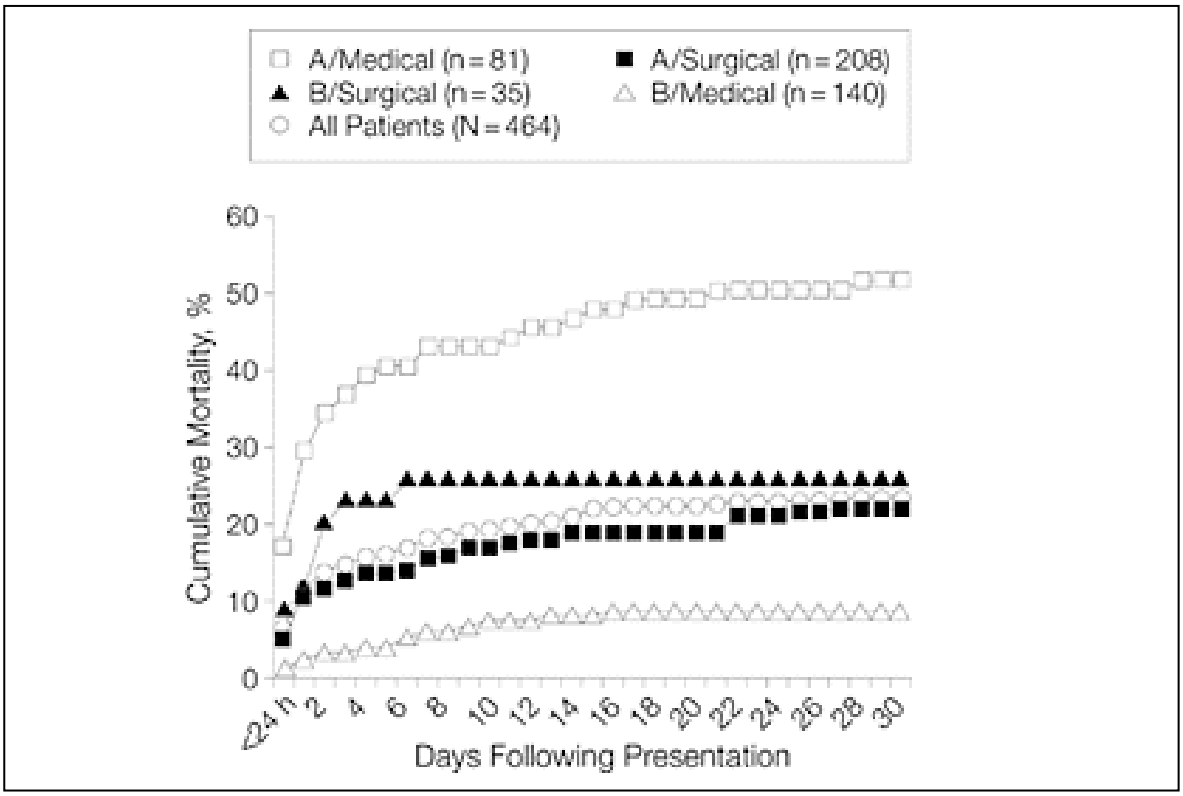

Graph adapted from Mehta *et al.* Mortality from both Type A and Type B versus time depending on medical or surgical management.(70) 30 day Mortality for AAAD is more than doubled if managed medically and not offered surgery (50% versus 20%).

Aortic rupture, stroke, visceral ischaemia and cardiac tamponade or circulatory failure are the most common causes of death (70).

Mehta *et al* have also published a risk score for death in patients presenting with AAAD (70). The most significant features at presentation are highlighted in the Table 7 below:

Table 7 Presentation features seen in AAAD associated with death

Variable	Overall (%)	Among Survivors (%)	Among deaths (%)	Score assigned	*p-value*	Death odds ratio (OR)
Age > 70	35.2	30	46.1	0.5	0.03	1.7
Abrupt onset pain	84.5	82.3	89	1.0	0.01	2.6
Abnormal ECG	69.6	65.2	79.5	0.6	0.03	1.77
Pulse deficit	30.1	24.7	41.1	0.7	0.004	2.03
Kidney failure	5.6	2.9	11.9	1.6	0.002	4.77
Shock / tamponade	29	20.1	47.1	1.1	<0.0001	2.97

A risk score of 1 results in a predicted and observed mortality of approximately 10%. A combined risk score of 4.5, corresponds to a risk of death approximated to 80%. These risk factors were statistically extracted from a retrospective analysis from the IRAD database, and then prospectively confirmed (70). Figure 28 below shows a graph of observed and predicted mortality based on AAAD risk score:

Figure 28 Graph showing observed and predicted mortality for AAAD based on a risk score

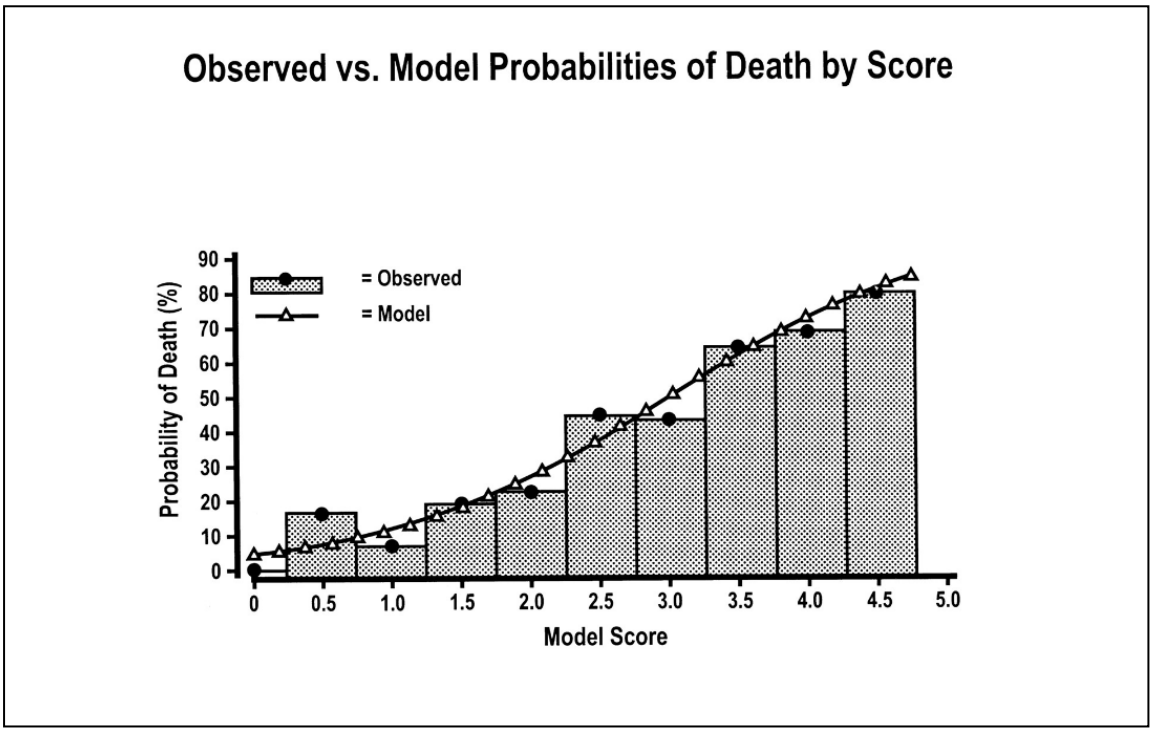

Adapted from Mehta *et al. (70)* Observed mortality versus predicted mortality for patients presenting with AAAD based on a risk score retrospectively extracted and prospectively confirmed from IRAD database. A risk score of 1 results in a predicted and observed mortality of approximately 10%. A combined risk of score of 4.5 = risk of death is around 80%.

1.3.2.2 Conventional AAAD surgical treatments

Currently no RCT have been conducted to guide the management of AAAD. Clinical pathways are therefore currently based upon registry data, consensus documents and local expertise.

Surgical resection of the ascending aorta is the standard management of AAAD (71). In case series of patients, only those with several co-morbidities and who were moribund or

refusing surgery are typically treated medically alone, with an in hospital mortality for these patients of 50% at 30 days (4).

28% of patients with AAAD in IRAD were treated medically because of co-morbidities (33%), patient or family choice (25%), advanced age (21%), or the presence of intramural haematoma only on imaging (21%) (67).

The principle aim of surgery for AAAD is to resect the ascending aorta and arch if affected by the intimal tear and replace it with a prosthetic graft (71). Repair or replacement of the aortic valve is also needed if substantial pathological change of the aortic root or valves exists. Depending on the state and anatomy of the coronary ostia, reconstruction of the coronary arteries may be required in some cases where aortic valve replacement is mandated.

The exact surgical approach taken depends on a number of factors:

Patient factors – preoperative condition, pre-existing pathological condition predisposing to dissection, extent of intimal tear and dissection, aortic root and aortic valve anatomy, coronary anatomy.

Surgeon factors – Surgeon experience, training and preference (71).

While AAAD patients share a common diagnosis every single patient will have a unique mix of anatomical and clinical parameters, and because patients present 24 hours a days they will often be met by a cardiothoracic surgeon who only performs a handful of type A repairs per year. In a number of countries as with most interventional and surgical procedures there has been centralisation of services to optimise outcomes by allowing

teams to be on call for a particular service at a tertiary or quaternary centre. As a result of the clinical and surgical variation many surgical approaches are used in large multi-centre series.

IRAD reported the results of surgical repair of AAAD in 682 patients treated at 18 tertiary centres in 6 countries (9). Techniques used included:

Supra-coronary aortic replacement in 399 patients (58.5%).

Aortic valve sparing operations in 58 patients (8.5%).

Aortic valve, root and ascending aorta replacement with coronary artery re-implantation performed in 101 patients (16.2%) by use of a composite aortic valve / aortic-valve conduit graft.

Right hemi—arch replacement was utilised in 168 patients (27.3%), complete arch replacement in 72 patients (11.5%).

An open procedure with hypothermic circulatory arrest was used in 597 patients (92%), with cerebral perfusion in 322 patients (51.4%). Overall the aortic valve was replaced in 152 patients (24.2%) and simultaneous coronary artery bypass grafting was performed in 100 patients (14.6%).

As has already been discussed in the previous section (1.3.1.8.5) there is considerable controversy in elective surgical repair of ATAA whether to repair or replace the aortic valve – this is also the case in AAAD surgery.

Suzuki *et al.* in their update on surgery for AAAD describe that there have been advances in operative methods, peri-operative management and that surgical outcomes are improving slowly, but that the in-hospital mortality is still unacceptable ranging from 10% - 30% in most series (3).

1.3.2.2.1 The techniques of aortic root repair in AAAD

1.3.2.2.1.1 Use of "Bio-glues"

Gelatin-resorcin-formaldehyde-glutaraldehyde (GRF) glue was created in 1966 and first utilised in aortic root reconstruction in 1977 by Guilmet *et al (72)*. Figure 29 below shows how bio-glues are utilised in the repair of AAAD:

Figure 29 Use of bio-glues in AAAD surgery

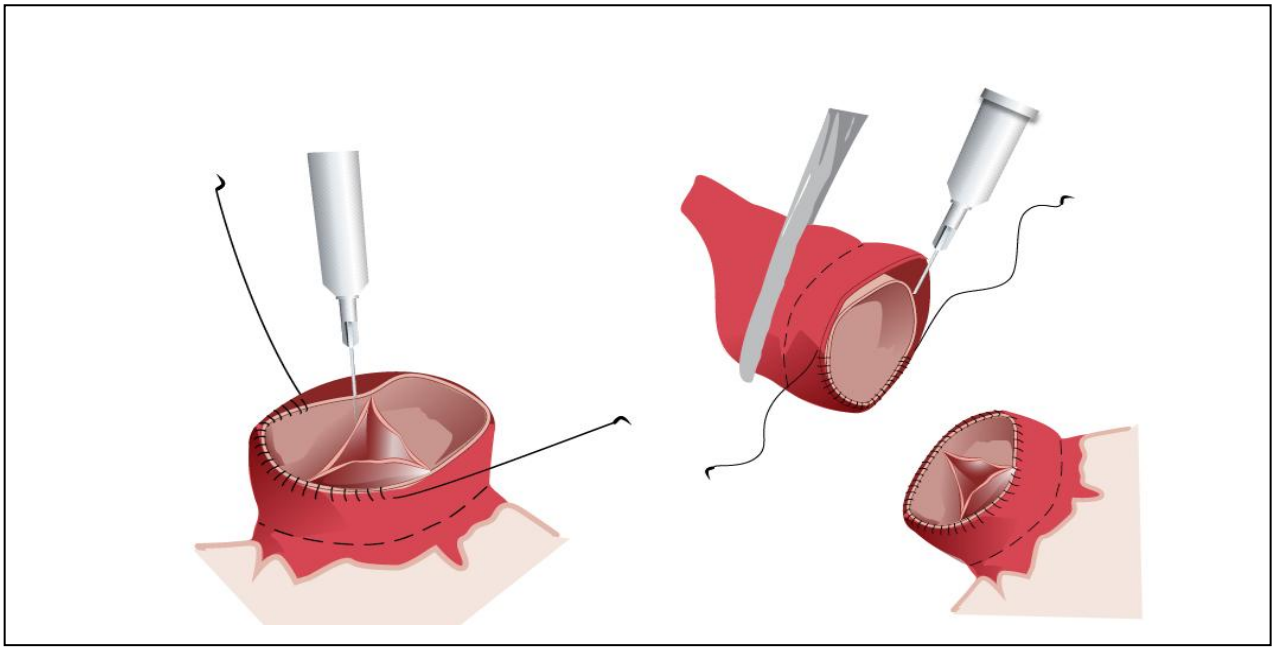

The bio-glue is applied between the intimal and media layers, to reinforce the aorta rendered fragile by the acute dissection, and also to strengthen the anastomosis.

In 1999 Bachet and colleagues reported 21% in-hospital mortality (39/204 patients) in operations using the GRF glue (73). Subsequently GRF had been used widely in operations for AAAD. There have however been reports of late toxic effects of the glue, and Kazui in 2001 reported re-dissection of the root in 4 of 57 patients (7%) who had undergone this technique (74;75). Re-operation revealed dehiscence of the proximal suture line. As a result of this GRF glue has fallen out of favour as it is felt that the toxic effects of formalin compromise an otherwise successful operation. A relatively similar story was seen with BioGlue^{TM} (Cryolife, GA, USA) composed of bovine serum albumin (BSA) with glutaraldehyde (76).

In 1994 Seguin *et al* reported one non-valve related early death (6.7%), but no late mortality after aortic valve repair with fibrin glue for AAAD *(77).* Suzuki *et al.* report that they have utilised fibrin glue with Teflon strips on the inner and outer surfaces of the aorta for reinforcement since 2003, with an impressive in hospital mortality rate of 15.9% (3). Nakajima and colleagues have adapted this technique by using a fabric neomedia and fibrin glue in patients undergoing supra-commissural aortic replacement. Aortic re-operation was not required in 98% of patients at 10 years (78). Fabric neomedia and fibrin glue technique is shown in Figure 30 below:

Figure 30 Fabric neomedia and fibrin glue use

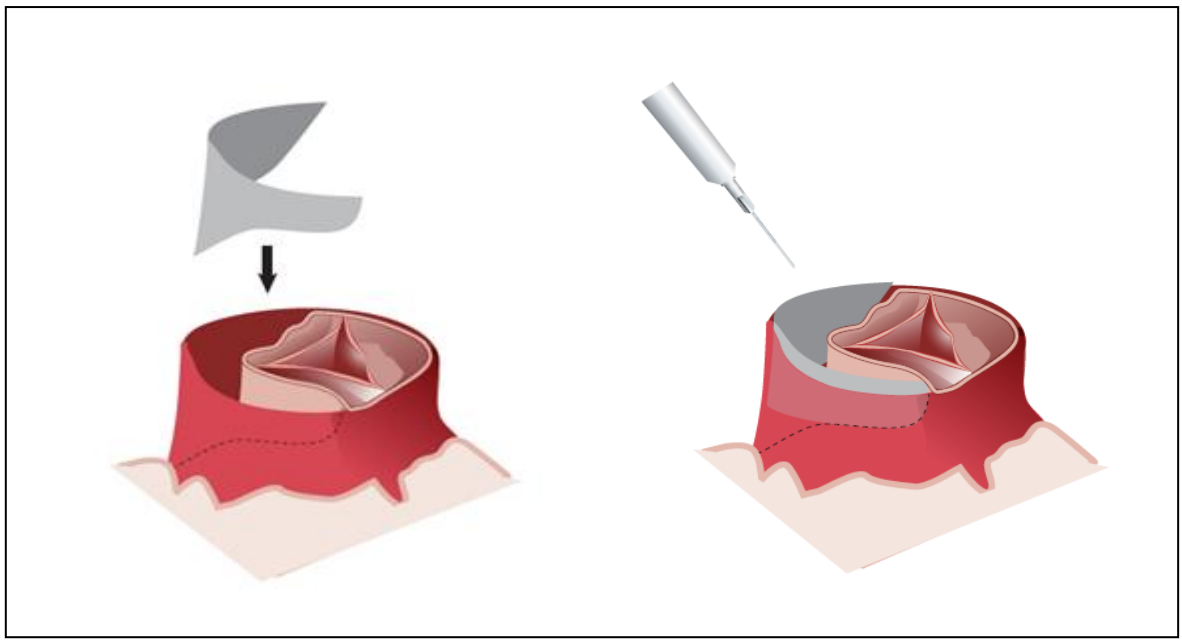

Nakajima and colleagues use a fabric neomedia and fibrin glue in patients undergoing supra-commissural aortic replacement (78). A bespoke cut piece of fabric neomedia is inserted between the intima and media, and then sealed in position with fibrin glue.

1.3.2.2.1.2 Adventitial inversion technique

Floten *et al.* described the adventitial inversion technique (AIT) to repair aortic dissection in 1995, and is described in Figure 31 below (79):

Figure 31 The AIT technique

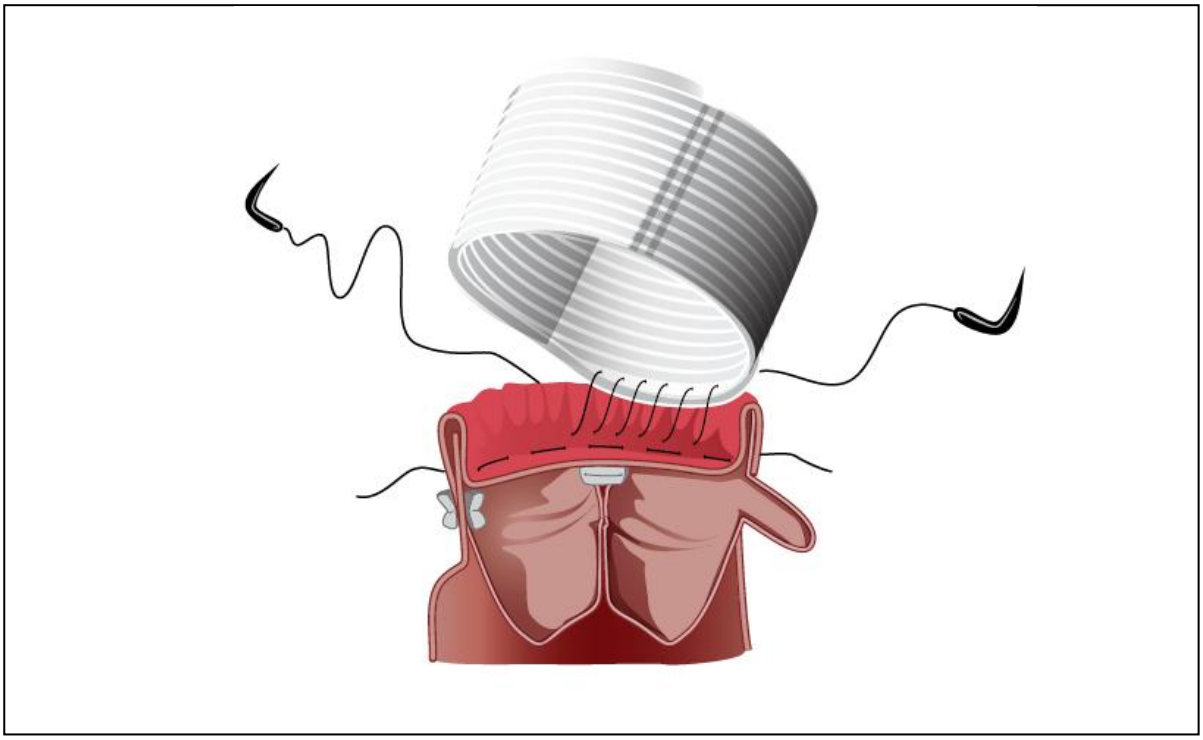

Adapted from Floten *et al .(79)* During the resection of diseased ascending aorta and inner curve of the arch, the margin of the intima is trimmed back 1 cm distal to the adventitial resection line. The redundant adventitia is then inverted into the aortic lumen and tacked to the luminal surface of the intima by horizontal 6-0 Prolene sutures. This creates a tough yet soft aortic cuff.

In 2005 Tanaka *et al.* reported using AIT in 18 patients with an overall in hospital mortality of 11.1% but no re-operation during the follow up period of 7-51 months. They concluded that while it appears safe with good short term data more operations and longer term follow up is required to validate the technique (80).

1.3.2.2.1.3 Composite Replacement

This technique has already been covered in section 1.3.1.8.2 on treatment of ATAA. The pros and cons versus more conservative but often more complex valve sparing techniques are exactly the same as in elective ATAA surgery. Ergin *et al.* compared 19

patients having composite radical root replacement (Group 1) with 54 patients having valve-preserving root reconstruction (Group 2). Despite Group 1 having higher risk features (more AR and coronary dissection involvement) the operative mortality of the 2 groups was the same (15.7% vs 12.9% NS). Group 1 also had better event free survival at 5 years (88 +/- 12% vs 63 +/- 9%) and at 9 years (88 +/- 22% vs 63 +/- 19%), thus they recommended that composite root replacement be utilised more frequently (81). The only drawback with patients treated with mechanical valve conduits is the need for lifelong anticoagulation which in itself carries a risk of bleeding and a rate of thrombo-embolic complications thought to be approximately 4 events per 1000 patient / years follow up (82).

1.3.2.2.1.4 Aortic valve sparing techniques

These techniques have already been described in detail within the ATAA section 1.3.1.8.3. In 2002 Leyh *et al.* reported that 30 patients with AAAD underwent valve sparing aortic root replacement (remodelling in 8 and re-implantation in 22). The mean follow up was 22.6 +/- 15.4 months. The overall 30 day mortality was 17% and late mortality 4%. During the observation period 4 patients (13%) required re-operation (83). Long term durability of the valve sparing repairs is a surgical concern. Not only that, but the results are very surgeon dependent and there appears to be a significant learning curve. Most of the published series of valve sparing aortic repairs are in patients undergoing elective aortic aneurysm surgery. In the 2002 series published by David approximately 12% of cases were in AAAD – it is therefore difficult to extrapolate elective outcomes and theoretical advantages into this very high risk AAAD cohort (84).

David (a pioneer of valve sparing aortic surgery) and Fazel from their paper in Current Opinions in Cardiology 2007 state:

"patients with AAAD may also benefit from the aortic valve sparing operation, but as these are complex operations they should be performed only in centres with much experience. Thus, the surgeon must be well trained in elective surgery to be confident using the technique when emergency surgery is performed for AAAD. We need to investigate whether these benefits will outweigh the potential risk for re-operation" (85).

1.3.2.2.1.5 Other controversy in AAAD surgery

Extent of the distal resection remains a controversy in AAAD surgery. The dissection frequently extends beyond the ascending aorta and arch, and thus theoretically the false lumen might remain patent after ascending aortic replacement. With the substantial mortality and morbidity associated with resection of large parts of the aorta, there is increasing interest in combining open surgical repair of the ascending aorta with endovascular stent grafting (86). These procedures might be combined or staged; however their exact role is unclear and are under investigation.

1.3.2 Overall Conclusions from literature review of AAAD

There are >7,000 documented cases of AAAD in the USA per year, and the incidence is increasing with better diagnostic identification and an aging population (62). Currently AAAD is a surgical emergency with a mortality rate within the first 24 hours of 1-2% / hour. Complications of AAAD include aortic rupture, AR, AMI, tamponade and malperfusion syndrome (2).

28% of AAAD patients are turned down for surgery, and medical management has a mortality rate of >50% at 30 days (2). Even with surgical repair mortality rates are approximately 10-30% at 30 days (3). The principle aim of surgery for AAAD is to resect the intimal tear and replace with a prosthetic graft (usually Dacron), ensuring coronary flow and aortic valve competence. In IRAD nearly 60% of patients had a "simple" supra-coronary replacement. 16% had aortic valve, aortic root and ascending aorta replacement, with coronary re-implantation. 8.5% had aortic valve sparing operations. 27.3% had a right hemi-arch replacement, while complete arch replacement was performed in 11.5% of patients (9).

A number of surgical techniques have been described, and operation choice is based upon patient, and surgeon factors. Valve sparing aortic valve repair surgery appears to have a role, but must only be performed by surgeons experienced in this technique as there is a steep learning curve.

1.3.2.3 Potential implications for ATAG design specification in setting of AAAD

The important facts with regard to designing an ATAG endovascular stent graft to treat AAAD are as follows:

AAAD is an emergency and must be treated quickly. An endovascular graft, trained staff and a theatre with x-ray equipment must be rapidly available because untreated AAAD has a mortality of 1-2% per hour. The manufacture of bespoke grafts will not be possible for this group of patients and we must have "off the shelf" grafts ready for this intervention.

An appropriately sized simple tubular graft starting at the STJ proximally and finishing distally before the RBCT might treat approximately 60% of AAAD (endovascular equivalent of a simple supra-coronary replacement). Success will depend on having an adequate proximal and distal landing zone for the ATAG.

Approximately 25%-35% of patients will require aortic valve intervention to render the aortic valve competent. The ATAG will either need to have an integrated valved solution, or a commercially available TAVI will need to be implanted after the ATAG has been deployed.

The ATAG will not be capable in itself of dealing with the 27% of patients that require right hemi-arch replacement, or the 11% requiring full arch replacement. It is too early to suggest how these patients will be optimally managed, but dedicated endovascular arch solutions are being developed and tested, and there is much interest currently with “hybrid” endovascular and surgical techniques to deal with arch anatomy.

1.3.3 Aortic sizes in AAAD

I now needed to understand the variation in aortic size in patients presenting with AAAD. This would have profound effects on the size of stent grafts required, and the subsequent size to which they could be stowed. For instance a 10 mm increase in deployed stent size could require a 2-4 F size increase in diameter of the delivery system. This full literature review of aortic sizes in AAAD also enabled me to understand what parameters remained unpublished and poorly understood (e.g. coronary associations / angulations) and this helped inform my measurement protocol for the CT work that I performed with Professor Qanadli.

In 2009 Parish *et al.* from Philadelphia published their data of 177 patients presenting with AAAD over a 10 year period (87). The ascending aortic measurements were taken retrospectively from TOE images performed pre-operatively. Measurements were taken at the anatomical landmarks shown in Figure 32 shown below:

Figure 32 Parish AAAD measurement protocol

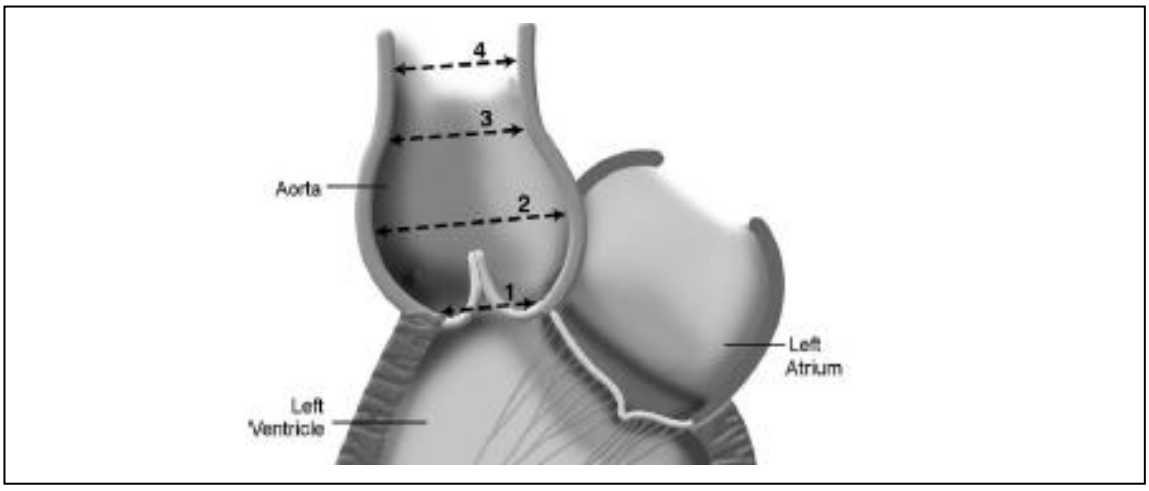

TOE aortic Measurements made 1 – Aortic annulus, 2 – Sinus of Valsalva, 3 – Sinotubular junction, 4 – Ascending aorta

Results were then compared to each patients predicted aortic dimension based on a large normative group corrected for age, sex and body surface area. Patients with known inherited connective tissue disease (Marfan syndrome, Ehlers Danlos etc) were excluded from this analysis as were those individuals with BAV.

The average maximal aortic diameter at any location was 53 +/- 10 mm (mean +/- SD). The maximum diameter occurred at the ascending aorta in 87.6% of patients, and 9.6% of patients in the sinus segment. Table 8 below reveals the observed diameters versus the predicted aortic size from the Parish AAAD cohort (87):

Table 8 Mean maximal aortic diameter at the time of dissection

Location	Observed diameter (mm) +/- SD	Predicted diameter (mm) +/- SD
Annulus	23 +/- 4	26 +/ - 4
Sinus	40 +/- 7	34 +/- 2
STJ	35 +/- 8	29 +/- 2
Ascending aorta	53 +/- 10	30 +/- 4

The graphical representation in Figure 33 below shows that 62% of this 177 non-marfan type AAAD cohort had a maximal aortic diameter of <5.5 cm (the current guideline for consideration of prophylactic aortic surgery). Over 20% had a maximal diameter <4.5 cm.

Figure 33 Maximum aortic diameter distribution

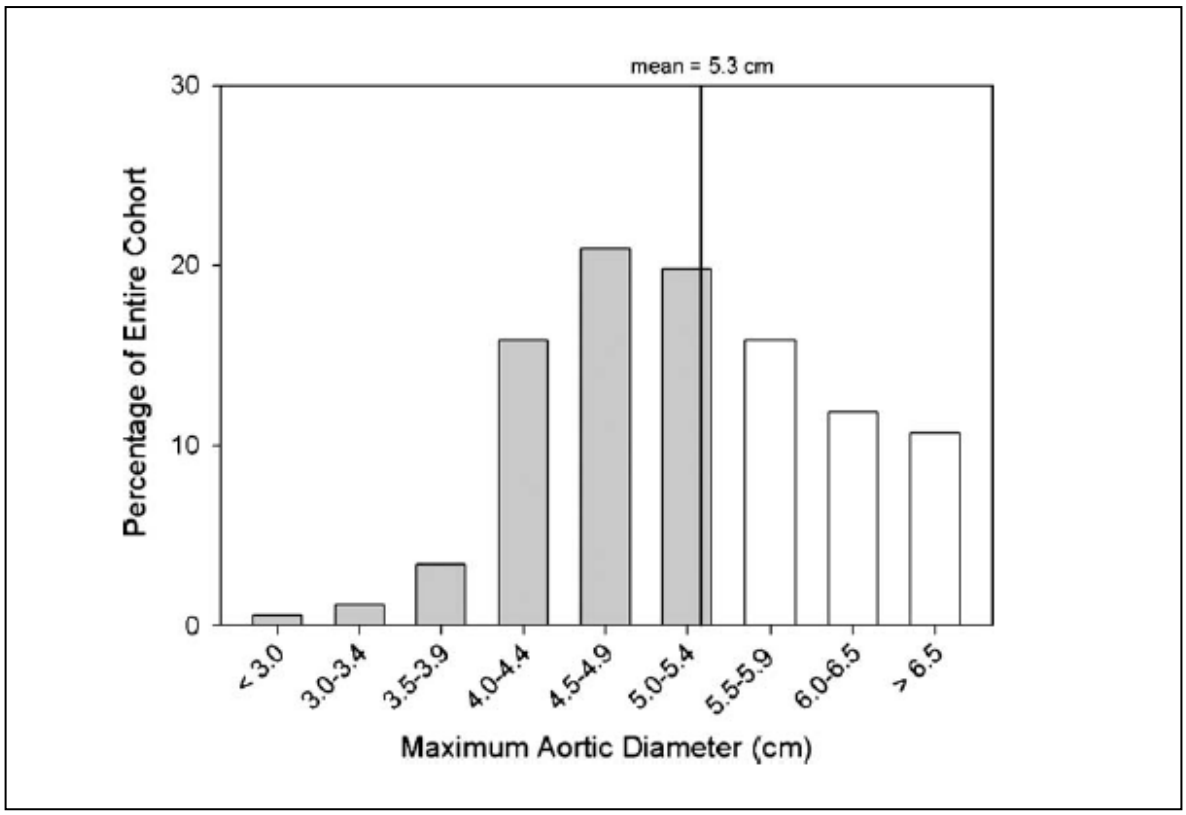

Adapted from Parish (87). The mean maximal aortic diameter in the Parish AAAD cohort was 5.3 cm. 62% (shaded bars) of the 177 non-Marfan AAAD cohort had a maximal aortic diameter of <5.5cm (the current guideline for consideration of prophylactic aortic surgery). Over 20% had a maximal diameter <4.5cm.

This study has important clinical implications, and its data is consistent with a similar analysis performed on the IRAD database (88). More than 60% of patients presenting with AAAD had maximal aortic diameters <5.5 cm (the current guideline recommendation size for elective prophylactic ascending aortic replacement). As a result the current surgical guidelines would fail to prevent the majority of aortic dissections seen in these large registry cohorts. Even with the more aggressive guidelines adopted for the Marfan syndrome patients (surgery > 4.5 cm) 20% of men and 23% of women in the Philadelphia cohort would not have qualified for preventative aortic replacement (87).

The Parish *et al.* study described above measured the maximal aortic size after the dissection had occurred. Although no data exist definitively demonstrating that aortic size immediately before aortic dissection is smaller than after dissection, it seems likely that this is the case.

Neri *et al.* attempted to determine pre-dissection aortic size from surgical specimens removed from over 200 patients at the time of AAAD (89). Perimeter of intimal layer was used as the measurement technique, as shown in Figure 34 below:

Figure 34 Inner layer measurement technique

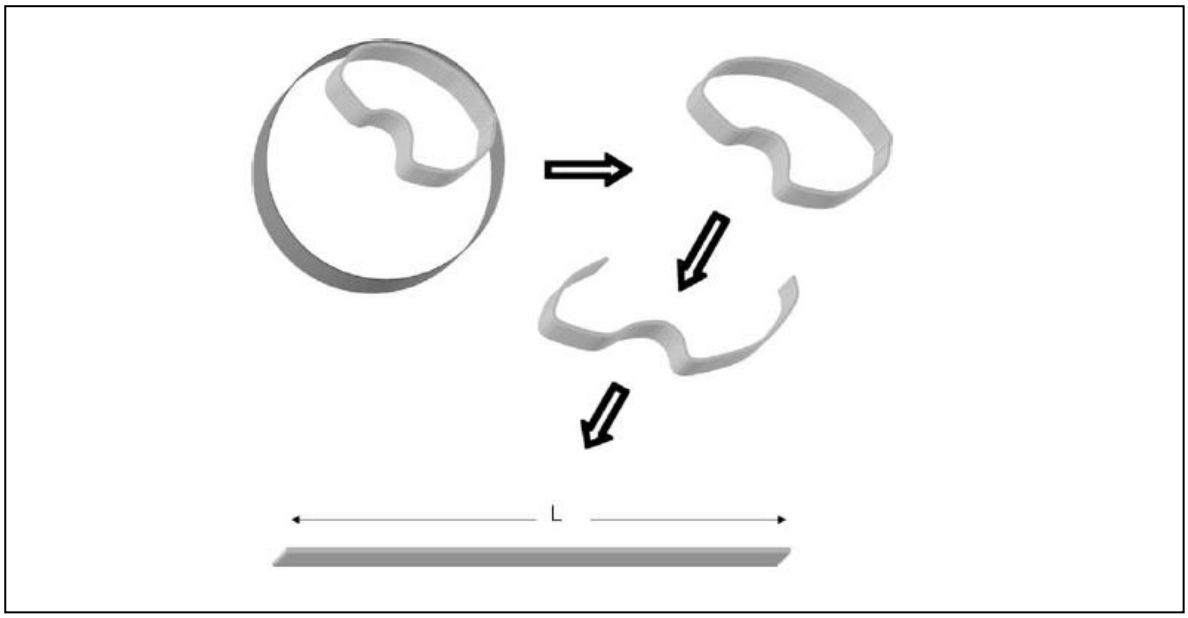

Adapted from Neri *et al (89).* Harvested cylinders of fresh aortic tissue were measured the inner layer of the true aortic lumen with a correction for the absence of perfusion pressure. L - perimeter of intimal layer.

The median ascending aortic diameter determined by this method was 4.1 cm (89).

These data would all seem to suggest that currently accepted aortic size guidelines are not a sufficient index for the risk of AAAD. To fully understand and predict those patients

at risk of AAAD we must study and understand the biomechanics of the ascending aorta. Dynamic mechanical factors such as aortic root motion, and the direction of twisting forces of the vessel may be important. Improved vessel imaging modalities including magnetic resonance angiography (MRA) coupled with finite element analysis (FEA) may provide us with better risk stratification in the future.

Further research is needed to develop effective algorhythms in the form of biomarker, genetic, or imaging strategies that can better identify patients with aortic sizes between 4-5 cm who are at the greatest risk from AAAD.

1.3.3.1 Conclusions about aortic size in AAAD important to ATAG design

From the literature currently available, the majority of aortic diameters in AAAD are between 4.0–6.5 cm, with a mean diameter of 5.3 cm (87). This covers approximately 85% of the population with AAAD, with 5% having a diameter of <4.0 cm, and 10% having a diameter greater than 6.5 cm.

This size variation and the need for the ATAG to be “on the shelf” will require ATAG to be developed in a number of different diameters (and lengths) to suit the aortic anatomy defined by pre-procedure tomographic imaging. Different stent designs may be required for these sizes, and also it is highly likely that different diameter delivery systems will also be required, as the larger the diameter of the deployed stent generally the greater the stowed diameter within the delivery system. During development we will determine the “maximal ATAG diameter” above which it is not technically feasible to make and stow a graft to a suitable diameter. There may also be potential financial restrictions where manufacturing for instance a 8 cm graft is not financially viable because of the large

development costs and the very small numbers of patients who will have this degree of aortic dilatation.

In the first instance ATAG design input will focus on developing a graft capable of treating patients with maximal aortic size of between 4-6.5 cm. One must also remember that if we choose to treat patients with grafts oversized by 20% (as is common in other parts of the aorta) this means that stent frames have to cover the maximal diameter of 48–78 mm. To develop grafts to this size and also enable stowing is technically very challenging. The largest commercially available graft for descending aortic treatment is the Medtronic Captivia^{TM} which is 46 mm in diameter and stows to a minimum diameter of 25 F (90). It must be remembered that descending thoracic aortic grafts are sized to the relatively "normal" aortic segment above and below the level of the dissection or aneurysm, a technique which if possible with landing zones we are likely to replicate.

1.4 "The endovascular revolution" - descending thoracic aortic disease, and aortic arch endovascular interventions - an overview of devices available and outcomes

In the treatment of AAAD there is an unmet clinical need for both patients turned down for surgery, (patients have a 50% in hospital mortality), but also those operated on with contemporary surgical techniques have a 10-30% risk of in-hospital mortality (2). Traditional AAAD surgery is hugely invasive, involves the risks of CPB and deep hypothermic arrest.

I wanted to understand what endovascular devices were available for treating other parts of the aorta, their design features, what had prevented them being utilised in the ascending aorta and what their mortality and morbidity outcome data was like compared to the previous gold standard treatments. Also I wanted to evaluate whether treating other parts of the aorta in a percutaneous way was superior to the more invasive surgical techniques.

1.4.1 Descending thoracic aorta endovascular stent grafting

Optimal treatment strategies for pathology of the descending thoracic aorta are still controversial (69). Open surgery is complex as thoracotomy, extensive surgical resection, left lung collapse, aortic cross clamping, and aortic replacement are all associated with considerable risks of visceral ischaemia and reperfusion, renal

ischaemia, hypothermia, and blood loss. As a result significant morbidity and mortality following open thoracic aortic surgery is well known especially in the acute setting (91).

Endovascular devices allow minimally invasive access to the thoracic aortic pathology. They can be inserted through a peripheral artery. Deployment of an endovascular stent graft for thoraco-abdominal aneurysm was reported by Dake *et al.* as early as 1994 and eventually in 1999 in the setting of acute type B dissection (92;93).

Thoracic endovascular aortic repair (TEVAR) has not been compared to surgery in RCT for patients presenting with descending thoracic aneurysm. Moreover the current literature is very heterogeneous with most reports being case series or registry data. Nevertheless, both short and mid-term outcomes after TEVAR in patients with descending thoracic aortic aneurysm are encouraging with significantly lower morbidity and early mortality when compared with open surgery (5;10). The rate of paraplegia and peri-procedural trauma are reduced as compared to open thoracic aortic replacement, although the incidence of stroke may be similar between the 2 approaches (6).

Jonker *et al* in 2011 performed a retrospective comparison of TEVAR versus open surgery in the repair of ruptured descending thoracic aortic aneurysms. The group found that the composite end point of death, stroke or permanent paraplegia was 36.2% in the open surgery group versus 21.7% in the TEVAR group (*p=0.044*) (94).

While TEVAR is considered potentially life-saving in patients with acute type B aortic dissection complicated by contained rupture or organ malperfusion syndrome, results in stable type B dissection were less supportive (93). The INSTEAD trial recruited 140 patients with stable type B aortic dissection and randomised them to either receive OMT

(n=72) alone, or elective stent graft placement in addition to OMT (TEVAR + OMT n = 68). The primary end point was all-cause death at 2 years.

There was no difference in all-cause death, with a cumulative 2 year survival rate of 95.6 +/- 2.5% with OMT, versus 88.9 +/- 3.7% with TEVAR + OMT (*p=0.15*). The trial however turned out to be underpowered. Three neurological adverse events occurred in the TEVAR group compared to one in the OMT group. The INSTEAD trial therefore supports the notion of a complication driven approach to TEVAR placement for patients that survive type B dissection (95).

The consensus from expert endovascular surgeons is that TEVAR does have an emerging role in the treatment of descending thoracic aneurysm, ruptured aneurysms and complicated type B dissection, but that endograft design and manufacture has not kept pace with the rapidly growing clinical ambition (1;96). Major challenges to be overcome include the rigidity of the endografts and delivery system. Non conformity of grafts may lead to graft instability and procedural failure. Current delivery systems are too large and inflexible to track through calcified tortuous vessels, and often require surgical exposure and iliac artery conduits to enable safe passage of the graft into the landing zone. The challenges of providing conformability and fixation in the aortic arch and the thoracic aorta are considerable, given the spiralling movement of the thoracic aorta with each ventricular contraction.

1.4.2 Currently available thoracic aortic endovascular grafts

I sought to understand the design features of currently commercially available descending thoracic aortic grafts - the materials utilised in the stents and the graft coverings, the stowage size and the delivery system attributes. I also wanted to understand the current techniques to avoid endoleak, stent migration and the relative performance. I wanted to see which mechanical and design features could potentially be incorporated into the ATAG, and at the same time identify those which had a low probability of success in the more challenging ascending aortic anatomy.

There are currently no available endovascular graft for treatment of the ascending aorta. All commercially available thoracic aortic grafts are designed for treating the descending thoracic aorta, and some are in clinical trials for treating the aortic arch. All currently available stent grafts have a self-expandable stent frame (generally z shaped nitinol stent frame), covered in a relatively non porous graft material (2).

1.4.2.1 Graft covering materials

Endovascular graft material must be durable and biocompatible, resist thrombosis and infection. The graft must act as a barrier to blood (preventing blood flow into the false lumen in dissection, and preventing pressure on the thinned aortic wall in aortic aneurysm). There are 2 commercially utilised stent graft coverings for descending thoracic and abdominal aortic endografts:

i) Woven polyester (PET / Dacron^{TM}), and

ii) ePTFE.

Both of these materials have been utilised in vascular applications for many decades.

1.4.2.1.1 Dacron (Polyethylene terephthalate (PET))

Dacron is the most commonly utilised endograft material (used in the Medtronic, Jotec, Cook, and Bolton grafts) and has a long history of vascular and endovascular applications. Figure 35 below shows 2 endografts with Dacron covering:

Figure 35 Endografts with Dacron covering.

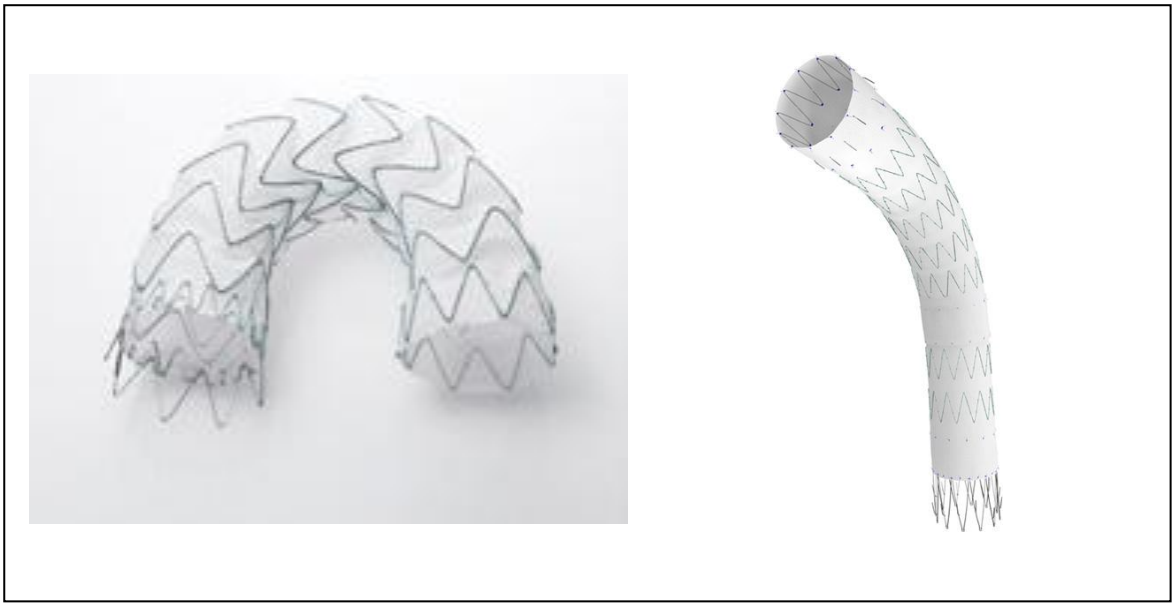

a) Medtronic Captivia graft b) Cook Zenith graft

Both stent grafts consist of z shaped nitinol stent frames with PET Dacron graft covering material, attached by sutures.

PET can be manufactured with a very thin profile (typically around 100 μm) (97). Drawbacks of the woven PET fabrics include an inability to stretch, a tendency to wrinkle easily and an inability to confirm to tubular shapes (98).

The biological response to PET vascular implants is characterised by a fibrous capsule on the outer surface of the graft with granulomatous tissue and abundant intracellular matrix infiltrating the fabric. The luminal surface is composed of compacted fibrinous material with absent endothelial lining except in the vicinity of anastomosis. A further drawback of PET is that when implanted in small vessels it induces an intense tissue reaction composed of concentric layers of eosinophils and lymphocytes, restricting the stent lumen, which can cause eventual thrombosis (99). PET elicits increased thrombogenicity when compared to ePTFE, and this has been explained by enhanced stimulation of macrophage pro-coagulant activity (100).

PET Dacron would seem to have a number of undesirable material properties that make it potentially sub-optimal for ATAG graft utilisation. These include:

i) An inability to stretch – which with the ATAG coronary projections is a highly desirable attribute given the potential variability in coronary ostia location. The material may also cope poorly being stowed to 18-24 F (6-8 mm) and then being expected to expand around the stent frame to a maximal diameter of 65 mm (i.e. 10 times expansion from stowed).

ii) Tendency to wrinkle and poor conformation. Studies have suggested that material wrinkle, and poor conformation to the aortic wall are positive predictors of endoleak risk. Once again in the ascending aorta with high exposure to both twisting and shear forces a poorly conformed stent material is more likely to result in endoleak and subsequent procedural complications.

iii) In small vessels (i.e. studied predominantly in 6-8 mm peripheral vessels) PET induces an intense inflammatory tissue reaction resulting in lumen loss and a significantly increased risk of thrombus formation and vessel closure. Given that potentially we will require the “arms” of the ATAG t-shirt to be stented into both the LMCA and the RCA ostium at a diameter of 3-4 mm, it is highly likely that PET Dacron would lead to coronary branch occlusion which is likely to result in a poor patient outcome.

iv) Dacron when joined to form branched grafts tends to be “hand sewn”. Sutures at haemodynamic stress points (like the attachment of the coronary branches) are likely to lead to increased risk of thrombus formation at the ostium of the coronary branches.

In summary it seems unlikely that the material properties of Dacron are suitable for a branched aortic graft with small (<5 mm) branches into the coronary arteries. It is important at this early stage that other materials are investigated and it is possible that the ATAG will require a novel material for the coronary sleeves with sufficient elasticity, and adequate prevention of cell migration / tissue ingression to prevent lumen stenosis and thrombosis.

1.4.2.1.2 ePTFE (Expanded Polytetrafluoroethylene)

ePTFE is chemically composed of carbon chains saturated with fluorine, this gives ePTFE conformational rigidity, stability and low surface energy, which results in low thrombogenicity and modest tissue reaction. ePTFE is utilised in the LeMaitre and Gore grafts, and has high strength, but low surface friction which can make stent migration a

problem. ePTFE grafts do not dilate over time and offer better resistance to infection when compared to the Dacron grafts, they are however more expensive to manufacture (101). Figure 36 below shows 2 commercially available ePTFE covered grafts:

Figure 36 Commercially available ePTFE covered grafts

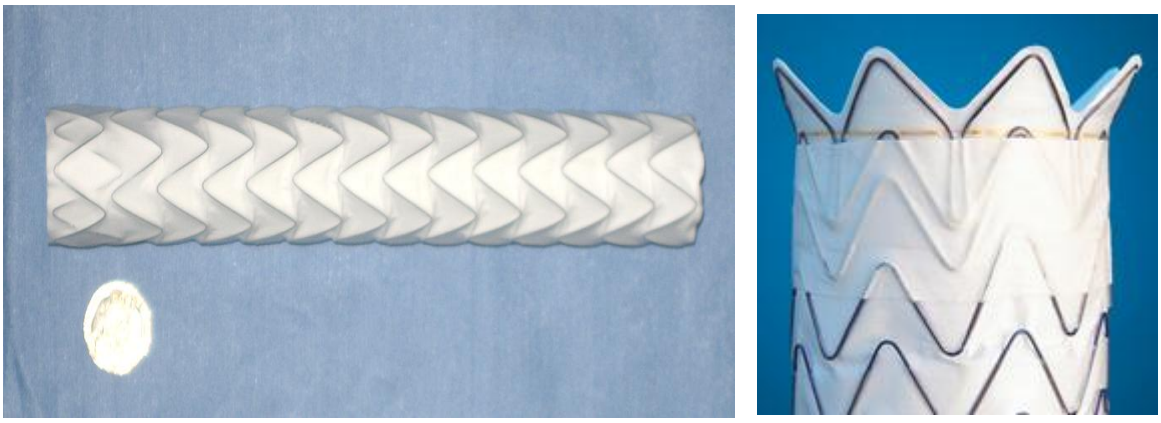

Commercially available ePTFE covered endografts. On the left side the LeMaitre TAArget thoracic graft next to a 20 p piece, and on the right hand side the Gore TAG thoracic graft.

ePTFE also exhibits some features which potentially make it unsuitable for use within the proposed ATAG graft. It is relatively rigid which in keeping with PET will make conforming of the coronary sleeves to the variability of coronary take off more challenging. Although better than PET with regard to thrombogenicity, 1 year patency rates in peripheral artery stenoses (femoral artery) are at best 80%, and this will not be acceptable in the coronary position. Part of the reason for this is that ePTFE grafts exhibit a scant neo-intimal layer except at the adjacent vessel surface. Endothelium has been found scattered through the lumen of the animal and human endovascular ePTFE

but it is never confluent or complete (102). It would seem therefore that ePTFE is unlikely to be a perfect material for our ATAG graft with coronary sleeves.

1.4.2.2 Design features of existing grafts dealing with branches

1.4.2.2.1 Uncovered stent portions

The proximal and distal ends of the stent grafts can either be covered with material as seen with the Gore and LeMaitre devices, or have some uncovered stent struts (like the Cook and Medtronic grafts in Figure 37 below). This allows the proximal end of the graft to sit across for instance the left subclavian artery (LSCA) without compromising flow into the side branch.

Figure 37 Uncovered proximal stent struts

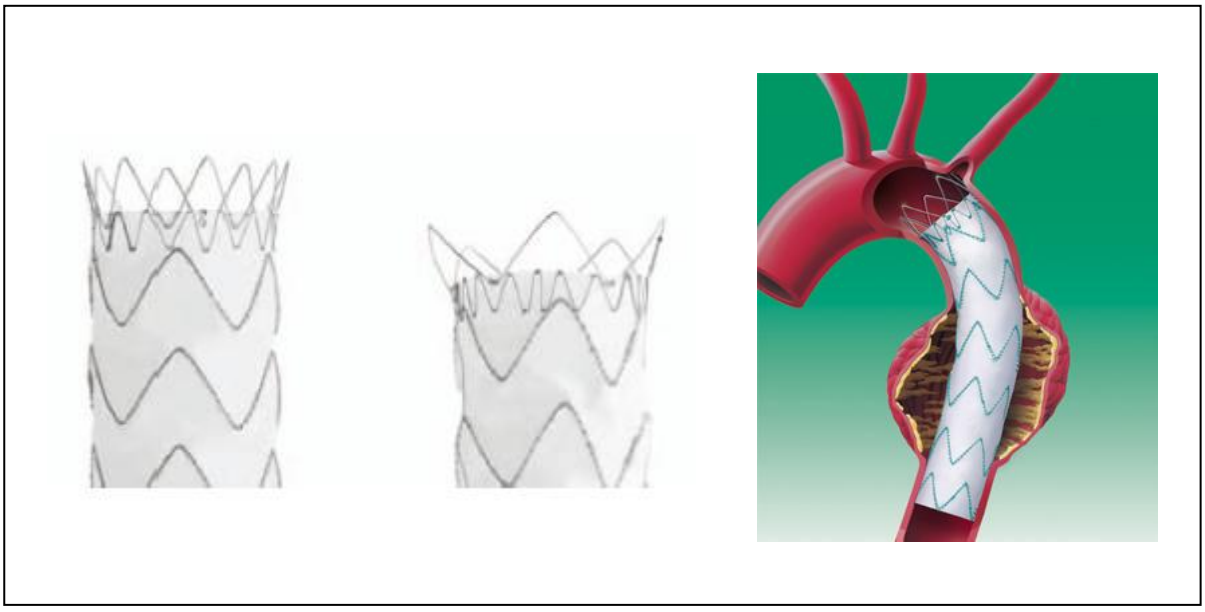

Having stent struts not covered with Dacron or ePTFE means that a seal can be achieved proximally (for instance lying across the LSCA), but that patency of the branch vessel can be maintained.

Alternatives to this include fenestrated grafts where holes in the fabric are aligned over the ostium of the side branch to enable uncompromised flow, and allowing access to stent the side-branch, optimising side branch flow and minimising endoleak risk. An example of a fenestrated graft is shown in Figure 38 below:

Figure 38 Fenestrated stent-graft

Two circular fenestrations can be seen in the graft material above, which oppose branches of the aorta allowing uncompromised flow into the branch arteries.

1.4.2.3 Anti-migration mechanisms

To prevent migration of conventional thoracic stent grafts there are 3 main strategies:

1) A proximal and distal flared portion to help anchor the graft in position, as shown in Figure 39 below:

Figure 39 proximal flared portion on Gore graft

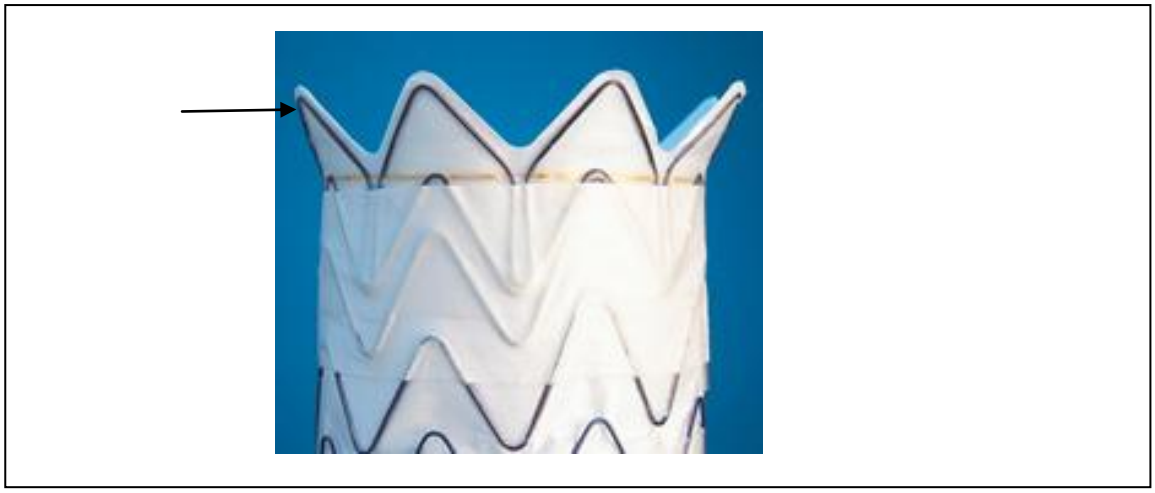

Proximal flared portion of a Gore endograft (arrowed).

2) Anti-migration barbs that imbed into the aorta. Figure 40 below shows the anti-migration barbs featured on the Cook TX 2 aortic endograft.

Figure 40 Anti migration barbs

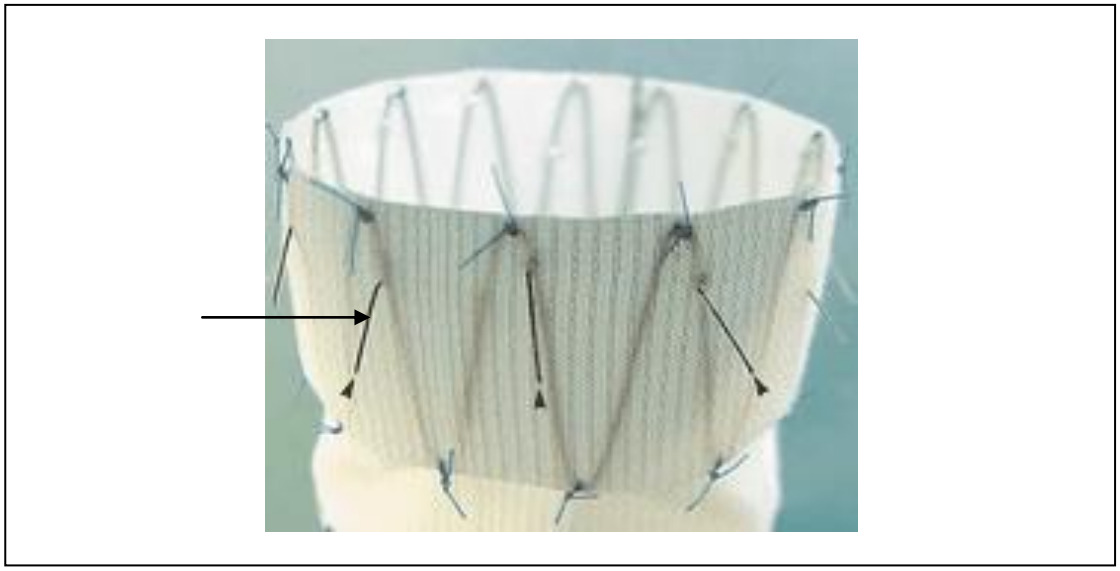

Anti-migration barbs are present on the Cook endografts (arrowed above).

3) Sufficient over-sizing to exert a constant outward radial force. Most commercially available thoracic stent grafts are over-sized to the vessel in their instructions for use (IFU) by 10-20%.

1.4.2.4. Stent sizing, availability and delivery systems

The method of measuring the adequate size of the stent graft in aortic disease is the subject of debate and according to a recent literature review is in "desperate need of a consensus" (96). This is especially the case in patients with aortic dissection. Currently interventional radiologists and vascular surgeons use a variety of methods. Some utilise the diameter of the proximal unaffected aorta and then oversize by anything between 10-20%. An alternative technique is to deliver a 10% larger graft than the average of the maximum and minimum diameters of the true lumen in acute dissection, or 20% in chronic dissection (103).

Choosing too small a stent-graft diameter can cause endo-leak (leak around the graft – see classification in section 1.4.2.5.4), or migration. Over-sizing may lead to infolding of the graft material, local trauma, retrograde propagation of the aortic dissection flap, and may lead to late erosion of the vessel wall.

1.4.2.5 Problems, failure modes, and applicability of thoracic aortic stent grafts

1.4.2.5.1 Mechanical failure of stent-graft

Once implanted the endograft is subjected to external forces imposed by the geometry of the tortuous aorta and the impact of phasic blood pressure. Mechanical failure of the

stent graft can occur in the form of metallic fracture, fabric tear, and suture breakage. A recent large series identified 60 patients (9%) with mechanical failure of the stent graft of the 618 patients who underwent stent-graft implantation. 43 patients (6.9%) had metallic stent fracture, 14 suture disruptions (2.3%), and 3 graft wear (0.5%). The average time to recognition of mechanical failure was only 19 months, with surgical conversion in 6 cases (104). At this time the clinical importance of any graft failure is not clear, and management of mechanical failure is on a case by case basis depending on clinical sequelae and risks versus benefits of re-intervention (either endovascular or open surgical).

1.4.2.5.2 Access issues and stroke

Although endovascular repair of the aorta avoids aortic cross clamping and is less traumatic than open surgery, the large calibre delivery systems often required can cause damage to access arteries. For patients with small peripheral vessels a surgically placed funnel bypass conduit may be required to the common iliac artery.

Cerebral ischaemic complication is reported to occur in 2.9-11% of stent graft procedures in descending thoracic aortic dissection, and is often associated with prolonged procedure time, manipulation of guide wire or device in the arch causing cerebral embolisation (105). This compares to the risk of stroke in carotid stenting in the contemporary CREST trial of 4.1% at 30 days (106). As graft technology becomes lower profile, delivery systems become more flexible, and cerebral protection devices become more advanced and established in practice we are likely to see a reduction in these complication rates.

1.4.2.5.3 Unintended side branch occlusion

Management of the aortic arch branches ranks among the most significant unresolved and controversial issues (107). Sufficient proximal anchoring and a landing zone of 2 cm is usually required to avoid type I endoleak, thus coverage of the LSCA or combined surgical extra-anatomical bypass of the aortic branches may be necessary.

1.4.2.5.4 Endoleak

Exclusion of the aneurysm sac is the main goal of endovascular stent graft treatment, and clinical success is defined by the "total exclusion" of the aneurysm. However, failure of the stent graft to totally exclude blood flow to the aneurysm sac may occur, and this is termed “endoleak”. Endoleak is a major cause of complications, causing continued pressurization of the aneurysm sac and may leave the patient at risk of an aortic rupture. Endoleaks are categorised into subtypes I – IV:

Type I or attachment endoleak is the most frequent complication associated with stent graft treatment of aortic dissection or aneurysm and may result in clinical failure eventually (108). The percentage of type I endoleak in the literature ranges from 1-44% (96). A proximal neck <2 cm from the LSCA and existence of an entry tear at the lesser curve of the aortic arch predispose to endoleak and a “bird-beaking” appearance.

The fate of type I endoleak is still a matter of debate. Some experiences have shown spontaneous closure of the leak, while others have shown continuous expansion of endoleaks and failure requiring additional stent graft deployment for sealing, spot coiling or conversion to an open operation. If endoleaks persist long term progressive

aneurysmal dilatation of the false lumen occurs requiring further ancillary procedures or conversion to a surgical approach.

Type II endoleak is where blood continues to flow into the aneurysm sac from collateral vessels.

Type III endoleak results from blood flow into the aneurysm sac due to inadequate or ineffective sealing of overlapping graft joints or rupture of the graft fabric. This type of endoleak usually occurs early after treatment, due to technical problems, or later due to device breakdown.

Type IV endoleak - blood flows into the aneurysm sac due to the graft fabric porosity.

Figure 41 below shows the current endoleak classification I-IV:

Figure 41 Diagrammatic representation of the endoleak

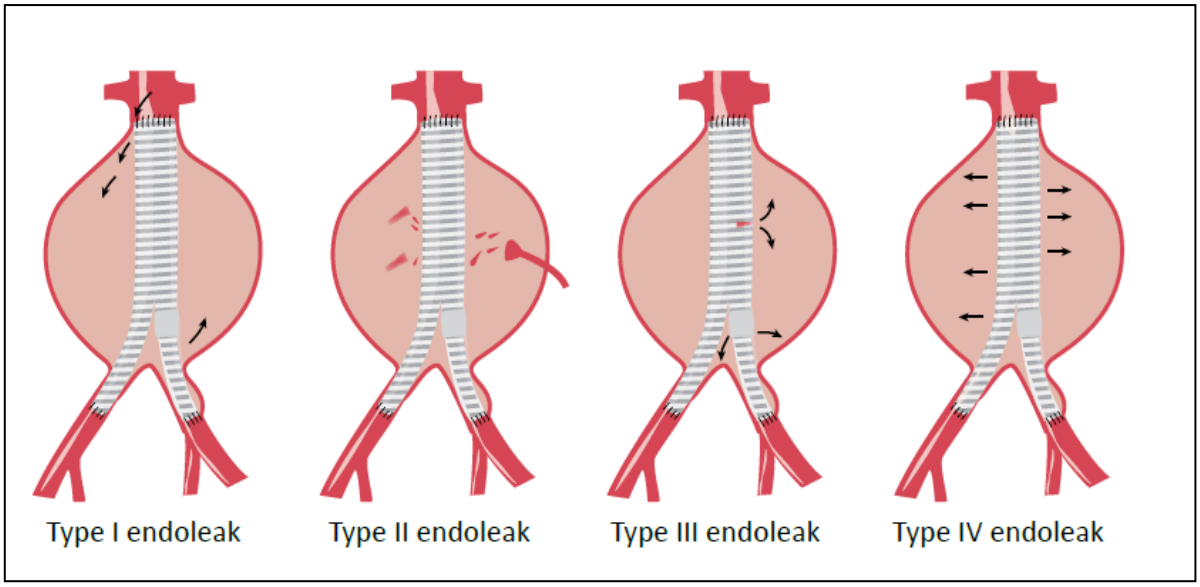

Type I or attachment endoleak is caused by a poor proximal or distal stent graft apposition allowing leak around the proximal or distal seal into the aneurysm sac. **Type II endoleak** is where blood continues to flow into the aneurysm sac from collateral vessels. **Type III endoleak** results from blood flow into the aneurysm sac due to inadequate or ineffective sealing of overlapping graft joints or rupture of the graft fabric. **Type IV endoleak -** blood flows into the aneurysm sac due to the graft fabric porosity.

1.4.2 Lessons learned from the review of currently available descending thoracic aortic endografts relevant to ATAG design specification:

1) All currently available descending thoracic aortic stent grafts utilise a self expanding (usually nitinol) “Z” shaped stent frame.

2) The majority are covered in a woven PET “Dacron” material, the rest covered in ePTFE. Both materials bring about an inflammatory response and cell adhesion resulting in lumen loss, which in small diameter vessels is important and can lead to graft

thrombosis and occlusion. Graft material choice will be very important for the ATAG if coronary projections are to successfully protect proactively the coronary flow. Materials choice is covered in detail within the device specification.

3) Thoracic and abdominal aortic grafts have a number of mechanisms to avoid branch occlusions. These include open cell uncovered stent portions (i.e. commonly utilised to cover the LSCA without compromising flow), and fenestrations to allow flow through the graft and into the branch vessel. It is unlikely that in the setting of ATAG open cell stents will be helpful, but certainly if protecting both coronary arteries with a stented "t-shirt" is too technically of physiologically challenging then one could use fenestrations over one or both coronary artery ostia.

4) As with all aortic endografts it is vital that once correctly positioned there is minimal migration. I think it is highly likely that the ATAG will integrate a flared portion at the proximal aortic valve end as this will allow it to optimise proximal seal to prevent endoleak. Anti-migration barbs are likely to be overly aggressive in the landing zone of the aortic root and may well interfere in a detrimental fashion with the aortic valve leaflets. In keeping with most thoracic endografts I think it is likely that the ATAG will be relatively "over-sized" - the exact amount assessed by further *in vitro* and *in vivo* experimentation.

5) ATAG will be exposed to all of the physiological stresses that descending aortic endografts experience. This will mean that the ATAG will be at risk of mechanical failure. During rigorous testing all component parts must be shown to be capable of withstanding these physiological stresses.

6) The commonest complications of TEVAR include vascular and stroke, and this represents the greatest risk to the potential ATAG patient. To minimise this risk the crimping profile and delivery system must have the lowest possible profile and be flexible, and ATAG implantation may utilise cerebro-vascular protection devices like those used in carotid stenting and those emerging in TAVI.

7) The ascending aortic anatomy poses many problems with regard to proximal and distal graft seal. Design must be meticulous to minimise endoleak, a complication known to increase re-intervention rates.

1.4.3 Innovations in arch endovascular stent grafts

Devices for treatment of the descending thoracic aorta have been commercially available for a number of years and are now 2nd or 3rd generation devices. With improving technology and tools interventional doctors are gradually moving more proximally into the aortic arch, where there are currently a number of devices in early clinical trials.

I felt it was important to understand the current innovations in the aortic arch for 2 reasons:

i) To give me an insight into contemporary endovascular management of the head and neck vessels

ii) If ATAG is to provide a solution for the ascending aorta in AAAD, about 35% of cases will have concomitant arch involvement and as such it would be advantageous if there was a completely endovascular solution (9).

Endovascular stent grafts have a role in the treatment of some patients with aortic dissection and aneurysmal disease in the descending thoracic and abdominal aorta. The arch of the aorta with its three branches creates a number of technical issues which must be overcome before successful endovascular stenting can become commonplace. I will now briefly outline some of the proposed solutions to treat by endovascular stent grafts the arch of the aorta. None of them have reached the level of accepted clinical practice or "gold standard" status, but some are in large scale clinical trials.

In 1999 Inoue proposed a branched aortic arch stent graft (109). This was the first proposed endovascular solution branched graft, and shown in Figure 42 below:

Figure 42 The Inoue branched aortic arch graft

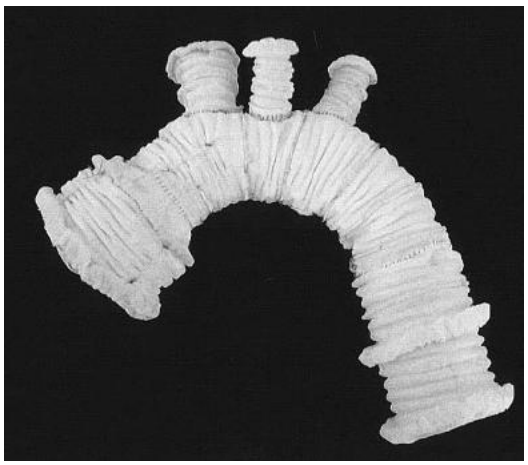

Photograph of the proposed Inoue branched aortic arch graft (109). It shows a material arch graft with 3 great vessel branches.

Inoue reported a procedural success rate of 60% in a series of 15 patients. There have been no large scale trials of this device since the FIM experience and many commentators cite that the procedure is very complex and not reproducible by the majority of interventional doctors (110).

In 2003 Tim Chuter reported *in vitro* experiments using a modular branched system, some of the designs are represented in Figure 43 below:

Figure 43 proposed drawings of the Chuter modular arch grafts

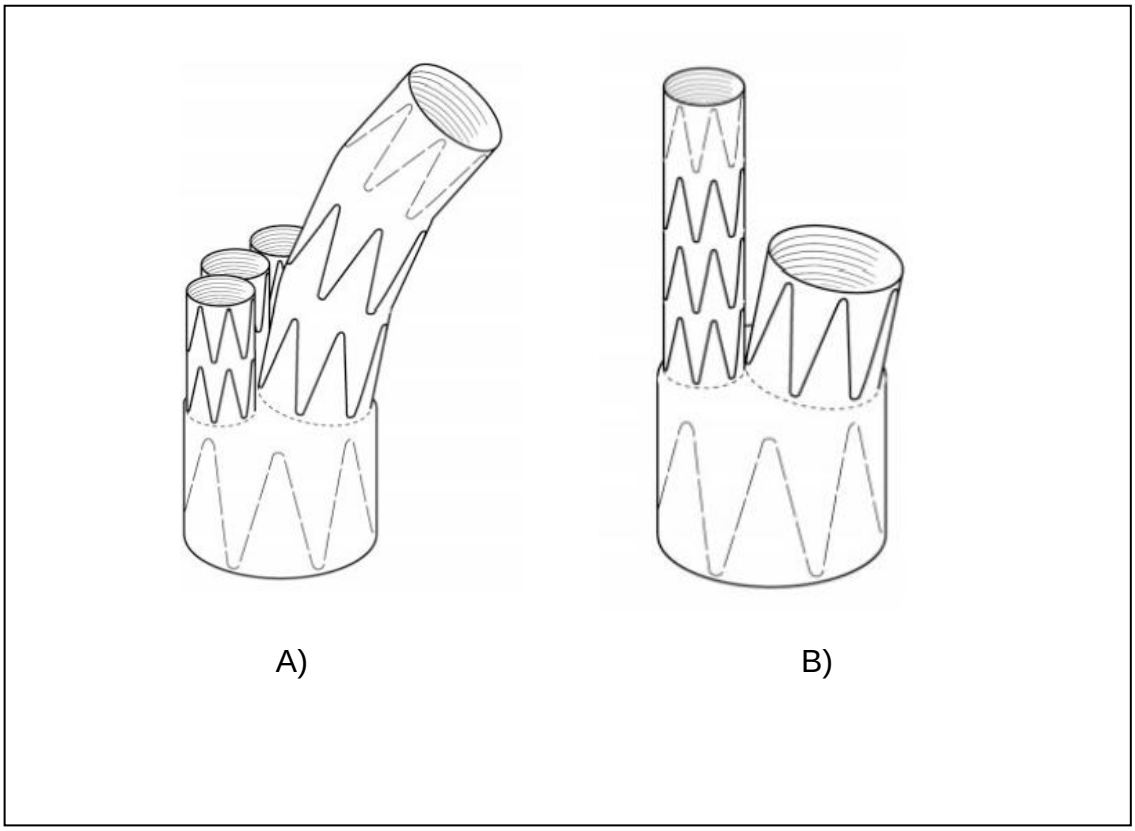

Adapted from Chuter *et al.(110).* Out of 4 designs tested only the simplest (B above) was deployable without difficulty or delay. B resembles essentially an upside-down version of a long-leg / short-leg bifurcated infra-renal stent-graft; even the delivery system had been used before to insert infra-renal stent-grafts.

WL Gore & Associates (Flagstaff, AZ, USA) are developing a branched graft with a limb into the LSCA, to avoid the need for LSCA occlusion or extra-anatomical bypass. This device is currently in clinical trial and shown in Figure 44:

Figure 44 WL Gore TAG branched device

The WL Gore TAG endograft above can be seen to have a dedicated branch for preserved flow into the LSCA, avoiding the need for extra-anatomic bypass, or coverage of the LMSA (111).

1.4.3.1 Hybrid aortic arch procedures

Another potential solution, albeit more invasive is a hybrid procedure with extra-anatomical bypass of a branch vessel, followed by endovascular stent-grafting covering grafted vessels. Figure 45 below demonstrates the theory of extra-anatomical bypass for the arch vessels followed by endovascular stenting across the grafted branches.

Figure 45 Diagram representing a possible hybrid procedure for the arch vessels.

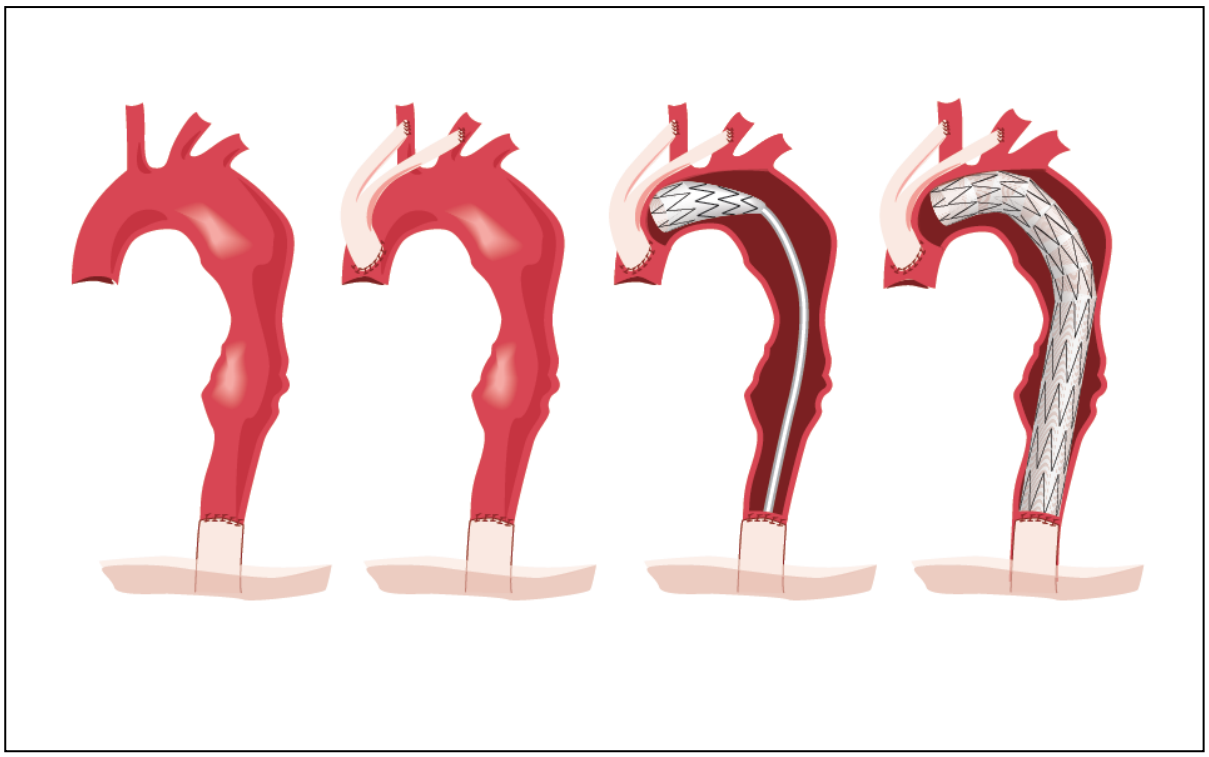

Extra anatomical surgical bypass, with surgically attached grafts from the aorta onto the RBCT and the LCCA followed by endograft treatment, across the origins of the bypassed arch vessels. Adapted from (31).

There are many potential variations of this and beyond the realms of this thesis for full discussion.

1.4.3 Endovascular solutions for the treatment of the aortic arch

Conclusion

In 2012 there is no accepted solution to treat the aortic arch in a satisfactory endovascular manner. Treatment strategies vary according to local expertise, physician preference, patient anatomy, access to particular devices and regulatory issues.

Most physicians now accept that covering the LSCA without extra-anatomical bypass is associated with an increased risk of stroke and paraplegia. Clinical trials are on-going to see if the LSCA and descending aorta can be treated with a branched graft (WL Gore and associates) (111).

Treatment of the RBCT and left common carotid is more difficult and currently most endovascular solutions for these anatomical situations involve extra-anatomical bypass first. As devices, materials, delivery catheters and techniques improve it may be possible that the arch may be treated in a totally endovascular manner, we await further device testing and clinical trials.

1.5 Percutaneous aortic valve therapies

When the ATAG project commenced in 2007 TAVI was still in its relative infancy with early stage devices, large delivery systems, and no RCT data available to guide clinical indications.

Because of the very close anatomical association between ascending aorta, aortic valve and coronary arteries and the potential in both AAAD and ATAA populations to require aortic valve replacement it is vital that the TAVI devices and data are well understood. To treat the 25% of AAAD patients with incompetent aortic valve function, the ATAG would either need to have a "valved" version that could be implanted and perform aortic valve function, or the ATAG would have to be "compatible" with commercially available TAVI devices so that before or after ATAG implantation, the aortic valve competence could be restored with TAVI implantation (9).

Below I present the 2 commercially available devices with safety and efficacy data available in 2012.

The first percutaneous aortic valve implantation in man was performed in Rouen, France by Alain Cribier in 2002 (112). Cribier delivered the valve via a 24 F sheath in the right femoral vein, the valve delivered in an ante-grade fashion through the inter-atrial septum to the aortic valve position without compromising the coronary arteries.

The valve was manufactured by Percutaneous Valve Technologies (PVT Inc, Fort Lee, NJ, USA), was made of a slotted steel with 3 bovine pericardium leaflets, crimped onto a

commercially available NUMED^{TM} 23 mm diameter balloon, and shown in Figure 46 below:

Figure 46 shows the first pericardial PVT valve

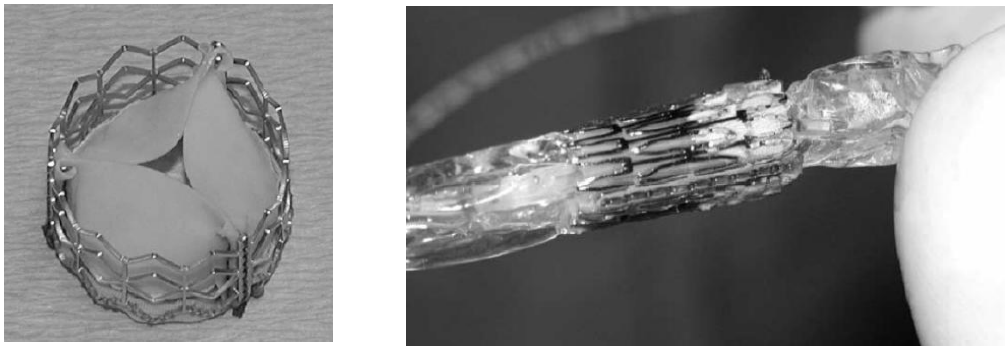

Photograph of the PVT valve (left), crimped down onto a 23mm NUMED balloon (right). Taken from the original description by Cribier (112).

Edwards Lifesciences Corporation (Irvine, California, USA) purchased PVT in January 2004, and since then the device has evolved dramatically. The Edwards Sapien XT valve has CE mark in Europe and regulatory approval (FDA) in the US for inoperable patients. It is currently in multi-centre, international RCTs (Placement of AoRTic TraNscathetER Valve Trial (PARTNER trials)). The current device, the Edwards Sapien XT is available in 3 sizes (23 mm, 26 mm, and 29 mm) and has a delivery system diameter of 18 F. The latest system Novoflex XT 18 F will pass through a specially designed eSheath^{TM} which is actually 16 F and "expands" to accommodate the larger delivery system. The Edwards valve can be delivered trans-femorally (Novaflex XT), and trans-apically (Ascendra 2 delivery system). Figure 47 below shows the current Edwards Sapien XT valve:

Figure 47 Current Edwards Sapien XT valve

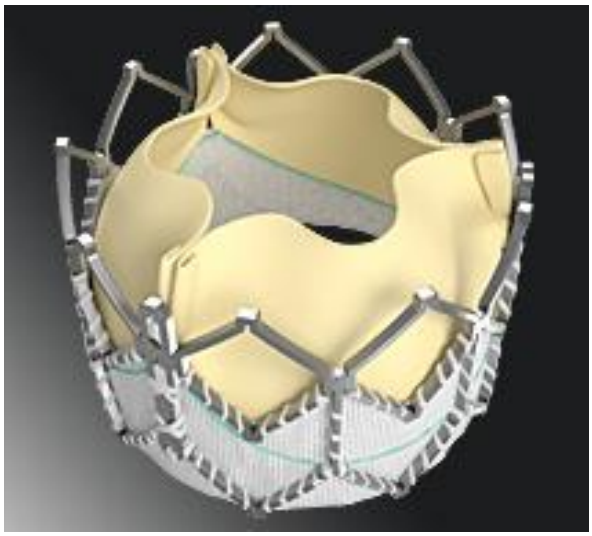

The Edwards Sapien XT valve has a cobalt chromium balloon expandable stent frame. Within the stented portion are 3 bovine pericardium valve leaflets which are treated using a Thermafix™ process to minimise subsequent calcification.

The other currently available CE marked percutaneous aortic valve is the Medtronic CoreValve™. In contrast the CoreValve frame is made from self-expandable nitinol. It is longer than the Sapien valve and has sections of differing diameters and radial strength to complement the differing portions of the ascending aorta and outflow tract. It is delivered similarly in a retrograde manner using an 18 F delivery catheter. Figure 48 below shows the Medtronic CoreValve:

Figure 48 Medtronic CoreValve revalving system

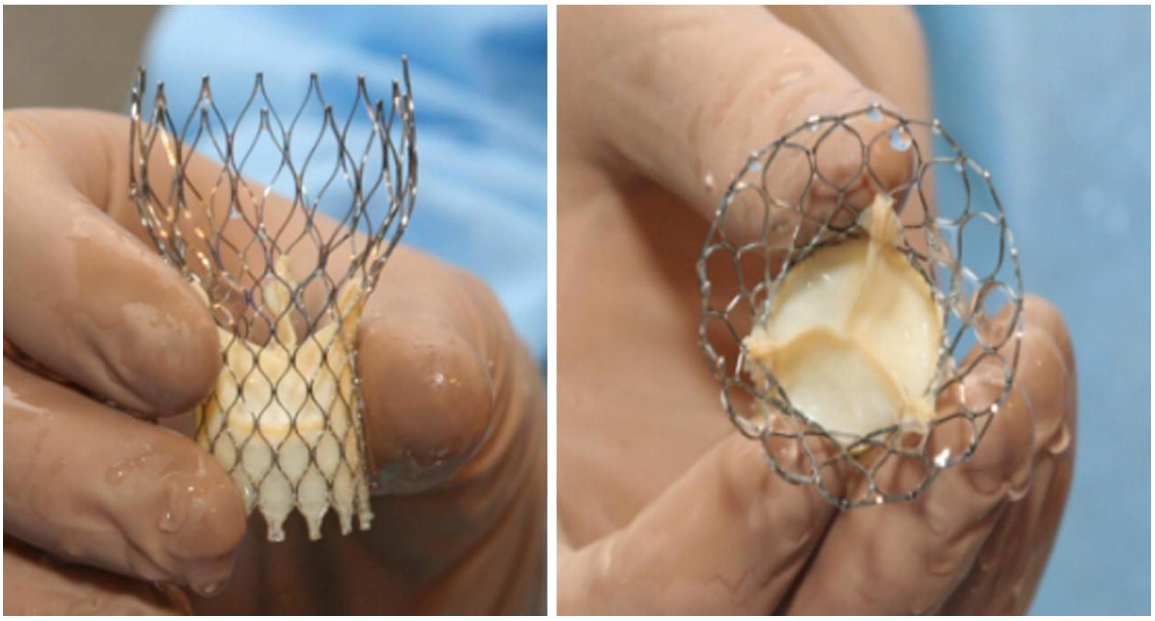

The CoreValve frame has three distinctive nitinol zones. 1) The inflow - radial force and frame elasticity are designed to maximise conformation and sealing to the native annulus. 2) Mid frame hoop strength designed to resist deformation and preserve geometry for leaflet co-aptation. 3) Outflow - Low radial force, which orients the valve to the aortic root to ensure optimal forward flow. Within the frame is attached a porcine pericardial aortic valve.

To date in early 2012 there have been approximately 20,000 Sapien™ and 20,000 Corevalve™ implantations worldwide. Both Edwards and Medtronic have ongoing large RCTs assessing the safety, efficacy and long term durability of their percutaneous valves.

1.5.1 TAVI data so far

The most robust RCT data so far published has been from the Edwards Lifesciences sponsored PARTNER trials utilising the Sapien balloon expandable valve.

1.5.1.1 PARTNER trial cohort B

Leon *et al* published the first results of the PARTNER B cohort in the New England Journal of Medicine in October 2010. 358 patients with severe aortic stenosis (AS) having been turned down for surgical replacement were randomised to either receive OMT including balloon valvuloplasty, or TAVI via the trans-femoral route. The primary end point was rate of death from any cause at one year (113).

At 1 year of follow up, the rate of death from any cause was 30.7% with TAVI, compared to 50.7% with OMT (hazard ratio with TAVI, 0.55 *p<0.001*). The rate of the composite end point of death from any cause or repeat hospitalization was 42.5% with TAVI compared to 71.6% with OMT (hazard ratio, 0.46; *p<0.001*). Among survivors at 1 year, the rate of cardiac symptoms (New York Heart Association (NYHA) class III or IV) was lower among patients who had undergone TAVI than among those who had received OMT (25.2% vs. 58.0%, *p<0.001*).

At 30 days TAVI, as compared with OMT, was associated with a higher incidence of major strokes (5.0% vs. 1.1%, *p = 0.06*) and major vascular complications (16.2% vs. 1.1%, *p<0.001*). In the year after TAVI, there was no deterioration in the functioning of the bioprosthetic valve, as assessed by echocardiogram.

1.5.1.1.1 PARTNER B Conclusion

In patients with severe AS who were not suitable candidates for surgery, TAVI, as compared with OMT, significantly reduced the rates of death from any cause, the

composite end point of death from any cause or repeat hospitalization, and cardiac symptoms, despite a higher incidence of major strokes and major vascular events.

1.5.1.2 PARTNER trial cohort A

Smith *et al* reported on the PARTNER trial cohort A in June 2011. 699 high-risk patients with severe AS were randomly assigned to undergo either TAVI with the Edwards Sapien Valve (either a transfemoral or a transapical approach) or surgical replacement. High risk was defined as patients having a Society for Thoracic Surgeons (STS) score of >10%, which correlates to predicted 10% risk of death with 30-days from the cardiac surgery (28).

The rates of death from any cause were 3.4% in the TAVI group and 6.5% in the surgical group at 30 days (p = 0.07) and 24.2% and 26.8%, respectively, at 1 year (p = 0.44), a reduction of 2.6 percentage points in the transcatheter group (p = 0.001 for non-inferiority).

The rates of major stroke were 3.8% in the TAVI group and 2.1% in the surgical group at 30 days (p = 0.20) and 5.1% and 2.4%, respectively, at 1 year (p = 0.07). At 30 days, major vascular complications were significantly more frequent with transcatheter replacement (11.0% vs. 3.2%, $p < 0.001$); adverse events that were more frequent after surgical replacement included major bleeding (9.3% vs. 19.5%, $p<0.001$) and new-onset atrial fibrillation (AF) (8.6% vs. 16.0%, p = 0.006). More patients undergoing TAVI replacement had an improvement in symptoms at 30 days, but by 1 year, there was not a significant difference between the groups.

1.5.1.1.2 PARTNER cohort A Conclusions

In high-risk patients (STS score >10%) with severe AS, transcatheter and surgical procedures for aortic-valve replacement were associated with similar rates of survival at 1 year, although there were important differences in peri-procedural risks, with major bleeding and AF being more common in the surgical approach and stroke and vascular complications being more common in the TAVI group.

1.5.2 TAVI discussion with relevance to the ATAG development

Within a decade of FIM, TAVI is now a recognised and proven treatment option in patients deemed high risk for conventional corrective surgery. Over the next 5 years ongoing studies will tell us more about the durability of these valves, and also whether they may have clinical benefit in lower risk patient groups and not just those at high risk for surgical valve replacement.

A thorough understanding of TAVI technology is vital as it is likely that the ATAG procedure will share many of the most frequent complications (vascular and stroke) and it will be interesting over the next few years to see how new devices are developed to minimise the procedural complications of the TAVI procedure (smaller sheaths, embolic filters) – some of these devices may also be suitable for the ATAG procedure.

The development of a covered ATAG may well be able to deal with and adequately treat the ascending aorta dissection flap, but the resultant AR from the dissection may need either an integrated valve within the ATAG graft (valved ATAG), or a hybrid approach using an established TAVI system following ATAG implantation.

1.6 Case reports of the ascending aorta being treated with an endovascular approach

In 2011 Sobocinski published "Endovascular approaches to acute aortic type A dissection: A CT-based feasibility study". The purpose of this paper was to determine what percentage of patients presenting with AAAD that could potentially be treated with a simple tubular endograft. Of a total of 102 patients analysed they deemed that an endovascular repair with a tubular endograft was feasible in 37 patients (36% of cohort). An additional 8 patients were also candidates for tubular endograft repair but would have required additional carotid-carotid bypass (8).

I will now review the case reports of AAAD in the literature treated by endovascular grafts concentrating on the type of graft, the sizes and the access routes utilised.

A literature review found tens of peer review journal published cases where a endovascular stent graft, designed for use in descending thoracic aortic aneurysms and type B aortic dissections, was used "off-label" to treat AAAD and aortic aneurysms / pseudo aneurysms. All were compassionate cases where the patient had no other treatment options and had been turned down for conventional surgical treatment.

There are currently at least 7 manufacturers in Europe of descending thoracic aortic stents with CE mark licensed for the endovascular treatment of the descending thoracic aorta. "Off-label", non licensed use of these devices poses a number of technical and anatomical challenges for both the device and its delivery by the interventional team.

1.6.1 Device challenges

The devices available are designed for deployment in the descending thoracic aorta, a site that is approximately 50 cm from the femoral artery sheath insertion point, often with a fairly straight run from femoral artery, through the iliac artery and retrograde up into the descending aorta. Having to manipulate the stent graft around the aortic arch and down into the ascending aorta is a large technical challenge for both the device (crimped stents can be very stiff and not want to track around the aortic arch), and for the delivery system. Not only that, but once the device and delivery system are in the "landing zone" of the ascending aorta there is the matter of accurate and precise device placement against a significant cardiac output. The landing zone is also in close proximity to the aortic valve and coronary arteries that must be avoided, and the RBCT that must be avoided distally.

1.6.2 Delivery system challenges

Over the last 5 years, with the rapid development of TAVI there has been significant innovation in both stent design, and also the manufacture of low profile, flexible, trackable delivery systems with transmitted torque for accurate positioning. There are a number of design features which have enabled better manipulation around the aortic arch and improved accuracy of deployment of TAVI at the delivery zone.

The Edwards Sapien XT^{TM} 18 F percutaneous aortic valve and delivery system have a novel "Retroflex^{TM}" feature, shown in Figure 49 below:

Figure 49 The Edwards Retroflex™ delivery system

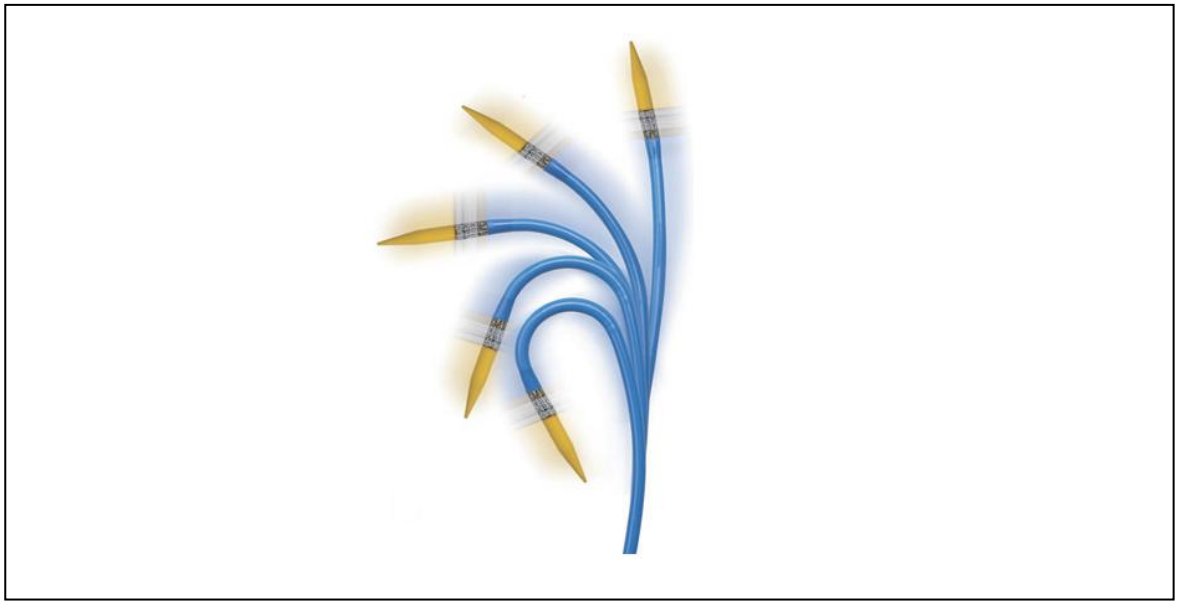

Turning a handle on the delivery system enables the catheter tip to bend and track more smoothly around the arch allowing a less traumatic passage of the device and delivery system to the landing zone of the aortic valve.

In contrast to the specially developed TAVI delivery systems, the thoracic stent graft delivery catheters are generally relatively short, and stiff. There are however case reports featuring most of the top graft manufacturers delivering grafts to the ascending aorta, and they share common anatomical features. All of the case reports published have a single intimal entry dissection flap, or aneurysmal portion of aorta in the straight part of the ascending aorta distant from both the coronary arteries, aortic valve and RBCT. An endovascular prosthesis is then delivered to the site with both proximal and distal portions apposing “relatively normal aorta”.

In one of the cases a Medtronic™ endovascular stent graft TC4646B 46 mm x 100 mm, was placed between the coronary arteries and the RBCT, to treat an aortic dissection in a 65 year old male with an intimal flap above the RCA. The patient was deemed unsuitable for open surgery however the implantation of this stent allowed the patient to

be discharged on the fifth day after the procedure and there were no subsequent complications (114).

While most cases published are technically successful at the time of procedure, there is still a considerable post procedure complication rate, morbidity and mortality. Another case utilised a Gianturco Z-stent (Cook Inc.) in a 46 year old Marfan syndrome female with AAAD with intimal flap above the RCA. However this led to severe cardiovascular complications 21 months after implantation with significant AR and impaired left ventricular function. The stent had to be removed and the heart valve replaced in a conventional manner (115).

In general the other published cases describe the use of stent grafts on average 40-46 mm in diameter and 55–100 mm in length (with the aim of not occluding the RBCT). Case reports included:

- 40 mm x 10 mm Excluder stent graft (W. L. Gore & Associates, Inc)(116)
- 55 mm x 22 mm Zenith (Cook Inc.)(117)
- 44 mm x 70 mm EndoFit (LeMaitre Vascular, Inc)(118)

One case report describes the use of a bespoke made stent:

- 46 mm x 85 mm custom stent (Jotec, Hechingen, Germany)(119)

The implantation route is generally via femoral or iliac artery access. Some cases describe more novel delivery access including trans-carotid and trans-apical

implantation, with the advantage of a shorter and straighter delivery route to the ascending aortic landing zone (29;118;120).

It is difficult to assess the true number of compassionate cases performed in the ascending aorta as well as relative success rates as there is likely to be publisher bias in that successful cases are more likely to be published hence skewing the published data. It is fair to say that as the devices become of a lower profile with more sophisticated delivery systems and with novel routes of access it is likely that we will see more "off-label" uses of thoracic aortic stents in the ascending aorta. Not only that but in the last 5 years the rapid development of TAVI has allowed us to understand the aortic valve, ascending aorta and coronary artery anatomy as well as the physiological tolerances and techniques for accurate deployment within this high risk area.

The cases described are of the most "straight forward" aortic anatomy. Routine endovascular treatment of ascending aortic syndromes will require the design of more sophisticated devices capable of conforming to a number of different anatomies and having special design features to maintain aortic valve competence, coronary artery flow, having a good proximal and distal seal, and being sized and deployed so as not to impinge on the great vessels.

1.6 Conclusion

In both AAAD and ATAA, where open surgery is not an option, and the ascending aortic anatomy is suitable; curative endovascular treatment is feasible using endografts designed for the descending thoracic aorta. Complications do however occur and in this short series appeared to be related to interruption of aortic valve function and stroke. At

present the long-term outcome is unclear, but endovascular stent treatment for AAAD is a promising option, at least for patients with multiple co-morbidities who are not candidates for conventional surgical repair.

In the future dedicated grafts like ATAG need to be developed to take into consideration the proximity of the aortic valve, coronary arteries and great head and neck vessels. Specially designed delivery systems are required to enable safe passage and accurate deployment of the graft in the ascending aorta. Embolic protection systems may be developed and deployed to minimize embolic stroke related to the device delivery.

1.7 Innovation in endovascular repair of the ascending aorta

In 2007 Tim Chuter a vascular surgeon and endovascular pioneer based in the United States published "Endovascular repair in the ascending aorta: Stretching the limits of current technology" (1). In his commentary in the Journal of Endovascular Therapeutics he describes the case reported in the same edition by Lin et al of stenting the ascending aorta to treat pseudo-aneurysm (29). He explains the theoretical advantages of the endovascular approach, but at the same time demonstrates the current limitations in the stent grafts to treat this challenging ascending aorta anatomy.

Currently available TEVAR grafts are too long, while abdominal grafts are too short and narrow. The delivery systems for these devices are also way behind in their development when compared to both the CE marked TAVI devices (Edwards Sapien Novaflex^{TM}, and the Medtronic CoreValve^{TM}). To circumvent the short comings with the

graft technology (poorly flexible grafts and rudimentary delivery systems) Lin and colleagues accessed the ascending aorta via a trans-carotid route. They shortened the nose cone (to prevent aortic valve disruption by the delivery system), and instead of delivering a bespoke or correctly sized stent grafts, instead delivered 3 x Zenith endovascular cuffs (short 32 mm stent grafts). This was only feasible in this patient because of the combination of large right carotid artery and normal size ascending aortic portion (32 mm). The stents were delivered by a 20 F delivery catheter inserted through a 22 F introducer sheath in the right common carotid artery. The problem here therefore is that if a 36 mm stent was required for example because of the more bulky size it would have required a 26 F introducer. Anything bigger in diameter would almost certainly not be feasible via the carotid route, and these sheaths (>8 mm diameter) need consideration of conduits to either the innominate artery or the iliac artery (29).

Chuter describes the ascending aorta as *"the new endovascular frontier, in which many cases of type A aortic dissection are potentially amenable to endovascular repair. However this tempting fruit will remain just beyond our reach until we have low profile stent grafts packaged within long, flexible delivery systems"(1).*

Chuter himself in collaboration with Cook Inc (Bloomington, IN, USA) is trying to develop and test a graft for ascending aorta treatment and it has a sleeve for each coronary artery. At the Royal Society of Medicine (RSM) "Aortic disease symposium" in October 2009 one of his collaborators presented a photograph of the Chuter ascending aortic prototype device, shown in Figure 50 below:

Figure 50 The Chuter ascending aorta prototype device.

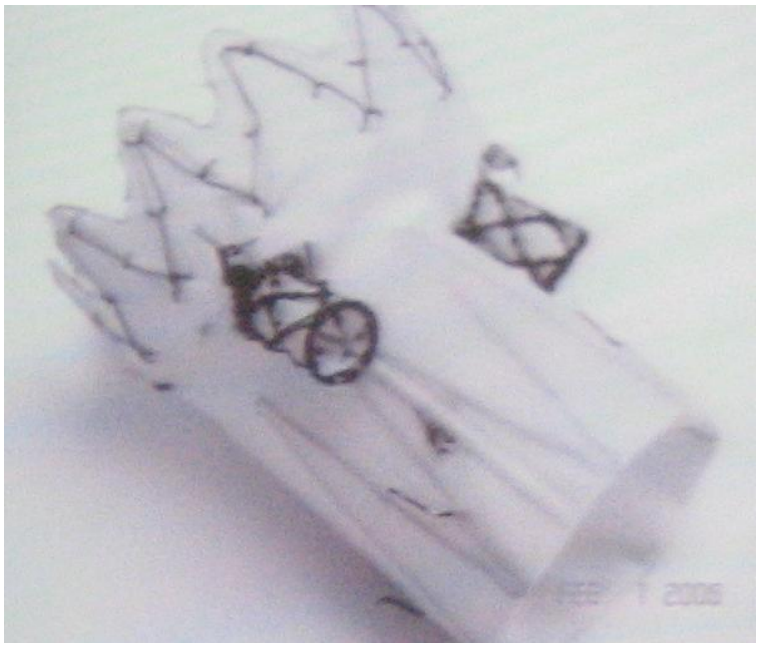

The Chuter ascending aortic stent-graft (unpublished photograph from RSM symposium) appears to have a zig-zag nitinol frame, covered in Dacron, with a proximal flare and 2 coronary Dacron sleeves.

This work is as yet unpublished, and the group do not appear to have any robust patent protection for what appears to be a “t-shirt” like stent graft with coronary projections. The stent appears to be self expanding, covered with a woven Dacron material (attached by sutures), with a significantly bulky material sewn into the coronary sleeves. As an interventional cardiologist I feel that this bulky device with a poor profile, would interfere with the aortic valve functioning (the proximal skirt appears too long), and the coronary sleeves would be extremely bulky to deliver to the coronaries and the material (a woven Dacron) is unlikely to be compatible with long term patency in the coronary sleeves (which would be a very significant failure mode). Chuter’s team described that during *in vivo* animal testing of the device in the porcine model there were no successful

implantations and cited a combination of device failures and that technically there were difficulties with the porcine model.

All of the above reinforces the facts that for successful treatment of the ascending aorta using an endovascular approach the following must be overcome:

i) The self expanding stent must be low profile, especially given the fact that the size needed to treat many aortic dissections may well be up to 65 mm in diameter (+ any over-sizing). The larger the stent graft the more bulky and greater the profile. There must be a great deal of investment in designing an aortic stent frame that has adequate radial strength characteristics, but that can be stowed within a flexible and deliverable sheath (likely to be <24 F as any size greater than this means that many patients may not have adequate sized vessels to allow stent delivery).

ii) The stent graft delivery system must be flexible and in an ideal word navigate around the aortic arch with a minimal amount of trauma. It must have predictable torque and allow precise and accurate delivery with reliable movement characteristics.

iii) The graft covering material must be biocompatible, impermeable to prevent endoleak, and to seal the dissection flap blood flow. It must be low profile, manufactured from a material which will not kink / crease, and that can be stowed to an efficient diameter when compared to the current industry standards which are Dacron and ePTFE.

iv) The delivery system and stent should not interfere with aortic valve function. If function is compromised the valve will either need to be rapidly replaced with a commercially available TAVI. The alternative is to develop a “valved ATAG” capable of treating the dissection / aneurysm, but at the same time replacing the aortic valve function.

v) The coronary sleeves must protect the coronary blood flow rapidly and have a low risk of in stent graft thrombosis. Again it is likely that given the coronary arteries are at their ostium in the range of 3-5 mm a thin and potentially novel material covering may be required that is not thrombogenic / platelet activating to retain long term patency and prevent coronary artery occlusion.

1.8 What might the future ATAG look like?

With the anatomical review completed and the pathophysiology and treatment modalities of AAAD and ATAA understood I now wanted to detail potential ATAG design features prior to formulating a 1st design specification.

1.8.1 Anatomical considerations

In keeping with all of the other endovascular treatments for vascular disease, a novel endovascular solution for ascending aortic disease should treat the disease process in a manner non-inferior to the currently accepted gold standard treatment (conventional surgery for AAAD i.e. match the 10-30% mortality at 30 days) as well as offering clinical advantages (less invasive, and shorter hospital stays). It is also conceivable that a less

invasive, percutaneous solution that avoids the need for sternotomy, CPB, deep hypothermic circulatory arrest could provide a therapeutic strategy to the 28% of all patients who present with AAAD and are denied life saving surgery because of advanced age or co-morbidities (with a 50% in hospital mortality) (67).

A broad variety of specific operative techniques will be required to combat the myriad of morphological possibilities for AAAD, driven by the original site of intimal tear(s), extension of and direction of false lumen proliferation and probably most importantly malperfusion syndromes. Proximal extension to the aortic valve or ostia of the coronary arteries requires replacement of the aortic valve or coronary artery bypass; these surgical techniques were reported in 24% and 15% of IRAD type A dissections, respectively (9).

Distal extension of the dissection beyond the replaced ascending aorta may require a hybrid endovascular procedure to seal the distal intimal tear; the optimal timing of this approach remains controversial and some experts prefer a staged approach (86;121).

1.8.2 The stent graft body design considerations

In its simplest embodiment the ATAG would consist of an appropriately sized self expanding or balloon expandable covered stent graft tube, which would be able to be deployed over the intimal tear with accuracy within the ascending aorta. It must have a landing zone proximally, opposing the aortic wall achieving an adequate seal and preventing endoleak, but at the same time not interfering with aortic valve function (if it is preserved) or coronary artery blood flow. It must also fall short of the first great head and neck vessel the RBCT.

In 2011 Sobocinski *et al.* suggested that based on CT angiography of the aorta, approximately 36% of patients presenting with AAAD could potentially be treated by a simple tubular endovascular stent graft (8). A schematic of "tubular ATAG" is represented in Figure 51 below:

Figure 51 Tubular ATAG

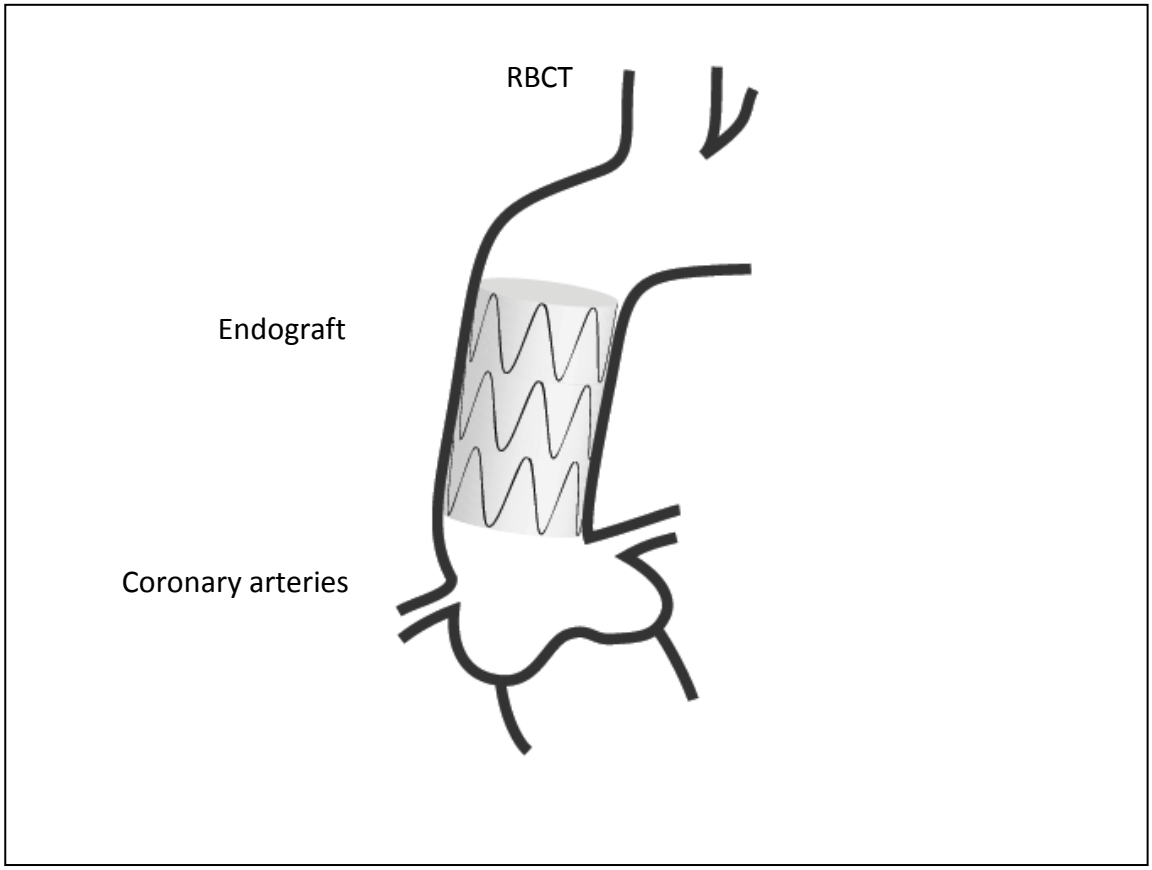

Schematic representation of a simple tubular graft from above the STJ to just before the RBCT. The tubular ATAG consists of an appropriately sized graft frame, covered in material, with a proximal seal above the coronary arteries and aortic valve, excluding the intimal tear, and a distal seal before the RBCT.

This tubular design however offers no proactive coronary flow protection, and its proximal portion is a straight edge, which if positioned slightly too low would run a reasonable risk of jeopardising coronary flow and potentially aortic valve competence. It would however

be the easiest to deploy and may suit an intimal tear within a few cm of the aortic valve with no coronary or valvular involvement – this is in essence what all of the endovascular treated AAAD case reports have demonstrated. This is likely to be the simplest embodiment of the ATAG.

1.8.3 Coronary artery protection considerations

The next consideration would be a graft capable of proactively protecting coronary artery blood flow. This could be done unilaterally; with a “sleeve” or arm into either one or alternatively an “inverted t-shirt” design with arms into both coronary arteries. While proactively ensuring coronary artery flow is a desirable device feature – it must not be forgotten that this will be technically challenging for both the device design, and deployment. Figure 52 below describes the 3 main possible coronary artery treatment solutions:

Figure 52 ATAG coronary artery design considerations

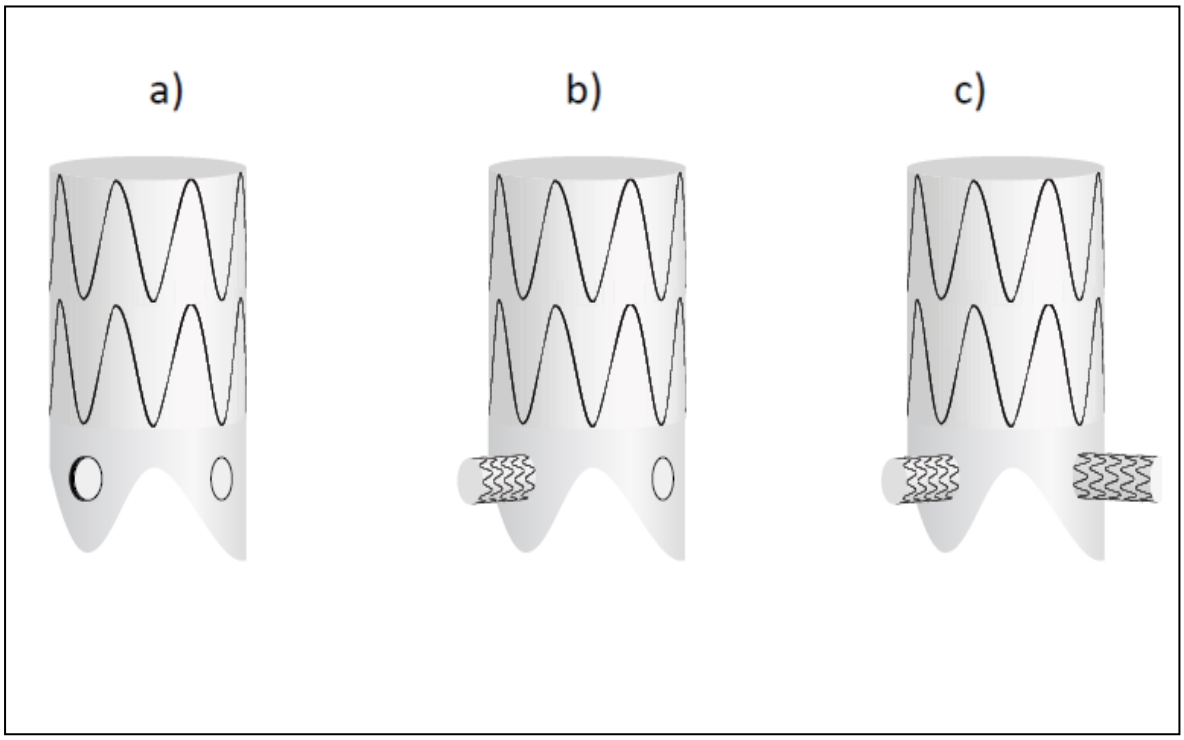

Potential ATAG coronary design considerations a) fenestrations over both coronary ostia allowing flow. b) fenestration over one ostia and a protective sleeve in the other. c) "Inverted t-shirt" graft ATAG with proactive sleeve deployment into both coronary ostia.

In the vast majority of patients the LMCA is the most important vessel, giving rise to both the LAD artery and the Cx artery, while the majority of intimal entry tears occur within 2 cm of the RCA ostium, as shown in Figure 53 below (122):

Figure 53 Site of intimal tear in Type A aortic dissection

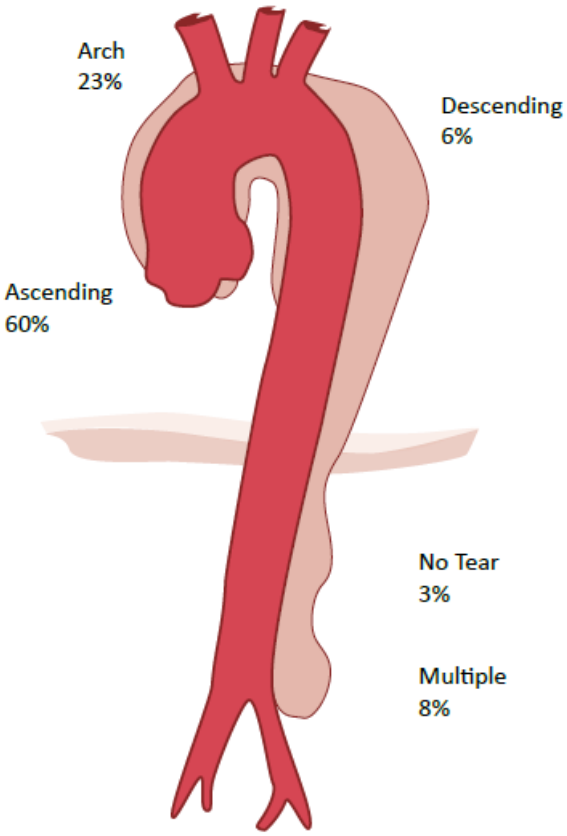

Site of intimal tear as described in the IRAD database(122). It can clearly be seen that the majority (60%) originate within the ascending aorta, 23% in the arch, 6% in the descending, and 8% have multiple tears.

One could therefore consider proactively protecting the coronary flow to the RCA (close to the site of many of the intimal tears), and have a fenestration within the graft over the ostium of the LMCA. This may allow the ATAG to protect coronary artery blood flow where the risk is greatest, but simplify the deployment process and risk to coronary artery flow disruption.

As has already been outlined much of the ATAG design specification concern is with regard to the very close proximity of the coronary arteries to the aortic valve. Figure 54 below from the Muriago paper on location of coronary orifices shows very clearly that the vast majority of coronary ostia arise within the sinus (i.e. below the STJ) (21).

Figure 54 Representation of location of coronary ostia

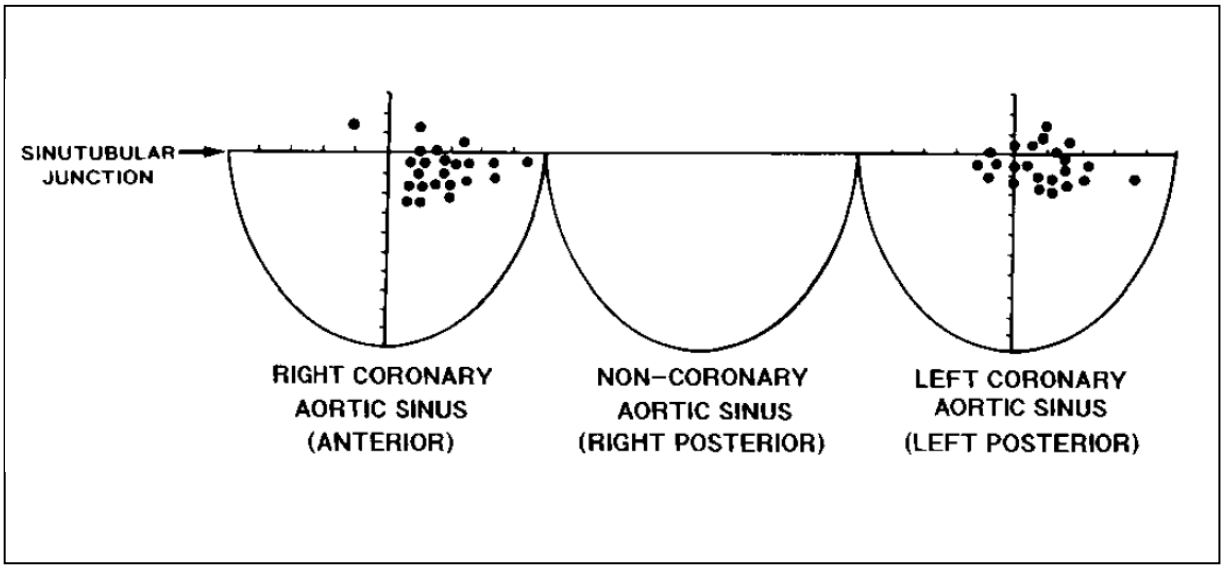

Adapted from Muriago *et al (21).* Figure shows the 3 aortic sinuses (anterio, right posterior and left posterior). RCA and LMCA orifices (dots) are not located in the centre of each aortic sinus, but instead there is a tendency for all orifices to be towards the zone of apposition of adjacent leaflets at the STJ.

If the ATAG is to proactively protect flow to the coronary arteries with a coronary sleeve or “inverted t-shirt” then this branch must come off of the main stent graft low down, and special design considerations may be required to mirror and fit the sinus anatomy so as to minimise the chance of aortic valve dysfunction. One potential consideration is the formation of a tri-lobed proximal portion in an attempt to mirror the natural sinus of Valsalva anatomy. This potential ATAG design is shown in Figure 55 below:

Figure 55 Potential ATAG design

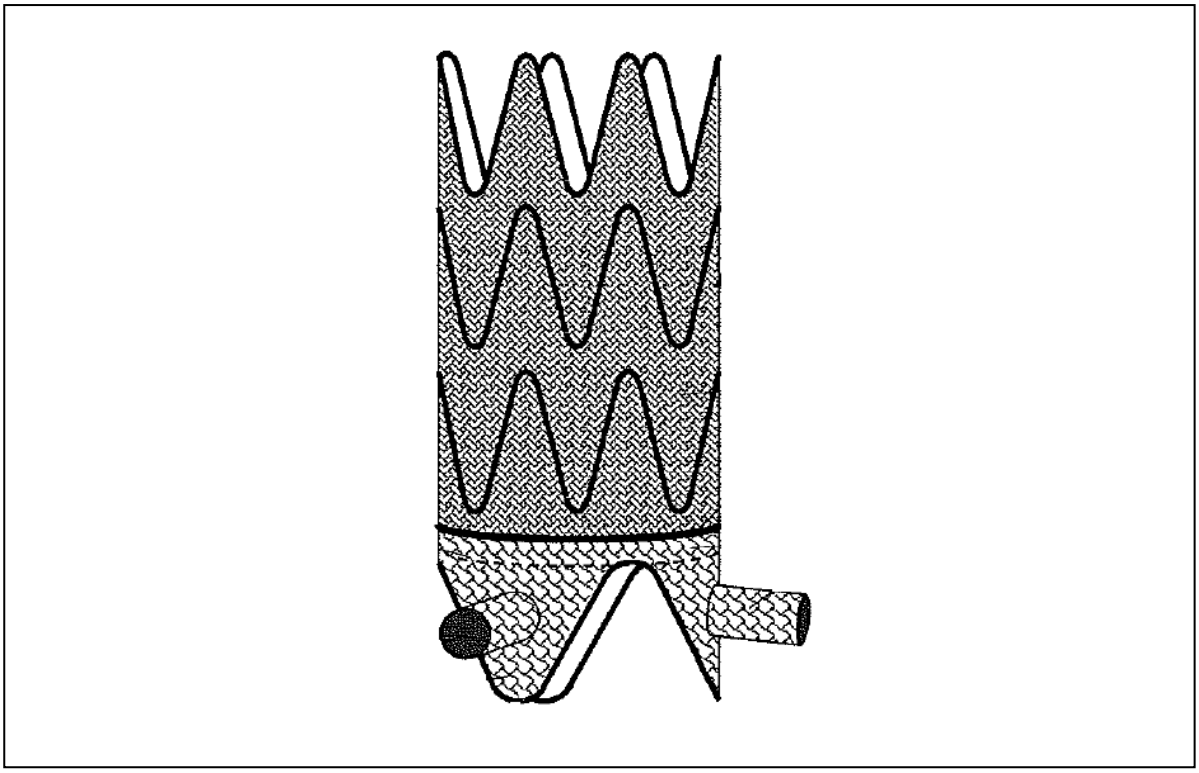

The proximal end of the ATAG device could have a tri-lobed appearance to mirror the anatomy of the sinuses of Valsalva enabling the proximal seal to conform and provide less risk of endoleak and potentially minimise aortic valve dysfunction.

Proximal end fixation is also an important consideration to enable a good proximal seal to prevent both endoleak and stent graft migration when exposed to physiological systemic pressures. Specific design features are likely to be required to enable a satisfactory proximal end "seal", whether that is in the form a "flare" or expandable ring portion - accepting that achieving a seal in this area with such proximity to the coronary arteries and aortic valve is not straight forward both from a design and procedural perspective.

If the ATAG is to proactively protect the coronary ostia with a sleeved "inverted t-shirt" then the material pushed with the stents into the coronary arteries must be as thin as possible (conventional woven Dacron material may be too thick, and its poor patency in

small vessels may be prohibitive). Any new material for this purpose must be strong, durable, biocompatible and be low profile for packing into the delivery system. It will also need to be potentially less rigid than Dacron displaying some flexibility with regard to coronary ostia position, and in small lumen diameters have less of a tissue ingression and inflammatory reaction to maximise medium to long term vessel patency.

1.8.4 Aortic valve considerations

All of the above design suggestions have been driven by the perceived need to avoid interfering with aortic valve integrity. However we know that nearly a quarter of all AAAD will have significant AR, which if the patients are treated surgically will require aortic valve replacement or repair to regain integrity (9). With TAVI rapidly gaining acceptance as a treatment strategy we have considered that after dealing with the intimal tear in the ascending aorta using the ATAG graft, one could then proceed on to deploy a commercially available TAVI to treat the AR which was either already present, or that was caused by the ATAG graft insertion. Bonhoffer *et al.* in their large series of percutaneous pulmonary valve replacements utilise a bare stent in the pulmonary outflow tract into which the Medtronic Melody percutaneous valve is implanted (123). The Seigburg group in Germany have already reported a case of iatrogenic AAAD during balloon valvuloplasty which was successfully treated by a CoreValve TAVI implantation without the need for surgery (124).

The next design and intellectual property approach is to consider integrating a functional aortic valve into the ATAG graft so that the proximal end of the valved ATAG device could be positioned either into or just above the LVOT, gaining a good proximal seal

potentially at the site of the aortic annulus (a relatively uniform size), extending through the aortic valve portion, where a new integrated aortic valve would provide valvular function, into a coronary area - giving coronary protection and then finally leading into an ascending aorta section providing intimal tear exclusion before the distal seal falling short of the RBCT.

The CoreValve^{TM} percutaneous re-valving programme has taught us important lesions that the lower we implant devices into the LVOT the greater the potential disruption of conduction in the bundle of His and the greater need for permanent pacemaker (PPM) insertion post TAVI. In the UK CoreValve registry the PPM implantation rate was 33% at 30 days post CoreValve TAVI (125). This is thought to have improved with the latest generation device and a slightly "higher" optimal CoreValve implantation position.

This aortic valve design feature was captured within our second patent filing as illustrated below in Figure 56 with an integrated valve within the ATAG device, termed the "valved ATAG". The site of proximal seal would most likely be at the level of the aortic annulus, and as the aortic valve function is being replaced there is potentially no need for the 3 feelers to fit into the natural sinus anatomy.

Figure 56 The Valved ATAG

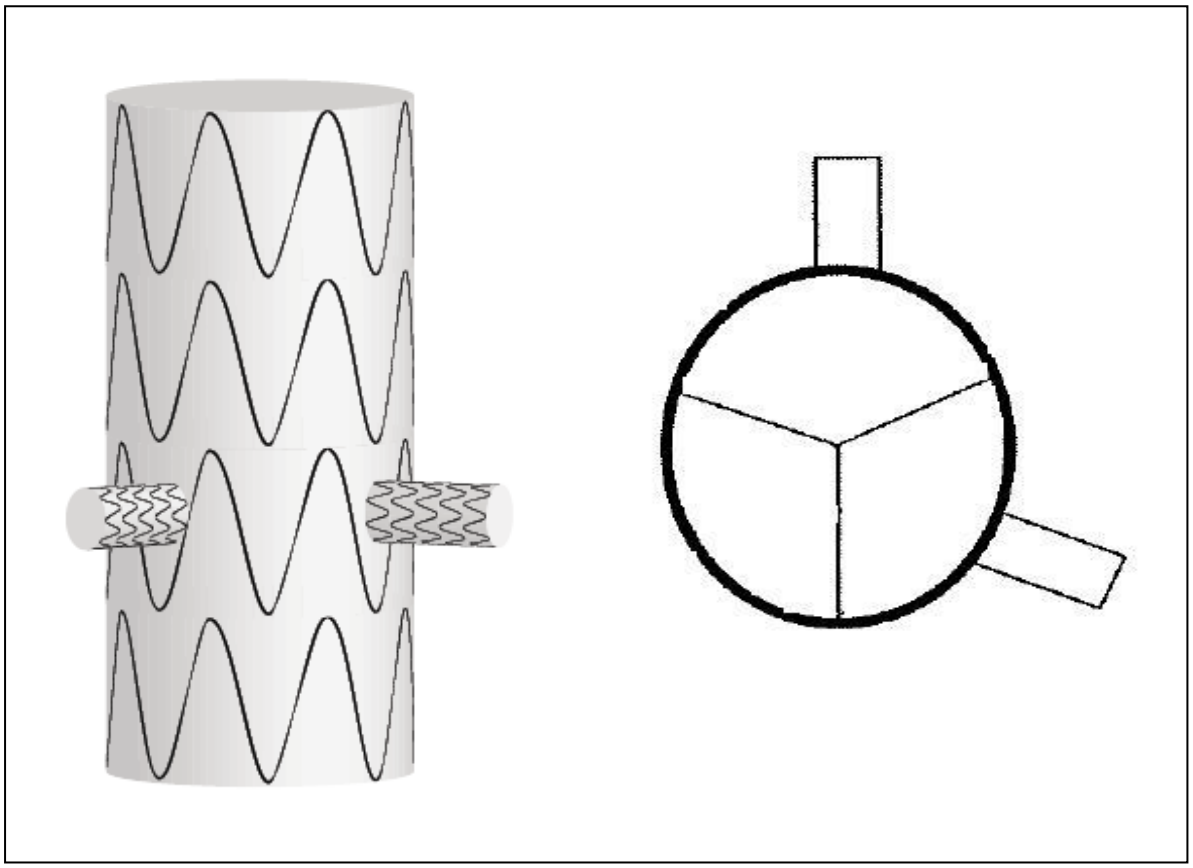

The “valved ATAG”. A proximal skirt will sit at the level of the aortic annulus forming a proximal seal. In the proximal section of the valved ATAG is a fully functional aortic valve. This leads into the coronary sleeve portions, and then into the ascending aorta endograft body.

1.8.5 Other anatomical considerations

As an interventional cardiologist I do not under-estimate the procedural challenges involved to successfully deploy an endovascular solution for acute ascending aortic syndromes. A super-imposed challenge is going to be the design of family of devices in different “off the shelf sizes”, or rapidly available to a cardiothoracic centre to enable treatment to the widest possible spectrum of anatomical variations.

Another possibility is that if the device becomes indicated for use in a more chronic and stable patient cohort then bespoke grafts could be manufactured on a patient by patient basis manufactured from 3D reconstruction information gathered from either the CT or MRI scans. This is currently the case in the descending thoracic aorta with endografts manufactured and dispatched within 6 days of order by the German based endovascular company Jotec (Hechingen, Germany).

1.8.6 Procedural considerations

It has always been the aim of the ATAG device from its very inception to be implanted using percutaneous techniques already established within the interventional cardiologist's repertoire – the aim of this to help support early adoption of the technique. One only has to look at the rapid rise in TAVI implantation rates to see that when interventional cardiologists can use existing skills, with a new device, and a significant patient benefit, adoption of the technique is extremely rapid.

ATAG can learn much from the incredible development of TAVI devices. Like TAVI the ATAG device if delivered truly percutaneously from the femoral artery must traverse the aortic arch and the delivery system must be low profile, trackable and the delivery must be precise and controllable. As the TAVI devices have evolved and become of lower profile the associated cerebro-vascular and vascular complications rates have also decreased. Both of the currently available TAVI devices utilise an 18 F delivery system and this is the profile that we are aiming for when we take ATAG into the FIM clinical trials. Achieving this goal will rely upon state of the art nitinol frame design, thin low

profile covering material, and an efficient and reliable stowing and deployment mechanism.

The device will be located into the landing zone using conventional “over the wire” techniques that all cardiologists are very comfortable with. Again we do not underestimate the potential challenges of delivering a graft device potentially with 2 coronary arms, and therefore up to 3 guidewires in total. The guide wires are likely to have specific design requirements to enable stability; the device, and the procedure will require meticulous guide wire care so as to avoid “wire wrap” and tangling as delivery will be impossible if this were to occur.

We anticipate that during the early FIM trials patients are likely to be under a general anaesthetic (GA), although again in a situation similar to that of TAVI after experience has been gained it may be a procedure that can be performed under conscious sedation avoiding all of the haemodynamic and respiratory risks of GA in this very sick patient cohort. Other shared features with TAVI programmes are that the ATAG will be best implanted by a “Heart team”, with interventional cardiologist, cardio-thoracic surgeon, imaging cardiologist, cardiac anaesthetist, endovascular specialist within a hybrid catheter laboratory under fluoroscopy with the aid of either intra-cardiac echo (ICE) or TOE.

Even if the procedure is successful at the time of implantation there will be many clinical and regulatory questions that must be answered and this information must be constantly collected during the development programme. What is the long term durability of the graft material? What is the durability of any integrated aortic valve? What is the percentage endoleak rate? Will the graft be prone to thrombosis? What is the coronary

sleeve patency long term? What is the optimal anti-platelet / anti-coagulation protocol for the ATAG device? How will we follow these patients up?

While currently we are not in a position to answer any of these questions we must be continuously collecting scientific data so that when the *in vivo* and FIM trials do arrive we are in a position to give our opinions and evidence based answers.

Chapter Two

Novel CT and MRI anatomical data collection in AAAD and ATAA

Chapter Two: Novel CT and MRI data

2.0 Novel CT and MRI anatomical data in AAAD and ATAA

In the previous chapter I have set the landscape in which ATAG is being developed. The endovascular field is one that is fast moving, and much of the practice seems consensus and registry data driven. I hope I have outlined the clinical problem of ascending aortic pathology, the current treatment modalities and their deficiencies.

Since 2007 TAVI has become more widespread and as interest has grown there has been an exponential growth in the anatomical literature relating to the aortic valve, coronary arteries and ascending aorta. Most data however focuses understandably on the TAVI patient cohort, and while this is interesting, very little still exists on either the AAAD or ATAA populations with similar details concerning aortic valve size, competence, coronary take off and angulation, and ascending aortic size.

In 2008 to enable design of our ATAG graft within our target population required the collection of novel anatomical data. To access sufficient numbers of these patients and the expertise to analyse CT and MRI images required collaboration with other institutions.

I collaborated with Professor Salah Qanadli an interventional radiologist at CHUV Hospital, Lausanne, Switzerland to measure anatomical variables in a 9 patient AAAD cohort that he had collected over 4 years. Accepting the limitation of small sample size I

felt that at the time in the absence of robust published data on the subject this would give me a tangible understanding of anatomical sizing and coronary angulation in this patient group.

I also collaborated with Dr Raad Mohiaddin CMR consultant at the Royal Brompton Hospital who has a large cohort of patients with Marfan syndrome ATAA which he follows up. There is a paucity of data on ATAA aortic size, aortic valve AV competence, coronary size and take off angulation, and if ATAG is going to be a potential treatment modality for ATAA in Marfan syndrome then devices need to be able to conform and treat the corresponding anatomy.

2.1 Aortic dimensions and coronary angulations measured in a 9 patient cohort presenting with AAAD

2.1.1 Study purpose

A retrospective pilot study to measure aortic dimensions by CT angiography evaluated on true lumen 2D centre line based reconstructions, 3D and multi-planar reconstructions (MPR) at multiple levels in the aorta as described by O'Neill *et al.* to help understand aortic and coronary anatomy in a patient population presenting to hospital with a diagnosis of AAAD *(126).*

2.1.2 Methods

2.1.2.1 Study Cohort

A total of 9 consecutive patients presenting to CHUV hospital in Lausanne, Switzerland between January 2007 and December 2010 with signs and symptoms of AAAD confirmed on CT scanning made up the study group.

2.1.2.2 CT cardiovascular imaging

All subjects were imaged using GE CT scanners within the CHUV radiology department. CHUV has a number of CT scanners and during the study period these were updated. As a result the temporal resolution and the speed of the scan generally improved with

time, the early scans being performed on a 16 slice CT, and the latest scans on a 64 slice GE CT scanner. None of the CT scans were ECG gated.

CT scans where collected from the archive and anonymised. Scans were reformatted using a GE Medical System Advantage Windows Workstation with version 4.3 software.

3.1.2.3 Measurements

The following patient characteristics in Table 9 below were collected:

Table 9 Patient characteristics

Age
Gender
Hypertension
Diabetes
Hyperlipidaemia
Smoking
Confirmed connective tissue disease / family history of connective tissue disease

Aortic measurements of aortic diameter and lengths are shown in Figure 57, and Table 10 below:

Aortic measurements (TK / SP supervised by SDQ)

Figure 57 Showing ascending aortic diameters and lengths measured

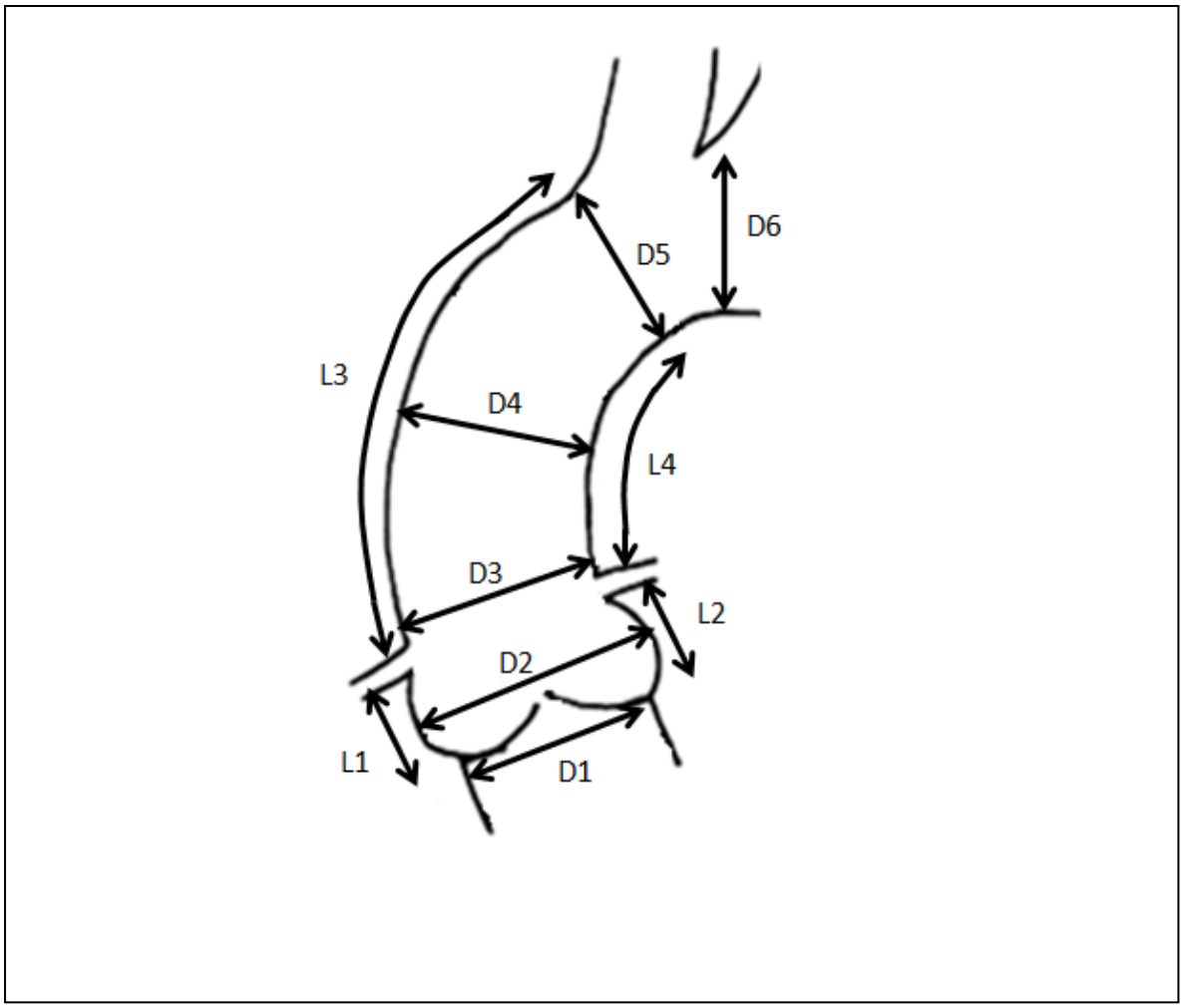

For all diameters a maximal and minimal measurement were made. D1 – annulus diameter, D2 – Sinus diameter, D3 – STJ diameter, D4 – Mid ascending aorta diameter, D5 – Diameter just proximal to RBCT, D6 – Mid aortic arch diameter. L1 – Length from annulus to RCA, L2 - Length from annulus to LMCA, L3 – Length from RCA to RBCT, L4 – Length from LMCA to point opposite RBCT,

Table 10 Aortic diameters and lengths measured

Number of aortic cusps
D1a Maximal annulus diameter (mm)
D1b Minimum annulus diameter (mm)
D2a Maximal sinus of valsalva measurement (cusp to cusp mm),
D2b Minimum sinus of valsalva measurement (cusp to cusp mm)
D3a Maximal sinotubular junction diameter (mm),
D3b Minimum sinotubular junction diameter (mm),
D4a Maximal mid ascending aortic diameter,
D4a Minimum mid ascending aortic diameter,
D5a Maximal diameter of aorta at RBCA,
D5b Minimum diameter of aorta at RBCA,
D6a Maximal mid aortic arch diameter (mm),
D6b Minimum mid aortic arch diameter (mm),
D7a Maximal descending aortic diameter (mm),
D7a Minimum descending aortic diameter (mm),
D8a Left Iliac artery maximal diameter (mm)
D8b Left Iliac artery minimum diameter (mm)
D8c Right Iliac artery maximal diameter (mm)
D8d Right Iliac artery minimum diameter (mm)

Table 10 Aortic diameters and lengths measured cont.
D9a Left femoral artery maximal diameter (mm)
D9b Left femoral artery minimum diameter (mm)
D9c Right femoral artery maximal diameter (mm)
D9d Right femoral artery minimum diameter (mm)
D10 Distance from annulus to site of intimal dissection tear (mm)
S1 Site of end of dissection flap
L1 Annulus to right coronary ostium (RCA mm),
L2 Annulus to left main stem coronary artery (LMCA mm),
L3 Length RCA to RBCA (mm),
L4 Length LMCA to RBCA (mm),

Coronary artery angulation measurements recorded are demonstrated in Figure 58 below:

Figure 58 Coronary artery ostia angle from aorta

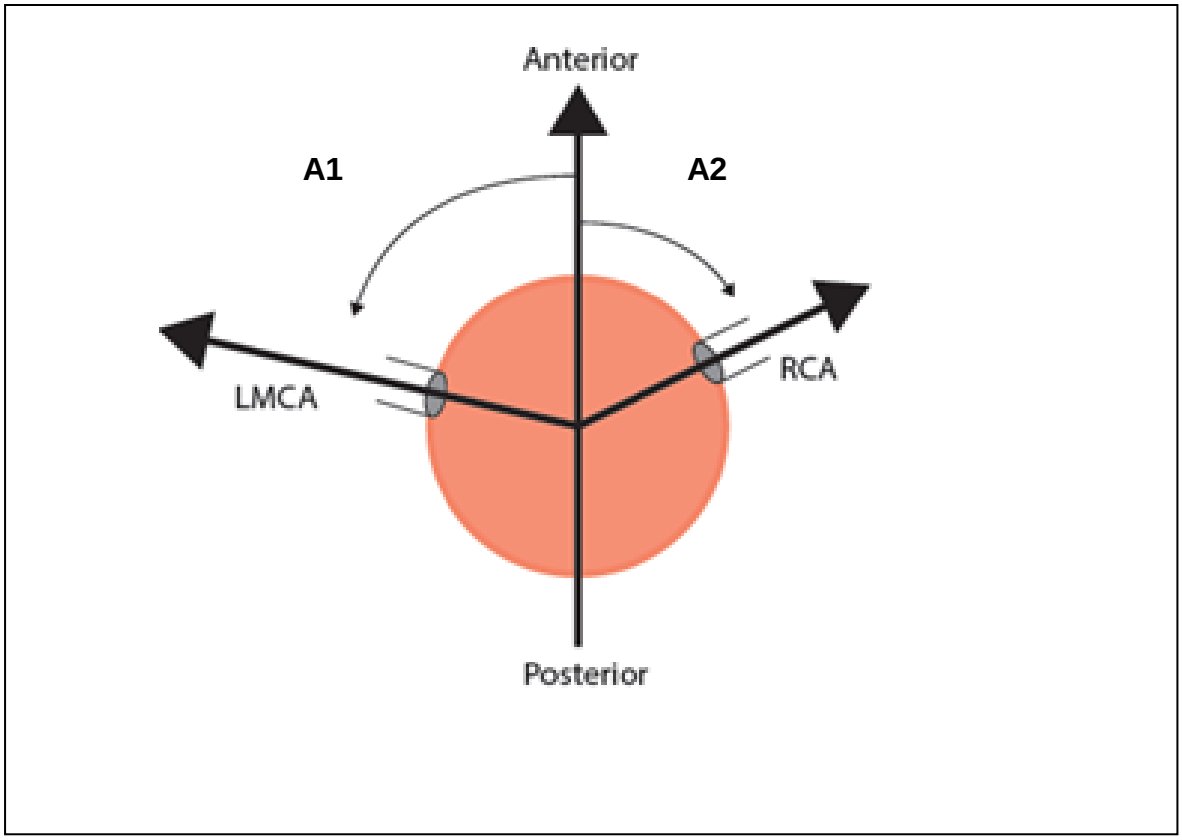

Coronary angle measurement with AP direction at 0 degrees. **A1** Angle of origin of the LMCA from aorta (degrees from AP), **A2** Angle of origin of RCA from aorta (degrees from AP), **A3** Delta angle between RCA and LMCA

2.1.3 Results

2.1.3.1 CT scanning information

One patient was scanned with a 5 mm thickness slice (least accurate), 2 patients with a 2.5 mm slice, 5 with a slice thickness of 1.2 mm, and one patient 0.6 mm. All scans were of adequate resolution and quality to make the desired measurements.

2.1.3.2 Patient demographics

The 9 patient cohort comprised 5 males and 4 females. The mean age was 64.8 +/- 12.8 years, (range 44-85). 3 patients were active smokers (33%), 1 patient (11%) was an ex-smoker, and 5 (55%) were non smokers. 8 of the 9 patients were hypertensive (89%), none suffered with diabetes, and 2 (22%) were known to be hyperlipidaemic prior to presentation. None had a known inherited connective tissue disorder.

2.1.3.2 Aortic Valve

All patients had 3 aortic valve cusps – there were no patients with a BAV.

Table 11 below shows the aortic dimensions:

Table 11 Dimensions in the 9 patient AAAD cohort

Parameter	Mean (mm)	Range (mm)	SD (mm)
D1a Max annulus diameter	27.4	24.4 - 31.3	2.1
D1b Min annulus diameter	22.7	19.0 - 26.2	2.8
D2a Max sinus diameter	33.3	29.5 - 41.1	4.2
D2b Min sinus diameter	24.9	20.2 – 28.7	3.6
D3a Max STJ diameter	43.1	31.4 – 56.6	7.7
D3b Min STJ diameter	40.2	26.9 – 54.4	8.4
D4a Max mid AA diameter	45.4	27.8 – 57.8	10.9

Table 11 Dimensions cont.	**Mean (mm)**	**Range (mm)**	**SD (mm)**
D4b Min mid AA diameter	41.6	24.9 – 51	8.9
D5a Max diameter Ao RBCA	45.6	33.8 – 63.3	9.7
D5b Min diameter Ao RBCA	40.9	28.4 – 58.2	9.8
D6a Max mid A Arch diameter	36.4	27.8 – 59.9	9.6
D6b Min mid A Arch diameter	30.9	25.8 – 34.5	2.8
D7a Max desc Ao diameter	32.9	25.3 – 40.1	5.1
D7b Min desc Ao diameter	31.5	24.7 – 39.9	5.0
D8a Max L iliac diameter	15.5	11.7 – 23.4	3.5
D8b Min L iliac diameter	14.9	9.9 – 16.3	6.6
D8c Max R iliac diameter	14.5	9.4 – 26.9	5.8
D8d Min R iliac diameter	12.8	8.4 – 15.6	4.2
D9a Max L femoral diameter	9.5	6.4 – 13.2	2.1
D9b Min L femoral diameter	8.6	5.9 – 11.7	1.9
D9c Max R femoral diameter	10.3	7.5 – 13.5	2.1
D9d Min R femoral diameter	8.5	6.2 – 11.2	1.9
D10 Distance from annulus to site of intimal tear	28.0	12 – 49.9	18.2
L1 Annulus to RCA	23.0	16.9 – 40.4	7.1
L2 Annulus to LMCA	23.8	20.1 – 30.2	2.9
L3 Length RCA to RBCA	64.6	23.6 – 100.6	19.8

Table 11 Dimensions cont.	**Mean (mm)**	**Range (mm)**	**SD (mm)**
L4 Length LMCA to RBCA	33.1	18.2 – 59.1	12.5
A1 Angle of origin of the RCA from aorta	-51.0	-84.1 to -26.5	18.8
A2 Angle of LMCA from aorta	111.5	78.5 to 137.4	22.3
A3 Angle between RCA and LMCA	162.5	131.6 to 201.8	27.5
S1 Site of end of dissection false lumen			
Femoral artery	3 / 9 (33%)		
Iliac artery	2 / 9 (22%)		
Aortic arch	2 / 9 (22%)		
RBCT	1 / 9 (11%)		
Distal descending aorta	1 / 9 (11%)		

2.1.4. Conclusions

Any conclusions that are drawn from this CT analysis must be tentative as the sample size is small (n=9). The difficulty with AAAD is that it is relatively rare and as such finding scans of adequate quality to assess can be difficult. I do think that this data does give us some understanding of the aortic sizes and in particular looking at the coronary orientation and the peripheral access vessels.

The mean age of this cohort (64.8 years) is similar to that reported in the IRAD database of 62 years. In this small group we had a slight predominance of males (55%) compared

to IRAD of 68%. 8 of the 9 (89%) patients had a known history of hypertension compared to the IRAD literature which suggests figure of 67%. (64;88;127;128)

The mean aortic annulus measurement is essentially normal at 25 mm **(normal = 24.5 mm)**, as is the mean diameter at the level of the sinuses 29.1 mm **(normal = 32 mm).**(129)**.** The STJ dilates to 41.65 mm **(normal = 29.7 mm)**, with corresponding mean mid ascending aortic diameter dilated at 43.5 mm **(normal = 32.7 mm)** (11). This is in very close agreement with the data from Neri *et al.* which in a much larger dissection cohort had a mean ascending aortic size of 41 mm (89). Parish *et al* using TOE measurements calculated a mean aortic diameter of 53 mm (87).

The aorta remains significantly dilated at the level of the RBCT at 43.5 mm, the level of the mid-point of the aortic arch at 33.6 mm, and at the descending aorta at 32.2 mm.

In this AAAD cohort the mean distance from the annulus to the RCA was 23 mm **(normal = 19.3 mm)**, and to the LMCA was elongated at 23.8 mm **(normal = 12.1mm)** (11). The angle between the origin of the RCA and the LMCA from the aorta was 162.5 degrees **(normal 154 degrees)**(24)**.** The angle between the orientation of the RCA and the LMCA had a standard deviation of 27.5, with 2 real outlying values. The lowest angle was 110 degrees and the largest was 202.

An important feature if we are to treat AAAD by percutaneous means is to ascertain the diameter of the access vessels i.e. the femoral and iliac arteries. Although calcification and tortuosity were not assessed in this study the diameter assessment showed a mean left common iliac artery diameter of 15.2 mm, common right iliac artery 13.6 mm, common left femoral artery diameter 9.1 mm and common right femoral artery calibre of

9.4 mm. All patients had a femoral artery diameter of >7.5 mm, which will comfortably accommodate an 18 F arterial access sheath.

Worthy of note is that in 3 patients the false lumen extended down to the femoral artery, and a further two down to the level of the iliac artery. It will be vitally important at the time of sheath implantation for ATAG delivery that the true lumen is selectively cannulated.

Discussion with regard to ATAG design specification for AAAD

This small pilot study has allowed me to measure accurately the aortic diameters, and discern the relationship between aorta, coronary arteries and aortic valve, in order to further develop the ATAG design specification. It must always be borne in mind that this is a small cohort with the inherent errors associated.

That said, the aortic diameter data is very much in agreement with the literature available from larger series, and the aortic diameter and peripheral vessels suggest a diameter that in the most part will accommodate a large sheath for ATAG device delivery.

Looking at specific mean aortic diameters, Figure 59 shows the mean aortic diameters from the AAAD cohort:

Figure 59 Mean AAAD aortic diameters at specific landmarks

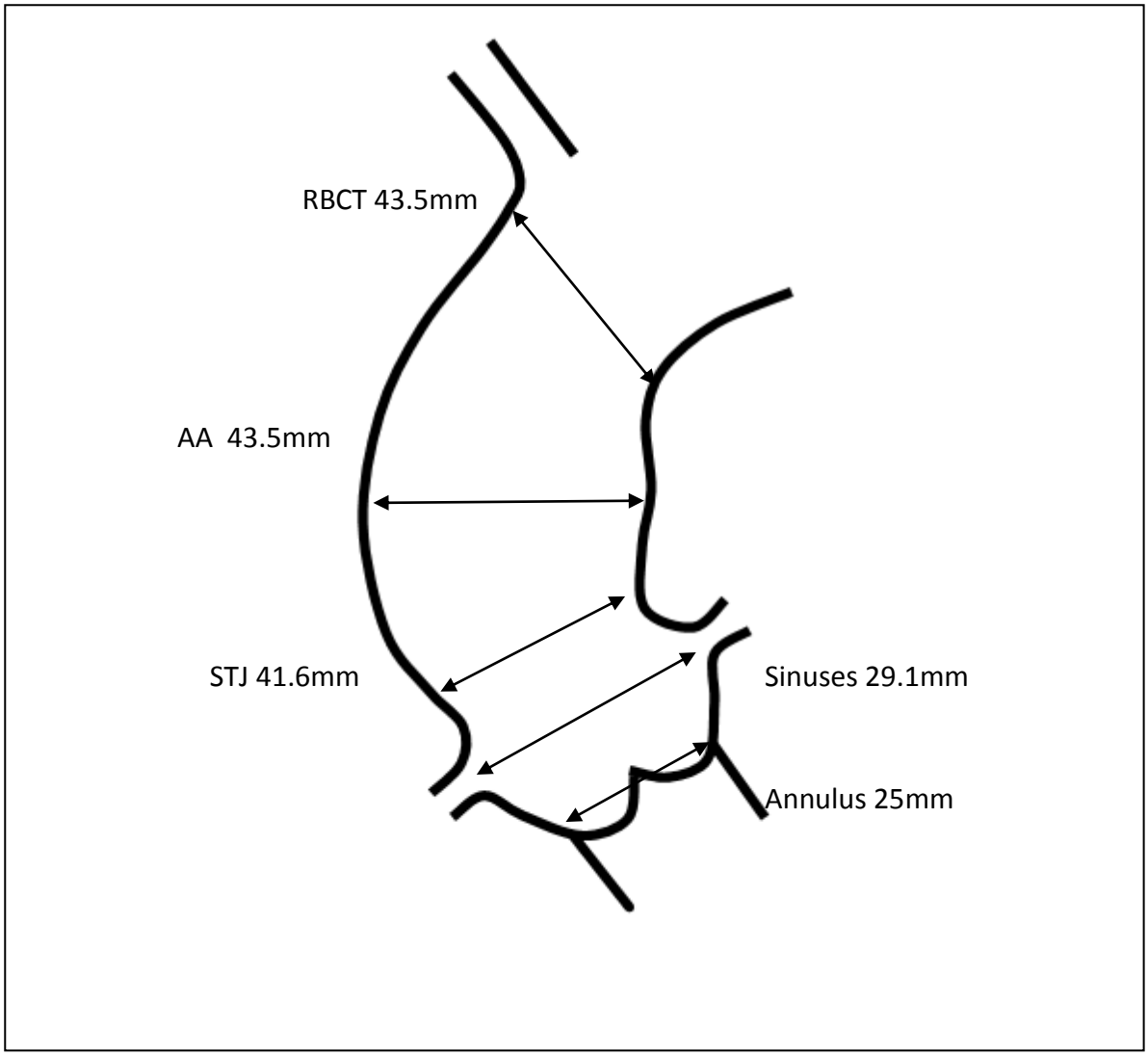

The AAAD cohort seems to have maintenance of normal aortic diameter at the level of the aortic annulus and sinuses. The STJ, ascending aorta and aorta at the level of the RBCT are all dilated at a mean diameter of 41.6 mm, 43.5 mm and 43.5 mm respectively.

This has important implications for ATAG design. If we are just to implant a simple tubular endograft as postulated by Sobocinski to treat at least one third of all patients then the endograft will be a uniform tube of around 40mm plus approximately 20% over-sizing (8).

If we are to design our ATAG as a t-shirt with one or more coronary branches then the proximal end will need to "cone down" to approximately 30 mm within the sinuses plus over-sizing. If the proximal landing zone is to be the aortic annulus as with the proposed "valved ATAG", then the proximal portion will measure 25 mm +/- over-sizing. If the valved ATAG would to be implanted at this site there is a clear consensus as to annulus measurements and sizing from TAVI experience and this is device specific. Our valved ATAG device is likely therefore to have a similar sizing protocol to the nitinol framed self-expanding CoreValve^{TM} revalving system (Medtronic, Santa Rosa, CA, USA).

The coronary angle data is novel and suggests a mean angle between RCA and LMCA of 162.5 degrees relatively similar to that seen in normal human aortas (154 degrees). As well as requiring ATAG main body grafts in different sizes we may also consider the need for proximal portions with different coronary angulations. As with any device it is important we are able to treat the majority of patient anatomies with this disease process, but there will always be patients particularly with the first device iteration that have anatomy beyond the realms of a device – the important thing is to understand the anatomical needs of the patient and treat as wider range of patients as is possible with the smallest possible range of off the shelf products. It is clear that to cover and treat both coronary ostia with a true "t-shirt" graft, the coronary sleeves must have some flexibility to treat a variety of angulations, and bench testing will elucidate the degree of angulation that the ATAG can comfortably treat.

The degree of AR was not assessed in this study, and this is something that I will seek to analyse from both TTE and TOE performed at the time as it has important implications as to the type of curative surgical or percutaneous procedure required (i.e. TAVI, or valved

ATAG). It is also likely that we will extend our pilot to more patients within the CHUV, so that we might get more of a wealth of reliable data to publish these findings – at the moment from this pilot the numbers are simply too small.

2.1.5 Recent data published on AAAD aortic size

The CHUV AAAD anatomical data were accumulated in 2010 while I was an interventional fellow on exchange in Switzerland. In 2011 Sobocinski published subsequent data in a larger group of patients outlining some very interesting anatomical measurements from a group of 102 patients presenting with AAAD (8). This paper represents the most current and detailed assessment of aortic anatomy in AAAD and is highly relevant to the design of ATAG, and as such I will now proceed to summarise Sobocinski's findings.

102 patients were enrolled across 5 centres in France with a clinical and CT diagnosis of AAAD between 2006 and 2009. Pre-operative CT scans were analysed and aortic measurements performed by 2 experience endovascular surgeons. Echocardiography was also performed on all patients to assess the degree of AR.

Mean age of patients enrolled was 64 years (36-85 years). 70% of patients were male, 71 % having a history of hypertension. Of the 102 patients enrolled in the study, 77% had a Debakey type I, 18% type II, and 5% retrograde type III. The Debakey classification is briefly described in Figure 60 below:

Figure 60 Debakey classification of aortic dissection

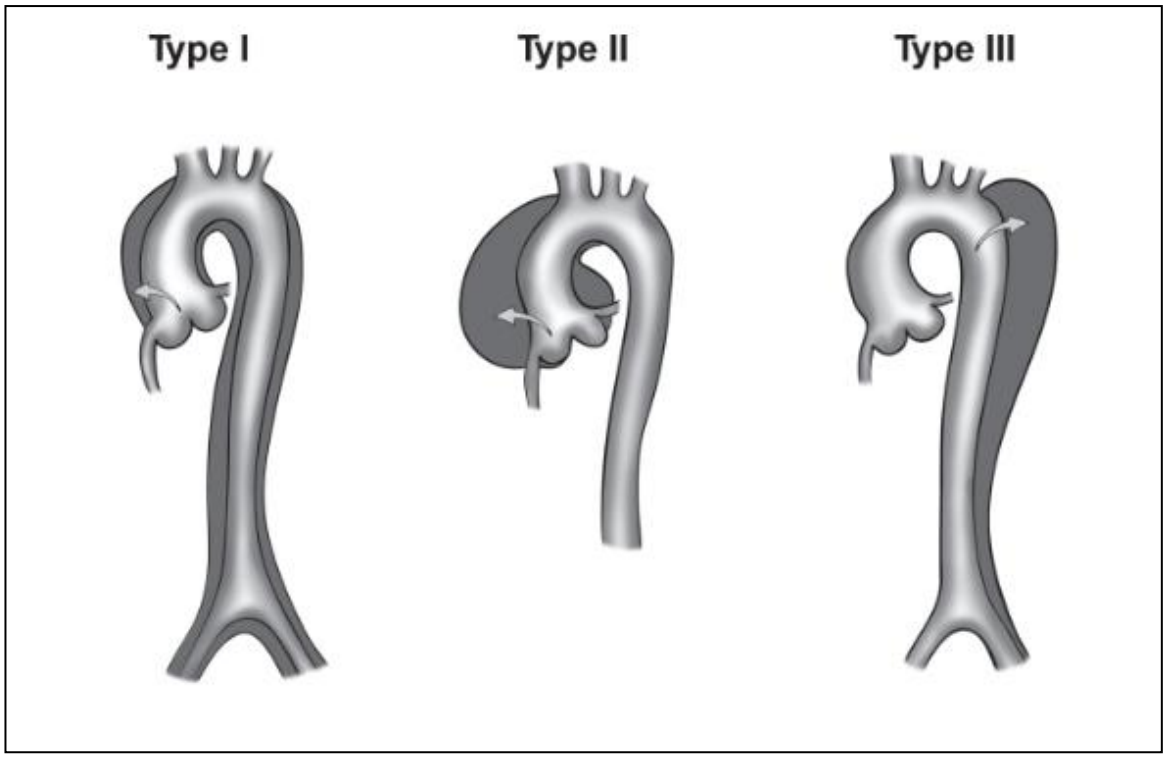

Type I – Originates in ascending aorta, propagates at least to the aortic arch and often beyond it distally. It is most often seen in patients less than 65 years of age and is the most lethal form of the disease. **Type II** – Originates in and is confined to the ascending aorta. **Type III** – Originates in descending aorta, rarely extends proximally but will extend distally.

Aortic regurgitation

44% of patients on echocardiography had no AR, 23% had grade I AR, 20% grade II, 8% grade III and 5% grade IV.

Operation performed

An ascending aorta replacement, a Bentall procedure and a Tirone-David procedure were performed in 70%, 29% and 1% of patients respectively. An aortic valve repair or

replacement was performed in 35% of patients. The mortality at 30 days was 24%. Table 12 below shows the aortic anatomical data (8).

Table 12 Sobocinski AAAD cohort anatomical data

	Mean diameter (mm)	Range (mm)
Aorta 15 mm above coronary (=STJ) True	38	22-78
Aorta 15 mm above coronary (=STJ) Total	46	28-93
Aorta diameter at RBCT True	35	19-67
Aorta diameter at RBCT Total	42	27-61
Distance from distal coronary to RBCT	85	40-130
Distance from distal coronary to Entry tear (ET)	28	0-128
Distance from ET to RBCT	59	0-118
Dissection extension length	373	20-699

The intended focus of the Sobocinski paper was to act as a CT based feasibility study to determine theoretically the proportion of patients presenting with AAAD in whom it might be possible to implant a tubular endograft between the coronary arteries and the RBCT to occlude flow into an ascending aortic entry tear. The goal of such an intervention in AAAD is to cover the entry tear redirecting the entire flow into the true lumen and therefore enabling the false lumen to collapse or even thrombose. Even if there are

multiple tears, simply covering the most proximal one is often sufficient to initiate remodelling and reverse malperfusion conditions.

This feasibility analysis suggests that 36% of patients presenting with AAAD may be able to be treated with a simple tubular endograft. A further 8% may be able to be treated the same way so long as they have an extra-anatomical bypass in case the endograft compromises the RBCT because of close proximity. These figures probably represent a conservative estimate given that criteria for feasibility included having a landing zone 20 mm from both the coronary arteries and the RBCT. The maximum true lumen size considered for endograft placement was 38 mm, given that currently the largest commercially available stent graft is currently 46 mm (i.e. taking into consideration a 20% over-sizing).

35% of patients required aortic valve repair or replacement because of echocardiographic Grade II – Grade IV AR. These data are in agreement with the larger IRAD database and suggest that to treat these patients adequately will require either TAVI following endograft treatment, or a valved ascending aortic endograft as proposed by the “valved ATAG”.

This paper also provides the most robust, in-depth analysis of entry tear location and the associated diameters of the aorta and great vessels in patients presenting with AAAD, and will help us in combination with our own and other published data to make the ATAG design specification.

Conclusions relevant to the formulation of ATAG design specification:

i) A simple tubular endograft covering the entry tear, with a 20 mm landing zone between both the coronary arteries and the RBCT will be suitable to treat 36% of patients presenting with AAAD (8).

ii) Up to 35% of patients presenting with AAAD are likely to require valve repair or replacement, so an endovascular solution for these patients will require either a commercial TAVI implantation following endograft insertion, or a valved ATAG endograft.

iii) The mean true lumen sizes in this cohort were 38 mm at the STJ, and 35 mm at the origin of the RBCT. Current commercially available endografts for the descending aorta have a maximal size of 46 mm, and as such if we are to treat the majority of AAAD with an endograft (taking into account the standard 20% over-sizing) we may well need to design and develop larger grafts which may pose technical challenges with crimping as well as delivery system size.

iv) The mean distance from the distal coronary artery to the RBCT is 85 mm (range 40-130). We will clearly need a variety of “off the shelf” endograft diameters and lengths. It is also possible that in keeping with practice in the descending aorta “extension cuffs” could be used at the distal end to ensure adequate coverage, but overlap and fall short of the RBCT.

2.2 A CMR investigation of the aortic anatomy of 62 patients with Marfan's syndrome and ATAA

There is little published data concerning ATAA coronary and aortic valve orientation and function. To understand this area better I collaborated with the largest Marfan syndrome patient group in the UK, based in London at the Royal Brompton Hospital and St Georges Hospital.

Dr Raad Mohiaddin is a Consultant MRI Cardiologist at the Royal Brompton Hospital, and he runs the MRI follow up service of the population with Marfan syndrome within this quaternary service. He has approximately 150 patients in annual CMR follow up, 62 of which have a dilated ascending aorta / ATAA.

Dr Anne Child is a clinical geneticist with an interest in Marfan Syndrome and forms part of the multi-disciplinary team managing all patients in Marfan syndrome follow up. She is based at St George's Hospital.

Professor Ho is a cardiac morphologist based at the Royal Brompton hospital.

I wrote the measurement protocol, but I received advice and support from all the collaborators listed above.

2.2.1 Study background

Aortic root size has important prognostic implications in patients with Marfan syndrome (130). Accurate measurements and follow up of the aortic diameters of patients with Marfan syndrome are required for informed decision making on the timing and nature of surgical treatment to the aortic valve and root.

Cardiovascular magnetic resonance (CMR) is becoming increasingly available, and has the clear advantages over CT scanning of clear visualisation with freedom from ionising radiation. It has become the gold standard for monitoring of aortic root dilatation providing guidance as to the prospective timing of prophylactic aortic root intervention.

CMR has many advantages, allowing cine image acquisition of the aorta and re-construction and measurements in any plane.

2.2.2 Study purpose

The purpose of this study was to measure aortic dimensions by CMR using planes transecting, as well as aligned with the axis of the aortic root to help understand aortic and coronary anatomy in a Marfan syndrome population with dilated aortic roots.

2.2.3 Methods

2.2.3.1 Study Cohort

Sixty-two patients with confirmed Marfan syndrome and dilated or aneurysmal aortas made up the study cohort, all patients were being actively followed up at the Royal Brompton Hospital, London.

2.2.3.2 Cardiovascular Magnetic Resonance

All subjects were imaged using a 1.5 Tesla system (Siemens Sonata, Erlangen, Germany). Images were acquired using Royal Brompton standardised aortic follow up protocol. The cardiac and standard aortic measurements were performed by AP and RM, all coronary and aortic valve measurements were performed by a single observer (TK, supervised by AP and RM), using CMRtools (Cardiovascular Imaging Solutions, London, United, Kingdom).

2.2.3.3 Measurements

Table 13 below shows the patient and cardiac characteristics measured:

Table 13 Patient and cardiac characteristics

Patient features (AP / RM)
Age, gender, Body surface area (BSA m^2)
Cardiac features (AP / RM)
Left ventricular diastolic volumes (LVDV ml)
Left ventricular systolic volume (LVSV ml),
Left ventricular ejection fraction (LVEF %),
Number of aortic cusps,
Degree of aortic regurgitation (AR grade 0-4),
Presence of mitral valve prolapse (MVP),
Degree of mitral regurgitation (MR grade 0-4)

Aortic measurements (TK supervised by AP / RM) shown in Figure 61, and tabulated in Table 14 below:

Figure 61 Aortic measurements from the 62 patient Marfan cohort

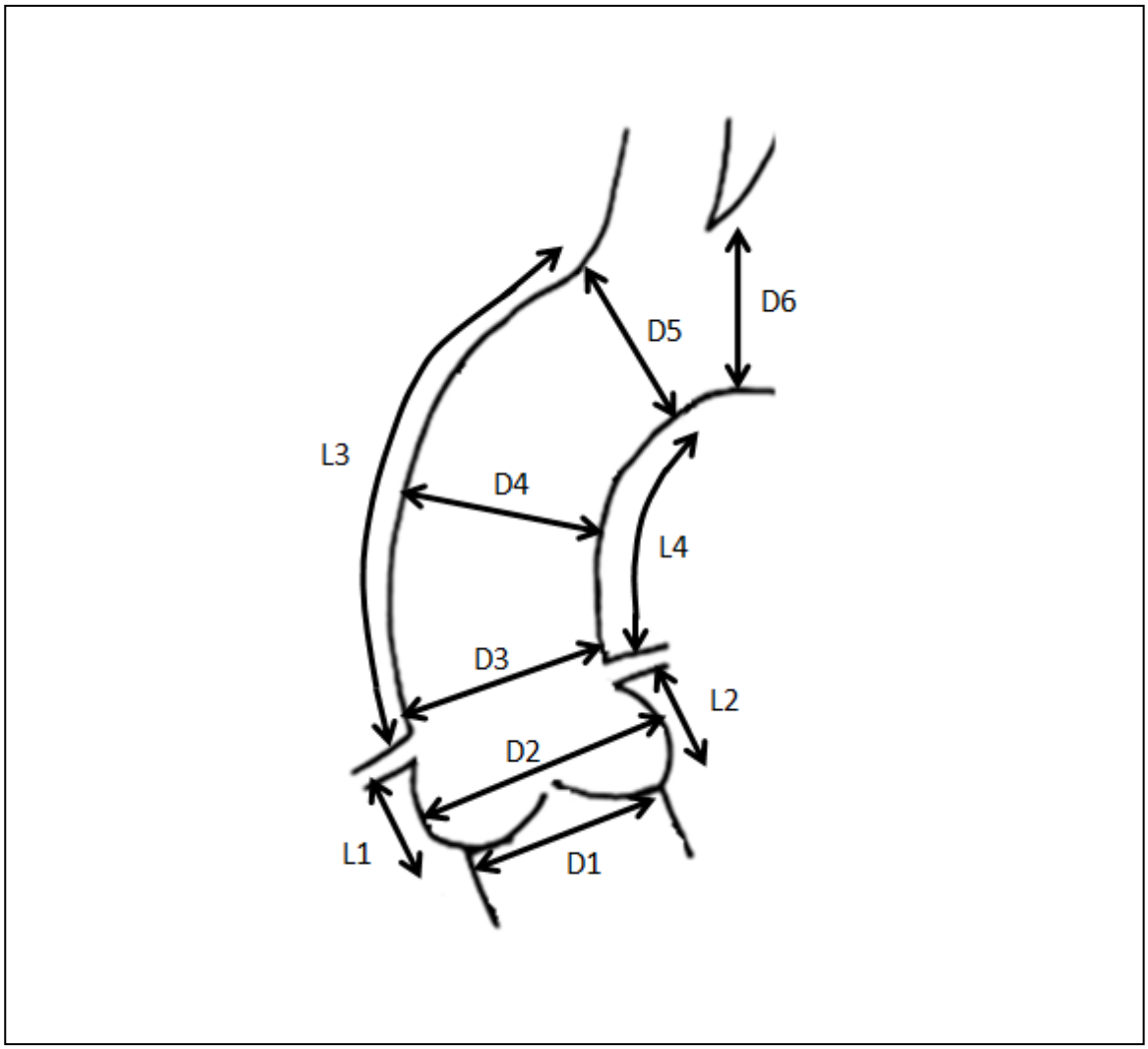

D1 – annulus diameter, D2 – Sinus diameter, D3 – STJ diameter, D4 – Mid ascending aorta diameter, D5 – Diameter just proximal to RBCT, D6 – Mid aortic arch diameter. L1 – Length from annulus to RCA, L2 - Length from annulus to LMCA, L3 – Length from RCA to RBCT, L4 – Length from LMCA to point opposite RBCT,

Table 14 shows aorta measurements performed

D1a Systolic annulus diameter in the 3 chamber view (mm)
D1b Systolic annulus diameter in the cross sectional plane (mm)
D2a Systolic sinus of valsalva measurement (cusp to cusp mm)
D2b Systolic sinus of valsalva measurement (cusp to commissure mm)
D3 Systolic sinotubular junction diameter (mm)
D4 Maximal systolic ascending aortic diameter (mm)
D5 Diameter of aorta at RBCA (mm)
D6 Mid aortic arch diameter (mm)
D7 Descending aortic diameter (mm)
D8 Aortic diameter at diaphragm (mm)
L1 Annulus to right coronary ostium (RCA)(mm)
L2 Annulus to left main stem coronary artery (LMCA) (mm),
L3 Length RCA to RBCA (mm),
L4 Length LMCA to RBCA (mm)

Coronary artery ostia angle from aorta

Figure 62 below shows the measurement of relative coronary ostia angulation from the aortic root in the AP plane:

Figure 62 Measurement of relative coronary ostia angle in the AP plane.

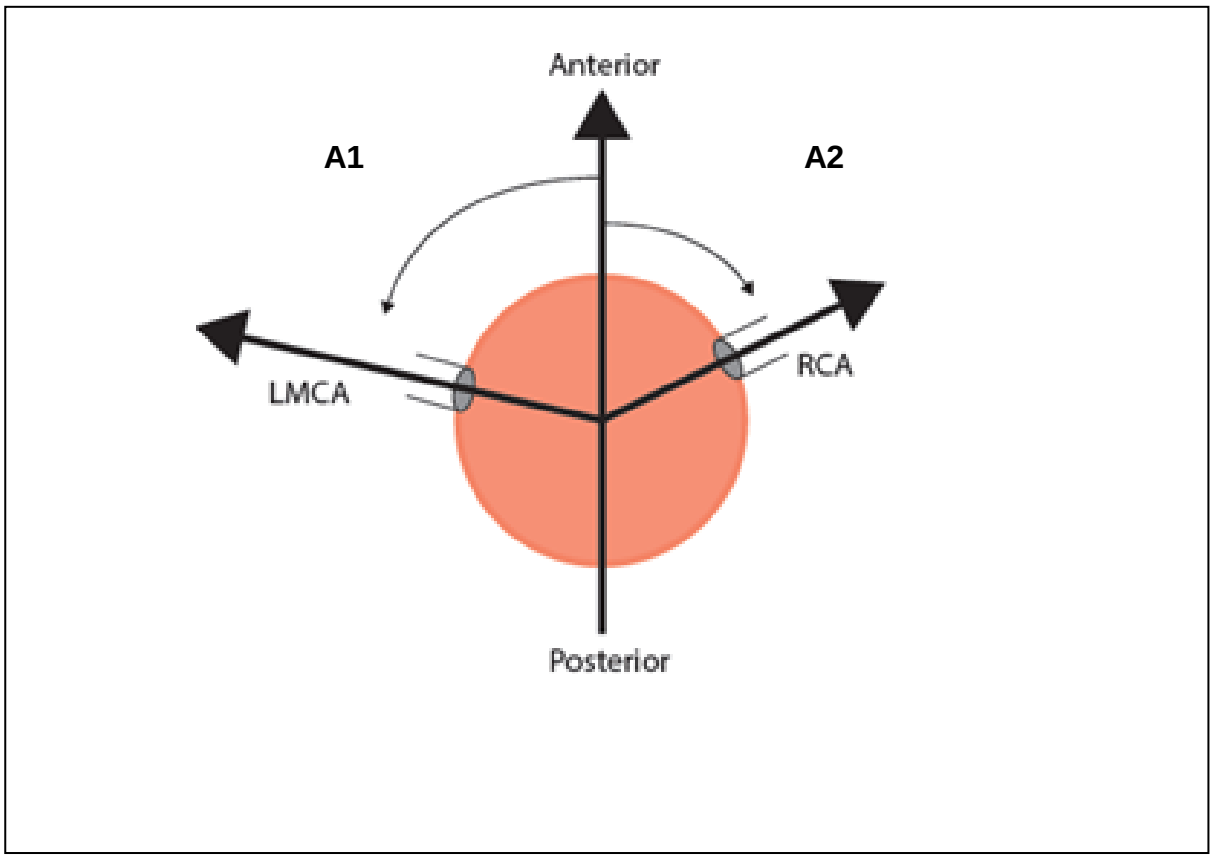

Coronary angle measurement with AP direction at 0 degrees. **A1** Angle of origin of the LMCA from aorta (degrees from AP), **A2** Angle of origin of RCA from aorta (degrees from AP)

Figures 63 – 66 below show the various planes in which aortic and coronary measurements were made:

Figure 63 Shows a still frame from an oblique sagittal MRI systolic frame

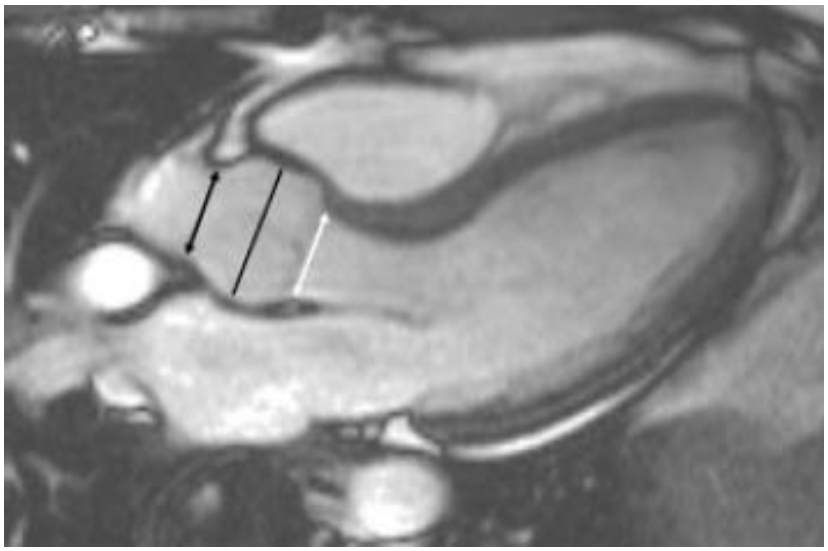

Oblique sagittal MRI systolic frame showing the levels of annulus, sinus, and STJ measurements (white arrow, black line, and black arrow, respectively).

Figure 64 shows oblique coronal LVOT still image

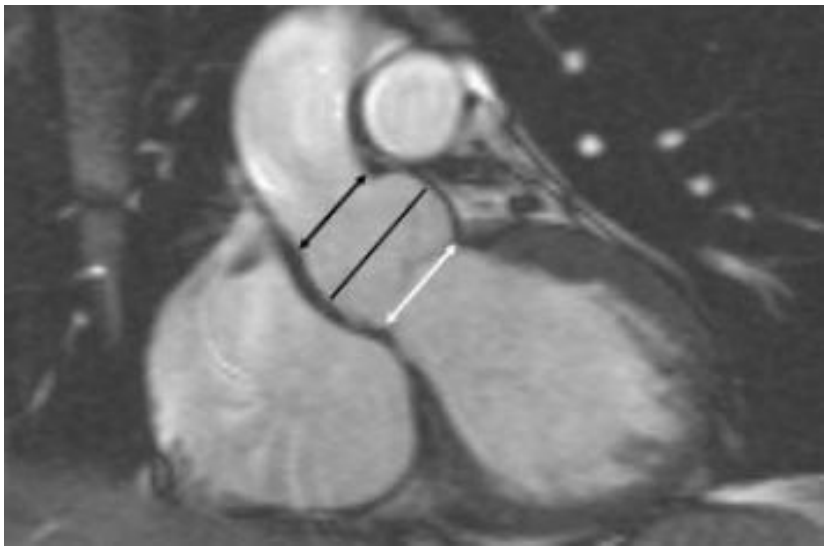

Oblique coronal LVOT cine showing the equivalent levels of measurement - annulus, sinus, and STJ measurements (white arrow, black line, and black arrow, respectively).

Figure 65 A systolic sinus plane MRI image, systolic frame

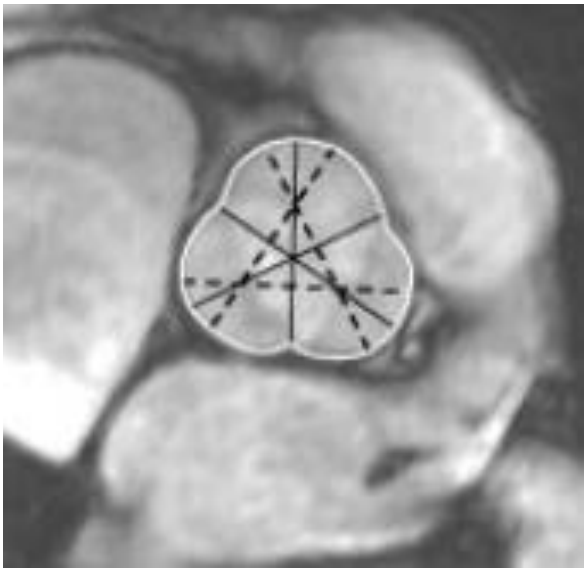

A systolic sinus plane image, systolic frame, showing 3 cusp-commissure and 3 cusp-cusp lines of measurement (continuous and dashed black lines, respectively)

Figure 66 Measurement plane for measuring the distance from annulus to coronaries

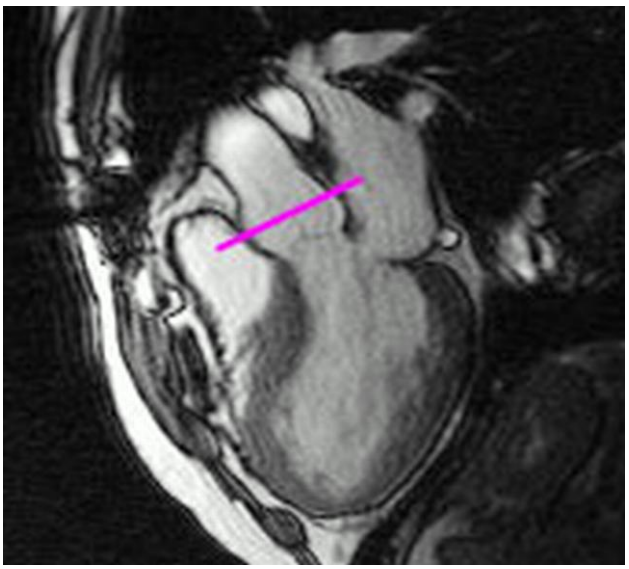

Measurement plane for measuring the distance from annulus to RCA and LMCA

2.2.4 Results

The patient cohort comprised 44 males and 18 females, with a mean age of 32 +/- 14 years, (range 18 - 64). Mean body surface area 2.1 +/- 0.23 m^2. Mean diastolic LV volume was 205 ml, with a mean systolic LV volume of 82 ml, giving a mean LV ejection fraction of 62 +/- 3.2%, (range 31 – 75).

3 patients were found to have a BAV (5% of the cohort), the remaining 59 patients having tricuspid valves. 33 patients (53%) had no AR. 21 patients (34%) had mild AR, 2 patients (3%) had mild-moderate AR, 1 patient (1.5%) had moderate AR, 1 patient (1.5%) had important AR, and 4 patients (7%) had severe AR. The 4 patients with severe AR all had grossly dilated aortic sinus measurements of 60 mm, 79.5 mm, 71 mm and 80 mm respectively.

22 patients (35%) had an associated mitral valve prolapse, giving rise to 10 patients (16%) having mild mitral regurgitation (MR), 2 patients (3%) with moderate MR, and 2 patients (3%) with severe MR.

2.2.4.1 Aorta and coronary measurements

Table 15 below documents the results of the aortic and coronary measurements in the 62 patient Marfan syndrome cohort:

Table 15 Marfan syndrome aortic and coronary measurements

Parameter	Mean	Range	SD
D1a Systolic annulus diameter 3 C (mm)	28.5	21-39	3.9
D1b Systolic annulus diameter in the X plane (mm)	29.4	24-39	4.3
Mean annulus diameter (mm) ((D1a + D1b) / 2)	28.9	22-39	3.9
D2a Systolic sinus of valsalva (cusp to cusp)(mm)	48.7	34-80	9
D2b Systolic sinus of valsalva (cusp to commissure)(mm)	46.9	34-80	9.7
Mean sinus diameter (mm)	48	34-80	9.2
D3 Systolic STJ diameter (mm)	37.7	23-85	11.5
D4 Maximal systolic ascending aortic diameter (mm)	34.1	21-115	15.1
D5 Diameter of aorta at RBCA (mm)	26.1	18-35	4.4
D6 Mid aortic arch diameter (mm)	22.9	16-37	4.8
D7 Descending aortic diameter (mm)	22.5	15-32	3.7
D8 Aortic diameter at diaphragm (mm)	19.8	13-27	3.6
L1 Annulus to RCA (mm)	20	14-36	4.7
L2 Annulus to LMCA (mm)	16.3	11-32	4.1
L3 Length RCA to RBCA (mm)	101.5	63 – 160	19.9
L4 Length LMCA to RBCA (mm)	59.6	40-85	10.2

Table 15 cont.	**Mean**	**Range**	**SD**
A1 Angle of origin of the LMCA from aorta (degrees from AP)	+124	+80 to +160	14.8
A2 Angle of origin of RCA from aorta (degrees from AP)	-18	-40 to -80	18
Angle between LMCA and RCA (degree total)	142	120-175	12.6

2.2.4.2 Discussion

Many patients with Marfan syndrome who have a dilated aorta are young. This is reflected by the mean age of this cohort being 32 years. Certainly the group appears to have a relatively large end diastolic volume, but with a mainly preserved ejection fraction (mean EF = 62%).

7% of the cohort had significantly dilated aortas giving rise to severe AR. A further 2 patients (3%) had either moderate or important AR with the mechanism of aortic dilatation. This is likely to represent patients who have presented later on in their disease process, rather than patients with an early diagnosis and serially followed. Screening would normally not allow diameters to exceed 4.5 cm before offering a surgical correction in an attempt to avoid the exponential risk of aortic aneurysm rupture and the associated aortic regurgitation.

4% of patients had moderate (2 patients) or severe MR (2 patients) secondary to mitral valve prolapse (MVP). MVP is associated with Marfan syndrome, and therefore it is no surprise to find this number in our cohort.

For the purposes of comparison Table 16 shows the Marfan syndrome aortic diameters compared to normal values:

Table 16 Marfan syndrome aortic diameters compared to normal values

Measurement	Marfan syndrome	Normal values
Aortic annulus (mm)	28.9	24.5
Sinus (mm)	48	32
STJ (mm)	37.7	29.7
Ascending aorta (mm)	34.1	32.7

All normal values are derived from the Qanadli data (11).

The mean aortic annulus measurement is a dilated at 28.9 mm, dilating further to a maximal diameter of 48 mm within the sinuses. The mean STJ measurement remains dilated at 37.7 mm, and by the ascending aorta the diameter is only mildly dilated at 34.1 mm.

In this Marfan syndrome cohort the mean distance from the annulus to the RCA was 20 mm **(normal = 19.3 mm)**, and to the LMCA was 16.3 mm **(normal = 12.1 mm)** (11). The distance from the LMCA to the RBCT was a mean of 59.6 mm **(normal = 52.9 mm)**, and

from the RCA to the RBCT was 101.6 mm (11). The angle between the origin of the RCA and the LMCA from the aorta was 142 degrees **(normal 154 degrees)** (24).

2.2.4.3 Conclusion

The pattern of dilatation of the Marfan aorta is well described, but this novel data has allowed documentation of the exact annular and sinus diameters, focusing also on the take off, distance and angulation of the coronary arteries. It would appear from these data that the Marfan syndrome aortic root dilates in a relatively uniform way maintaining relatively normal angulation between the LMCA and the RCA. Most of the dilatation seen is at the level of the sinus, and STJ, and that by the mid portion of the ascending aorta, diameters are virtually back to normal values.

I think we should not be too concerned by the very large diameter of 4 of the cohort and their associated severe AR. With aggressive screening protocols these diameters and the concomitant AR will not been seen as surgery / treatment options will be offered before this degree of dilatation has occurred. We must also be realistic that in the first instance the ATAG device is not primarily for ATAA patients, but the unmet clinical need of AAAD. Not only that, but the ATAG device will not be capable of treating all anatomies, and rather like TAVI there will always be patients that fall beyond the treatment realms of any new percutaneous device.

Conclusion on ATAA data and relevance to potential ATAG design

Although the ATAG is being designed in the first instance as a device to treat the unmet clinical need of patients presenting with AAAD, there is no doubt that as endovascular

therapies evolve, devices and delivery systems improve ATAA could become a cohort capable of being treated by ATAG, avoiding the need for invasive cardiothoracic surgery. That said this novel ATAA data provides us with a number of patient and anatomical challenges:

i) The Marfan syndrome cohort are generally young with little co-morbidity. The mean age of this study group was 32 years. As has already been outlined because these patients are in regular follow up they are generally stable and surgery is elective with a relatively low risk. Any percutaneous solution for ATAA would need to have a similarly low procedural risk but also display long term durability which may prove challenging.

ii) The pattern of the aortic dilatation is different to that of AAAD. Marfans display "*annulo-aortic ectasia"*, where the annulus dimension is dilated (mean 28.9 mm) leading into a dilated sinus (mean 48 mm), dilated STJ (mean 37.7 mm) into a relatively normal sized mid ascending aorta (mean 34.1 mm). This anatomy poses a number of device design challenges:

- Achieving an effective proximal endograft seal will be difficult in the dilated sinuses.

- The proximal end of the graft will be relatively large for endovascular stents. The mean sinus dimension in this cohort was 48 mm, meaning that even the average aorta will potentially require a 58 mm endograft with 20% over-sizing. This poses device, crimping and stowing as well as delivery challenges.

- The graft will also need to have a cone-shape, given that at the proximal end it will be around 58 mm and by the mid ascending aorta the diameter will be closer to 40 mm (with 20% over-sizing).

- The “valved ATAG” may suit the ATAA where the proximal seal is at the mildly dilated aortic annulus, and then the distal seal is at a relatively normal part of the aorta prior to the RBCT (in a similar fashion to descending and abdominal aortic endovascular exclusion). So long as the coronary perfusion is maintained and the new valved portion competent the ATAG would not necessarily need to be in contact with the most dilated portion of the aorta in the sinuses. The valved ATAG would also enable satisfactory treatment of the 5% of patients with BAV, and the 10% of this cohort who had at least moderate AR, which would normally require treatment.

- Despite the annulo-aortic dilatation the angle of the coronary arteries to one another is relatively preserved at 142 degrees (normal 154 degrees, range 120-175).

Chapter Three

ATAG device specification

PoC ATAG graft and delivery manufacture and testing

Chapter 3: ATAG device specification and PoC build

3.1 ATAG "inverted t-shirt" device specification

Now that the pathophysiology, anatomical data and current treatment modalities and deficiencies have been established for AAAD and ATAA, I will now utilise this data to develop an general ATAG device specification.

3.1.1 General device specification

The ATAG is a proposed endovascular stent graft designed to treat AAAD, where there is a large unmet clinical need (the 28% of patients presenting who are turned down or who refuse a surgical approach) (67). It is also possible as our experience grows that like in the rest of the vascular tree the ATAG device could become a treatment modality for ATAA, although the currently well established surgical treatments have a low operative morbidity and mortality (7).

The key feature of ATAG is the insertion of a covered aortic endograft near the aortic valve. Chapter 1.8 discussed generically the design possibilities with regard to maintenance of aortic valve function, protection of coronary artery flow, and exclusion of the intimal tear. As has already been discussed, a simple tubular endograft will only be feasible to treat approximately 36% of AAAD patients, as the remainder have diseased segments too close to the aortic valve, coronary arteries, or RBCT (8).

It was decided early on in this project that one embodiment of ATAG should try to proactively protect flow into both coronary ostia with the delivery of an “inverted t-shirt” ATAG graft with 2 covered coronary sleeves attached to the main graft body. If during testing the device and or the procedure is too technically or physiologically challenging then we can always retreat to a position where only one or none of the ostia are proactively protected. Professor Rothman is always keen to focus on the “device end game”, and if this is found to be over-zealous or not technically feasible during testing a more simple solution can be sought.

As a coronary interventional doctor commonly occluding flow during LMCA and RCA coronary intervention I am comfortable that I have the time available to deploy stents into both LMCA and RCA – the question is while the body commonly tolerates temporary LMCA or RCA occlusion, will it be able to cope with relative no flow simultaneously and potentially for a more prolonged time with no ischaemic pre-conditioning?

The Muriago paper on normal coronary ostia position emphasises proximity of the coronary ostia in essence at or within the aortic sinuses, as a result if we are to successfully deploy coronary branches, the ATAG main graft stent will have a very short proximal section with attachment of coronary stents to minimize interference with the aortic valve apparatus in the sinuses of Valsalva. The front section will be relatively short, sitting within the sinuses, minimising aortic valve interaction and maximising the chance of maintaining valve competence (21).

The graft will be delivered in one percutaneous intervention.

3.1.2 Intended use

The intended use is for a percutaneously delivered stent graft to treat acute aortic syndromes of the ascending aorta – namely AAAD. It will need to adequately cover the intimal tear in the ascending aorta at the same time proactively protecting coronary artery flow and preventing interference with aortic valve function. If the aortic valve is already significantly incompetent, or becomes so during the ATAG implantation, subsequent delivery of a commercially available TAVI is possible. We have also captured within our intellectual property and we will seek to simultaneously develop a "valved ATAG" where the proximal fixation point will be at the aortic annulus and that the ATAG will have a fully functioning percutaneous aortic valve within its proximal end.

3.1.3 Indication

The ATAG is intended to be used in patients with AAAD. Patient anatomy (particularly aortic dilatation) is likely to necessitate a number of "off the shelf" sizes (diameters and lengths, and possibly coronary angulations). In the acute setting bespoke stent graft design based on CT / MRI data will not be possible because of the acute nature of treating AAAD and the 1-2% mortality per hour after diagnosis associated with this pathology (58).

3.1.4 ATAG device attributes

ATAG device attributes are summarised in Table 17 below:

Table 17 ATAG device attributes

A self-expanding Nitinol aortic stent graft with an "inverted t-shirt" configuration integrating 2 coronary sleeves, covered in a biocompatible material
The covering of the graft shall have two side branches attached. These coronary side branches with integral balloon expandable stents (covered side arm stents) shall protect the coronaries and shall ensure coronary perfusion.
The coronary side branches are of different diameters (LMCA 4.5 mm, RCA 3.5 mm). Colour coding for left and right is required to minimize confusion and avoid incorrect placement. There will be a single radio-opaque marker on the left coronary balloon, and a double marker on the right coronary balloon. Fluoroscopic markers will be vital in anterior / posterior and left / right orientation process.
The device will prevent blood flow into the false lumen through the intimal tear, and protect the aortic wall from the pressure of the blood and as such a good proximal and distal seal will be needed to prevent endoleak and the graft covering material must be biocompatible but also relatively impermeable to blood.
The ATAG graft will be inserted over a central 0.038" superstiff guide wire (positioned in the left ventricular cavity), and the coronary sleeve stents will run over 2 x 0.014"coronary guide wires (perhaps specially designed and configured) already placed into the LMCA and RCA
The graft shall be delivered via percutaneous vascular access most likely the femoral artery, if the delivery sheath is 18 F or less, but other routes may be viable including iliac or femoral conduit, and direct aortic implantation especially during the development phase when the delivery system may be larger than 18 F.
It is our aim that the diameter of the stowed graft should be 18 F by the time we reach our FIM cases.
The graft should minimize any compromise of the aortic valve or it would require re-valving (utilizing a commercially available TAVI device). If AR is present at commencement of case it is possible a "valved ATAG" may be able to treat the intimal tear and the concomitant AR.
The graft will need to be visible during fluoroscopy and ultrasound examination ICE / TOE
The graft shall have flexible coronary region to allow some variation in patient's coronary angle anatomy.

Table 17 ATAG device attributes cont.
The coronary stents should be attached as close to the leading front end of the lobes as possible to minimize the amount of lobe sitting in the sinuses with potential to disrupt the aortic valve. The coronary stents will be attached with an angle of approximately 150 degrees between them so as to match the standard coronary angulation. The attachment mechanism must allow for some coronary angle variability.
The first device will be 65 mm in total length so when in position it will comfortably end before the RBCT to avoid compromise of blood flow to this vessel.

3.1.5 Method of operation

The following describes the theoretical steps of implantation of the ATAG device in the treatment of AAAD with an intimal tear in the ascending aorta:

- ATAG device will be stowed to 18 F (stowage is likely to be performed in a sterile ice bucket to aid nitinol contraction). All of procedure under taken using aseptic sterile techniques, with patient under GA.
- Insertion of right femoral arterial 18 F sheath, pre-closed with suture based closure device (Prostar ^{TM} Abbott Vascular, USA). Insertion of right radial artery (RRA) 6 F sheath for pigtail catheter to allow injection. Left femoral vein insertion of 6 F sheath with insertion of a temporary pacing wire (TPW) in to the right ventricle for rapid ventricular pacing to allow reduced cardiac output during deployment and therefore greater deployment accuracy and precision.
- Systemic anticoagulation and anti-platelet loading. (Regimens to be elucidated)
- 2 x 260 cm 0.014” coronary guide wires, one positioned into each coronary artery using standard guide catheters (wire into distal LAD and RCA). A 260 cm x

0.038” Amplatzer Superstiff type guidewire with a pre-formed curve inserted into the left ventricle (LV). Guidewires may be modified to provide additional stiffness where the device will enter the coronary ostium, and an anchoring technique to keep the wire fixed within the vessel during the positioning of ATAG.

- Sterilised stowed ATAG device in delivery catheter placed into sterile operating field. Central guide wire fed into the central delivery catheter lumen, both coronary guide wires fed into coronary sleeves. Care taken to correctly align the guide wires and avoid twists or wire-wrap.

- The ATAG is likely to take up the “diving man” position with coronary arms facing forwards, as shown in Figure 67 below:

Figure 67 ATAG taking up the “diving man” position

.

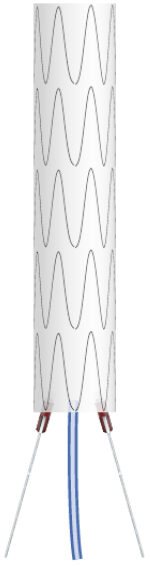

Stowed ATAG with central wire and 2 coronary guidewires running though the coronary sleeves, within OTW push rods, taking up the “diving man” position with coronary arms pushed forward like a man preparing to dive.

- ATAG device within delivery catheter passed through sheath into femoral artery, into aorta, around arch and pushed towards ascending aortic landing zone. Ensure wires are unwrapped and that the coronary projections are aligned to respective coronary ostia.
- Decision to implant at correct landing zone.
- Rapid RV pacing allowing relative low cardiac output state.
- Distal part of sheath retracted to allow proximal (aortic valve end) of the device to flare to free the coronary arms to reach the coronary arteries.
- Coronary sleeves pushed into both coronary arteries and stents within each dilated into coronary ostia allowing graft fixation. The LMCA stent will be delivered and stented in position first, before implantation of the RCA arm.
- Rest of ATAG body graft delivered.
- RV pacing stopped.
- ATAG delivery catheter withdrawn
- Check shot using pigtail catheter from RRA to globally look at coronary flow and degree of AR (can be confirmed with TOE or ICE)
- Selective coronary angiography to check sleeve stent patency using left and right coronary guide catheters. Post-dilatation can occur if flow sub-optimal or stents under-deployed. Intra-vascular ultrasound (IVUS) of the LMCA / RCA may be helpful to ensure stent deployment.

- Aortic valve integrity must be critically assessed by aortic pressure trace / fluoroscopy and TOE. Assess need for implantation of a commercially available TAVI.

- Remove all guide wires, and sheaths and manage the puncture sites in the routine manner.

- If the aortic valve is affected or re-valved the TPW may be left in for 48 hours post procedure depending on the pre-procedure ECG and perceived risk of bradyarrythmia / heart block.

3.2 Proof of concept (PoC) device specification

3.1 has already detailed a general ATAG device specification. To prove the ATAG concept (that a graft with 2 coronary sleeves can be deployed), it was decided to design an "inverted t-shirt" ATAG that could be deployed within a normal sized glass aortic model.

The PoC model has a number of functions:

i) To prove that the concept is feasible and identify future technical challenges for development.

ii) To prove to potential investors that this is a technological reality and to seek further development funding.

iii) To reduce to practice to allow for intellectual property (IP) filing i.e. IP is not just an idea but can be realised in the real world.

iv) To generate new ideas and solutions from problems encountered strengthening IP position.

It is vital that if at this first hurdle design specification simplifications are accepted, they must be acknowledged and plans for the "real life complexities" considered later in the specification process.

This design specification intended to prove the "inverted t-shirt" ATAG concept and percutaneous delivery from femoral artery within a "normal sized" human adult glass

aorta model (Farlow Scientific Glass, CA, USA), under first direct vision and then under fluoroscopy. Figure 68 below shows a photograph of the glass aortic model:

Figure 68 shows a photograph of the glass aorta

Photograph of the glass normal sized aortic model (Farlow Scientific Glass, USA). For the purposes of PoC demonstration I mounted it upon a piece of hardboard for stability.

Figure 69 below shows a diagram of the glass model with dimensions:

Figure 69 Diagrammatic representation of aorta glass model dimensions (mm)

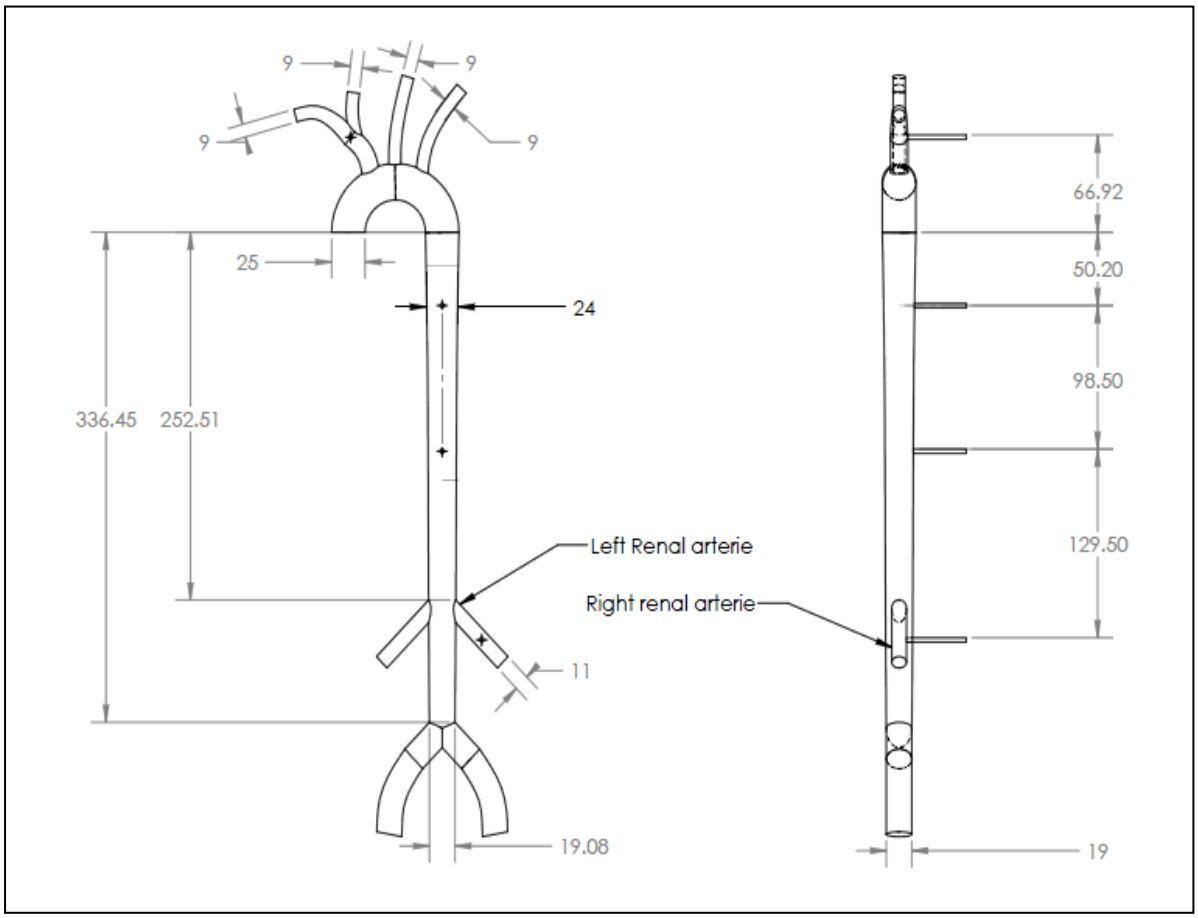

Despite the glass model being purchased as have "normal aortic anatomy", actually it has a constant ascending and arch aortic size of 25mm, and a descending aortic diameter of 24mm. The coronary arteries in this model come off at 180 degrees to one another. Simplifications in the design specification had to reflect this simplified aortic model anatomy.

The PoC device design specification is split into 2 main parts:

i) The ATAG endograft (inverted t-shirt graft with body for aorta and 2 coronary sleeves)

ii) The ATAG delivery system for delivery to the proximal aortic landing zone, around the arch of a glass aortic model from “a femoral access sheath”.

3.2.1 ATAG graft body

It can be clearly seen in Figure 69 that the “normal” glass vascular tree has simplified dimensions when compared to the normal human aorta. With an ascending aortic diameter of 25mm, taking into account the current TEVAR graft over-sizing by approximately 20%, the PoC ATAG graft would have an expanded diameter of 30mm to provide continuous external radial force to maintain the graft in position once deployed (in keeping with current clinical practice).

The ATAG graft itself is further subdivided into 3 sub-components:

i) Self expanding nitinol body frame

ii) LMCA and RCA stent projections (inverted t-shirt configuration)

iii) ATAG graft covering material

Table 18 below outlines the ATAG PoC graft design specification:

Table 18 ATAG PoC graft specification

ATAG diameter stowed in sleeve	6 mm (18 F)
Diameter of main body when deployed	30 mm
Diameter of proximal aortic lip	30 mm
Diameter of RCA sleeve / stent	3.5 mm
Diameter of LMCA sleeve / stent	4 mm
Length of coronary sleeves	8 mm
Angle between coronary branches	180 degrees
Vertical Offset between coronary sleeves	0 mm
Length of ATAG main body	55 mm

To reflect the glass aortic model into which PoC ATAG is to be implanted, the device specification has a number of anatomical simplifications, when compared to the potential AAAD treatment population. The glass model has a relatively constant diameter throughout aortic root and ascending aorta of 25 mm. It also has a simplified aortic root with LMCA and RCA coming off at an angle of 180 degrees to one another, which we know is not found in the AAAD cohort (Section 2.1.3).

The LMCA had a stented diameter of 4mm (rather than the literature which supports 4.5mm) as this is the diameter of expired stents available. For ease of manufacture I placed the LMCA and the RCA sleeves at the same level with no “offset” (11). The graft

will be a straight tube and not have any inherent aortic curve, and finally in a theoretical attempt to minimise aortic valve interference the coronary sleeves will be attached as close to the proximal end of the ATAG body as is technically feasible.

3.2.2 Coronary Stents / sleeves

The stented portions within this PoC model comprised a 4 mm x 8 mm bare metal stent into the LMCA and a 3.5 mm x 8 mm bare metal stent into the RCA. For simplicity I elected to manually sew the covering material to the stents and then attach them with fine 6.0 sutures to the graft body. I acknowledge that having a suture line at the ostium of both the LMCA and RCA is far from ideal and that this is unlikely to feature in the final product, given the potential risk of thrombus formation and the mechanical forces at this critical point.

3.2.3 ATAG graft covering material

Currently available thoracic stent grafts are either covered with a woven polyester (PET Dacron), or ePTFE. We could have utilised Dacron as it is readily available, cheap and easy to use, but at the time of device build I was working with Andrew Pacey a medical engineer working for Advotek Medical Devices, Herts, UK. Advotek had developed a silicone-coated polyester for another application. It appeared to have greater elasticity, and be less stiff when compared to Dacron and I felt that this might offer some flexibility advantage compared to Dacron with regard to coronary angle variability in this first model.

3.2.4 ATAG delivery system

3.2.4.1 Product description

The following describes the proposed delivery system for the ATAG PoC graft.

3.2.4.2 Delivery Catheter

The delivery catheter has 3 main components:

1) Central Shaft - The shaft that the graft is stowed around. It tracks over the 0.038" stiff guide wire (which has been placed into the LV cavity).

2) Push Rods - Incorporates balloon shafts and stents. Used to deploy each of the coronary sleeves with stents. Left and right push rods (graduated hypo-tube) identified with marker bands and 2 different coloured hubs. Each of the push rods to be fitted within a 0.075 mm PTFE liner to ease guide wire movement through lumen. The balloons are Over the Wire (OTW) construction, with variable shaft stiffness to aid tracking. Hydrophilic coated inner diameter to aid the deployment. These might have a monorail configuration eventually, if adequate "pushability" of the coronary sleeves can be achieved.

3) Outer retractable sleeve. A PTFE outer sleeve over the complete length of the device was used to act as the pod into which to stow the graft. Deployment of the graft would be realised by relative retraction of the outer sheath and pushing of the inner central shaft / graft allowing graduated expansion of the ATAG graft.

Figure 70 below shows a schematic diagram of the proposed ATAG with delivery system prior to crimping:

Figure 70 Schematic diagram of the ATAG graft with delivery system prior to crimping

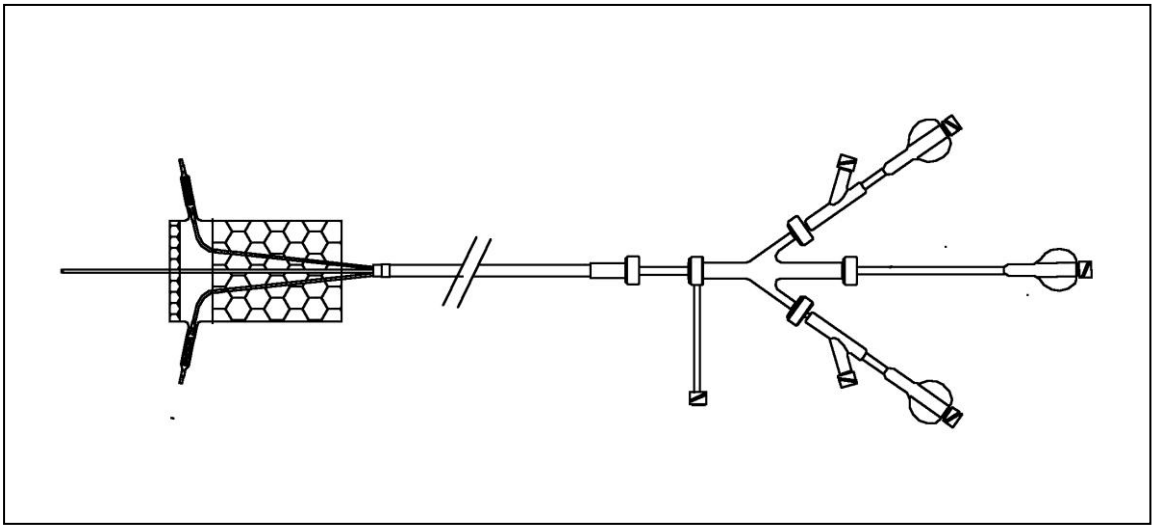

Figure above shows ATAG graft body prior to crimping, with 2 coronary sleeves. Within the coronary sleeves are 2 OTW push rod balloons, for deployment of the coronary "arms". The delivery catheter tracks over 3 wires, 1x 0.38" central wire within the LV cavity and a 0.014" coronary wire in each coronary artery.

3.3 ATAG Proof of concept device build

Now that both the device specification and the design had been specified for the PoC ATAG, it was time to build the PoC device. The endograft was made with support from 2 medical engineers at Advotek Medical Devices, while I designed and built the delivery system.

3.3.1 ATAG “t-shirt” graft with coronary sleeves

As already discussed, currently available thoracic aortic stent grafts consist of a nitinol self expandable frame and either Dacron or ePTFE graft material. For the purposes of PoC we could have quite easily and legitimately “adapted” a commercially available stent graft, changing it to the desired size and length, and then adding the coronary sleeves. Instead however with Leena Jaatinen, a PhD student with Advotek medical devices it was decided to build our ATAG PoC graft with some bespoke made parts and the rest from “off the shelf” expired materials in a “make and do manner”.

3.3.1.1 Nitinol frame

All current commercially available aortic stent grafts utilise nitinol in a “zig-zag” formation. To achieve this pattern, firstly nitinol wire (Euroflex SE508; http://www.nitinoleurope.com) of an appropriate thickness must be formed into a zig-zag shape using a brass former. Figure 71 below shows nitinol wire being bent around the brass former. The nitinol and former is then heated to 500^{o}C in an oven for 15 minutes before being rapidly cooled in water.

Figure 71 Nitinol wire on brass former

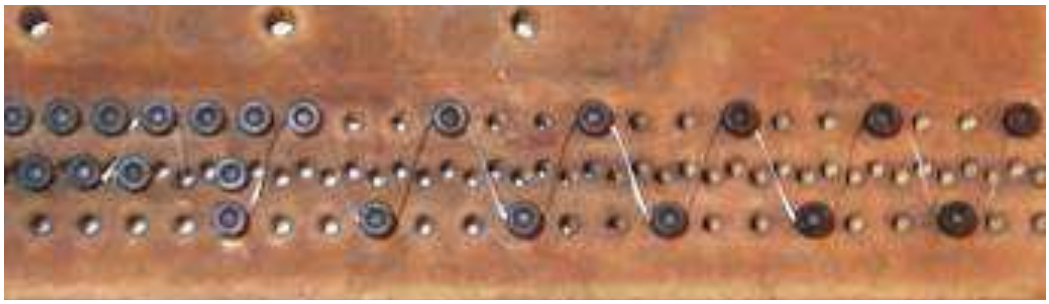

Nitinol wire of an appropriate thickness is bent around the brass former in a zig-zag pattern.

The first 2 devices built as shown in Figure 72 had inadequate radial strength, firstly because the nitinol wire used was too thin (0.15 mm), and then with appropriate wire thickness (0.4 mm), the zig-zag pattern was too sinusoidal and rounded at the apex (12 cycle pattern), with reduced resultant radial strength.

Figure 72 The first 2 PoC ATAG builds

a)

b)

a) First ATAG graft lacked radial strength as you can see the nitinol frame cannot even hold open the graft material b) was better but still inadequate.

The third graft that was made had the correct dimensions and adequate radial strength for the purposes of PoC demonstration. No formal radial strength testing was performed at this early PoC stage. The PoC ATAG consisted of 5 zig-zag nitinol bands, 4 of which were made from 0.4 mm diameter wire, and 1 frame was made of 0.23 mm wire - this was the centre band. Figure 73 below shows the bend radius of the zig-zag brass former:

Figure 73 Bend radius of the zig-zag pattern of nitinol brass former

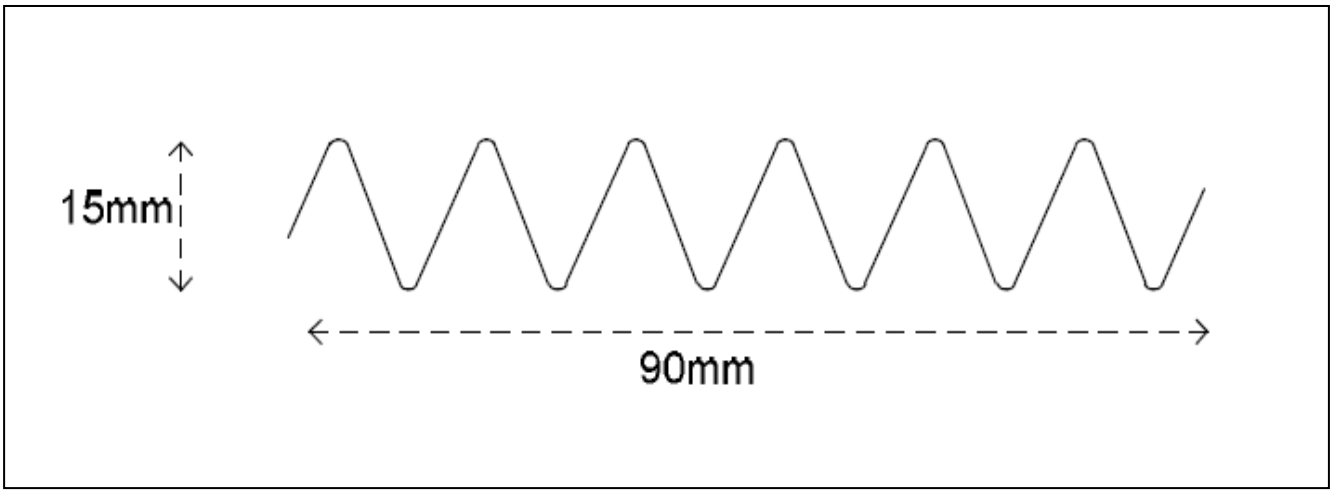

Figure shows the bend radius of the zig-zag pattern of nitinol on the brass former.

3.3.1.2 Graft material

Advotek had recently produced a polyester fabric material impregnated with silicone rubber. For the purposes of the PoC ATAG only this material was ideal. It was cheap, readily available, could be sewn easily to nitinol frame, and as compared to Dacron had some elasticity in its form allowing potentially some flexibility for the coronary arms.

It is unlikely that this material would be used in later generations as it does not have a vascular regulatory dossier (for CE Mark and FDA approval process), and currently lacks the thickness profile required for low profile crimping and stowing.

The fabric is formed into a tube by wrapping and sewing the seam to form a tube using cotton thread. The wire bands were then sewn into the outside of the graft material to create a 30 mm diameter tube.

3.3.1.3 Coronary sleeves

The coronary sleeves consist of tubes made of the graft fabric, formed into a tube and sewn at the seam. A 4 mm hole was made at the LMCA and a 3.5 mm hole at the RCA ostium of the main body graft, inside the bend of the bottom frame. The sleeves were sewn around each hole. A 4 mm x 8 mm expired stent, and a 3.5 mm x 8 mm expired stent were then sewn around the sleeve to make the "inverted t-shirt". More complex discussion about potential coronary sleeve designs is covered in 4.5.2.

3.3.1.4 Design output specification

The first PoC ATAG endograft had the following properties in Table 19 below:

Table 19 ATAG PoC design output specification

ATAG graft diameter	30 mm
ATAG graft length	55 mm
LMCA sleeve	4 * 8 mm stent
RCA sleeve	3.5 * 8 mm stent
Angle between stents	180 degrees
Distance coronary sleeve from proximal frame	3 mm

Figure 74 below is a diagrammatic representation of the PoC ATAG device, and Figure 75 shows the first PoC device build:

Figure 74 Diagrammatic representation of the PoC ATAG device

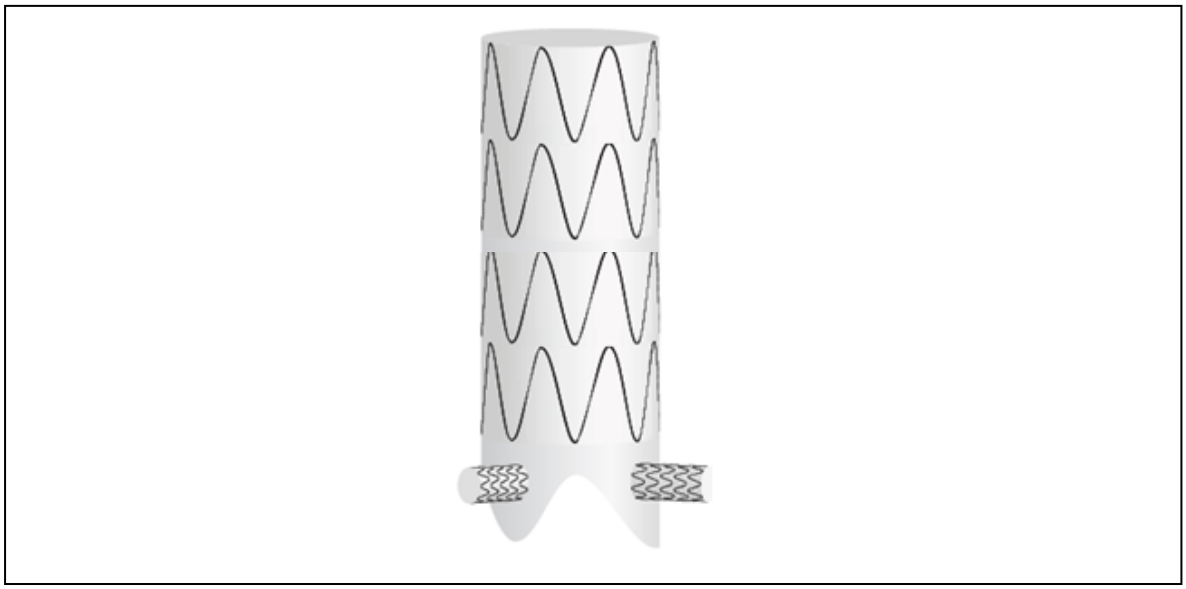

The PoC ATAG consists of a stent body which is covered in graft material. Attached to this body are the 2 coronary stented sleeves at and angle of 180 degrees to one another. They are attached low down on the main body graft.

Figure 75 First PoC with "adequate" radial strength and coronary side-arms attached

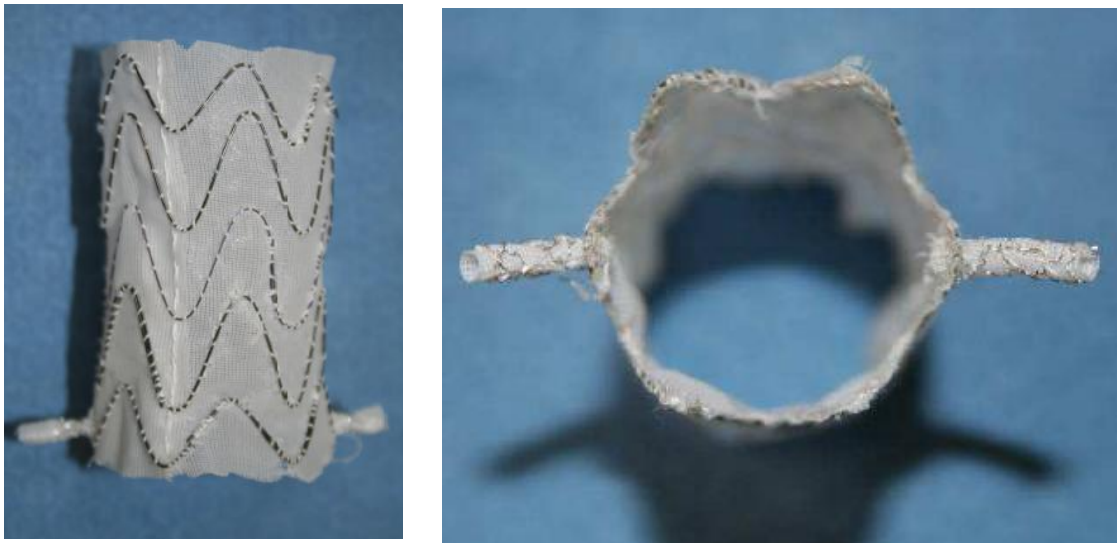

Photographs of the PoC ATAG with adequate radial strength utilising 5 zig-zag bands of formed nitinol, hand sewn to polyester silicone graft material. Low down on the ATAG graft, 2 coronary sleeves with integrated coronary stents are attached to protect coronary artery flow.

3.3.1 Conclusion

The manufactured PoC ATAG endograft fulfilled our design specification for the purposes of proof of concept. There are a number of deficiencies and simplifications that we accept in this first model including:

i) Simplified graft dimensions for the purpose of demonstration in the glass model.

ii) Untested radial strength just to allow demonstration that the technique is feasible.

iii) The use of an untested material covering that has no regulatory dossier and that is too thick for further testing.

iv) The attachment of coronary stents using material and fine sutures, at a point where there is huge mechanical stress and blood flow turbulence, which *in vivo* is likely to lead to mechanical failure and high risk of thrombus formation.

v) The coronary branches attached at an angle of 180 degrees to one another to match the glass model, rather than attached at 155 degrees which we know from anatomical review to be the normal coronary angulation.

All these simplifications are accepted in this first iteration, but must be factored in for later device prototypes.

3.3.2 Simple delivery system and stowage

From the very outset I did not underestimate the complexity of accurate and precise delivery of the ATAG to the landing zone just above the aortic valve, avoiding aortic valve incompetence, while proactively securing both LMCA and RCA flow with the sleeves and stents of the ATAG “inverted t-shirt”.

Before being able to design and specify a delivery system capable of deploying ATAG in the correct landing zone I felt that I had to make a simplified aortic model and break the delivery system down into the necessary constituent parts. Within the Appendix are the details of the preliminary fact finding delivery system testing, enabling me to define the length of system components, procedure sequence and potential complications.

This enabled me to develop the following PoC delivery system, as shown in Figures 76 – 81, breaking the system down into its constituent parts (described as a) – c):

Figure 76 Photograph of delivery catheter parts

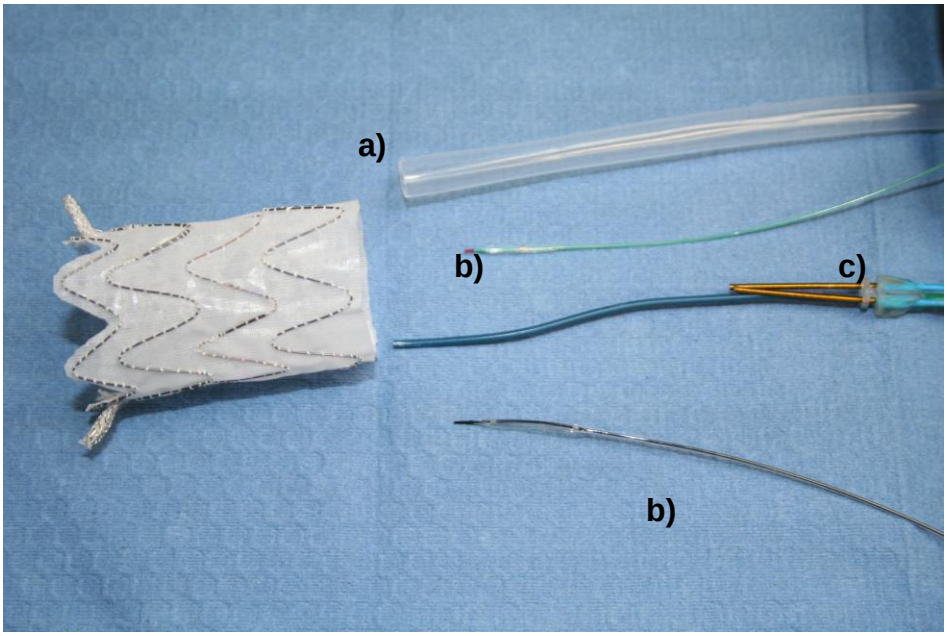

Delivery catheter constituent parts a) Retractable silicone sleeve, b) 2 x OTW balloon push rods and c) central core delivery catheter, with housing for the central 0.038" guidewire, and 2 sleeves to accommodate the 2 X OTW balloons

.

a) Graduated retraction of the silicone tube sleeve (Figure 77 below) would allow the proximal end of the graft to gradually expand releasing the graft in a controlled manner. In this first iteration it would rely upon controlled manual pull-back of the sleeve. In later iterations this sleeve retraction could be made more controlled with a graduated pull-back wind mechanism on the handle.

Figure 77 silicone tube sleeve

An outer retractable silicone tube sleeve (OD 6mm, ID 5mm), manual pull back would allow gradual release of the ATAG

b) Two push rods with integrated OTW balloons. For the purposes of this PoC I utilised 2 x expired Ninja™ OTW balloons (3 mm x 15 mm, Cordis Bridgewater , NJ, USA). The balloon shaft is made of a graduated hypo-tube as drawn in Figure 78 below:

Figure 78 Laser cut profile of the hypo-tube and Ninja OTW balloon

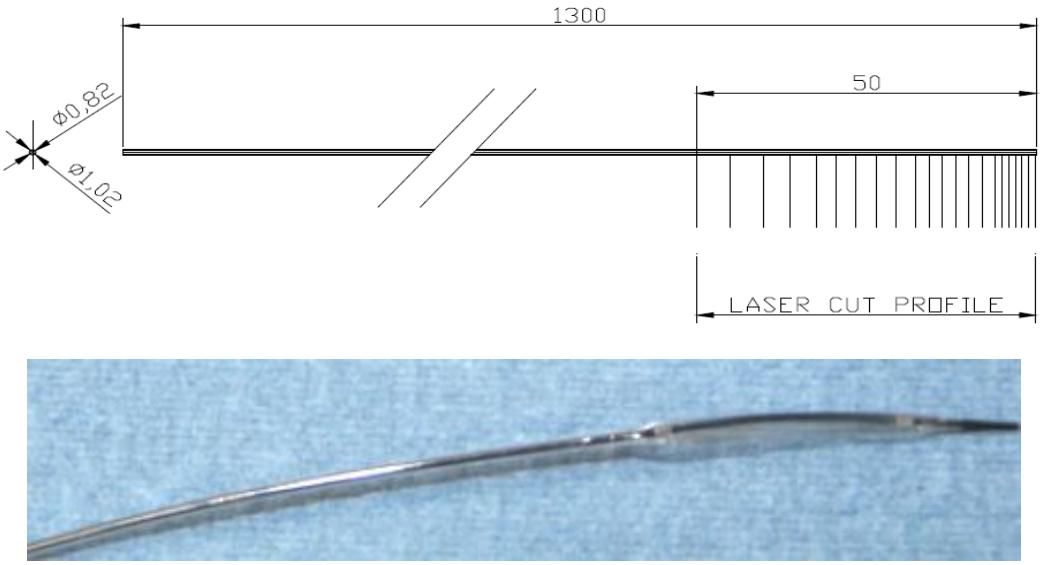

Graduated laser cut hypo tube forms the central core of the push rod, with a balloon section and marker bands added.

Figure 79 below shows the central core delivery catheter:

Figure 79 The central core delivery catheter

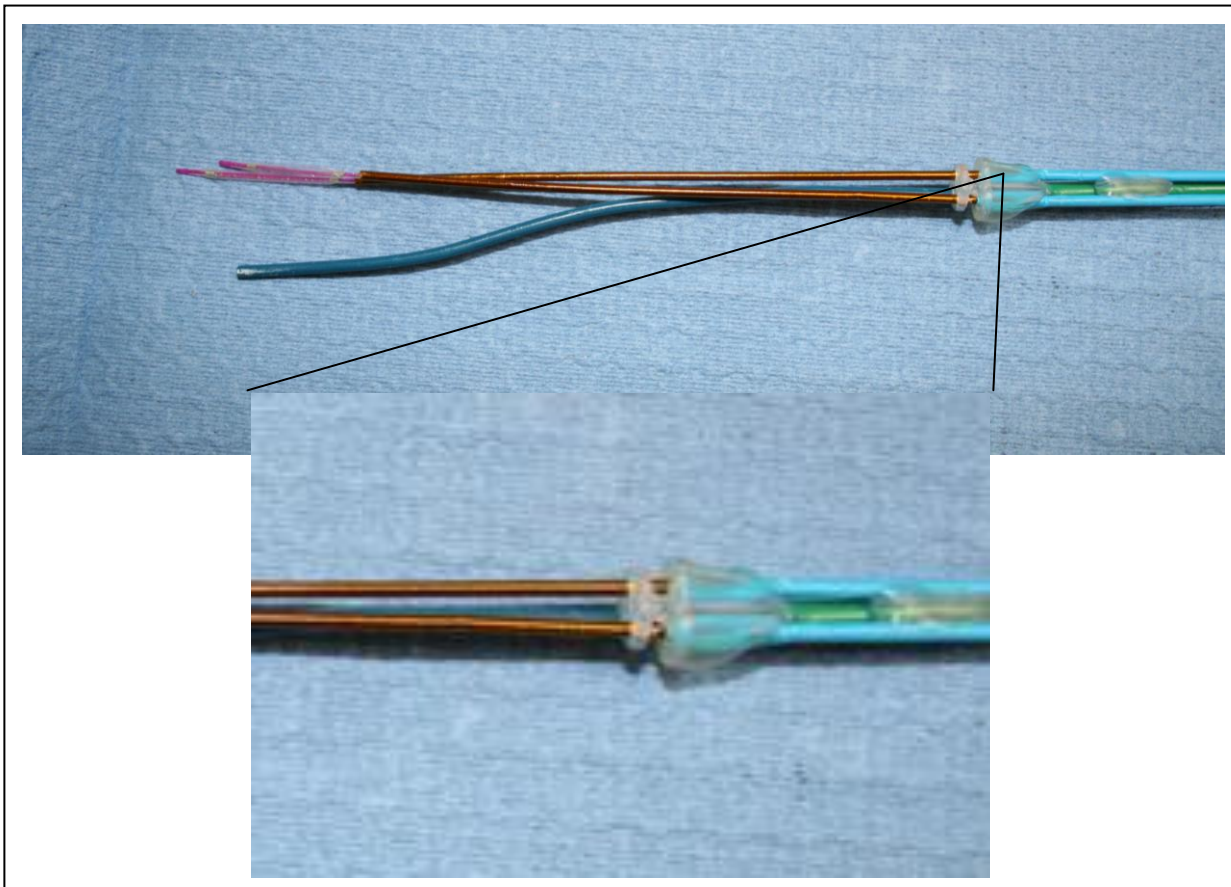

The central core of the delivery catheter is triple lumen in design. A central lumen for the 0.038" LV wire, with left and right channels for the coronary "push rod / OTW balloon sleeves". These sleeves were made from braided polyamide, allowing smooth movement and transmission of push from the OTW balloons within.

The 2 x OTW balloon push rods are inserted into their support sleeves as shown above. At the time of ATAG stowing, orientation of the ATAG stent graft to the correct coronary sleeve push rod / OTW balloon is vital.

During testing it became clear that the outer retractable sleeve would kink upon traversing the arch of the aorta (>180 degree bend). This made controlled retraction of the sleeve and subsequent delivery of the ATAG impossible as the sleeve would kink and catch on the nitinol frame of the graft.

I designed around this by inserting a layer of braided material, which upon traversing the arch would not kink and would allow smooth passage of the outer sleeve enabling controlled retraction and device deployment. Figure 80 below shows the integration of braided kink resistant material into delivery system:

Figure 80 shows the addition of the grey braided kink resistant material

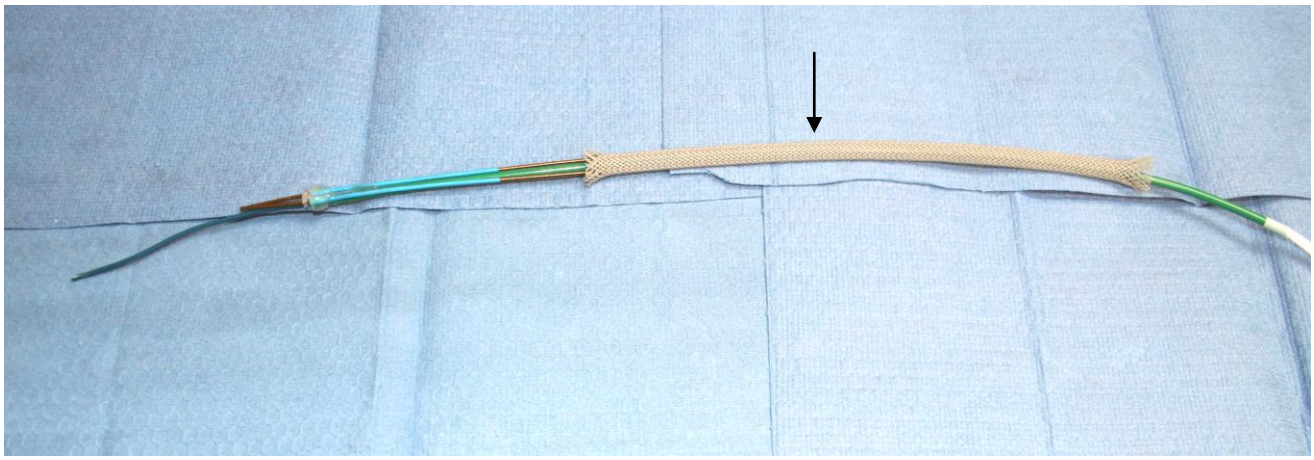

Integration into delivery system of grey braided material (arrowed), which prevents friction and kinking of the retractable silicone tube during passage around the aortic arch.

Figure 81 below shows the completed delivery system with the addition of the retractable silicone sleeve:

Figure 81 shows the addition of the clear silicon 6mm retractable sleeve

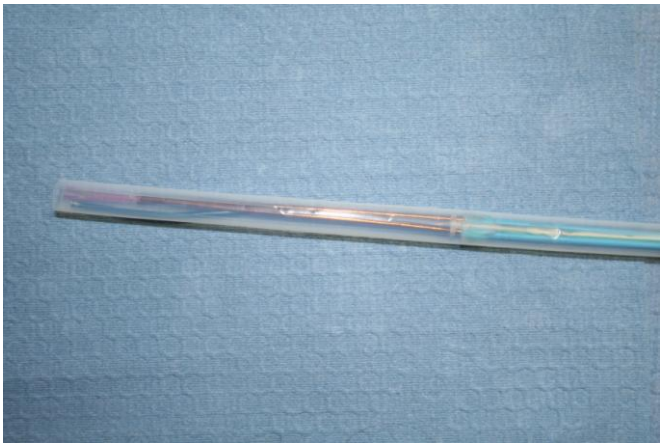

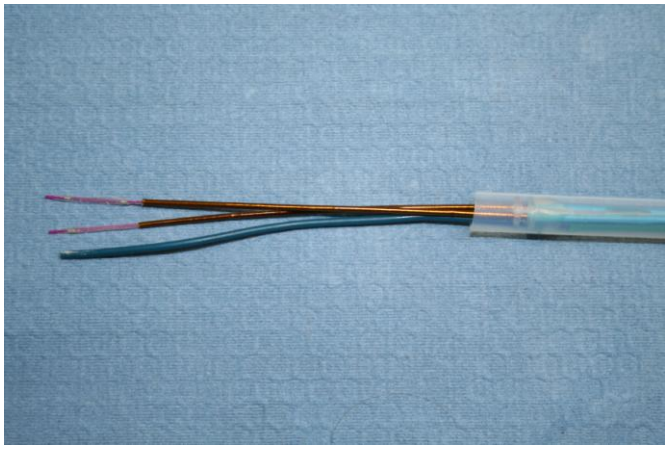

Outer silicone sleeve (clear tube) can be easily retracted over the central delivery catheter. A Central 0.38" core lumen can be seen (blue), as well as the 2 * OTW balloons within the gold polyamide sleeves.

3.3.2.1 ATAG endograft loading instructions

Loading instructions of the PoC ATAG device are demonstrated in Figures 82 a) – d) below:

Figure 82 a) ATAG loading 1

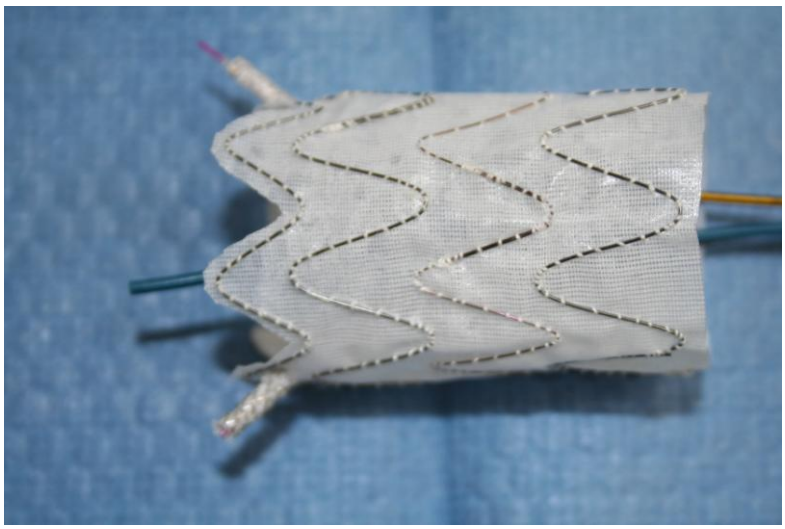

The graft is placed over the central shaft and the OTW balloon push rods are loaded through the coronary sleeves. It must be ensured that the push rods and graft are in the correct orientation (L and R).

Figure 82 b) ATAG loading 2

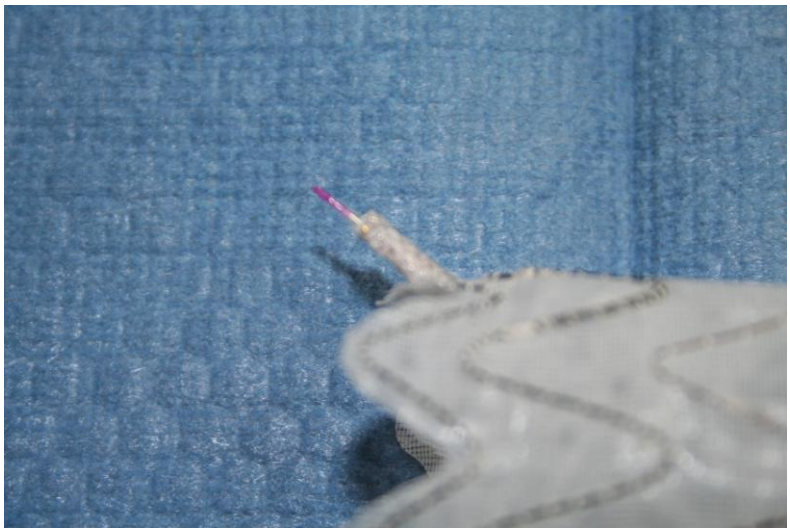

The push rods are positioned so that the balloon collar is around 1mm distal to the sleeve. ATAG coronary sleeve stents are crimped onto the deflated OTW balloon pushrods by hand.

Carefully load the graft by folding the frame inwards from the distal stent, compressing the wave form. With care load each band taking care not to catch the frame on the sleeve or displacing the crimped stents on the side arms or the balloons. Figure 82 c) below shows the ATAG graft frame being folded inwards into the silicone deployment sleeve:

Figure 82 c) ATAG loading 3

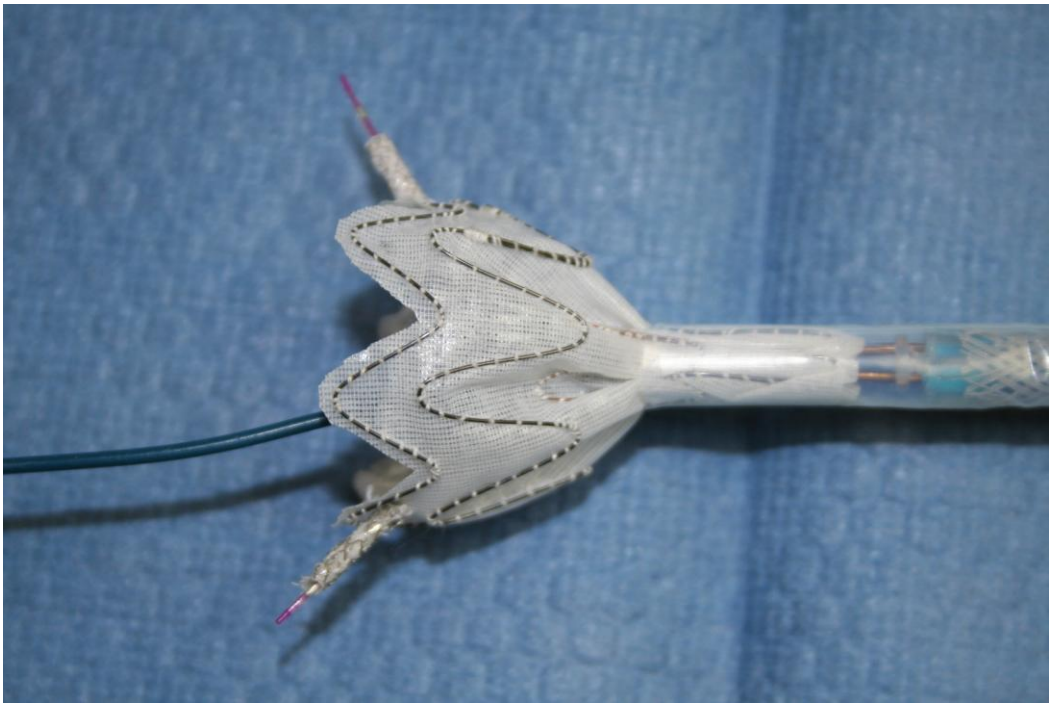

Load the final section of the graft in to the sleeve taking care not to stress the crimped stents on the side arms.

Figure 82 d) below shows the fully loaded ATAG graft taking up the “diving man” position with coronary sleeves facing forwards:

Figure 82 d) ATAG loading 4

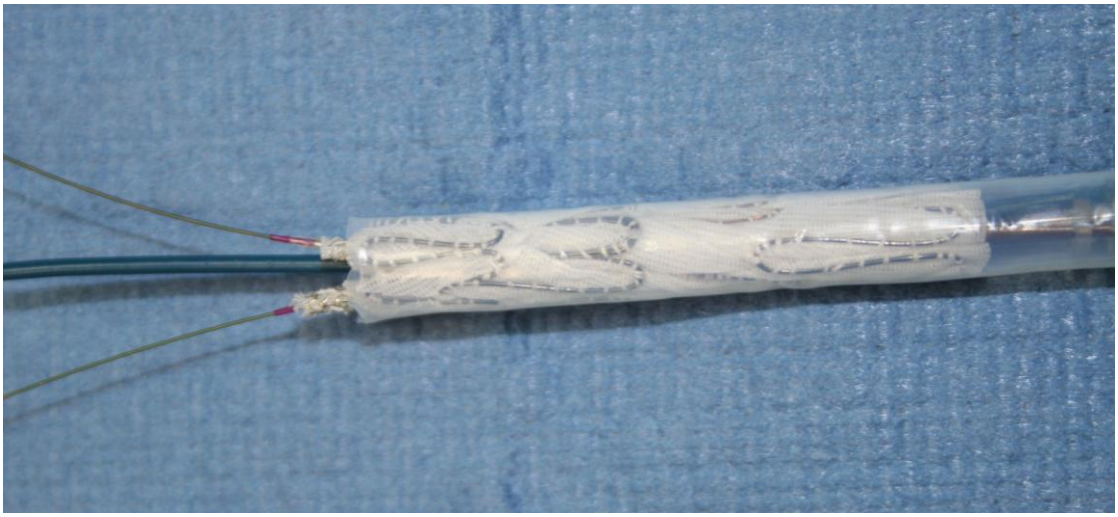

Continue until fully loaded – the coronary sleeves take up the “diving man” position with arms pushed forwards. Coronary 0.014” guide wires (already fixed in RCA and LMCA) can now be fed through the coronary OTW balloons / push rods. The 0.038” superstiff guidewire can then be fed through the central lumen (0.38” wire already fixed in LV cavity). The device is now ready for insertion.

3.3.2.2 Steps of ATAG deployment

Figures 83 a) – d) detail the steps of ATAG deployment from within the stowed delivery sheath, once the device has been advanced to the implantation zone within the aortic root:

Figure 83 a) ATAG deployment

Retraction backwards of silicone delivery sheath 10 mm to allow the coronary sleeves to move towards the LMCA & RCA

Figure 83 b) ATAG deployment

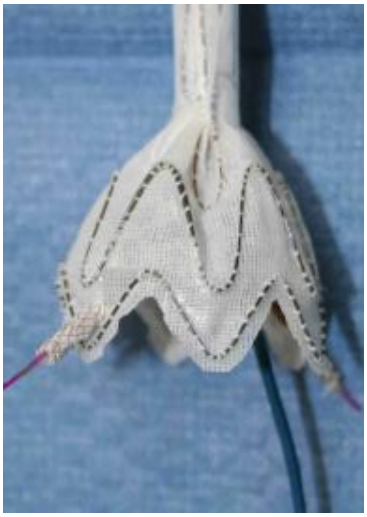

Further retraction of the outer sleeve, the coronary push rods and balloons are pushed forwards engaging the stents within the LMCA and RCA. The LMCA balloon is then inflated to fix the LMCA stent sleeve in position, before being repeated on the RCA.

Figure 83 c) ATAG deployment

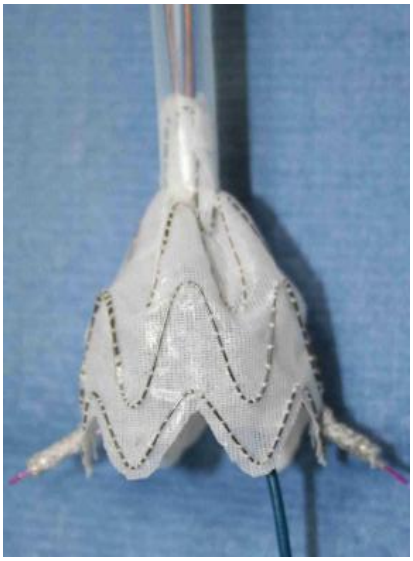

With the LMCA and RCA coronary sleeves and stents deployed, further retraction of the outer sleeve releases the ATAG

Figure 83 d) ATAG deployment

Deployment of ATAG and removal of the delivery sheath

3.3.2.3 Proof of concept ATAG device build conclusions

The manufactured PoC ATAG graft fulfilled our design output specification, accepting that it has some deficiencies and simplifications, that will need to be optimised later in the device development process.

Likewise the delivery system is simple, but would appear to have all of the necessary components to enable successful proof of concept within a bench test glass aorta.

3.4 PoC ATAG *in vitro* testing (glass model)

Having detailed both device and design specification, and built a prototype device satisfying the output specification for the PoC ATAG endograft and delivery system, it was now time to test whether I could truly prove the concept by implanting percutaneously a branched aortic endograft with 2 coronary sleeves into a normal sized glass model aortic root from femoral access over the wire using a percutaneous delivery system firstly under direct vision and then under fluoroscopic guidance.

3.4.1 Aim

To prove the concept of whether delivery of the PoC ATAG "inverted t-shirt" graft (main aortic body with 2 coronary sleeves as described in 3.2) with delivery system is feasible in a glass aorta model under both direct vision and fluoroscopy.

3.4.2 Methods

The test rig comprised a "normal" sized adult male glass aortic model (Farlow Scientific, California, USA) from the LVOT to the femoral arteries. The model was then fixed to hardboard. The delivery was performed in air without fluid flow which would overcomplicate this first PoC. Deployment would first be performed under direct vision, and once practiced, repeated under fluoroscopy in a similar manner.

3.4.3 Results

3.4.3.1 Results in glass model under direct vision

Standard 130 cm x 0.014" coronary guide wires were delivered via at Judkins left 4 (JL4) catheter to the LMCA, and via a Judkins right 4 (JR4) catheter to the RCA from access within the right femoral artery. These guide wires were then "clamped" at the coronary arteries so that they would not retract on insertion of the ATAG device. A 130 cm x 0.038" Amplatzer Superstiff wire was then placed through the aortic valve and into the "left ventricle" where it was secured. Figure 84 a) – g) show the stages of ATAG deployment in the glass model.

Figure 84 a) ATAG PoC deployment 1

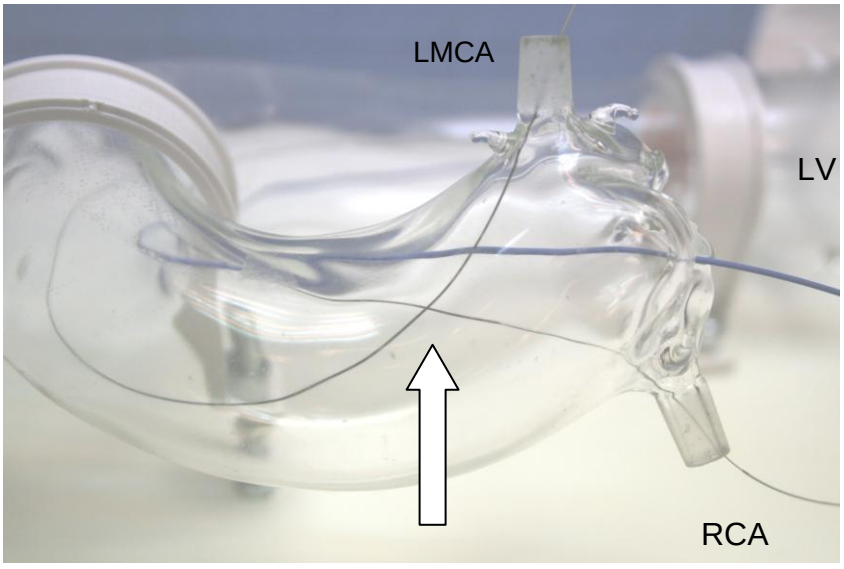

The left coronary wire at 12 o'clock in the picture hugs the "outer" curve of the aorta in the arch segment, while the RCA guide wire at 5 o'clock hugs the inner curve leading to a crossing point in the centre of the aorta about 2cm above the coronary arteries (arrowed). This must be "uncrossed" if the ATAG is to be delivered without complication. In addition the position of the LV wire has important implications for technique used to "unwrap" the LCA and the RCA wire.

Figure 84 b) ATAG PoC deployment 2

With the wires in position (LMCA, RCA, and LV) all 3 wires are then fed into the stowed ATAG device outside of the patient / glass model.

It is vital at this point that the marked guide wires are inserted into the correct side and that there is no visible wrapping of the wires. Once the device is loaded upon all three guide wires with both distal wire fixation (clamped) to avoid retraction and proximal wire fixation by operator assistant the ATAG within delivery catheter is advanced up the descending aorta, and around the aortic arch. See Figure 84 c) below:

Figure 84 c) ATAG PoC deployment 3

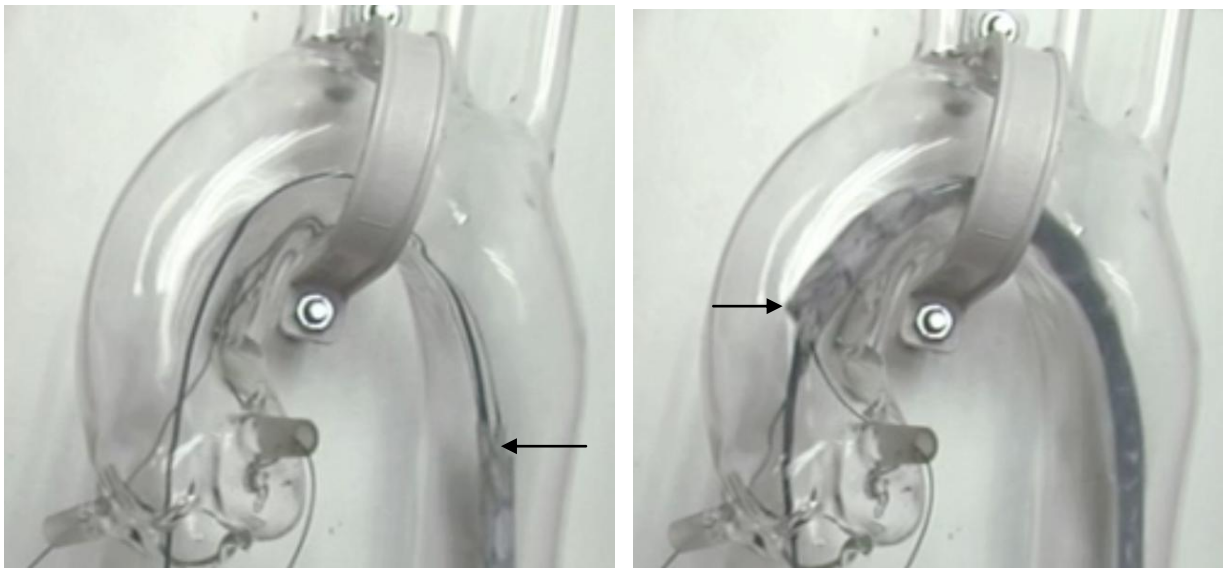

ATAG device on guide wires advanced around arch and towards landing zone (arrows denote proximal end of ATAG device)

ATAG is then pushed into the ascending aorta just above the “landing zone”. At this point because of wire wrap visually it was obvious that the device would advance no further and as such the central LV wire was withdrawn from the LV and back into the central lumen of the delivery catheter. The delivery catheter was then rotated 180 degrees clockwise to un-wrap the 2 coronary wires before the LV wire was then replaced back into the LV and fixed.

Once the wires are “uncrossed” it is possible to re-advance the ATAG so that the proximal end is within the aortic sinuses, and the coronary sleeves are pointing towards the appropriate coronary ostia, as shown in Figure 84 d) below:

Figure 84 d) ATAG PoC deployment 4

Following the “unwrapping wire manoeuvre”, the ATAG device is advanced forward so that the proximal flared end is within the aortic sinuses and the coronary sleeves are aligned towards the coronary ostia.

Figure 84 e) ATAG PoC deployment 5

The sheath of the delivery system is then partially retracted and the proximal nitinol flared graft self-expands.

It is important to retain position of the graft while the delivery catheter is retracted as there is a tendency otherwise for the graft to move upwards towards the RBCT. The coronary stent sleeves are then advanced by pushing the pushrods into the coronary arteries, to anchor position, and protect coronary artery blood flow. The LMCA is stented first followed by the RCA as shown in Figure 84 f) below:

Figure 84 f) ATAG PoC deployment 6

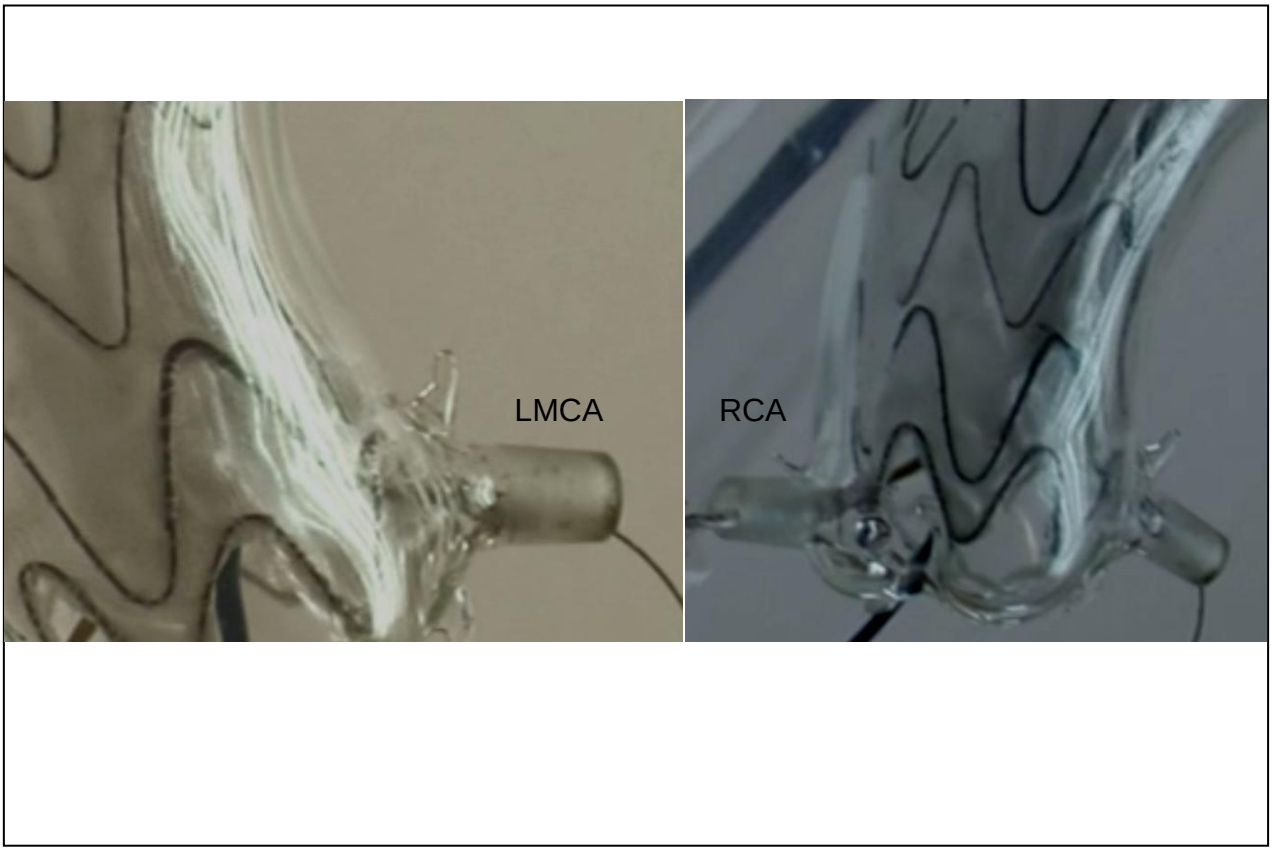

The LMCA sleeve is inserted first, once in position the balloon is inflated to high pressure (18atm) to deploy the integrated coronary sleeve stent. This is repeated for the RCA.

Figure 84 g) ATAG PoC deployment 7

Once the ATAG has been secured proximally with LMCA and RCA coronary sleeves, the delivery system is fully retracted allowing full expansion of the entire ATAG graft. The ATAG delivery sheath is then withdrawn over the guide wires and removed from the glass circulation. Finally the 2 coronary guide wires and the LV guide wires are removed to leave the device in situ. The graft position did not change with removal of the delivery system and the 3 guide wires.

3.4.3.2 ATAG delivery in glass model under fluoroscopic guidance

After numerous “trial runs” to perfect the procedure technique under direct vision it was decided to reproduce the ATAG *in vitro* glass model delivery without flow, but under fluoroscopic guidance. The methods and techniques utilised were identical to that of the deployment under direct vision, but the glass model was covered so that the operator (TK) had to rely upon fluoroscopic imaging in the AP position to guide deployment.

First the 2 coronary guidewires and the LV guidewire were inserted into position and fixed as in the direct vision experiment as shown in Figure 85 a) below:

Figure 85 a) ATAG PoC fluoroscopic deployment 1

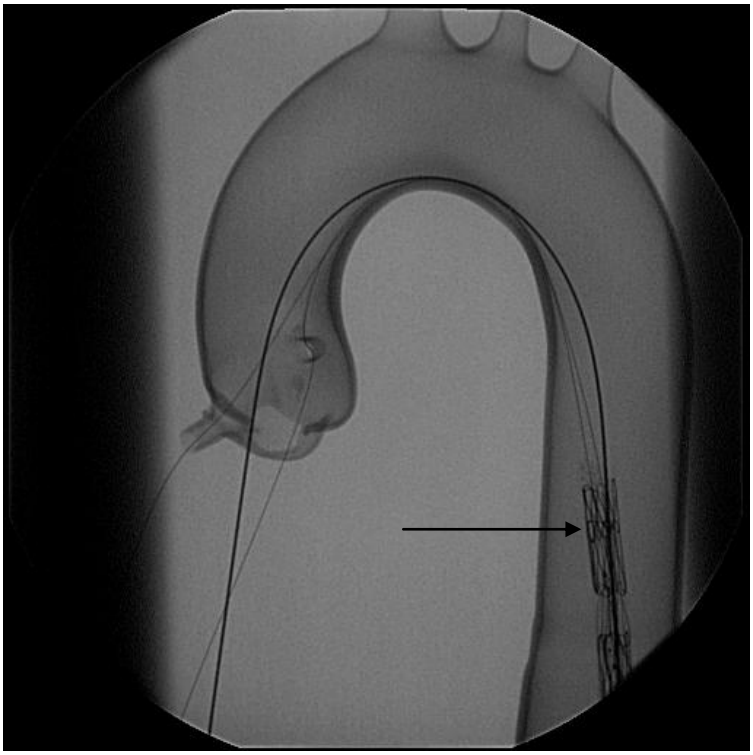

Insertion of RCA and LMCA coronary guidewires (0.014"), and LV superstiff guidewire (0.38"). When the wires are fixed in position the device is loaded on the 3 guidewires and inserted into the model and pushed up into the descending aorta (arrow shows position of ATAG tracking on the 3 guidewires within the descending aorta).

Figure 85 b) ATAG PoC fluoroscopic deployment 2

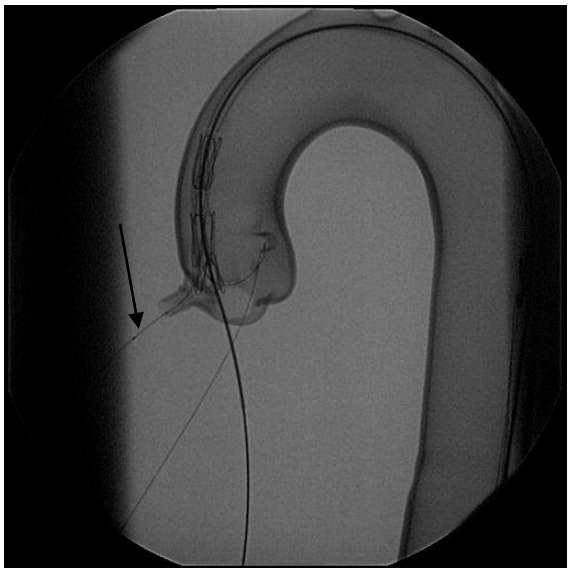

ATAG passed up and over arch under fluoroscopy. It can be seen here that the RCA balloon has moved forward from the crimped stent (arrow), this was rectified by pulling the balloon catheter back approximately 10mm until it was back within the stented portion of the RCA ATAG sleeve.

Figure 85 c) ATAG PoC fluoroscopic deployment 3

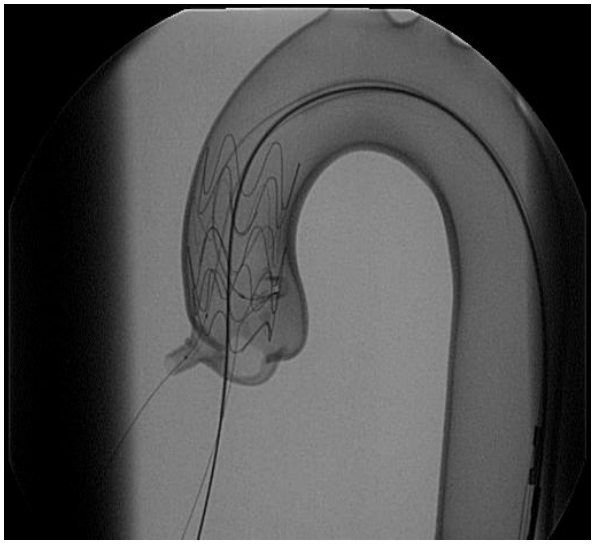

With the wire wrap removed (LV wire withdrawn into delivery catheter, followed by 180 degree clockwise delivery catheter rotation, and replacement of the LV wire) the delivery sheath was retracted allowing self expansion of the nitinol graft.

Figure 85 d) ATAG PoC fluoroscopic deployment 4

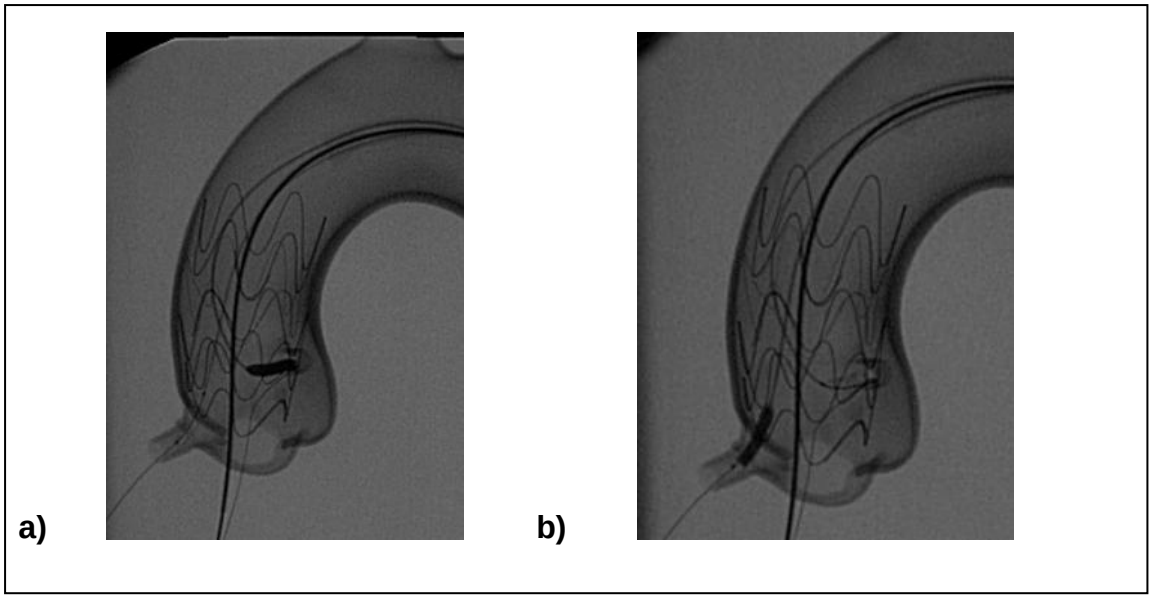

a) The LMCA sleeve balloon was then pushed into the LMCA and inflated, followed by b) similar procedure with the RCA. The silicone sleeve was then fully retracted allowing full deployment of the main ATAG body within the ascending aorta.

Figure 85 e) ATAG PoC fluoroscopic deployment 5

A still image of the final implantation position, with both coronary sleeves implanted into the appropriate coronary ostium, and the ATAG graft in its fully expanded form. The delivery catheter has been retracted into the descending aorta, and the guide wires are still in situ.

For the purposes of this PoC all radiographic acquisitions were performed in the AP position, but it is anticipated that *in vivo* and future implantations multiple imaging angulations will be required to ensure optimal positioning.

3.4.4 Proof of concept Conclusions

I have shown that a self expanding nitinol graft can be manufactured, with a silicone / polyester graft covering and 2 covered coronary sleeves in an “inverted t-shirt” formation. This graft can then be crimped into a 6 mm (18 F) delivery catheter, with a central core guide wire (0.038”) and 2 x OTW balloon push rods. When stowed the device and delivery system can be advanced over 3 fixed guide wires into a glass model vascular system via the femoral artery.

The device and delivery system can be advanced up the aorta and around the aortic arch, to a position 2 cm above the coronary arteries. This is the point at which the LMCA and the RCA guide wires “cross”. Uncrossing requires retraction of the central LV guide wire and then a 180 degree clockwise rotation of the delivery catheter and graft. The coronary sleeves of the ATAG then point towards their respective coronary ostium. The central LV guide wire can then be replaced into the LV before advancing the device to the implantation site.

ATAG implantation is achieved by retracting the outer deployment sleeve allowing expansion of the proximal end of the ATAG graft and the push rods can then be pushed into both LMCA and RCA, followed by further retraction of the sleeve. Once achieved both the coronary push rods are advanced into the coronary ostia and then the balloons

inflated to secure the t-shirt sleeves into the coronary arteries. This process was first practiced under direct vision and then successfully performed under fluoroscopic guidance.

3.4.5 Discussion of PoC ATAG delivery in a glass aorta

The PoC ATAG device has successfully proved that the concept of an “inverted t-shirt” graft with a triple lumen delivery system and coronary push rod sleeves is feasible under both direct vision and fluoroscopy in an air filled normal anatomy glass aorta from the femoral artery with fixed coronary and LV guide wires. There are however a number of important limitations of this testing that must be discussed moving forward to both dynamic flow *in vitro* testing and subsequently *in vivo* testing:

3.4.5.1 Limitations

i) All 3 guide wires were actively fixed in their positions in the LV and 2 coronary arteries. This will not be possible to replicate *in vivo*. The exact forces placed on the guide wires by the delivery system and device must be thoroughly investigated on the benchtop so that guide wires can be designed with specific “holding” features, whether this is a “noodle” wire in the coronary artery, or a “screw in wire” into the LV cavity. I believe that a specific guide wire for the purpose will need to be designed and tested and supplied with the ATAG device. It may well also provide new intellectual property.

ii) The glass aorta was filled with air and not fluid. The graft and delivery system moved very smoothly around the air filled aorta and was lubricated with

silicone oil. In the real *in vivo* situation there will be pulsatile blood flow at around 120 mmHg moving against the device, in a likely atheromatous, tortuous and heavily diseased and irregular aorta. This will provide significant obstruction to the advancing of the delivery system. At the point of implantation I have already eluded to the fact that cardiac output will be temporarily reduced by rapid RV pacing or other means so as to allow the most accurate and precise delivery possible.

iii) The wire crossing is a real technical issue, and while under direct vision it is extremely straight forward to "uncross", it is very difficult under fluoroscopy. One must also bear in mind that the fluoroscopic image was of superb quality as there was no soft tissue to absorb or scatter the x-rays. I do not underestimate the challenge of uncrossing the wires and allowing straight passage of the ATAG device into the landing zone. Work will have to focus on design of the marker aspects of the next generation ATAG and delivery systems to enable exact orientation in 3 dimensions in multiple fluoroscopic views, as once committed to sleeve retraction and coronary implantation one must be sure that all parts of the device are correctly aligned.

iv) The delivery system must allow 1:1 reliable rotational movement of the device i.e. 180 degrees clockwise rotation of the delivery system handle brings about an identical movement of the delivery system tip and ATAG graft, allowing exact and precise changes to orientation. I think also rather like a "trans-septal needle" has an arrow pointing to the relative direction of the puncture needle the ATAG delivery system will also have an arrow informing us of the orientation of the delivery system and device.

v) In an air filled model there was no pressure on the time taken to deploy the graft. In the first *in vivo* cases time will be absolutely critical, as coronary ischaemia time, and rapid RV pacing time must be minimised otherwise cardiac arrest may well ensue and without prompt return of coronary circulation / cardiac output resuscitation may be impossible.

vi) This particular glass model did not have an aortic valve, so it was impossible to determine whether any of the ATAG deployments would have impinged and interrupted the aortic valve integrity, which might lead to severe AR requiring TAVI implantation. The next *in vitro* trials will be performed in a silicone model with intact aortic valve leaflets, so that these questions can be better addressed. As has already been discussed a valved ATAG has also been intellectually protected.

vii) Although macroscopically the ATAG graft looked as though it had been deployed in the "correct" position with the coronary sleeves in the coronary arteries I have no idea as to the potential degree of reduction in coronary blood flow due to the stents / material. The PoC does not provide any indication as to the likelihood of endoleaks acutely which will have considerable bearing on the acute success of the implantation. This work will all need to be covered in further *in vitro* and *in vivo* testing protocols.

3.5 ATAG deployment videos

Videos of both ATAG implantations in the glass model under direct vision, and under fluoroscopy are found in the accompanying CD attached to this thesis.

3.6 Project management, funding, academic collaborations and industrial partners – an update

The ATAG project was commenced in September 2007. At that time Professor Rothman (MTR) and I (TK) formed the clinical team. We were supported financially by £50k proof of concept funding by NHS Innovations London (NHSIL) for the first 12 months. NHSIL also helped us with Intellectual Property management (Dr Andrew McCulloch, AM) and general project management (Dr Torsten Struntz TS).

Following successful proof of concept testing (TK / MTR), NHSIL awarded us a further £75k for further development work of the ATAG 2nd generation (2G) device with the aim of early *in vitro* work. During this period I wrote as co-applicant with Professor Rothman, and was successful in winning an NIHR invention for innovation (I4I) grant for £743,000 over 3 years to allow our development plan to be taken through further *in vitro* assessment, delivery system refinement, and finally *in vivo* animal trials. (Further development plan attached as NIHR application form, within Appendix).

There are 2 major academic collaborators:

i) Professor Stephen Greenwald – QMUL professor of cardiovascular mechanics and an expert in flow rig set up, physiology and testing.

ii) Professor Dan Brockman – Royal Veterinary College (RVC), Professor of small animal surgery, with a special interest in cardiac surgery. I also collaborated with Dr David Connelly a small animal cardiologist with an interest in TOE,

and Mr Michael Boyd who has undertaken many *in vivo* trials at RVC Camden campus.

Torsten Struntz (project manager NHSIL) was appointed ATAG project manager and searched for industrial partners with the expertise in stent design, laser cutting, graft covering materials and development of delivery systems. After consulting and having a number of quotes from the UK, US, and other European companies we felt that Qualimed (www.Qualimed.de) a German company based near Hamburg offered us the best “one stop product development shop”. All further ATAG device development work is directed and driven by TK / MTR in collaboration with Thomas Nissl and the engineers at Qualimed, funded by NHSIL and the I4I grant.

It was always my intention that I would design and produce the 2G ATAG graft, but that all subsequent project work including 3G ATAG, delivery system iterations and *in vitro* and *in vivo* work would be performed by my successor.

Chapter Four

2G ATAG design specification, device build and mechanical testing

Chapter 4 : 2G ATAG specification, build & testing

4.0 2nd Generation (2G) ATAG design specification

Chapter 4 will now build on the experience of the PoC testing and design and specify a second generation (2G) ATAG device. I will then describe the 2G ATAG device build and mechanical testing all performed at Qualimed's facility in Hamburg, Germany.

With the lessons learned from the proof of concept model, financial backing from NHSIL and NIHR, and a commercial engineering collaboration with Qualimed I re-specified the ATAG design brief for the 2G device. Qualimed were contracted to perform the medical engineering work, producing devices to my design specification. I will now describe in detail the deficiencies of the PoC ATAG and potential design iterations for the 2G device.

4.1 Deficiencies of the PoC ATAG and potential 2G iterative improvements

1) The PoC nitinol self expanding frame while adequate in function for the purpose of proving the concept would be unlikely to possess the radial strength necessary to provide adequate proximal and distal seal, and as such I was keen to design a more bespoke nitinol frame that could have radial testing formally performed and ensure that it was comparable to competitor aortic devices. The PoC graft had no

longitudinal stent attachments and as such the graft could shorten or concertina under the compressive forces of delivery.

The PoC graft very labour intensive to manufacture and if this could be mechanised it would make large scale manufacture later in the development cycle more straight forward.

Design iteration for 2G device

2G ATAG would be laser cut from nitinol tubing with a purpose built stent frame design theoretically capable of treating aortic dimensions from 25 mm to 65 mm. It will be designed to have similar radial strength to its competitors (descending thoracic grafts and CoreValve frame), and will be formally tested against commercially available grafts. The stent design will incorporate longitudinal struts to minimise graft shortening.

2) The PoC endograft covering material was too thick for use in the next generation graft and with no vascular regulatory dossier use of this material would be extremely high risk from a regulatory perspective. While both Dacron and ePTFE are utilised in competing grafts in the descending aorta, because of the coronary branch angulation variation, and small coronary vessel size I felt that we should consider a novel covering material that may confer some material advantage.

Design iteration for 2G device

The material investigated for use in this 2G device is electro-spun polyurethane (PU) made by a company in Israel (Nicast, Lod, Israel). They are world leaders in

electro-spinning technology and have a commercially available and CE marked PU product in the vascular domain called AVFlow™. I collaborated with both Qualimed who would design and manufacture the nitinol frame, and Nicast who would coat the endograft with electro-spun PU. I hoped that it might have beneficial effects upon graft stowing, flexibility of coronary angulation, and long term coronary sleeve patency - a concern with small vessel Dacron and ePTFE grafts.

3) The design of the proximal (aortic end) of the PoC endograft is sub-optimal. To allow proximal seal the endograft may benefit from a proximal tri-lobed "flare" engaging the proximal portion into the sinuses of Valsalva, attempting to mirror the native anatomy.

Design iteration for 2G device

The proximal portion of the ATAG will have 3 sinus "feelers" extending into the 3 sinuses of the aortic root, mirroring the anatomy in an attempt to minimise aortic valve incompetence and also attempting to improve proximal sealing to decrease the risk of type I endoleak.

4) The coronary artery branches need to be attached as low down as possible on the endograft so as to minimise aortic valve disruption. The attachment of the coronary sleeves on the PoC model was also inadequate being hand sewn with a join at the ostium of the coronary artery.

Design iteration for 2G device

In an ideal world the coronary sleeves and integrated stents will be "attached" to the main aortic endograft by being electro-spun into a single one piece "t-shirt" configuration.

4.2 General design brief for 2G ATAG

This device specification is planned for implantation into a "normal" sized bespoke manufactured silicone aortic model with functioning aortic valve leaflets (Elastrat, Geneva, Switzerland). Normative values were taken from the paper on aortic sizes published by Parish *et al.* in 2009 (87). The silicone model I developed and Elastrat manufactured had the following diameters as shown in Table 20 below:

Table 20 Bespoke made silicone model aortic diameter

Location	Normal aortic diameter (mm)
Annulus	26
Sinus	34
STJ	29
Ascending aorta	30

Normal aortic sizes taken from Parish *et al*. (87).

4.2.1 Device description

Key feature of the ATAG is the insertion of a covered aortic endograft near the aortic valve. The graft will have covered coronary stents attached to the main graft body (inverted t-shirt configuration) that protect the coronaries and allow perfusion. The important feature is that the main graft stent has a very short proximal section with attachment of coronary stents to minimize interfering with the aortic valve apparatus in the sinuses of Valsalva.

4.2.2 Intended use

The intended use is for a percutaneously delivered stent graft to treat diseases of the ascending aorta. ATAG will need to proactively protect the coronary arteries and maintain the aortic valve competence. The device is intended to treat primarily AAAD in a percutaneous fashion.

4.3 Design requirements

4.3.1 ATAG stent graft main body

Table 21 below shows the ATAG stent graft frame design requirements:

Table 21 ATAG stent graft frame design requirements

Item	Requirements
Description	Self expandable nitinol main body Stent (electro polished) and laser cut
Stent Design:	QM653 – a Qualimed stent frame design
Architecture:	Open cell design, cylindrical with flaring at the proximal end to ensure pressure fit, longitudinal bars to maintain longitudinal position, but allow arch flexibility.
Indicated for diameter	To fit normal aorta bespoke silicone model (Elastrat, Geneva, CH). Data from Parish *et al (87)* Sinus of Valsalva = 34 mm, Ascending aorta 30 mm therefore with 20% over-sizing main endograft 36 mm flaring to 42 mm at the proximal end within sinuses.
Nominal Stent Lengths:	Total stent length 60 mm: 50 mm cylinder, max 10 mm flaring end;
Principle Drawing of Stent design:	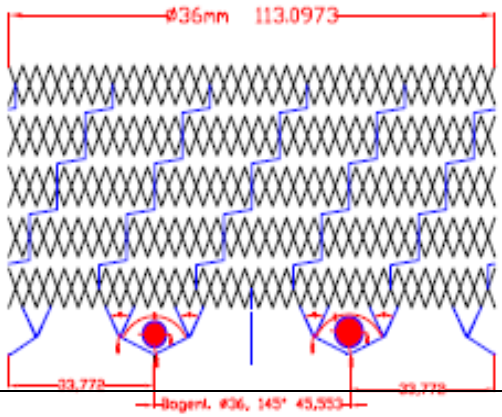
Crimping diameter	Start with 24 F, goal 18 F (stowed graft)
Radial Force:	Radial force has to be at least as high as the force of competitor products
Radio-opacity	The Stent has to be radiopaque; the stent body needs x-ray markers on the proximal “feelers” which facilitate the correct positioning of the proximal portion into the sinuses, as well as distal stent end. The attached coronary side branch stents should also be radio-opaque, and be mounted on balloons with markers 2 rings for RCA and 1 ring for LMCA to allow orientation.

Table 21 ATAG stent frame cont.	
Further mechanical properties	High flexibility: stent has to be able to turn over the arch of the aorta 180° without cracking Flexibility at least as high as competitor products (CoreValve™)
Further important feature	A very short proximal section with attachment of coronary stents to minimize interfering with the aortic valve apparatus in the sinuses of Valsalva

4.3.2 Coronary side branch stents

Table 22 below describes the coronary side branch design requirements:

Table 22 Coronary side branch stent design requirements

Item	Requirements
Description	Balloon expandable Stent (electro polished) stainless steel
Stent design	Qualimed current stent design
Architecture:	Tbc
Indicated for diameter	3.5 mm RCA, 4.5 mm LMCA Coronary sleeves will be attached at an angle of 150 degrees to one another
Nominal Stent Lengths:	8 mm
Foreshortening	max. 5% (Current coronary Stents 3 mm on the market shortened during expansion by 0 – 7.8% [Schmidt et al 2005 (Biomedizinische Tech)]
Recoil (mean value):	Recoil should be within the range of current coronary stents (max 5%)
Radial Force:	Higher than QualiMed in-house set target due to accomplished benchmark: ≥ 1500 mN for an 18 mm long Stent

4.3.3 Graft material

4.3.3.1 Electro statically spun Polyurethane (PU)

Unlike PET and ePTFE, PU's are a complex and diverse group of related compounds. PU's can be rigid or soft, depending on their composition. Electro-spun PU is a fibre forming polymeric material. Electro-spinning involves giving a polymer in solution an electrostatic charge and releasing this solution in a jet fired at a moving grounded structure (in this case the stent placed onto a mandrel). The jet accelerates and is thinned by the electric field and results in small diameter filaments that collect as a non-woven fabric on the grounded structure by evaporation of a solvent.

Graft porosity depends upon the angle of winding, pitch angle, thickness of the filament and number of layers. There are currently no endografts utilising PU as a covering material, and historically PU's in vascular prostheses have failed because of biodegradation. More recently in PU's such as *Chronoflex*^{TM} (Polymedica, Woburn MA), the polymer chain sites deemed at risk of cleavage are replaced for chemical groups resilient to degradation. Given the potential disadvantages of both PET and ePTFE as already documented I felt from an early stage exploring a novel cardiovascular graft material that may have properties more suited to the ascending aorta and the aorto-coronary junction might provide part of the answer to developing a successful branched stent graft in the ascending aortic position.

The theoretical advantages of PU for ATAG are as follows:

PU can be spun very thin (<100 μm), yet be extremely strong and robust. PU can also be designed to be less rigid than both PET and ePTFE, and therefore conform more smoothly to the curvature of the aorta. Being more conformable and elastic may provide advantages at the coronary ostia with regard to being able to treat more variability of coronary angulation. Electro-spinning can create multi-porosity layers throughout the graft material, with differing pore sizes and different permeability on the luminal and aortic surface.

I do not under-estimate the potential work involved within this experimental process, but Nicast (Lod, Israel) our PU industrial partners are a world renowned PU electro-spinning company who already have a commercially available PU vascular graft (AVFlo) - a haemodialysis implantable fistula membrane which means that much of the regulatory and manufacturing know how has already been overcome. Table 23 below details the ATAG graft material design requirements:

Table 23 ATAG graft material design requirement

Item	Requirements
Description	Electro spun medical grade polyurethane by Nicast (Lod, Israel)
Raw material	Medically biocompatible polycarbonate urethane
Material thickness	Aim for <100 microns if possible.
Joint method	Coronary arms to be electro spun by Nicast and then attached by glue to the main graft body in the first instance.

4.3.4 2G ATAG delivery system

Before formal *in vitro* flow rig or *in vivo* testing of the 2G ATAG device, a 2G delivery system must be developed. While this development is beyond the scope of this thesis, I expect it to possess all of the basic components of the PoC delivery system, but have a lower profile, be more flexible, have 1:1 torque characteristics allowing delivery to be more precise, accurate, controllable and less traumatic to the native aorta.

4.3.5 ATAG 2G Design specification conclusions

The 2G ATAG has been designed to be delivered and tested in a normal sized bespoke made aortic silicone model with “functional aortic valve”. As the device and the delivery system improve this silicone aorta can be integrated into an *in vitro* pulsatile flow rig.

The 2G endograft has a number of design improvements compared to the PoC device. These include:

i) Laser cut electro-polished nitinol frame with higher radial strength, built in longitudinal tie bars to prevent stent longitudinal shortening.

ii) A novel thin electro-spun PU endograft covering.

iii) A tri-lobed flared proximal portion to sit more naturally within the sinuses of Valsalva.

iv) Coronary sleeves to be electro-spun in a similar fashion to the endograft and these to be attached low down on the body frame to minimise disruption of the aortic valve.

4.4 2nd Generation ATAG build and stent body mechanical testing

Qualimed have a very experienced team of medical device engineers that have previously developed similarly sized stents for non-cardiovascular applications namely the trachea and oesophagus. They have also developed a number of bare metal, drug eluting and biodegradable coronary stents. They are highly experienced in regulatory approval and their unit near Hamburg, Germany has all the necessary developmental, testing, manufacturing, and CE mark approvals facilities.

This section describes the mechanical properties of nitinol, setting the scene for the 2G ATAG build and radial strength testing of the evolving 2G device. I performed all of the testing documented at Qualimed's facility in Germany.

4.4.1 The properties of nitinol and radial strength testing

Nitinol (Nickel-Titanium alloys) exhibit a combination of properties which make these alloys particularly suited to self-expanding stents. Nitinol stents are manufactured to a size slightly larger than the target vessel and crimped down into a delivery system of relatively small diameter. After deployment they position themselves against the vessel wall with a low chronic outward force. They resist radial compression forces.

4.4.1.1 Super-elasticity and shape memory in Nitinol

Super-elastic nitinol appears macroscopically to be very elastic. However the mechanism of deformation is different from conventional elasticity. When a stress is applied to nitinol, and after a modest elastic deformation the material yields to its applied stress by changing its crystal structure. When the stress is removed the material recovers its original shape and crystal structure.

Shape memory is a result of thermal phase transformation. When super-elastic nitinol is cooled to below a critical temperature (the transformation temperature, which is dependent on alloy composition and processing) it also changes its crystal structure. The material can be plastically deformed in the low temperature phase, but the original shape can be restored by heating above the transformation temperature. Self expanding nitinol stents are manufactured with their transformation temperature set to around 30 degrees centigrade (^{o}C). They can easily be crimped at low temperature into a delivery system, and upon delivery to the vascular site (temperature 37 ^{o}C) the stent expands to its original dimensions and conforms to the vessel wall.

4.4.1.2 Material considerations

Nitinol is an alloy composed of 55% nickel and the remainder titanium. The properties of solid state transformation which can be triggered thermally or mechanically is dependent on the composition and processing of the material and adds a further layer of complexity to material composition, specification and subsequent properties.

4.4.1.3 Biocompatibility and corrosion

Nitinol requires controlled processing to achieve optimal shape memory and super-elastic properties. In 1999 the medical community and device industry were alerted to the issue of corroded nitinol graft scaffold (131). To prevent nickel corrosion *in vivo* it is now generally accepted that nitinol is electro-polished.

4.4.1.4 Material specific device characteristics

The most unusual property of nitinol alloys is *stress hysteresis*, which results in a device feature termed *"biased stiffness"*. This phenomenon is explained in the following stress / strain curve derived from a crimping / deploying cycle of a nitinol stent graft as described in Figure 86 below:

Figure 86 Hoop force curve for stowing and then expanding a nitinol endograft

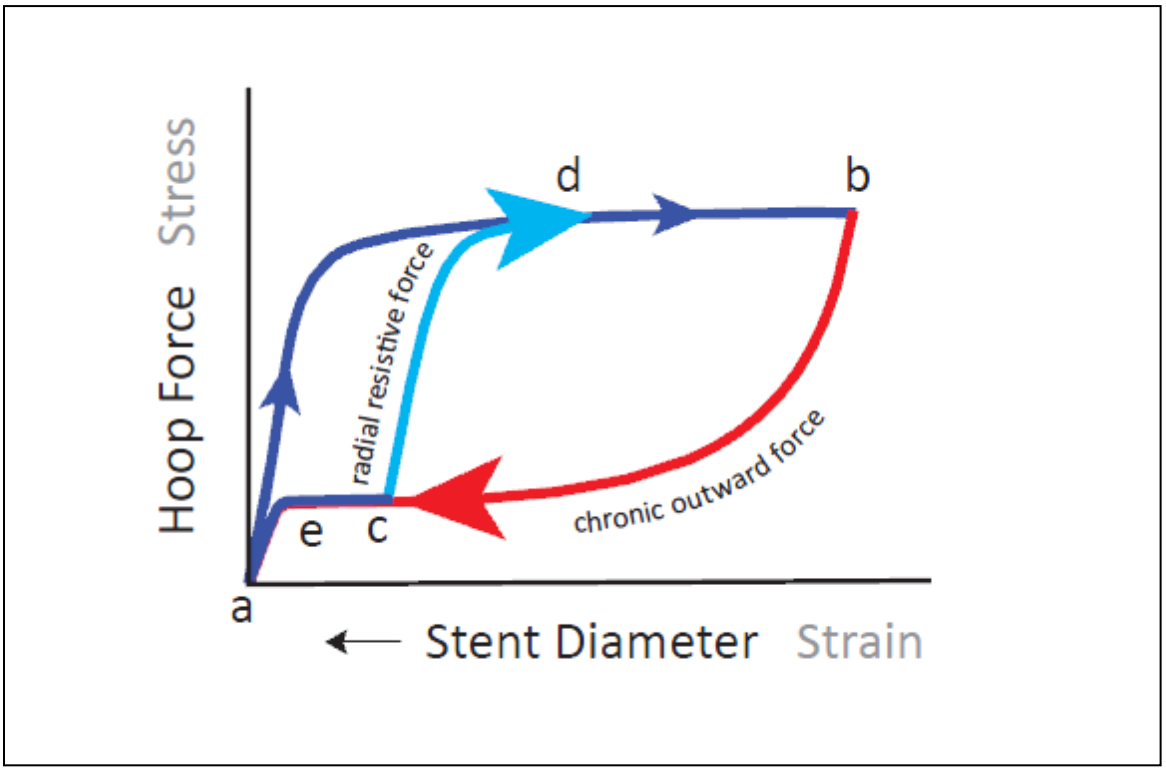

Note the x-axis is reversed i.e. increasing stent diameter from right to left. A stent of a given size larger than the vessel (point a) is crimped into a delivery system (point b, having followed the dark blue curve). After insertion into the target site the stent expands (along the red curve) until it opposes the vessel (point c). At this point further expansion of the stent is prevented. Since the stent did not expand to its pre-set shape it continues to exert a low outward force termed *chronic outward force*. It will resist recoil pressure, or external compression forces with forces dictated by the loading curve from point c to d, termed radial resistive forces (132).

The hoop force curves will be presented for the ATAG 2G graft and competitor endografts later in this section.

4.4.2 Radial strength testing

Given the problems experienced with relative poor radial strength in the PoC, in association with our engineering partner Qualimed, it was decided to perform a first 2G ATAG manufacture run purely to test whether the graft body had the appropriate radial strength when compared to competitor devices.

Following the original ATAG specification document Qualimed made the first prototype laser cut nitinol stent frame from 5 mm hollow nitinol tubing. Only the graft body was cut (without proximal flare) and was 36 mm in diameter (30 mm + 20% over sizing), picture shown below in Figure 87.

Figure 87 First Qualimed laser cut ATAG body frame

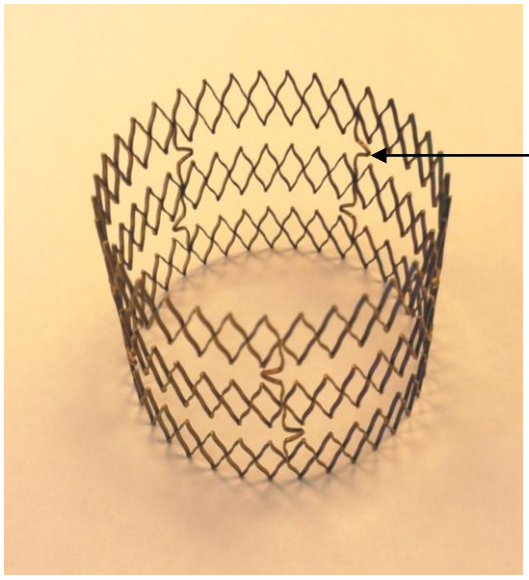

The first 2G ATAG design consisted of 3 closed cell rings joined by 5 “tie bars” (arrowed) which give longitudinal strength but allow for flexibility of the graft during delivery around the aortic arch.

For the purposes of radial strength testing the middle ring was used although it was still attached to the outer rings by longitudinal tie bars.

4.4.2.1Aim

To test the radial strength of the ATAG nitinol cut stent frame body against competitor devices:

i) a descending thoracic stent graft (Medtronic Talent graft) and

ii) the CoreValve aortic re-valving system ™ nitinol frame.

4.4.2.2 Methods

The constriction (hoop strength) method is a standardised method to determine the radial strength of stent grafts by applying a traction force to a flat collar around one segment of the stent. The temperature for this procedure has to be physiological (37°C). The force necessary to constrict the stent to 75% of the original diameter is called radial force. It is measured in milli Newton (mN). The hoop strength testing rig set up is shown below in Figure 88.

Figure 88 Radial hoop strength testing rig

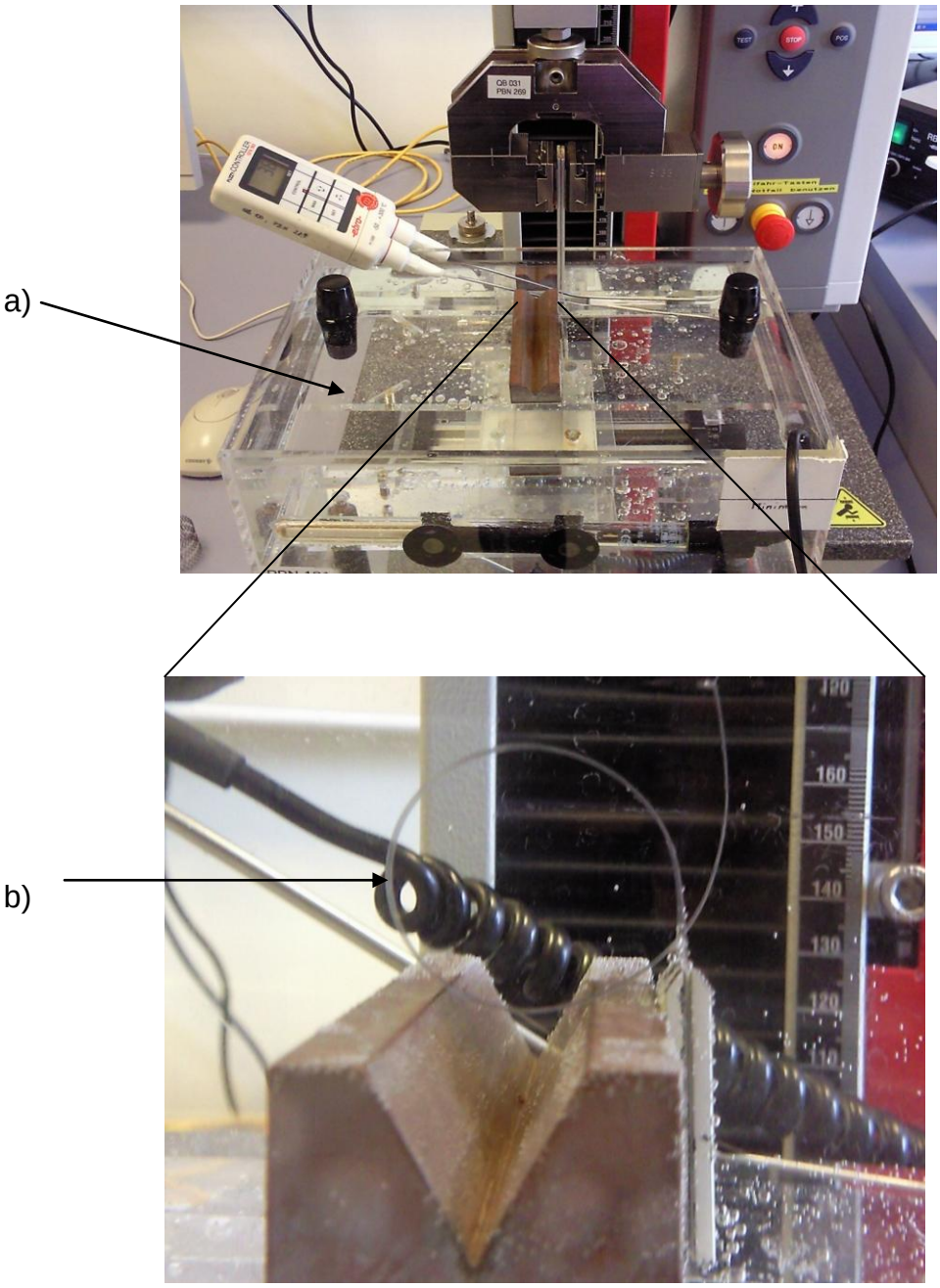

Radial strength testing performed in a water bath (a) at 37°C, using the constriction loop method (b). The loop is wrapped around the stent, while one end is clamped in a jaw, the other attached to the bottom of the water tank. The jaw is moved upwards with a velocity of 50mm / min until the stent diameter is 25% of its unloaded diameter ($d_{initial}$). This characteristic point is reached, when the jaw has pulled the collar by an amount of $\Delta L=0.25*\square*d_{initial}$.

The computer records the data from the force measuring station. A chart showing the radial force versus elongation of the collar is automatically generated. Table 24 below shows the hoop strength rig set up:

Table 24 Hoop strength set up

Initial Stent diameter	36 mm
Width of constriction hoop	20 mm
Constriction	25%
Change in length	27,5 mm ($\Delta L=0.25*\pi*d_{initial)}$
Jaw velocity	50 mm / min
Load at start	0.1 mN
Temperature	37°C (water tank)

Full macroscopic and microscopic photographic documentation of the first ATAG stent frame, the Medtronic Talent stent, and the CoreValve re-valving system ™ frame can be found within the Appendix.

4.4.2.3 Radial strength testing results

For each of the grafts tested a hoop force curve is produced. Measurements were repeated at least twice and an average hoop force measurement calculated.

The average hoop force for each graft is important, but more information about the stiffness and graft characteristics can also be measured from the graphs. For each graft test I have then measured from the graph the force required to deform the stent 10%, and 20% of the diameter, and then on the re-expansion curve (the lower of the 2 curves) the amount force that the graft is still exerting at 20% and 10% constriction – this gives an indication of the amount of chronic external force that the graft might impart upon the vessel wall if oversized by 20% and 10%, as is the current standard in aortic stenting.

Hoop force curves, and the subsequent 10% and 20% analyses are shown in Figure 89 a) and b) for the 2G ATAG, Figure 90 a) and b) for the Talent graft, and Figure 91 a) and b) for the CoreValve system below:

Figure 89 a) Radial Strength of centre ring portion of ATAG graft

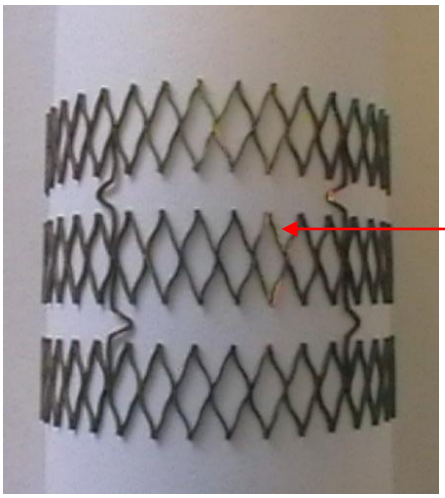

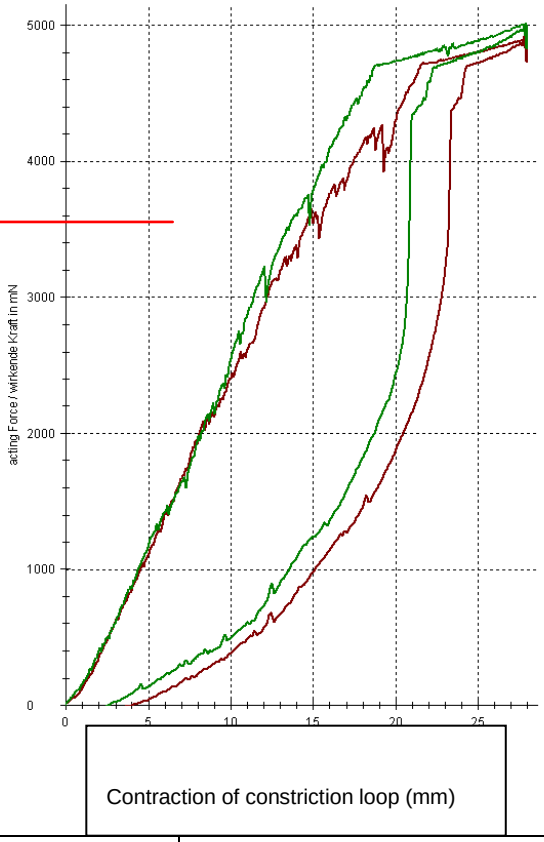

Legende	Nr	Radial Force mN	Remarks/Bemerkungen
	1	4921	Ø - Reduction/Reduzierung 2
	2	5009	Ø - Reduction/Reduzierung 2

Force required to achieve 25% graft diameter reduction.

Mean value = 4965 mN

The x axis here denotes the contraction in mm of the constriction loop. The y axis is the force required to bring about this constriction and is measured in mN. The axis labels for all other graphs are similar.

Figure 89 b) Radial Strength of centre ring portion of ATAG graft

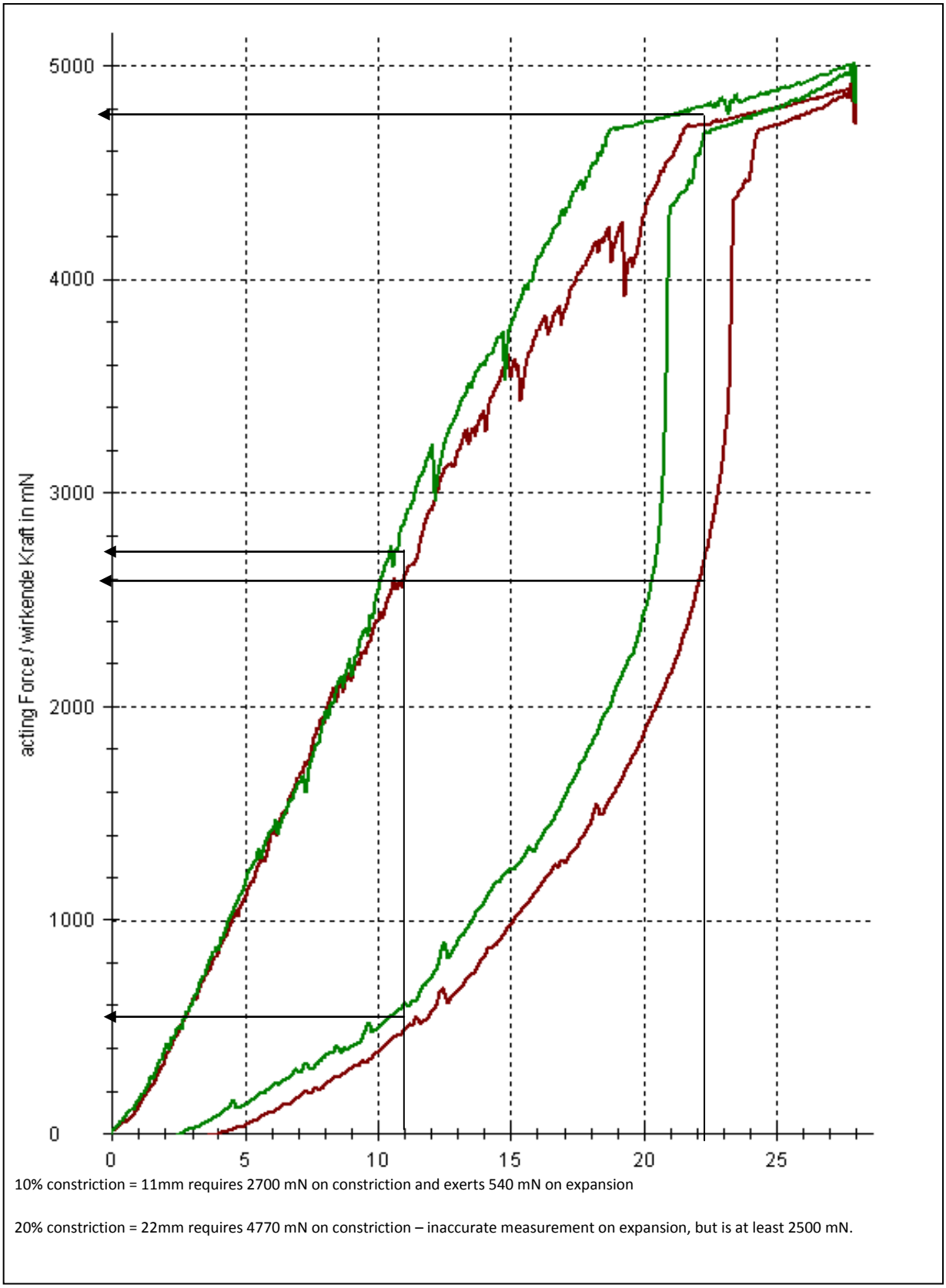

10% constriction = 11mm requires 2700 mN on constriction and exerts 540 mN on expansion

20% constriction = 22mm requires 4770 mN on constriction – inaccurate measurement on expansion, but is at least 2500 mN.

Figure 90 a) Radial Strength of Medtronic Talent graft (with Dacron woven covering)

Constriction of the 2nd distal segment

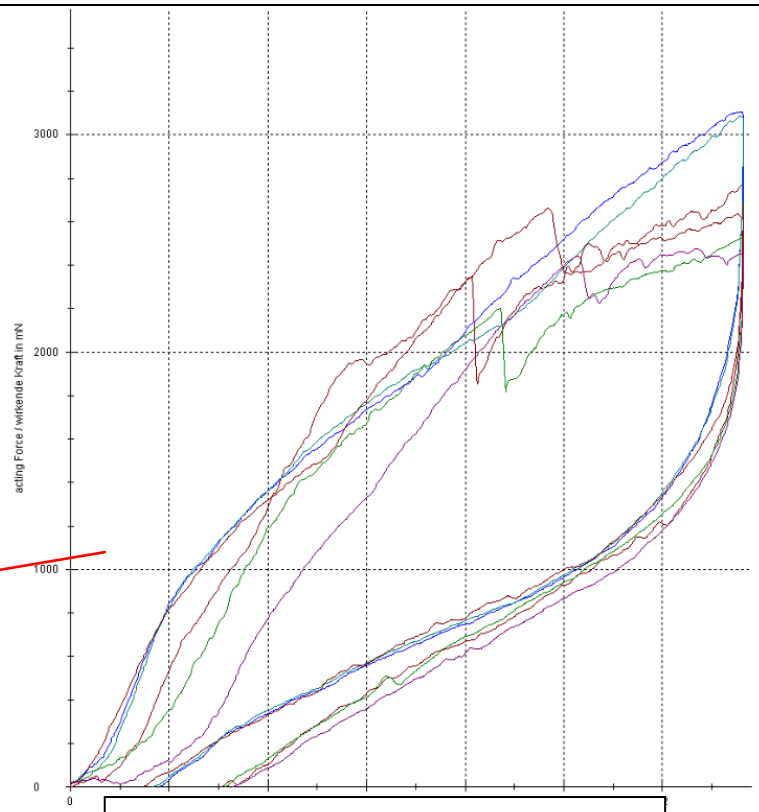

Legende	Nr	Radial Force mN	Remarks/Bemerkungen
	1	2770	Ø - Reduction 25%_Ø 17,38_2nd segment distal
	2	2525	Ø - Reduction 25%_Ø 17,38_2nd segment distal
	3	3106	Ø - Reduction 25%_Ø-17,38_2nd segment distal_90° rotation
	4	3086	Ø - Reduction 25%_Ø 17,38_2nd segment distal_90° rotation
	5	2476	Ø - Reduction 25%_Ø 17,38_2nd segment distal_180° rotation
	6	2660	Ø - Reduction 25%_Ø 17,38_2nd segment distal_180° rotation

Force required to achieve 25% graft diameter reduction.

Mean value of 6 measurements = 2771mN

Figure 90 b) Radial Strength of Medtronic Talent graft with Dacron covering

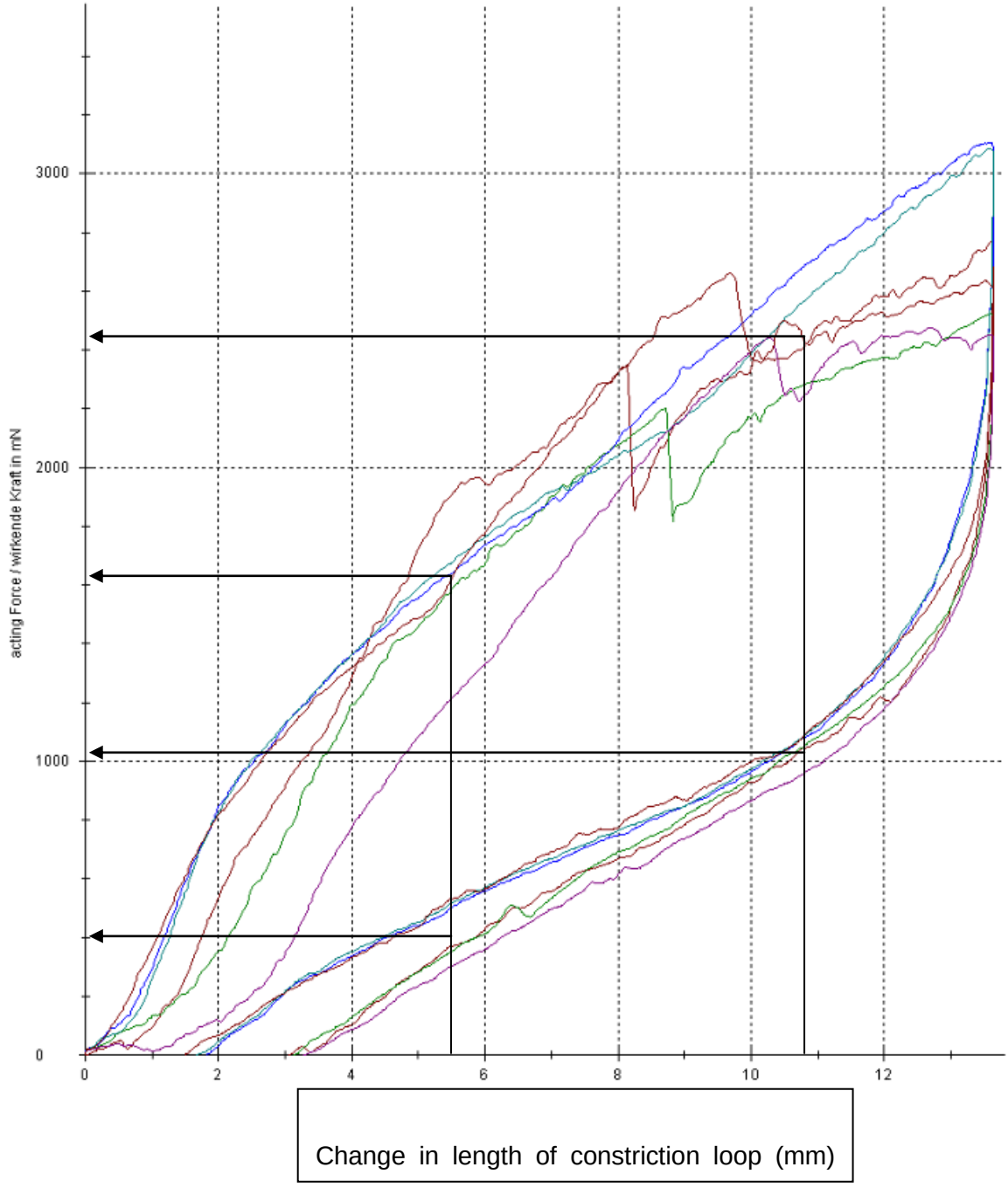

10% constriction = 5.4mm requires 1620 mN during constriction and 400mN during expansion

20% constriction = 10.8mm requires 2430 mN during constriction and exerts 1020 during expansion

Figure 91 a) Radial Strength of Corevalve Re-valving TAVI system Nitinol frame

Constriction at the smallest diameter

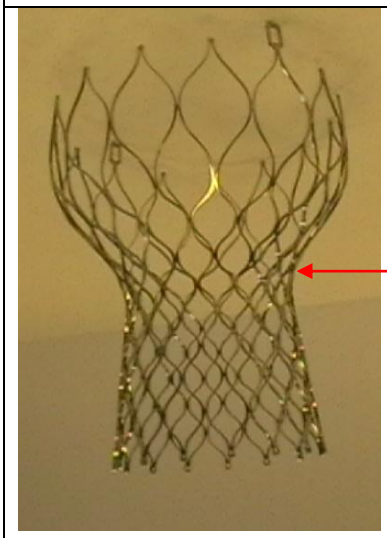

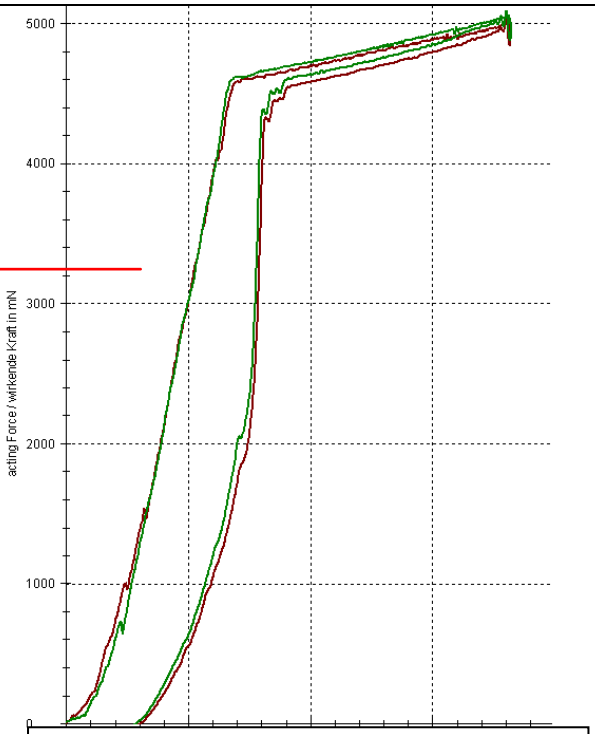

Legende	Nr	Radial Force mN	Remarks/Bemerkungen
	3	5030	Ø - Reduction/Reduzierung 25%
	4	5095	Ø - Reduction/Reduzierung 25%

Force required to achieve 25% graft diameter reduction.

Mean value of 2 measurements = 5063 mN

Figure 91 b) Radial Strength of Corevalve Re-valving TAVI system Nitinol frame

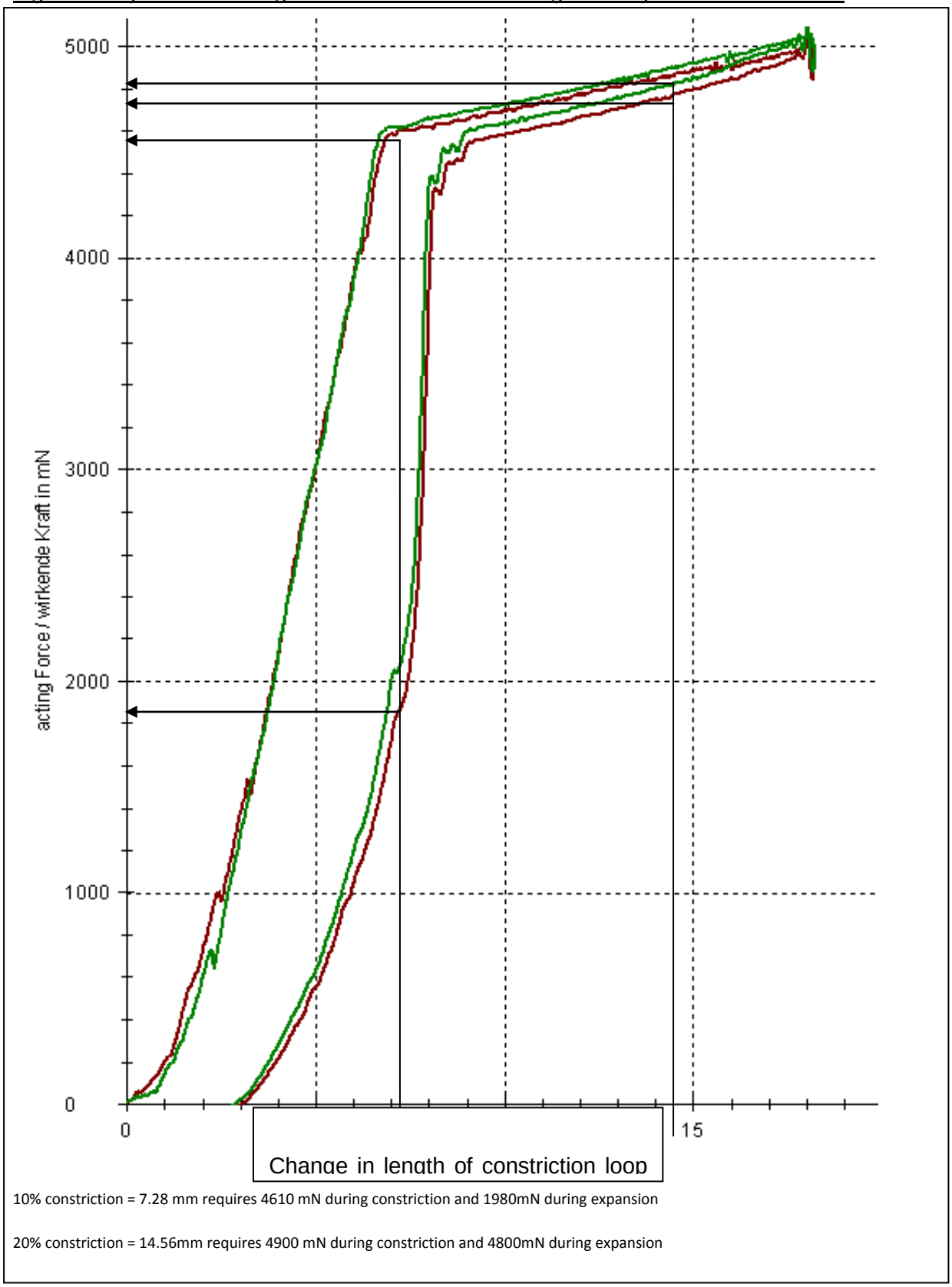

10% constriction = 7.28 mm requires 4610 mN during constriction and 1980mN during expansion

20% constriction = 14.56mm requires 4900 mN during constriction and 4800mN during expansion

Constriction testing was only possible at the smallest diameter of the Corevalve frame (the area aligned to the coronary arteries – as the constriction loop would slip from all other positions)

4.4.2.4 Conclusion

When only the force needed to deform the stents by 25% of their diameter is taken into account the basic 2G ATAG (4965 mN) would seem to have a similar radial strength to the CoreValve™ nitinol frame (5063 mN), and nearly twice the radial strength of the Medtronic Talent graft (2771 mN). In terms of adequacy of radial strength to oppose the arterial wall it would seem that the current ATAG stent design has sufficient hoop strength when compared to the most anatomically similar device on the market (CoreValve™).

These values alone however do not reveal the full picture. The shapes of the curves are also important, and inside the real patient's aorta it is the re-expansion profile (i.e. the lower curve) force that will be exerted chronically on the aortic vessel wall. It is the relative stiffness that affects the shape of these curves with the CoreValve™ being stiffer than both the ATAG and the Talent graft. This relatively increased stiffness can be attributed to the frame design of the CoreValve™.

As can be seen in Figure 92 below the CoreValve has a completely closed cell structure, compared to the more open ring structure of the ATAG with longitudinal tie bars. It is this closed structure that gives the CoreValve its radial strength, particularly at its mid-point which is not in contact with the aortic wall, but instead takes up a concave shape opposite the coronary arteries.

Figure 92 Medtronic CoreValve™ frame

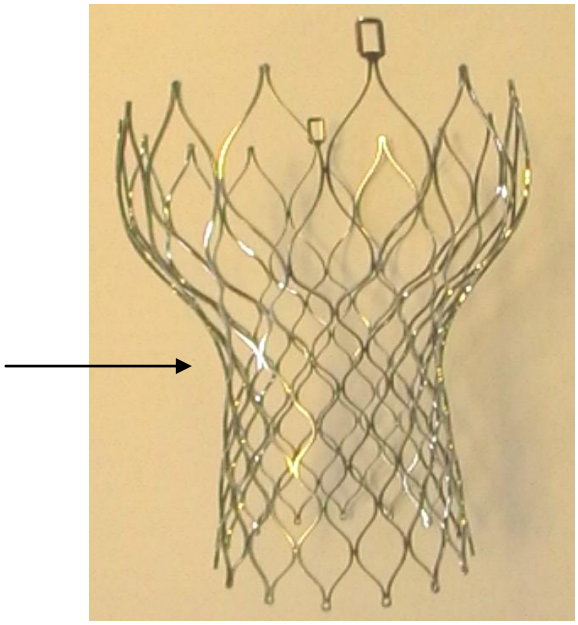

The CoreValve frame is completely closed cell and the mid portion, which is not in contact with the aortic wall has the highest radial strength (arrowed)

When we compare the CoreValve to the ATAG and the Medtronic Talent graft we see obvious differences. The basic 2G ATAG has 3 rings which are joined by 5 tie bars, when testing radial strength on the middle ring therefore the tie bars enable the 2 circumferential rings either side to impart additive radial strength. In comparison the Talent graft which has a longitudinal bar running the entire graft length attached to the material and then to the circumferential rings. As such any force measurement is provided predominantly by the ring around which the hoop is attached. It is possible that the Dacron material attached to the Talent graft could provide some additional radial strength as like the tie bar it allows some transmission of the hoop forces onto the circumferential nitinol rings at either side of the one being tested. Figure 93 below highlights the longitudinal design differences between the 2G ATAG and the Talent graft:

Figure 93 shows 2G ATAG and Talent graft

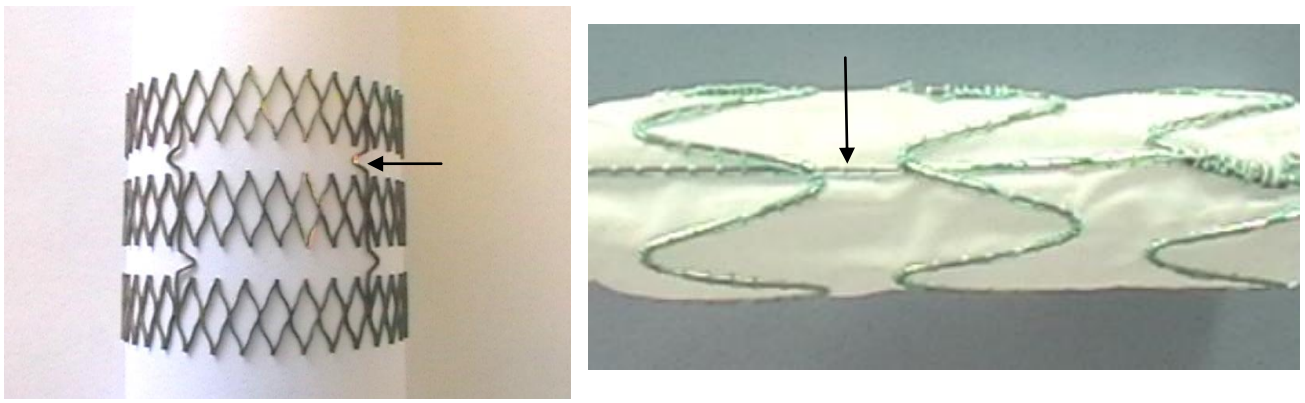

ATAG basic graft (left) with 3 circumferential rings and 5 longitudonal tie bars (arrowed on left). The Talent graft (right) is sewn onto a Dacron graft which also has a single longitudinal bar (arrowed on right) sewn along its length to give it longitudinal strength and prevent longitudinal shortening / concertina effect.

As mentioned above, the shape of the force / deformation curves is also important, particularly on the re-expansion profile as for instance the 20% re-expansion profile (measured from the graphs) essentially mimics the implantation of a 20% oversized endograft into a target vessel. As can be seen from the relative data the stiffest device the CoreValve still exerts an outward force of 4800 mN when deformed by 20% on the re-expansion phase. It is important to stress that this part of the CoreValve is not in contact with the aortic wall.

At 20% re-expansion the ATAG exerts at least 2500 mN, and the Talent graft 1020 mN against the aortic wall. At this early stage of the 2G device development I think it can be reasonably concluded that the 2G ATAG radial strength is sufficient to prevent vascular recoil, but the exact nature of forces involved is highly dependent on stent design, nitinol properties and chemical treatments. It is important as we proceed with ATAG design

iterations to keep all of these mechanical characteristics in mind, ensuring that while the radial strength of the ATAG is adequate it does not expose the already diseased aortic wall to additional long term stress and strain.

4.4.3 2G ATAG stent graft manufacture with 3 semi-lunar "feelers"

The simple 3 ringed ATAG body stent with 5 interconnecting longitudinal bars has proven radial strength at 25% diameter reduction when compared to a CoreValve nitinol stent frame, and twice the radial strength compared to a Medtronic Talent endograft.

With Qualimed I now moved towards making the full 2G graft stent with 3 proximal flared feelers in an attempt to mirror the aortic valve sinus anatomy and allow attachment of the coronary sleeves as close to the proximal end of the graft as possible.

Moving forward it was also important to iterate the stent design. Professor Rothman was concerned that if the 2G ATAG body had longitudinal bars at the same point on the circumference (as in Figure 93), then this could make the graft relatively inflexible as it passes around the aortic arch. Qualimed therefore spaced out the longitudinal bars, off setting them and making the device more flexible within the arch of the aorta. Qualimed's 2G ATAG with sinus feelers is shown in Figure 94 below:

Figure 94 Drawing of compressed nitinol 2G ATAG Frame

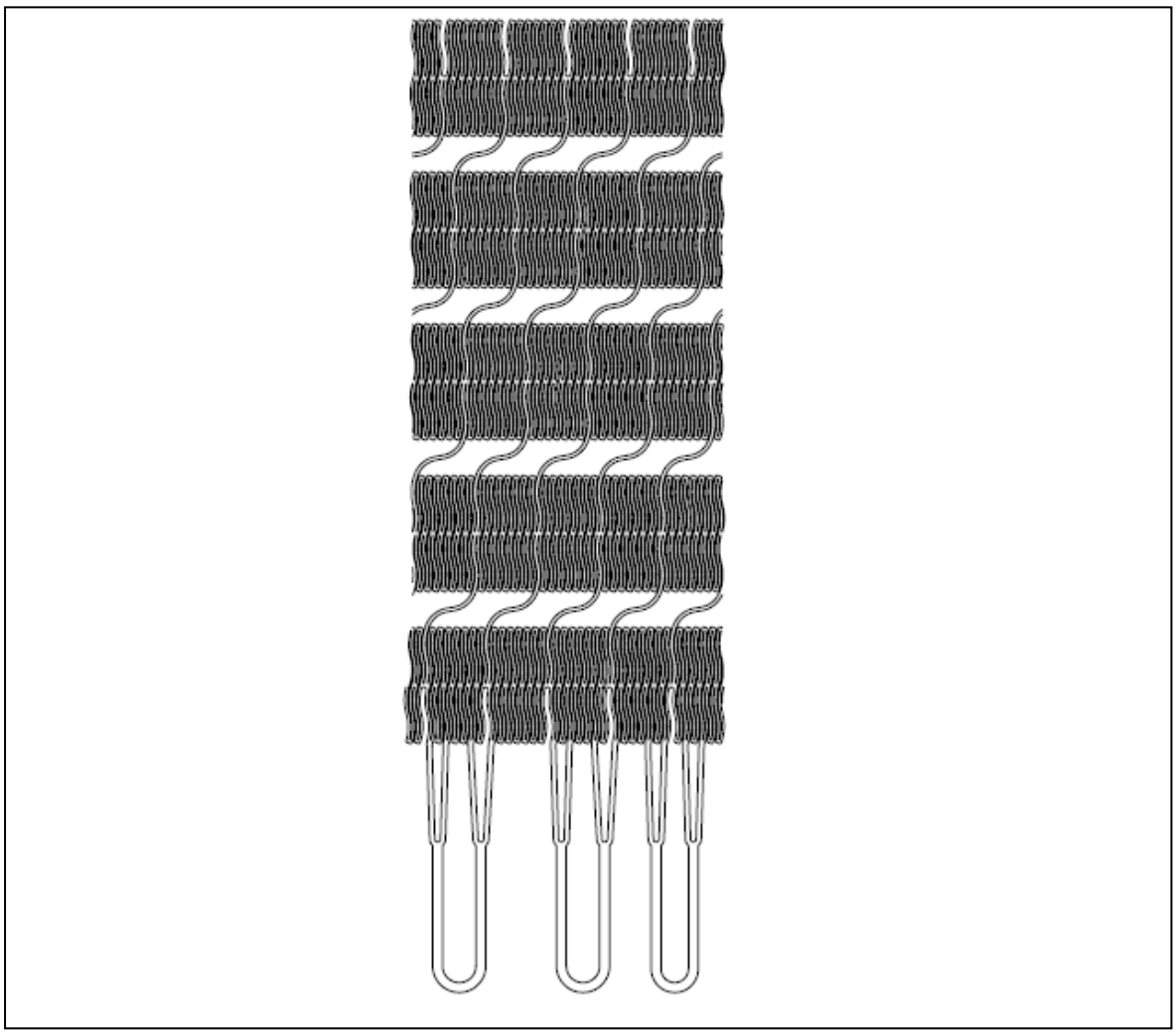

2G ATAG with proximal “feelers” and off-set longitudinal tie bars

Figure 95 below shows photographs of the first build 2G ATAG with sinus feelers:

Figure 95 Photographs of 2G expanded stent frame

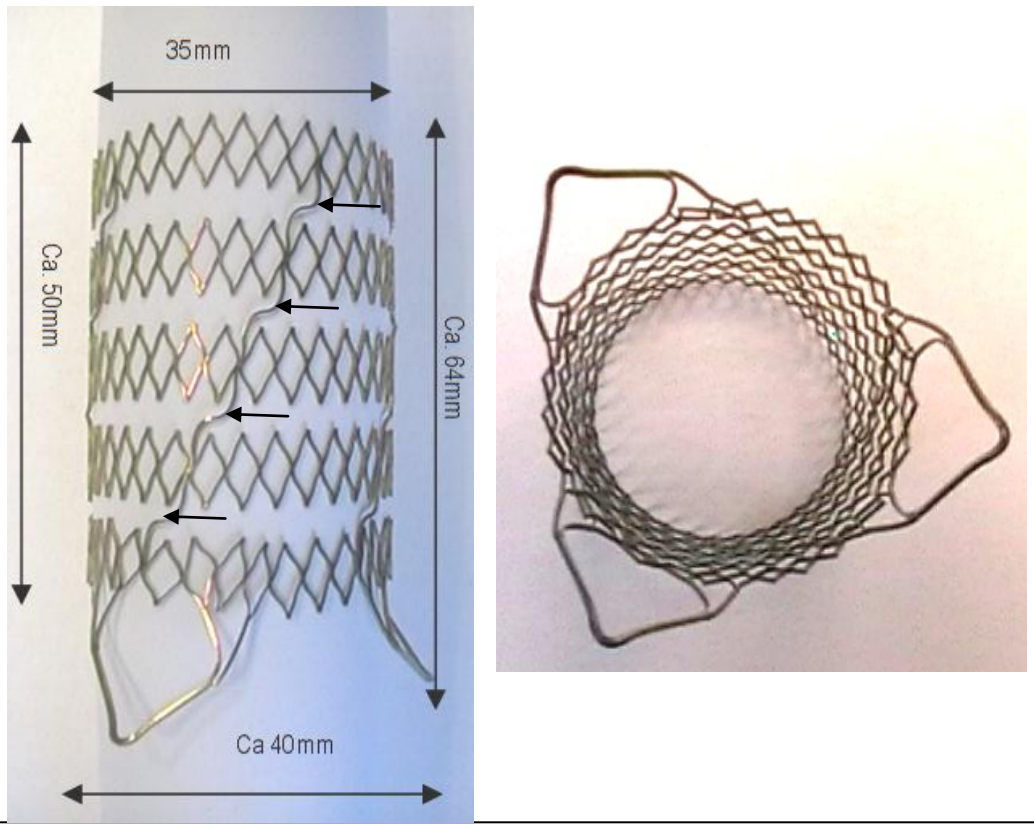

2G ATAG with sinus feelers expanded frame with measurements and arrows showing off-set longitudinal tie bars

4.4.4 Radial strength of uncoated 2G ATAG with sinus “feelers”

4.4.4.1Aim

To test the radial strength of the 2G ATAG nitinol cut stent frame graft with 3 “feelers”, and staggered longitudinal tie bars.

4.4.4.2 Methods

The constriction (hoop strength) method was used in an identical manner as already described in section 4.4.2. Figure 96 below shows the 2G ATAG with sinus feelers within the constriction loop:

Figure 96 2G ATAG with sinus feelers within the constriction loop

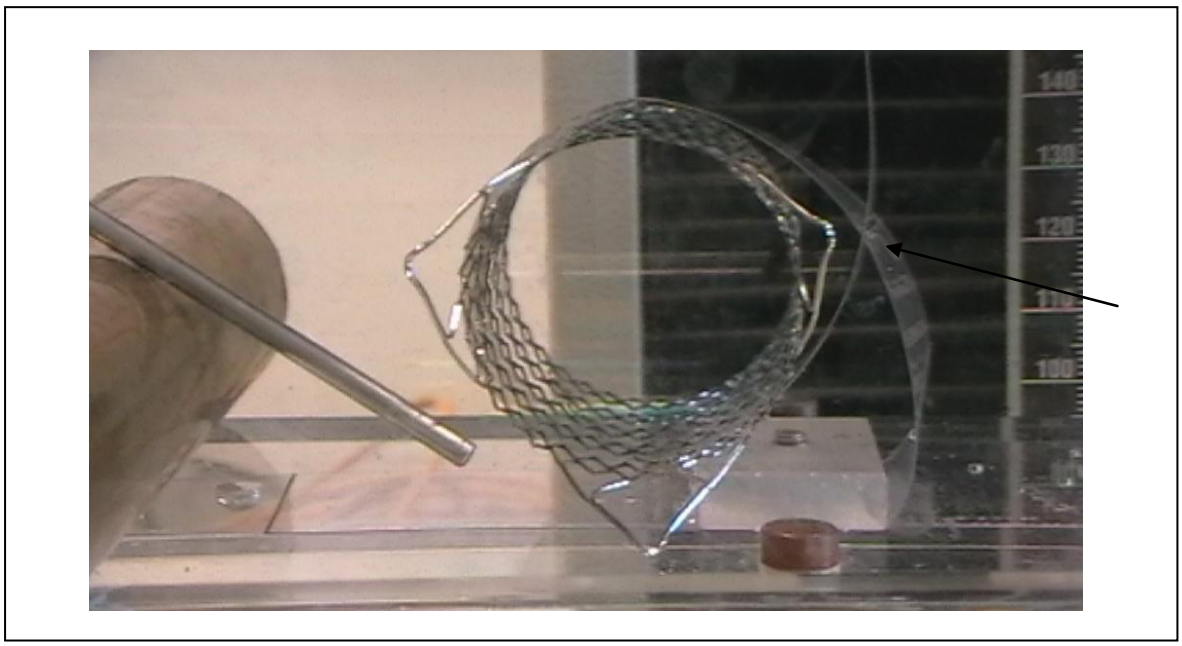

4.4.4.3 Results

The radial strength was tested over the middle ring as documented below in Figure 97 a) below, and the constriction / re-expansion profile at 10% and 20% measured in Figure 97 b):

Figure 97 a) Radial strength of 2G ATAG with sinus feelers

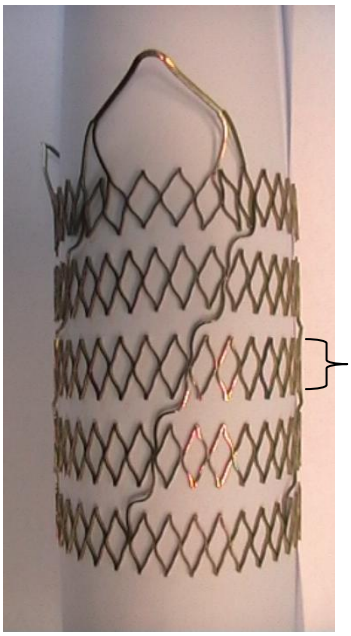

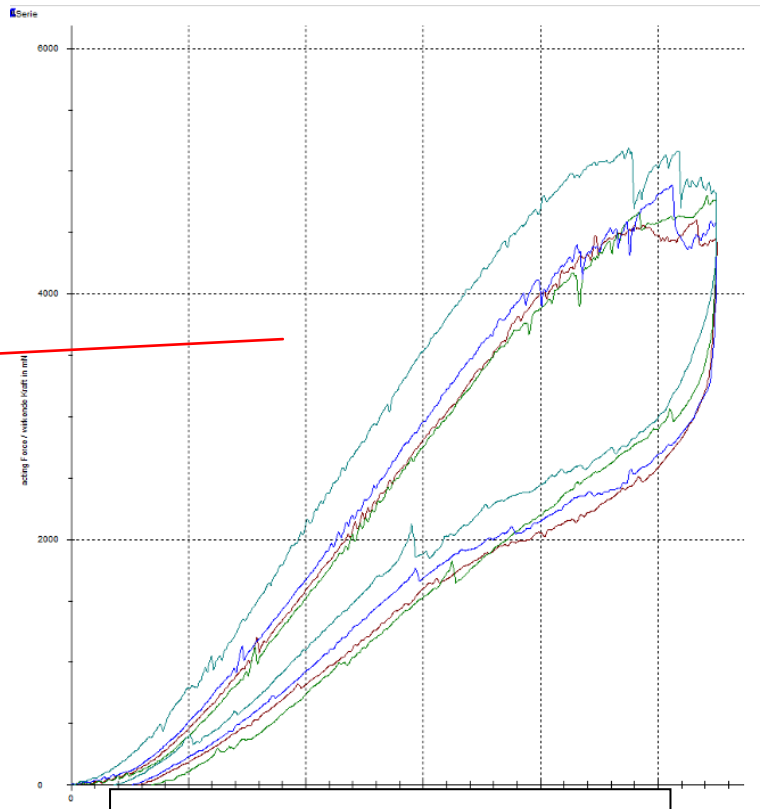

Change in length of constriction loop

	8	4601	Ø - Reduction 25%; Sample 3; A100954A
	9	4802	Ø - Reduction 25%; Sample 3; A100954A
	10	4886	Ø - Reduction 25%; Sample 3; A100954A
	11	5189	Ø - Reduction 25%; Sample 3; A100954A

Mean value [mN]

Force required to achieve 25% graft diameter reduction.

4870 mN

Figure 97 b) Radial strength results of 2G ATAG

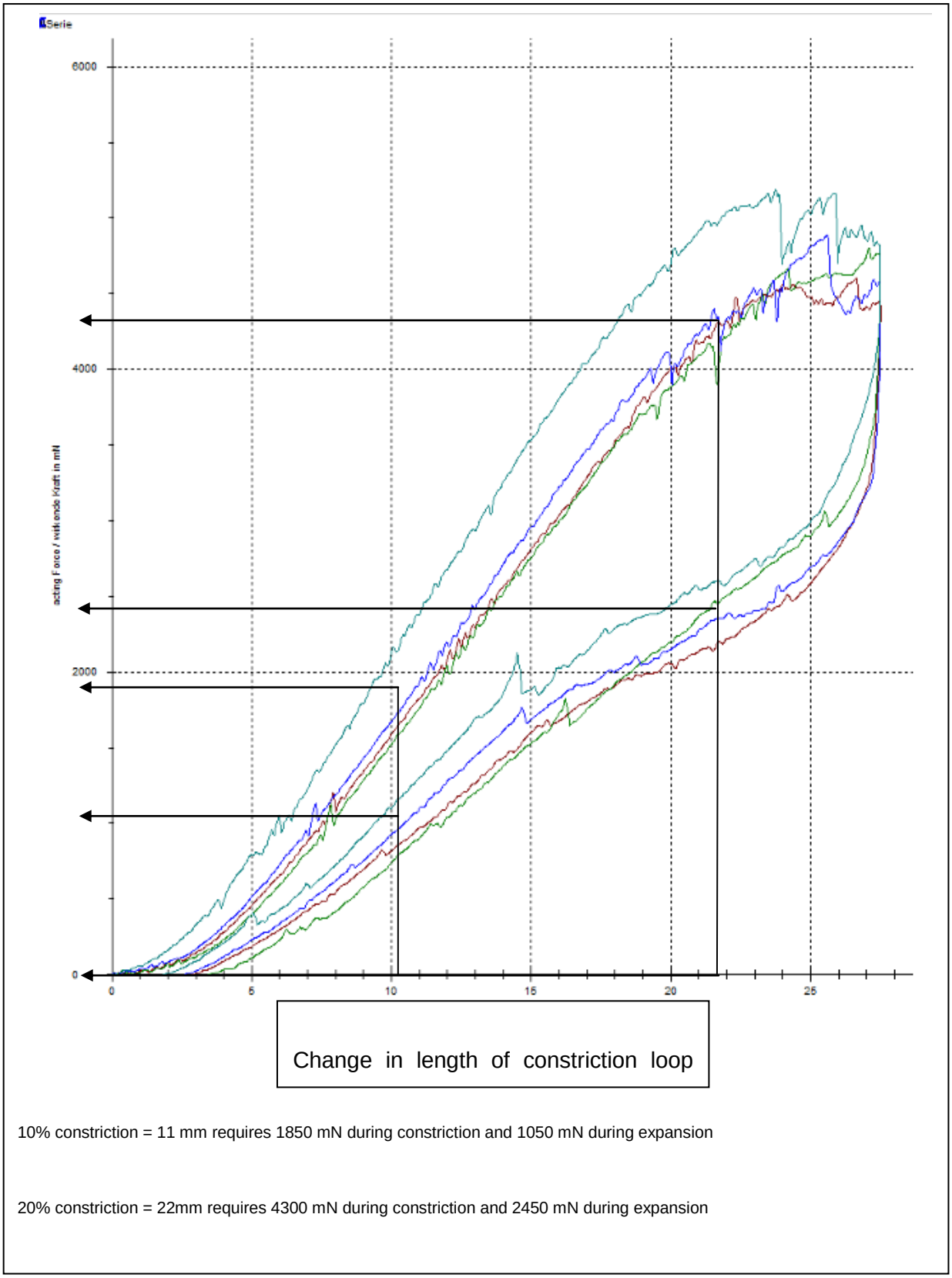

10% constriction = 11 mm requires 1850 mN during constriction and 1050 mN during expansion

20% constriction = 22mm requires 4300 mN during constriction and 2450 mN during expansion

4.4.4.4 Conclusion

The tri-lobed 2G ATAG stent graft, with spaced longitudinal tie bars has essentially identical radial strength as compared to the simple 3 ring structure with 5 longitudinal bars at the same circumferential point.

A 25% diameter reduction requires 4870 mN of force, and a 20% re-expansion profile of 2450 mN is also similar to the original 2G ATAG of at least 2500 mN.

4.4.5 2G ATAG with PU covering - further testing

The 2G ATAG with sinus feelers was then sent to Nicast (Lod, Israel) a company with an expertise in electro-spinning devices with PU. In order to electro-spin the PU onto the nitinol frame I designed and Qualimed made a spinning mandrel (design shown in Figure 98 below).

Figure 98 Diagrams of the 2G ATAG mandrel for electro-spun PU coating

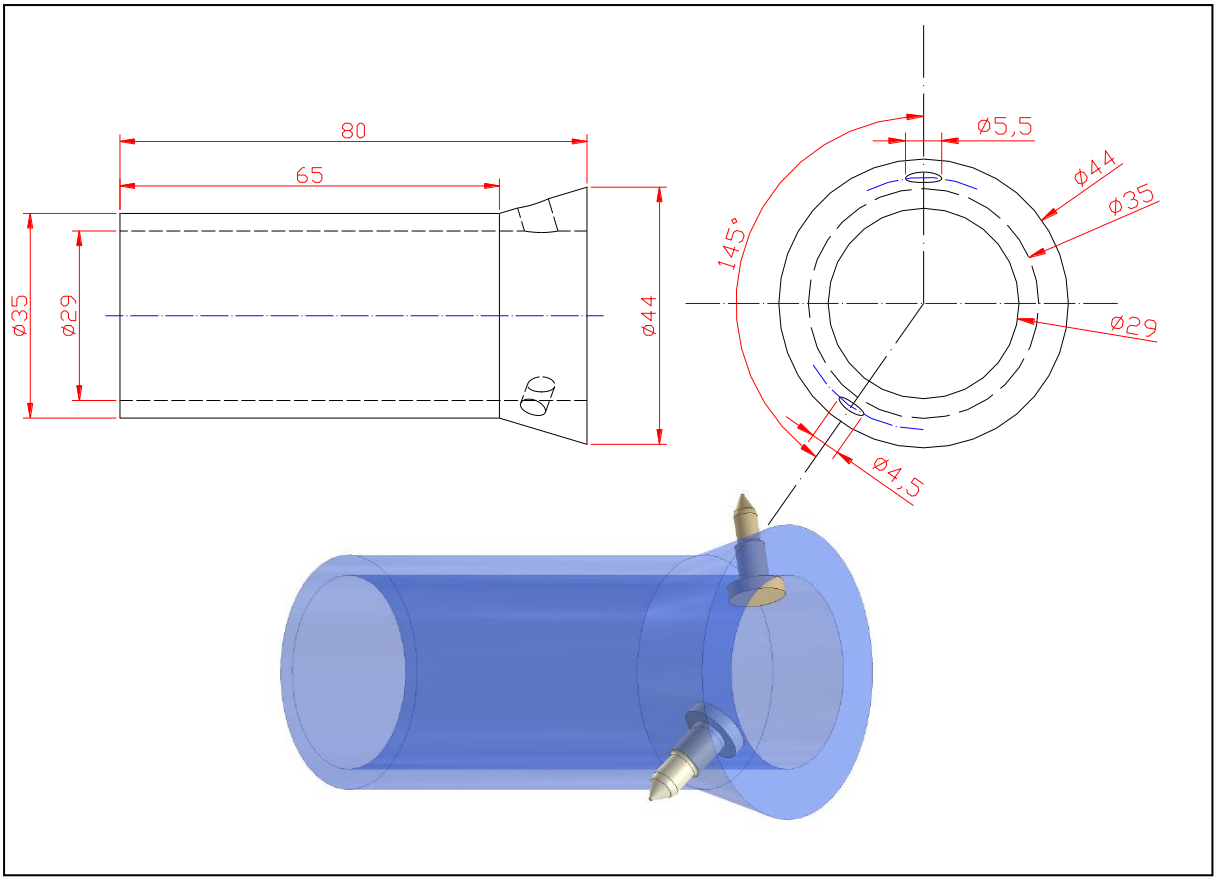

The blue diagram represents a 2D model of the mandrel, onto which the 2G ATAG with sinus feelers will be placed. There are projections for the coronary sleeves at an angle of 145 degrees to one another. With the 2G ATAG nitinol frame placed over the mandrel, the PU will be electro-spun onto the moving mandrel ensuring a homogenous graft covering onto the nitinol stent frame.

Nicast had already confirmed to us that at this time it was not technically feasible to electro- spin the ATAG “inverted t-shirt” in one piece and that the graft body would be coated and then the coronary sleeves would have to be attached by glue. This was the accepted solution for the 2G device. The reason for this is that currently the mandrel can only move in 2 dimensions to cover a standard stent in a homogenous PU covering. To coat the coronary sleeves as well would necessitate the mandrel moving in 3 dimensions – this is not currently possible. The aim was that the uniform electro-spun material would

have a thickness of <200 μm in the first 2G prototype. Ideally in further iterations and bench-testing we would like to get the PU coating thinner, <100 μm for the purposes of stowing, but a trade-off would be made against material properties.

4.4.5.1 2G ATAG with electro-spun PU graft covering

Qualimed manufactured 2 x 2G ATAG stent graft devices and both were sent to Nicast for PU electro-spinning. The first stent was covered with a 110 μm PU material, the second graft with a 200 μm covering as shown in Figure 99 below, and documented in Table 25:

Figure 99 2G ATAG with electro-spun PU coating.

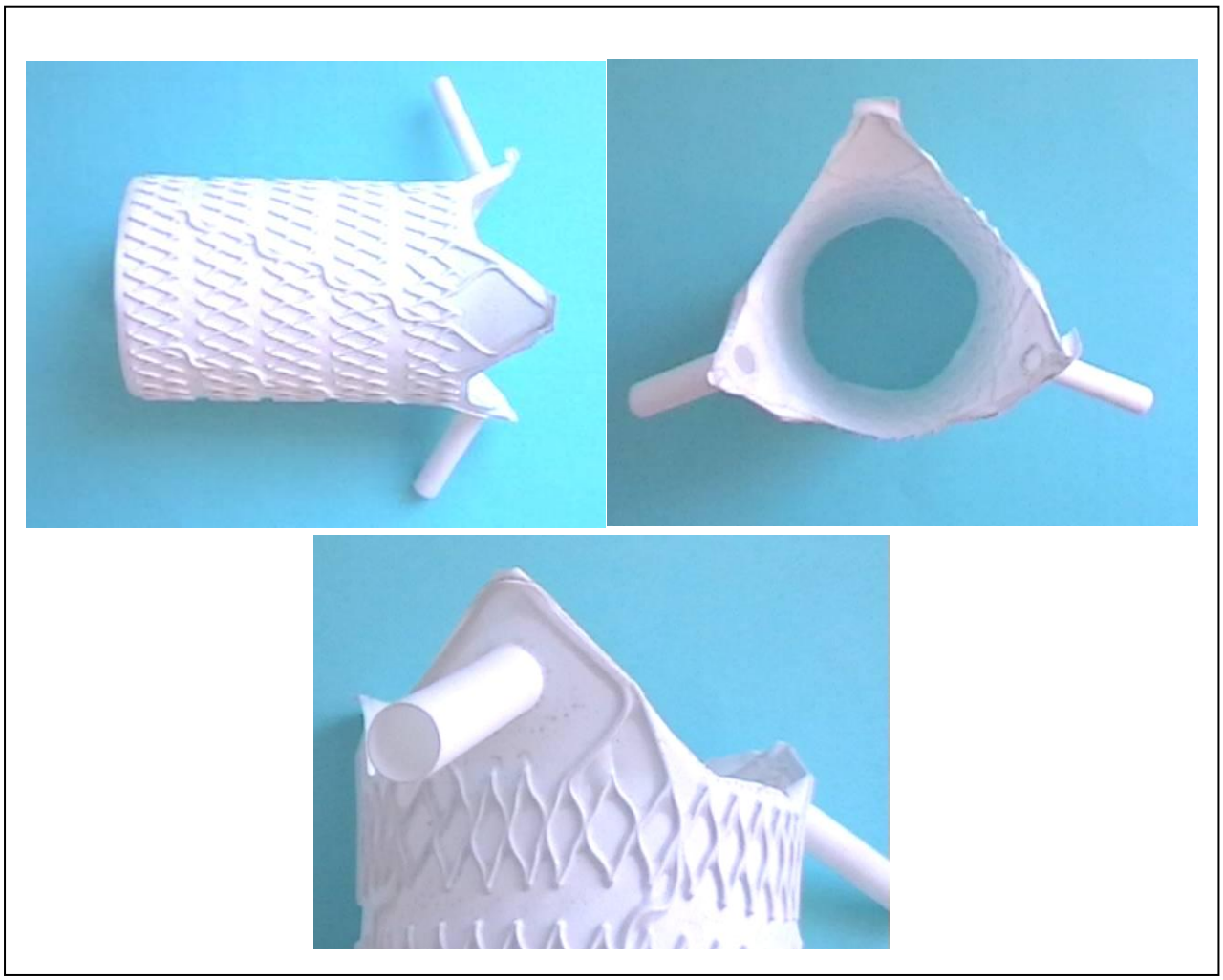

Table 25 2G ATAG PU covered product description

Sample	Description	Lot No. Nicast	Lot No. QualiMed	Polymer Type	Coating Thickness	Glue type
1	Coated Aorta Stent with glued coronary side branches	ME09 1138	A100954A	ChronoFlex-medical grade polyurethane	110 ± 10 µm	Polymer solution made of ChronoFlex plus Titanium Dioxide 5%
2		ME09 1139			200 ± 10 µm	

4.4.5.2 Electro Spun layer configuration

The PU has 3 discrete electro-spun layers with differing characteristics:

1) Inner (lumen) layer characterized by porosity about 60%, pore size 0.5–3 µm , fibre diameter 0.5–1 µm, layer thickness about 45% of total thickness.

2) Barrier layer is a non porous film, layer thickness is about 10% of total thickness.

3) Outer layer = Inner layer.

The stent itself is encapsulated inside of the barrier layer, in the middle of the coating.

4.4.6 Radial strength of the 200μm PU covered 2G ATAG

4.4.6.1 Aim

To test the radial strength of the 2G ATAG nitinol cut stent frame body with PU covering.

4.4.6.2 Methods

The constriction (hoop strength) method was utilised as already described in 4.4.2.

4.4.6.3 Results

It must be stated that in fact the constriction method for measuring radial strength in an endograft where a material is tightly attached to a nitinol graft provides only a limited amount of useful data, as the PU material allows the constricting load to be spread over the nitinol rings either side of the ring being tested. Therefore although this was performed, comparison of these results with those obtained from the bare metal stent are of limited value.

As before the hoop force, deformation curves for the 200 μm PU covered 2G ATAG are shown in Figure 100 a) and b) below:

Figure 100 a) Radial strength results of 2G covered ATAG

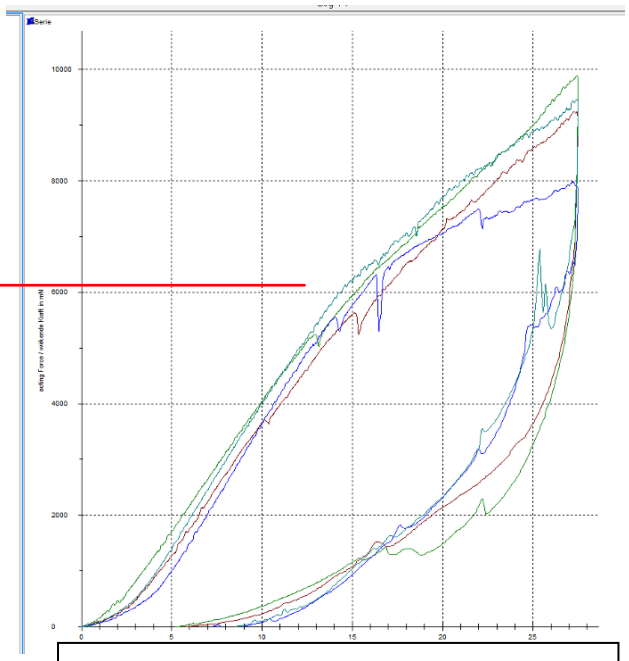

Change in length of constriction loop

Legende	Nr	Radial Force mN	Remarks/Bemerkungen
	1	9244	Reduction/Reduzierung 25% Sample 1; coating thickness 200µm
	2	9884	Reduction/Reduzierung 25% Sample 1; coating thickness 200µm
	3	7984	Reduction/Reduzierung 25% Sample 1; coating thickness 200µm
	4	9452	Reduction/Reduzierung 25% Sample 1; coating thickness 200µm

Mean value [mN]

Force required to achieve 25% graft diameter reduction.

9141mN

Figure 100 b) Radial Strength result of 2G covered ATAG

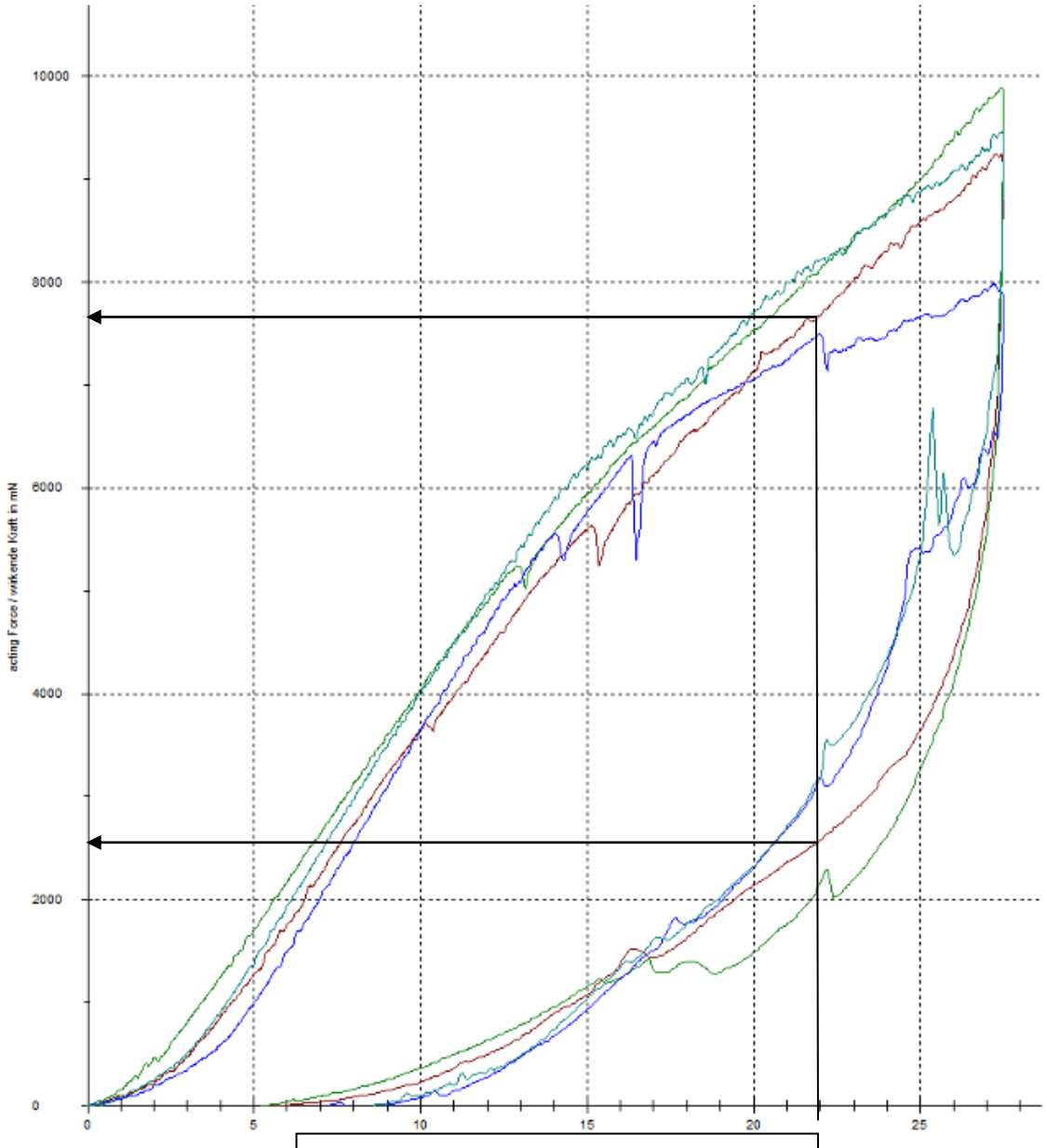

20% constriction = 22mm requires 7800 mN during constriction and exerts approximately 2500 mN during re-expansion

4.4.6.1. Conclusions

The standardised hoop strength as measured by constriction method for the PU covered 2G ATAG is 9141 mN, as compared to 4870 mN for the identical but uncovered 2G ATAG graft, 5063 mN for the CoreValve TAVI frame, and 2271 mN for the Medtronic Talent aortic Dacron covered stent frame. The PU 200 μm coated 2G ATAG graft has an apparent radial strength almost twice that of the uncoated graft, as the PU acts as a continuous longitudinal link giving the graft more combined radial strength, by spreading the load over a greater length of the device.

The re-expansion profile at 20% is essentially the same as the uncovered graft i.e at 20% re-expansion, the force that remains exerted on the vessel wall at the graft / vessel interface is approximately 2500 mN (the same as the uncovered 2G ATAG).

Also worthy of note in this testing protocol is that the covered 2G PU covered ATAG graft behaved in a robust manner and serial manipulations and constrictions at 37^{o}C in water did not result in any damage to the frame or PU covering.

4.4.7 2G PU covered ATAG stowage testing

4.4.7.1 Aim

To assess the minimum stowed diameter of the 2G ATAG with and without the 200 μm PU graft covering.

4.4.7.2 Methods

Using a commercially available circumferential stent crimper (similar to a disposable device which is used to crimp the Edwards TAVI), and Kalte 75 a spray which cools nitinol to -55^{o}C the 2G grafts were crimped and then transferred into a suitably sized hollow piece of clear plastic tubing (to act as a stowage sleeve).

4.4.7.3 Results

The uncovered 2G ATAG frame could be crimped to 6 mm, which allowed stowing into a 22 F (7.3 mm) delivery sheath (see Figure 101 below):

Figure 101 shows the uncovered 2G ATAG frame crimped to 6mm

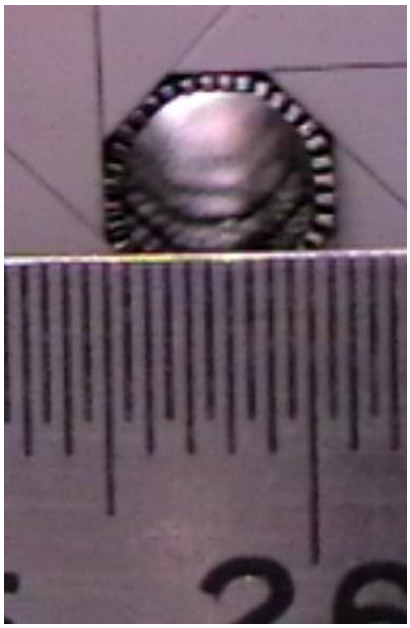

The 200 μm PU covered 2G ATAG could be compressed to 7.5 mm and stowed into a 28 F (9 mm) outer diameter delivery pod as shown in Figure 102 below:

Figure 102 Stowage of the 200 μm PU covered ATAG

4.4.7.4 Conclusions

Stowage testing of the 2G PU covered ATAG reveals that the current minimum stowage diameter is 9 mm or 28 F, which is approximately 3 mm and 10 F larger than our specified design input. It will be vital in further iterations that the device profile and stowing diameter is reduced to allow greater deliverability and minimise vascular complications.

4.4.7.5 Stowage testing discussion

It must be remembered that this is the first ATAG graft that we have manufactured to a high specification, and that this is a highly iterative process. We accept that 28 F is significantly larger than our original design brief, but this at least now gives us a stent design, and electro spun covering that we can now optimise as we move forward.

The first CoreValve^{TM} percutaneous aortic valve graft implanted into humans was a 25 F device which took just 2 years and 2 generations before it was 18 F as is now commercially available. Not only does the CoreValve^{TM} easily crimp to 18 F but it also has a porcine pericardial tri-leaflet aortic valve attached within the lumen. I expect similar advances over the next development cycle with the ATAG system.

The proposed ATAG prototype and the CoreValve^{TM} frame do have some generic similarities. They are both nitinol frames with diamond shaped cells. The ATAG has open cell structure with longitudinal tie bars making it more flexible versus the more rigid CoreValve architecture. I have tested the prototype ATAG against the CoreValve nitinol frame and find the following as shown in Table 26 below:

Table 26 Average nitinol stent design characteristics

Characteristic	2G ATAG prototype	CoreValve
Material thickness (μm)	489	420
Strut width (μm)	204	310
Connector width (μm)	246	420

Moreover I believe that the special ATAG 'honeycomb' design is new and crucial points will lie in the detail. For instance the application of the wave design allows for different segment widths matched to the flexural load with a single laser cut pattern.

With regard to the PU graft covering 200 μm is the starting thickness and it will be interesting to work with Nicast to see if adequate performance can be achieved with a thinner layer which again will lower the overall profile of the device.

A vital part of the future 3G ATAG design and development will be devoted to minimising the stent graft and covering profile to minimise the stowing diameter, allowing easier vascular access and minimising vascular and embolic complications.

4.5 Potential 3G ATAG device iterations

The formal design of a 3G ATAG device is beyond the scope of this thesis, but following on from all of the anatomical research and the testing of the 2G device I do have some recommendations for possible design iterations that might be considered within the 3G ATAG development process.

4.5.1 Proximal aortic seal designs

I think from the outset I have stressed the importance of the ATAG proximal stent design. The 2G sinus "feelers" are probably too long and too "pointed". I think the 3G ATAG may benefit from having the coronary sleeves attached to a more sinus shaped "feeler" protruding less into the sinus of Valsalva. They may also have less outward flare force and be "softer", reducing the risk of damaging the aortic valve apparatus.

If softer less flared sinus feeler design is incorporated, proximal endograft seal may be worse increasing the risk of endoleak. To mitigate against this, design iterations may be mandated just above the coronary arteries to ensure a seal at this point with a more flared portion or a self expanding cuff at or above the STJ to help seal so that proximal endoleak is less of a problem.

The concept of a "valved ATAG" is desirable for a number of reasons, and during 3G ATAG development a "valved ATAG" development programme will run simultaneously. The reason why having an integrated aortic valve is so attractive is that in both the AAAD and the ATAA cohorts the annulus segment size is less variable, enabling annulus

proximal seal to be achieved, without the worry of interference with the aortic valve. Published data also suggests that the aortic valve will be incompetent and need repair or replacement in between 25-35% of all AAAD presentations, thus providing a suitable treatment modality for this mechanical complication (8).

I do not underestimate the cost and development time required to integrate a functioning aortic valve into the ATAG, but conceptually I believe it may be mandated in the end user ATAG device, and for this reason is covered in our intellectual property.

4.5.2 Coronary sleeve considerations

Coronary entry and coronary sleeve stenting requires further bench test experimentation. Currently coronary artery flow is secured by stenting 2 coronary sleeves as branches off the main ATAG graft. The ability of the coronary sleeves to adapt to coronary distance and angulation rests within the flexibility and elasticity of the PU material – bench testing with different coronary angulations and distances will help to inform as to whether this is sufficient. Future coronary sleeve embodiments may consist of design features with the aim of increasing the range of coronary distances and angulations that are treatable. Potential design features might consist of a) conical coronary segments and b) stepped concertina segments as represented in Figure 103 below:

Figure 103 Possible coronary sleeve designs

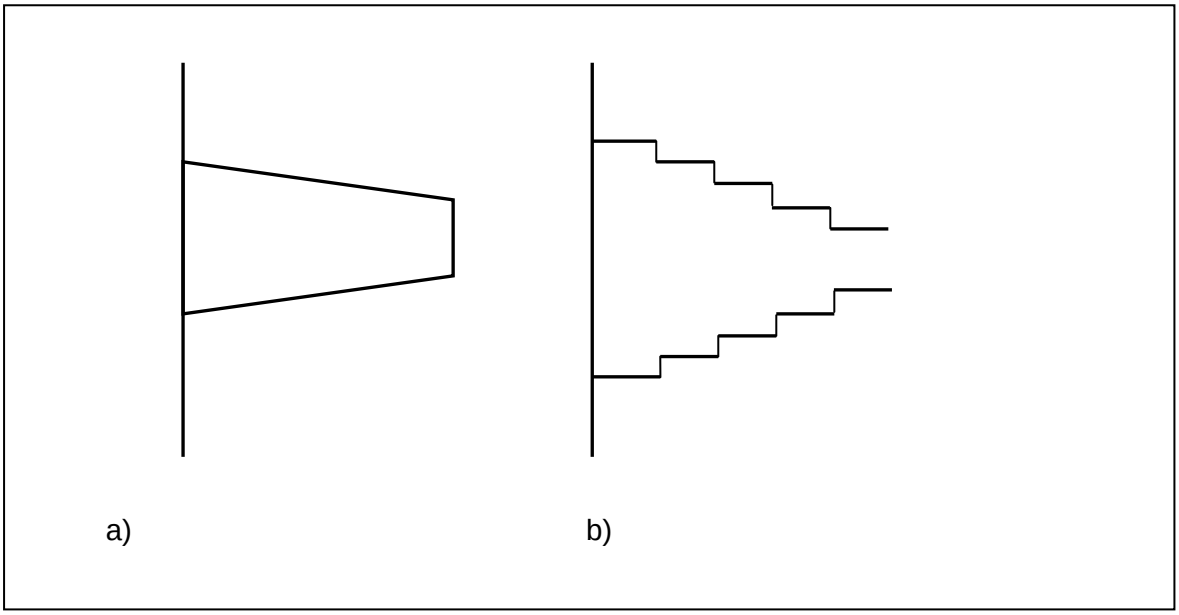

Possible coronary sleeve designs, with the aim of increasing the range of angulations and lengths that each device is capable of treating effectively. a) Conical coronary sleeves b) Stepped concertina effect of sleeve material.

At this point in time it is still too early to suggest whether protection of the coronary flow in the manner I have outlined is technically feasible and / or physiologically tolerated in both animal models and human patients. We must optimize the design and deployment characteristics, and have undergone significant *in vitro* delivery work before consideration of a first *in vivo model.* As has already been outlined in the design specification if protecting both coronaries in a proactive way is not feasible we will retreat to a less ambitious design.

Even if stenting of the LMCA and RCA using the “inverted t-shirt” ATAG is possible we will need to test the material durability and its risk of fatigue and thrombus formation / restenosis. Further work will involve platelet and coagulation activation, as well as suggested strategies (heparin, aspirin and clopidogrel) to maintain long term patency. There is already interest in attaching molecules to the PU surface to increase

endothelialisation and improving long term patency rates (133;134), and one must consider whether a drug eluting layer could provide protection against re-stenosis.

While currently the coronary sleeves require gluing to the main ATAG body frame I am hopeful that within the 3G ATAG a one piece electro-spun T shirt will be possible integrating both coronary sleeves.

4.5.3 Iterations related to aortic curvature

The first 2-3cm of the ascending aorta is relatively straight and can be managed using a straight graft (like the CoreValve^{TM}). After this proximal portion there is curvature in 2 dimensions, a factor that has partially been taken into account with the 2G ATAG design, but relies upon the stent frames ability to flex to conform to the shape of the aorta in this region, with an open cell design connected by staggered longitudonal struts as already described in Figure 95.

Optimisation of the longitudonal strut geometry is required to maximise endoluminal apposition and is reflected in our future work packages and will allow for optimal graft shape minimising the formation of “wrinkles”.

The formation of “wrinkles” of the graft covering material may also be material specific. Four of the seven main descending thoracic aortic endografts use Dacron woven material as their covering (Medtronic Valiant, Bolton Medical Relay, Cook Zenith, and Jotec Evita). They all have rudimentary Z shaped stents, Dacron material and the grafts have developed little since their inception. The grafts themselves often have significant

infoldings of material even when placed in a straight tube (see Figure 104 below of Medtronic Talent graft)

Figure 104 Medtronic Talent graft

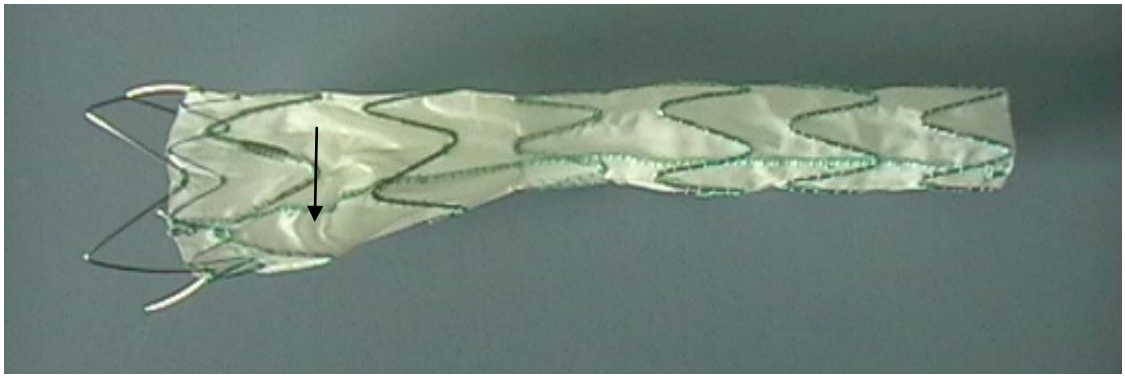

Medtronic Talent graft with Dacron covering showing material infolding (arrowed)

When treating the ascending aorta, protection of the coronary arteries and aortic valve is likely to require a more sophisticated graft, capable of conforming to the curvature of the aorta, lined with a covering that is novel, thin, flexible, strong, biocompatible, thrombus resistant and impermeable.

The 3G ATAG may well have a shorter inner aortic curve, or at least tie bars which can compress on the inner curve compared to expanding on the outer curve, in an attempt to allow better apposition of the ATAG graft and covering material to the aortic wall, which is likely to improve the distal seal and minimise distal endoleak.

Further information on the aortic angulation in 3 dimensions will be required, and will be obtained most readily from CT or MRI angiography.

4.5.4 3G ATAG profile

Much design consideration with 3G ATAG will focus on reducing the overall stowing profile from the current 28 F towards our original aim of 18 F. The 3G stent frame needs to be stowable with reduced profile, while maintaining radial strength. The graft material must be as thin as possible while maintaining its barrier function, and being robust.

4.5.5 Radio-opacity and optimizing visualization

As 3G ATAG moves towards more sophisticated testing, stent radio-opacity and visualisation under fluoroscopy must be prioritised. As has already been shown visualisation and orientation in 3 dimensions is vital for successful deployment and as such we must focus on these factors. Current designs have radio-opaque markers on ends of the graft, coronary balloons and stents (with L and R orientation). Only through further testing and simulation will it become clear whether this is adequate or whether more sophisticated markings are required.

4.5.6 Guide wire specification

One of the major limitations of the PoC deployment *in vitro* model was that once the guidewires were in both coronary arteries and LV cavity, they were fixed in position, a manoeuvre that cannot be replicated *in vivo.* Attention must be focused on bench testing

and determining the amount of force ATAG imposes on the guide wires within the coronary arteries and LV cavity when the device is advanced up the aorta and around the arch into the landing zone. With this information it will be possible to design coronary and LV guidewires with specific properties to keep them in position and allow ATAG advancement. Possible guidewire designs include balloon securing wires, noodle wires, and possibly a screw in LV wire.

4.5.7 Sizing protocol

Over-sizing is likely to be device specific and we will need to work hard during bench tests to evaluate radial strength and propose an evidence based over-sizing protocol for the ATAG instructions for use.

Chapter Five

Development of a simple *in vitro* flow loop, and investigating the most suitable *in vivo* animal model for future work

Chapter 5 : Development of *in vitro* and *in vivo* models

5.1 Development of a simple *in vitro* flow loop

In vitro assessment of a new vascular endoprosthesis is a vital part of testing for both regulatory and device and delivery system design / iteration. The next phase of the ATAG iteration and testing (documented within the successful NIHR grant and beyond the scope of this thesis) would involve flow rig analysis of implantation and device behaviour resulting in further iterations of both the ATAG device and the delivery system.

There are commercially available flow rigs (http://www.blockwise.com/robopulse) capable of replicating human physiological conditions including arterial wave form, blood pressure, temperature etc, but at $100,000 are beyond the reasonable budget of this project.

To develop my own simple flow rig I collaborated with Professor Steve Greenwald who is Professor of Cardiovascular Mechanics at QMUL with the aim of building from scratch a basic prototype flow rig which could then be improved and optimised by my successor for ATAG testing with the Elastrat silicone aorta.

5.1.1 Flow rig experiment 1

5.1.1.1 Aim

To set up a simple *in vitro* flow rig with semi-physiological conditions.

5.1.1 2 Simple In vitro flow rig specification

- To be able to implant ATAG into cylindrical aortic portion with coronary artery branches
- Flow rig to utilise water in first iteration (less viscous than blood)
- Water to be a physiological human body temperature of 37^{o}C
- Have a flow rate of 5 litres / minute (L/min) up to a supra-physiological 14 L/min to potentially test possible migration / stent stability and fixation characteristics
- To be capable of delivering a constant mean pressure of 80 mmHg (phasic pressure / flow beyond the realms of this simple flow rig)
- Pumped return system

5.1.1.3 Materials and methods

5.1.1.3.1 Materials

Table 27 below details the materials used in the simple flow rig:

Table 27 Materials for flow rig

32 mm Internal Diameter (ID) rigid Perspex tubing
3.5 mm ID rigid Perspex tubing (RCA)
4.5 mm ID rigid Perspex tubing (LMCA)
Perspex bonding cement
20 mm ID clear silicone tubing
13 mm ID clear silicone tubing
22 mm white plastic plumbing pipe
Flow regulator / 22 mm Tap
37^{o}C thermostatically controlled water bath
Electric DC water pump capable of > 5 L/min
10 litre storage tank

5.1.1.3.2 Methods

A 32 mm internal diameter (ID) Perspex tube 15 cm long was chosen for the implantation zone (IZ) to simulate the ascending aorta. To this 2 coronary artery portions were attached – a 4.5 mm Perspex tube for the LMCA and a 3.5 mm Perspex tube for the RCA. The coronary arteries were attached at an angle of 155 degrees to one another, representing essentially “normal” ascending aortic and coronary size and geometry. It was accepted that Perspex tubing could not take into account the natural curvature of the ascending aorta, the shape of the sinuses, take off angle of the coronary arteries, or the elastance / physical properties of the native aorta. Figure 105 shows the Perspex IZ:

Figure 105 Shows the Perspex IZ

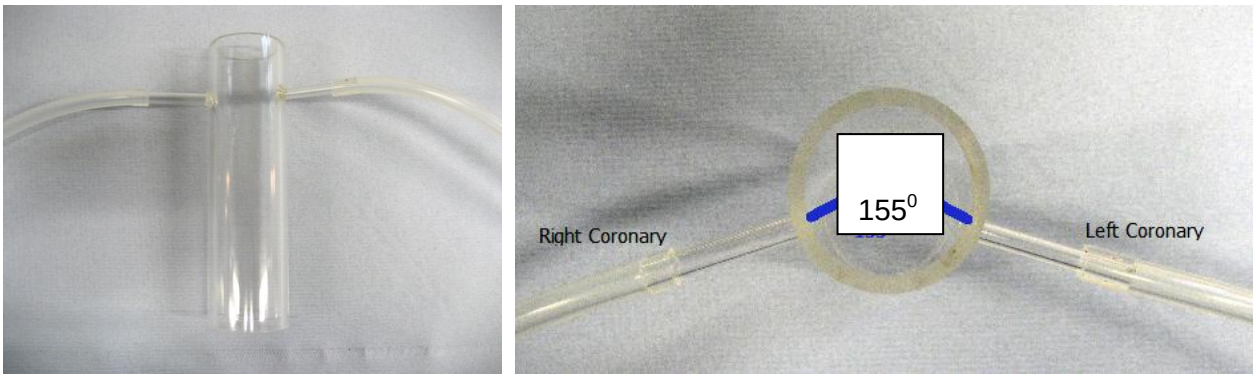

Photographs showing Perspex aorta with LMCA and RCA branches attached by bonding cement at 155 degrees to one another.

This Perspex area will form the ATAG IZ. It will be supplied by an aortic inflow where physiological warm water (37^{o}C) will flow through the graft at a rate of 5 L/min. Using only gravity this device can really only test the device in one of two ways:

i) High flow, low resistance / pressure – the tubing would allow approximately 14 L/min, but at a very low pressure.

Or

ii) High pressure between 80-94 mmHg but with low / no flow i.e. the hydrostatic pressure created from water being 2-2.5 m above the implantation zone with resistance after the IZ increasing pressure.

The majority of the tubing making up the circuit is a 20 mm ID silicone tube. There are joining portions of 22 mm plastic tubing – allowing the integration of flow regulator taps.

A thermostatically controlled water bath was used as a reservoir for the 37°C water which was then pumped into a 10 L storage tank suspended 2 metres above the graft giving gravitational pressure and flows through the graft implantation zone. Figure 106 and 107 below show the experimental set up:

Figure 106 First flow rig experimental set up

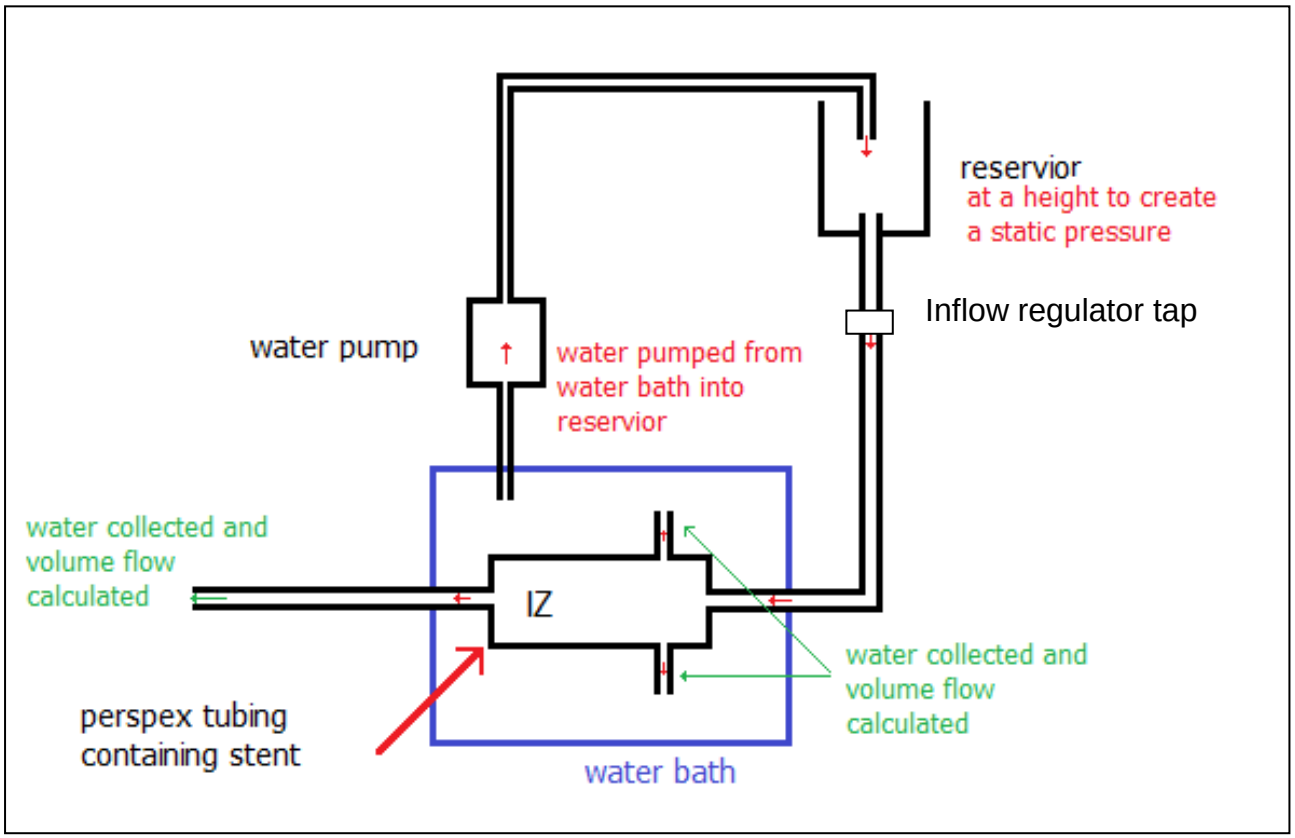

A 10L reservoir for storing the water is placed at 2-2.5 metres above the IZ. This leads into a inflow regulator to control flow. Water passes into the IZ and can flow either straight through the IZ, or through the attached coronary Perspex branches. Water is collected from all routes and the volume over time measured. The 37 degree water bath also acts as a reservoir connected to an electrical water pump recycling water up to the elevated reservoir.

Figure 107 Photograph of experimental set up

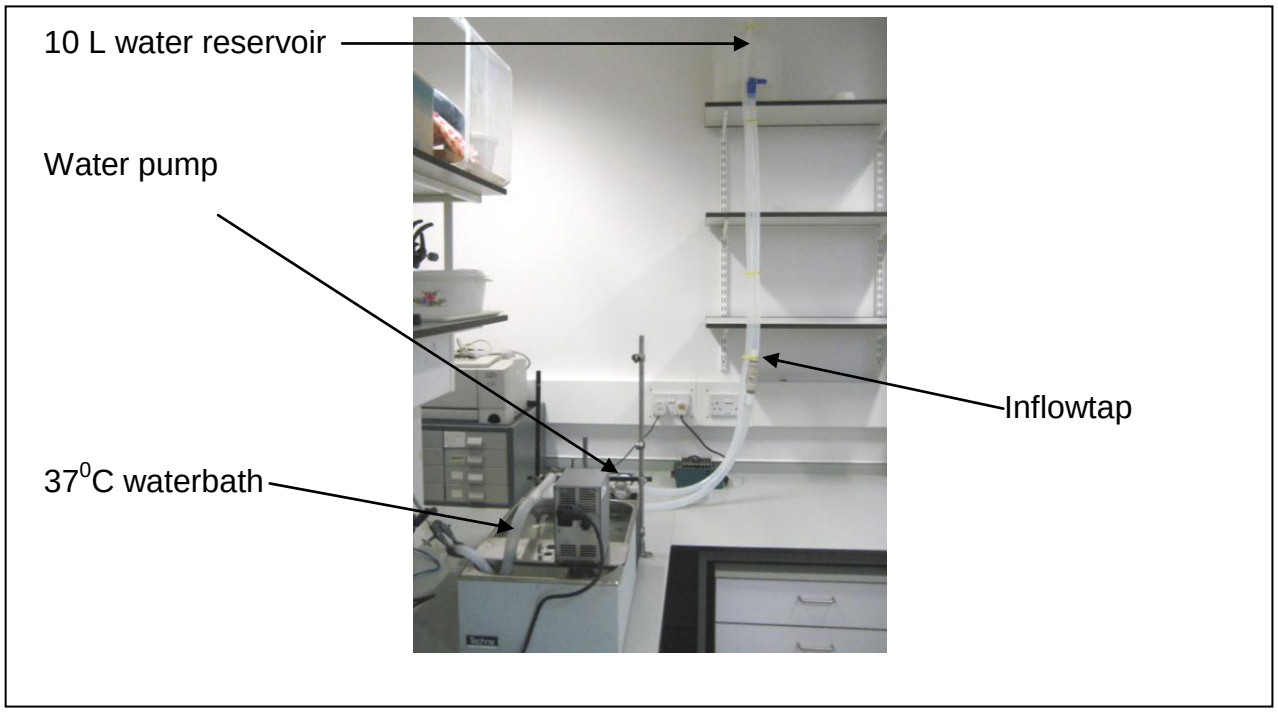

Flow per minute was measured by collecting the water that had run through the system during a 15 second period, weighing it (1 litre weighs 1 Kg) and multiplying by 4 to get L/min.

5.1.1.3.3 Result

5.1.1.3.3.1 Temperature

Over the testing period, with continuous circulation the water bath remained at a constant temperature of 37 +/- 1 ^{o}C.

5.1.1.3.3.2 Flow measurement

Flow could easily be adjusted (adjusting flow regulator tap) to allow a reliable “circulating volume” / min. Table 28 below shows the flow of water through the IZ in L/min when the angle of the inflow regulator tap is adjusted:

Table 28 shows angle of inflow tap against total flow through IZ

	Angle of inflow regulator tap (^{o})	Flow in L/min
1.	45	1.45
2.	60	4.56
3.	70	6.42
4.	68	5.61

A volume of 5.6 +/- 0.14 L/min (measured by the total weight of water (Kg) from outflow over a minute period), could be reproduced with the flow regulator tap at 68 degrees angulation as shown in Table 29 below:

Table 29 Reproducibility of flow measurements

Run	Flow in L/min
1	5.76
2	5.49
3	5.58
Mean	5.61
Standard deviation	0.14

5.1.1.3.3.3 Pressure assessment

Pressure wire assessment of the pressure within IZ revealed essentially a hydrostatic pressure of 80 mmHg when the storage vessel was placed at 2 m height, and the outflow from the IZ and coronaries was clamped (i.e. static pressure). The maximal constant pressure that could be created by this flow loop within this lab was 94 mmHg with the storage reservoir at 2.5 m above the IZ, and the outflow of the graft clamped (i.e. high pressure, no flow). The pressure at the IZ during flow of 5.6 L/min was approximately 20 mmHg.

5.1.1.4 Conclusions

During this first simple flow rig experiment I had set up a circuit capable of reliably pumping 5.6 L/min of water at 37^{o}C through a mock aortic root, with 2 coronary arteries

at a pressure of 20 mmHg. The greatest hydrostatic pressure that could be created was 94 mmHg (with no flow and outflow clamped). Flows of around 14 L/min could be achieved with the inflow tap completely open, and no distal resistance.

5.1.2 Flow rig experiment 2

5.1.2.1 Aim

To implant the ATAG into the specially made Perspex “ascending aorta IZ”, as documented in 5.1.1).

5.1.2.2 Methods

The 2G ATAG did not contain coronary stents, but instead cylindrical sleeves of Nicast PU material with a material thickness of 152 μm.

Figure 108 below shows a photograph of the 2G ATAG with PU covering:

Figure 108 Photograph of the proximal end of the 2G ATAG with coronary sleeves

The 2G ATAG device was manually inserted into the Perspex IZ, with each coronary sleeve positioned into the respective coronary artery.

5.1.2.3 Results

The 2G ATAG with PU coronary sleeves (but no coronary stents) was successfully implanted manually into the Perspex ascending aorta as shown in Figure 109 below:

Figure 109 Shows 2G ATAG implanted into the Perspex ascending aorta

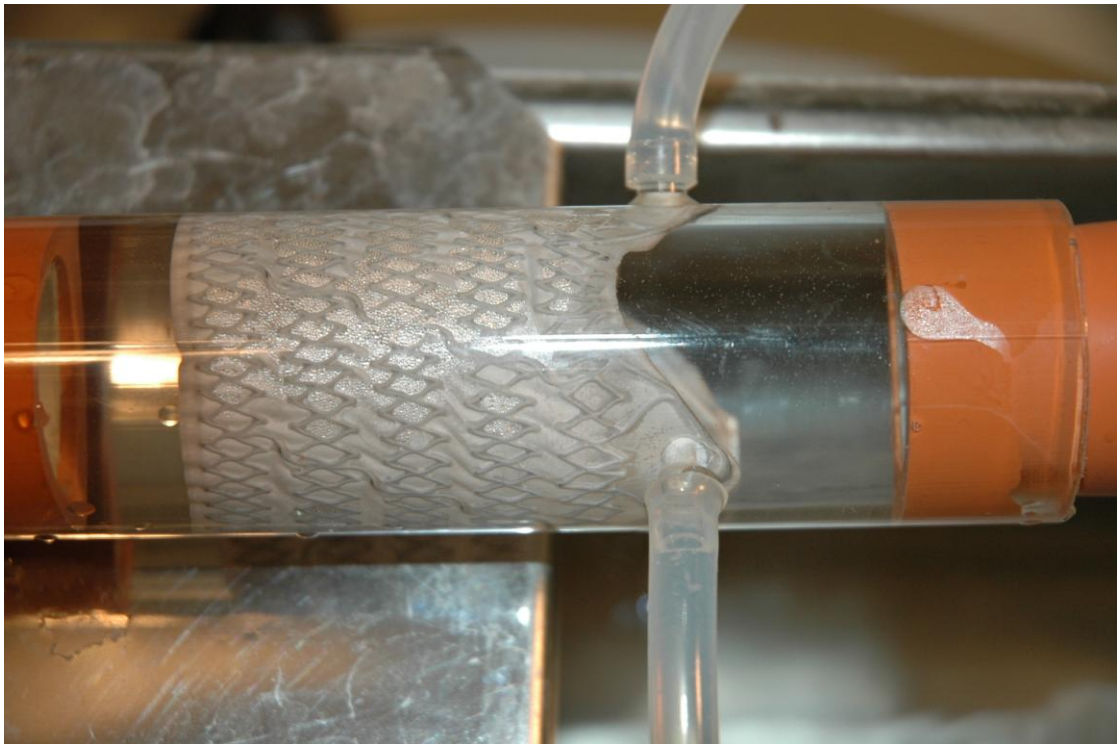

It was noted however that the coronary artery sleeves collapsed down precipitating major flow of fluid around the graft and not through it, as shown in Figure 110 below:

Figure 110 Involution and collapse of the PU materials within the coronary ostia

I decided to stent the branches in place as detailed in the design specification. This was achieved using a 4.5 mm stent in the LMCA and a 3.5 mm stent in the RCA. Both stents were from my expired stock and were cut to around 8 mm in length, as shown in Figure 111 below:

Figure 111 Coronary stents inserted to LMCA and RCA PU coronary sleeves

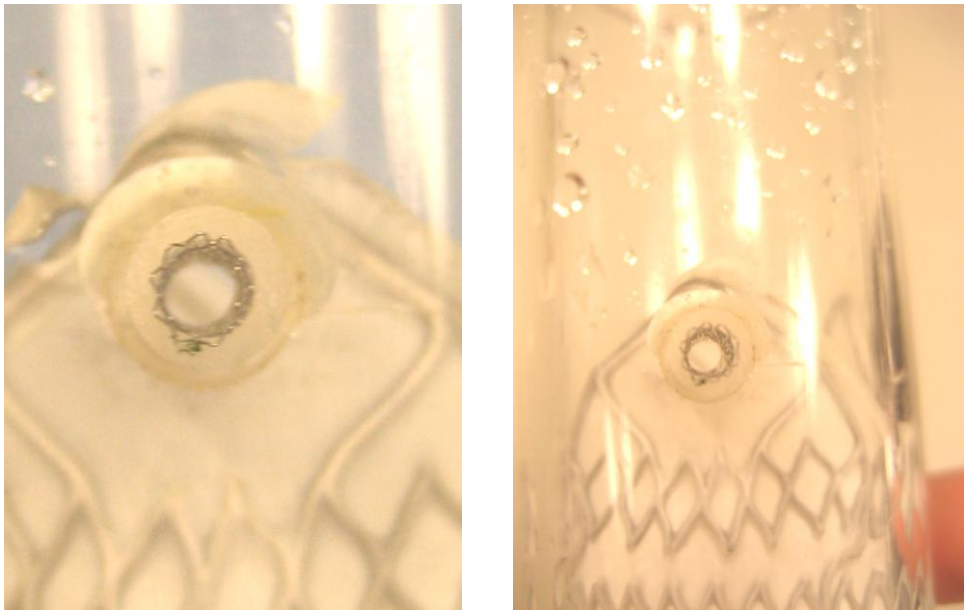

Implantation of coronary stents into the Nicast PU sleeves resulted in a seal between the ATAG graft and coronary arteries so that the predominant flow came through the stent graft and sleeves.

Using water as the fluid at 37^0C it was impossible to rule out that some may “bypass” the sleeve and come around, but this is likely to be minimal.

5.1.2.4 Conclusion

It was possible to implant the 2G ATAG graft into the IZ of the Perspex model, but the unsupported coronary sleeves involuted allowing predominant flow around the graft rather than through it.

It was rectified by stenting the coronary sleeves into the LMCA and RCA resulting in macroscopically the majority of the flow through the coronary arms.

5.1.3 Flow rig experiment 3

In the human, the coronary circulation receives approximately 5% of the cardiac output at rest (135). With resistance only placed on the inflow or outflow of the main ATAG graft the relative coronary flows were supra-physiological (between 20% and 57%), coronary flow being the path of least resistance.

5.1.3.1 Aim

Using flow regulators (resistance valves) on the main outflow and the coronary outflows create the most physiologically correct simple flow rig possible (proportional flow through the aortic stent and coronaries). i.e. create a mock circulation with a total cardiac output of around 5 L/min, with 95% going through the main stent graft body and 5% through the coronary arteries.

5.1.3.2 Methods

With ATAG already implanted in the IZ, and coronary sleeves stented, by serially testing the flow rig with water, adjusting the flow resistance of outflow, and both coronary arteries to achieve a physiological cardiac output as documented above.

Figure 112 below shows the ATAG with stented coronary portions implanted within the Perspex IZ:

Figure 112 covered ATAG inserted into IZ of Perspex aorta

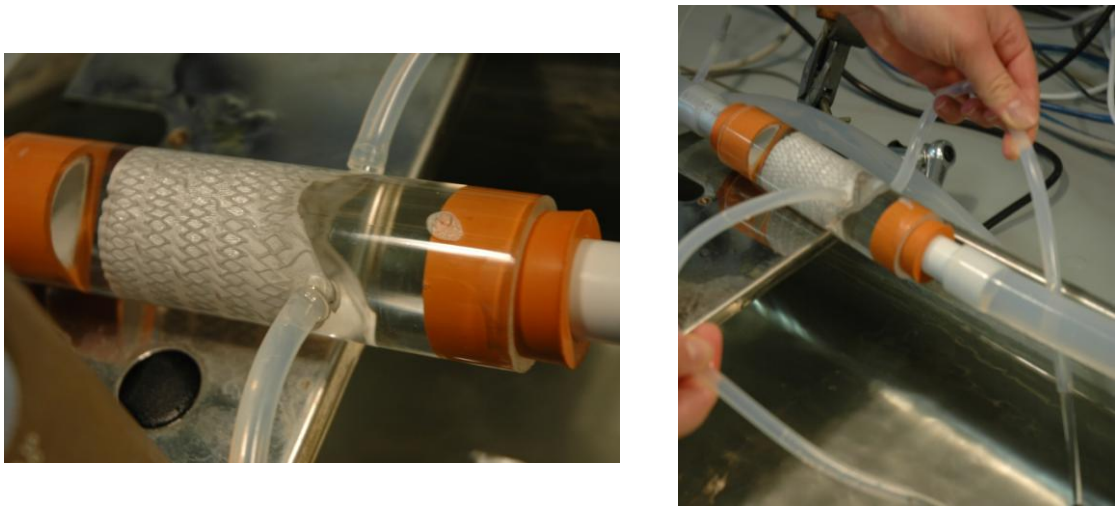

ATAG implanted into the IZ, and the coronary sleeves stented in position. With silicone tube attachments to the coronary Perspex sleeves coronary flow could be easily collected and measured:

5.1.3.3 Results

Table 30 below shows flow of water through the main aortic stent and through the coronary arteries:

Table 30 physiological coronary flow achieved with the simple flow rig

Flow through end of Stent in 15 sec (ml)	LMCA flow in 15 sec (ml)	RCA flow in 15 sec (ml)	Total Flow Through Stent (ml/min)	Percentage total flow through Left Coronary (%)	Percentage total flow through Right Coronary (%)	Percentage of Total Flow through Both Coronaries (%)
1208	53.2	44	5220.8	4.07	3.37	7.44

Using water within the flow loop the most physiological set-up managed was a total cardiac output of 5.2 L/min, with 7.4% of the cardiac output going down the coronary arteries – this is clearly supra-physiological as normally 5% of cardiac output fills the epicardial coronary arteries at rest, but was the best we could reliably achieve with this simple flow rig set up.

5.1.3.4 Conclusion

With water as the loop fluid and resistance taps on the aortic outflow and both coronary artery outflows it was possible to create a flow loop with physiological proportions of fluid flow through the main stent body and through the coronary arteries.

5.1.4 Experiment 4 ATAG flow rig testing with contrast under fluoroscopy

5.1.4.1 Aim

To visualise the flow of contrast through the ATAG graft and coronary sleeves under fluoroscopy within a flow loop.

5.1.4.2 Methods

The flow rig from experiment 3 was set up in the cardiac catheter laboratory of the London Chest Hospital, with a flow of 5.5 L/min, with similar coronary and outflow resistances. Just proximal to the ATAG graft a 6 F pigtail catheter was inserted through a 6 F sheath to inject iodinated contrast (by a automatic contrast injector at 20 ml / second for 2 seconds) through the graft to be captured on fluoroscopy. Experimental set up is shown in Figure 113 and 114 below:

Figure 113 shows flow rig set up in cath lab

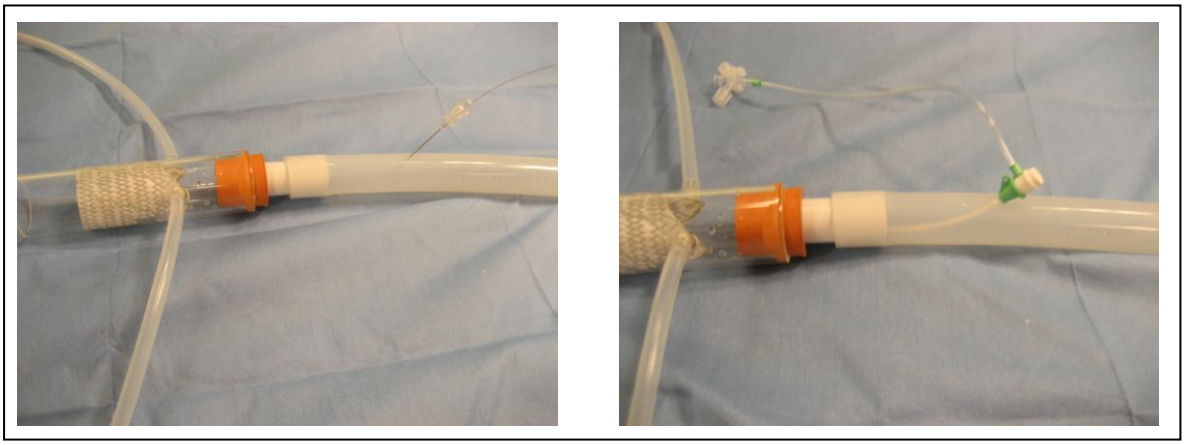

Left picture reveals the introducer needle in the silicone tubing proximal to the implantation zone (ascending aorta), using the Seldinger technique a wire is passed through the needle and into the silicone "aorta". Over the wire a 6 F arterial sheath is inserted into the silicone artery.

Figure 114 Pre-contrast fluoroscopy image of the ATAG

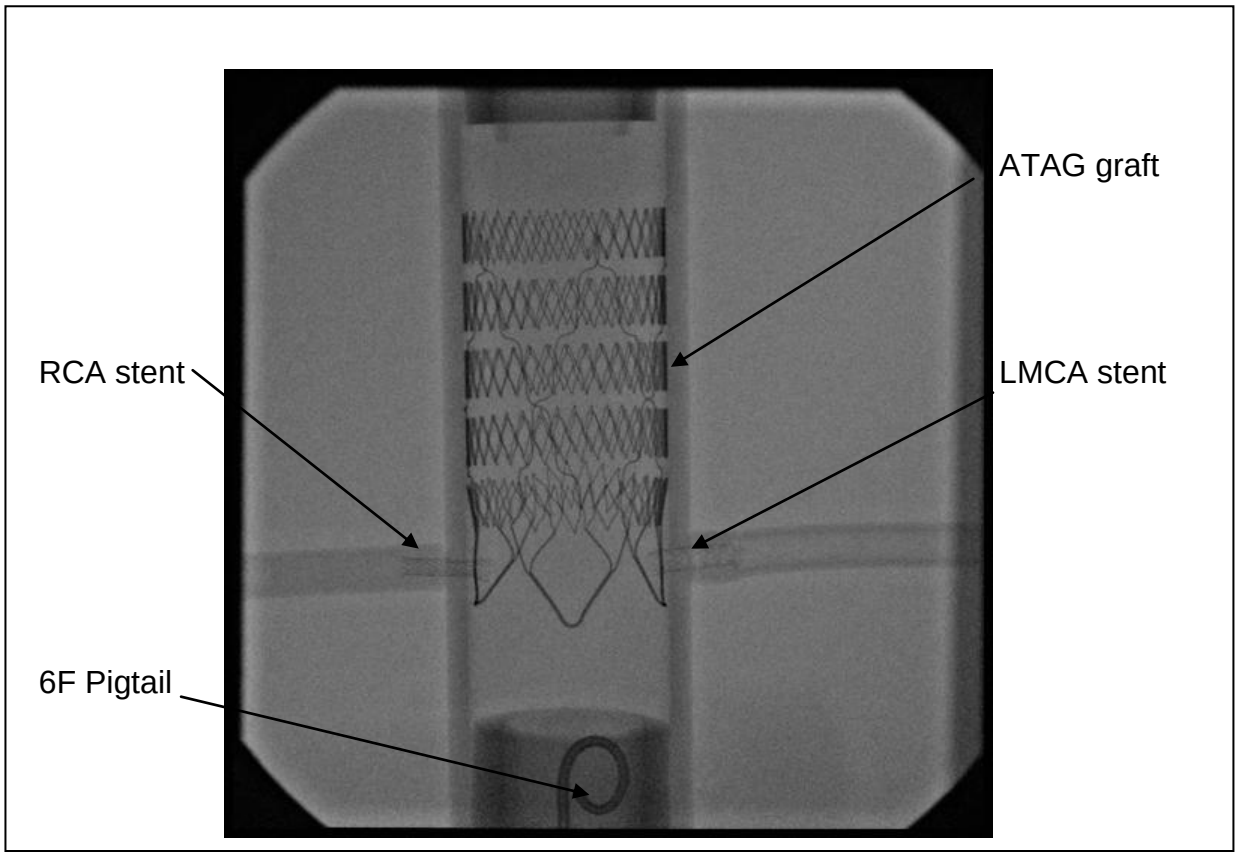

5.1.4.3 Results

CD ROM attached to this thesis documents the video captured fluoroscopy, a still image is shown in Figure 115 below:

Figure 115 Still fluoroscopic image from the contrast injection into ATAG

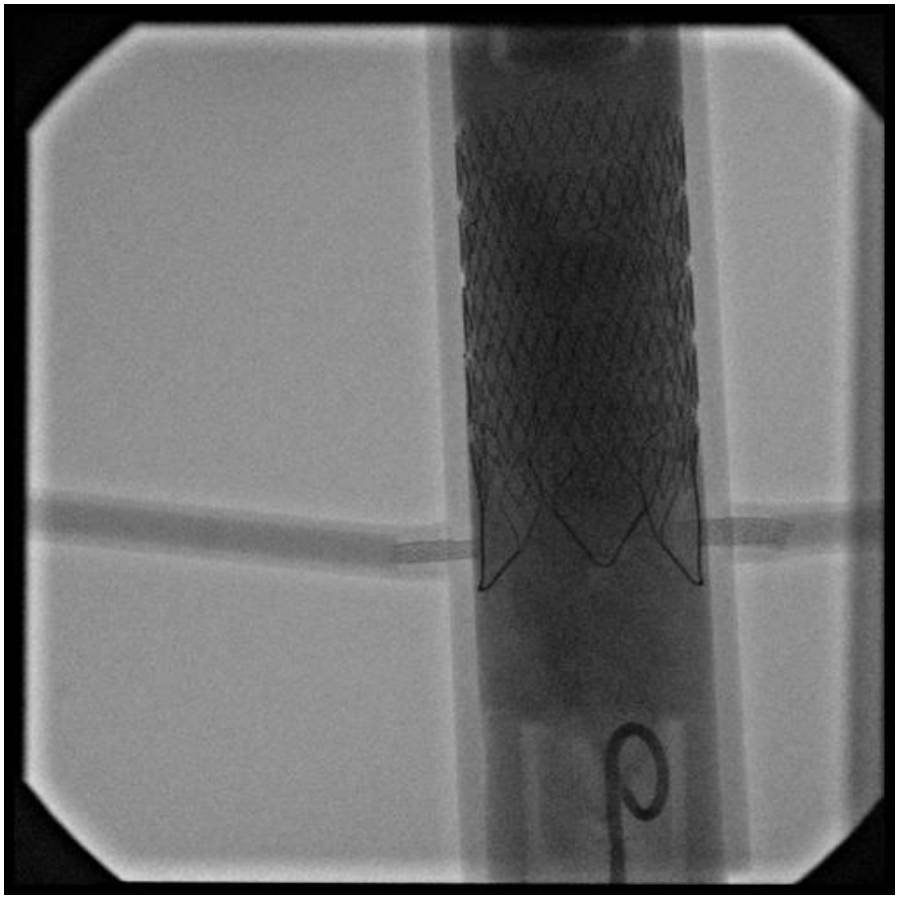

It appears contrast travels through the coronary arteries and stent graft body. The ability to detect and quantify endoleak is impossible by this means, and would be better achieved under direct vision with the use of a dye tracer, which would be seen to track outside of the graft material.

5.1.5 Conclusion and discussion

The set up of an extremely simple flow loop with variable coronary and outflow resistances enabled me to get a first “understanding” of flow loop dynamics, and really acted as an introduction to further more complex pulsatile flow rigs with resistance and capacitance.

I was able to set up a flow rig with a maximal flow of 14 L/min and low pressure, as well as a maximal pressure of 94 mmHg with no flow (outflow tap closed = hydrostatic pressure from 2.5 metres). In both of these scenarios there appeared to be no migration of the ATAG graft macroscopically, although we must accept that the lack of migration may have had much to do with the materials used in the loop (i.e. Perspex and PU).

I was also able to set up a flow rig with physiological cardiac output and correctly proportioned flow through the main graft and into both coronary arteries.

The flow assessment under fluoroscopy added little to our understanding of the graft, apart from its radio-opacity. Endoleak cannot be formally assessed, although contrast could clearly be seen to track behind the 3 proximal “feelers”, implying that proximal seal would not have been sufficient in this case. It must however be pointed out that because of constant size of the Perspex model and no sinus dilatation the specifically designed feelers were unable to take up their anatomical position and potential proximal seal. This will be better assessed within future work *in vitro* testing utilising a silicone anatomically correct model (Elastrat, Geneva , CH), with integrated aortic valve.

5.2 Animal model selection for ATAG *in vivo* studies

The successful NIHR grant for further ATAG testing and development will take the 3G ATAG once built into in-vivo trials (beyond the scope of this thesis). During numerous meetings with Professor Brockman and Dr Connelly it became clear that the selection of an appropriate animal model for ascending aortic ATAG work is not straight forward.

While most TAVI valve and coronary stent testing had been performed in porcine models there are a number of issues that make the porcine ascending aorta less favourable as a model for testing ATAG. There is also a lack of robust published anatomical data about the ascending aorta in all animal models. I first decided to do a literature review on published aortic dimensions of potential animal models.

5.2.1 Possible animal models

The 3 animal species models most frequently utilised to test new cardiovascular devices are – ovine, porcine, and bovine. A literature review of aorta size in these 3 animals species revealed the following, summarised in Table 31 below:

Table 31 An overview of animal model aortic sizes

Animal model	Aortic size (mm)
2-5 year old ovine (55-95 Kg)	32.9 (range 28.3 – 39.7)(136)
1 year old porcine (30 Kg)	19 (range 19 – 25)(137;138)
4 month old bovine (120 Kg)	37.2 (SD +/- 9) (139)
Adult bovine (300 Kg)	60 (SD +/- 4)(139)

At first glance the ovine aorta may look promising for ATAG testing in that the ascending aortic size is similar in an adult sheep to that of an adult human. The porcine model would seem to have a relatively small aorta, and the juvenile bovine model has a good sized aortic diameter (37.2 mm), but if implanted at this size the ATAG would not be capable of expanding and keeping pace with the natural growth of the aorta resulting in the animal outgrowing the aortic graft.

There are also follow-up implications. Most regulatory *in-vivo* studies have at least 6 month follow up. The gold standard in aortic follow up like in human beings is either MRI or CT aortography. It is not possible to CT or MRI scan any adult animal > 120 Kg and as such for the reason of growth and sheer size the bovine model is impractical for regulatory ATAG testing.

A single echocardiographic ascending aorta diameter does not tell the whole story with regard to optimal *in-vivo* model for the implantation of ATAG. In the absence of

published data on animal model aortic size / length, coronary and aortic valve anatomy I decided to obtain cadaveric samples of all three species and perform my own examination and measurements.

5.2.2 Cadaveric measurement of ovine, porcine, and bovine aortic and coronary dimensions

5.2.2.1 Introduction

As can be seen from the literature review above there is a paucity of accurate and reliable aortic, great vessel and coronary anatomical data to allow us to pick the best *in vivo* ATAG animal model for further prototype development. As a result I decided to obtain cadaveric samples of sheep heart and aorta (termed “pluck”), as well as pig and cow from Smithfield livestock market, City of London.

5.2.2.2 Aim

In cadaveric sheep, pigs and cows to dissect and accurately measure aortic diameters and distances of great vessels, comparing them to the known human reference vessels.

5.2.2.3 Methods

Cadaveric animal heart and aorta were obtained. The aortas were dissected using scalpel and fine scissors, and then diameter and length measurements were made by a single operator (TK or SP assisted by Professor Brockman) using callipers capable of measuring to the nearest 0.1 mm.

5.2.2.3.1 Aorta and coronary measurements

The following measurements were made in all 3 animal cohorts, as shown in Table 32 below:

Table 32 Aortic and coronary measurements taken in each animal model

Ascending aorta diameter (mm)
LMCA ostium diameter (mm)
RCA ostium diameter (mm)
Distance from RCA to first great head and neck vessel (mm)
Distance from LMCA to first great head and neck vessel (mm)
Diameter of the first great head and neck vessel (mm)
Diameter of the mid aortic arch (mm)

5.2.2.4 Experiment 1 - ovine measurements

5.2.2.4.1 Study population

Measurements were performed on 4 adult 60-70 Kg sheep plucks consisting of the heart, ascending aorta and aortic arch. Plucks had been frozen and then thawed prior to measurement.

5.2.2.4.2 Results

The ovine ascending aorta is short, giving rise to a single great head and neck vessel - the brachiocephalic trunk. This then divides into the left and right subclavian arteries, and a branch that then gives rise to both the right and left common carotid arteries (see Figure 116 below):

Figure 116 Ovine heart and ascending aorta

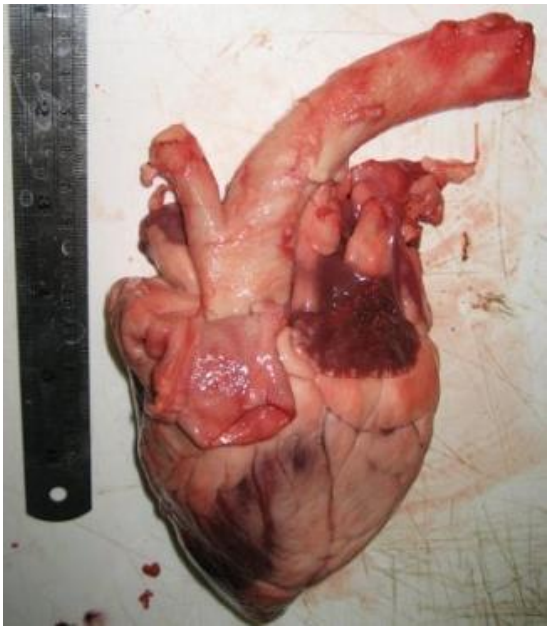

The ovine ascending aorta is short, giving rise to a single great head and neck vessel - the bracheo-cephalic trunk. This then divides into the left and right subclavian arteries, and a branch that then gives rise to both the right and left common carotid arteries

Table 33 Ovine aorta and coronary measurements

Sample	Ascending Aortic diameter (mm)	LMCA diameter (mm)	RCA diameter (mm)	Distance from RCA to 1st branch (mm)	Distance from LMCA to point opposite 1st branch (mm)	Diameter mid aortic arch (mm)	Diameter of the 1st aortic branch (mm)
1	20.8	6.9	2.8	23.8	14.1	14.2	11.2
2	22.2	7.7	2.3	20	11.4	16.5	12.2
3	19	7.8	2.7	14.8	12	16.1	9.5
4	17.4	5.9	1.9	16.2	12.5	12.6	9.8
Mean	**19.9**	**7.1**	**2.4**	**18.7**	**12.5**	**14.9**	**10.7**
SD	2.09	0.88	0.41	4.05	1.16	1.80	1.26

5.2.2.4.3 Conclusion

The measurements of the vasculature of adult sheep plucks from 60–70 Kg animals suggested many anatomical differences to that seen in the human population.

The measurements showed the average ascending aortic diameter was smaller at 19.9 +/- 2 mm, whereas an average normal human ascending aortic diameter is 32.7 ± 4 mm (11).

The anatomical features of the sheep were also different; the average LMCA diameter was 3 times that of the RCA, 7.1 mm and 2.4 mm respectively. Sheep also have one

large common branch off the aortic arch compared to three in humans. This vessel also branches off earlier leaving an average ascending aortic length of only 18.7 mm compared to 92.6 mm in humans (11).

5.2.2.5 Experiment 2 - porcine measurements

5.2.2.5.1 Study population

Measurements were performed on 3 adult 60-70 Kg porcine plucks consisting of the heart, ascending aorta and aortic arch. Plucks had been frozen and then thawed prior to measurement.

5.2.2.5.2 Results

The porcine aorta also has a different great vessel anatomy when compared to both the human and the ovine model. The porcine ascending aorta gives rise to 2 arch vessels, a brachiocephalic trunk and a LSCA as shown in Figure 117 below:

Figure 117 2 aortic arch vessels in the Porcine animal model

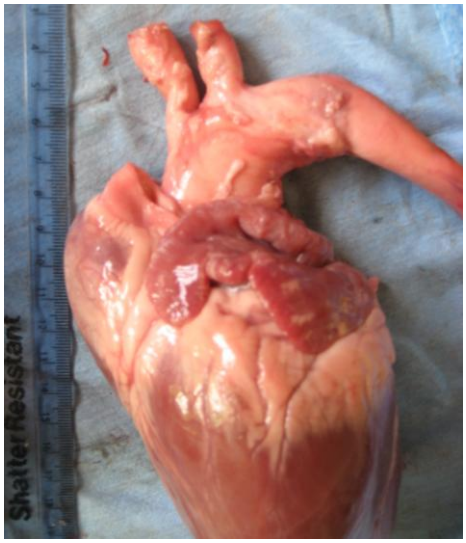

Table 34 Porcine aorta and coronary measurements

Sample	Asc. Aortic diameter (mm)	LMCA diameter (mm)	RCA diameter (mm)	Distance from RCA to 1st branch	Distance from LMCA to point opposite first branch (mm)	Diameter aortic arch (mm)	Diameter of the 1st aortic branch (mm)
1	19.7	8.3	N/A*	N/A*	38	N/A*	N/A*
2	21	8.6	4.0	38	40	17.5	10.2
3	19.7	6.4	4.0	32	35	16.6	9.2
Mean	**20.1**	**7.8**	**4.0**	**35**	**37.7**	**17.1**	**9.7**
SD	0.75	1.19	0	4.24	2.52	0.64	0.71

**The 1st heart was cut in half so not all the measurements were available (N/A)*

5.2.2.5.3 Conclusions

There are differences between the porcine model and the normal human aorta. The ascending aorta is smaller with a mean diameter of 20.1 mm. The LMCA is larger at 7.8 mm, and nearly double the size of the RCA ostium (4.0 mm). The distance from the coronary arteries to the first great head and neck vessel is shorter (35 mm and 37.7 mm).

The aortic arch consists of 2 branches:

1) The first, a brachiocephalic trunk, which then splits into the right subclavian artery and a cephalic trunk that then further splits into the right and left common carotid arteries.

2) The left subclavian artery.

The anatomical finding of the 2 branch aortic arch is shown in Figure 118 below:

Figure 118 Diagrammatic representation of porcine aorta and branches

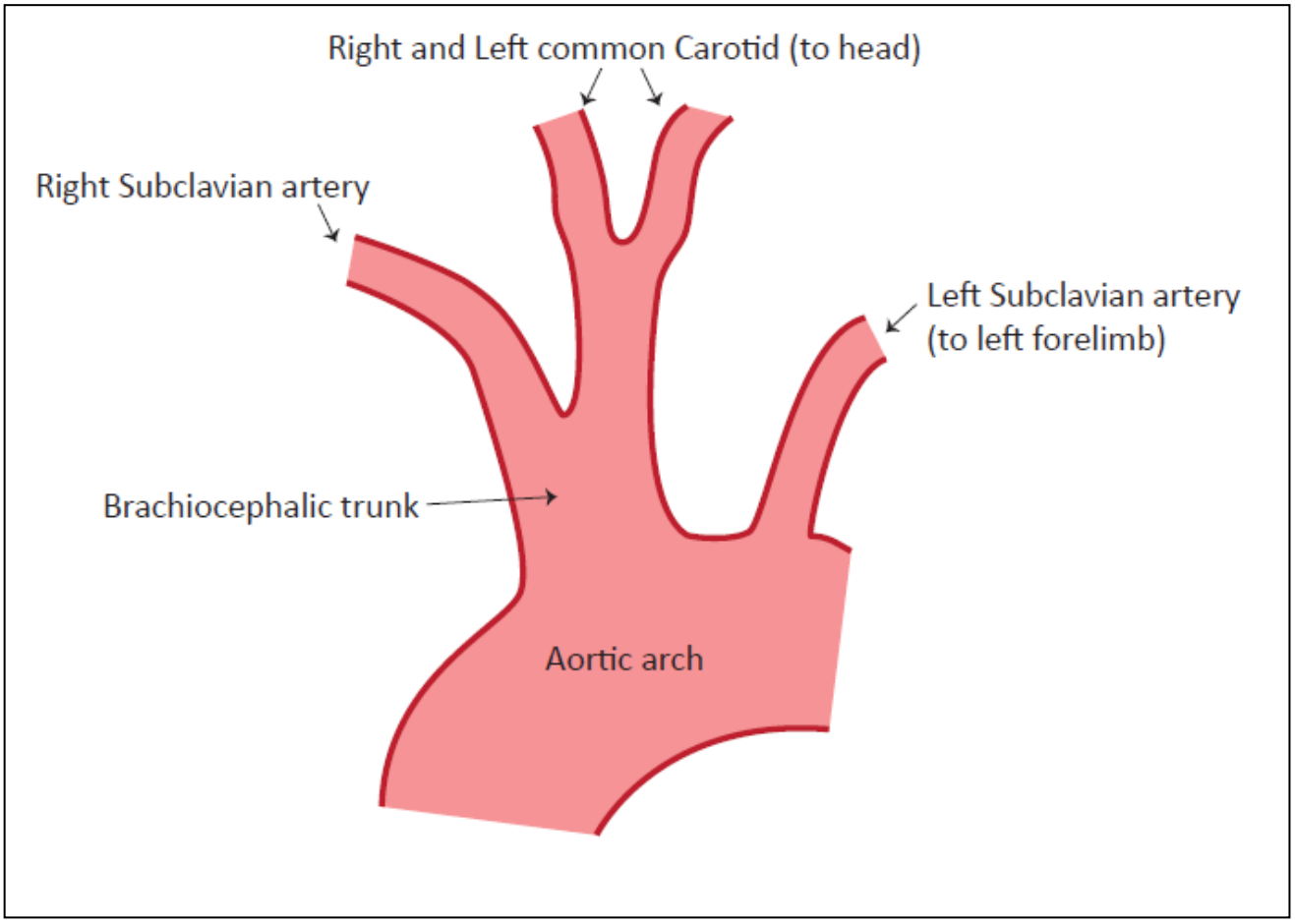

The porcine aortic arch gives rise to a brachiocephalic trunk, which then splits into the right subclavian artery and a cephalic trunk that then further splits into the right and left common carotid arteries. The second arotic arch branch is the left subclavian artery.

5.2.2.6 Experiment 3 Bovine aorta (Juvenile calves 140-150 Kg, 26-28 weeks old)

5.2.2.6.1 Study population

Measurements were performed on 3 juvenile 140-150 Kg calf plucks consisting of the heart, ascending aorta and aortic arch. Plucks had been frozen and then thawed prior to measurement.

5.2.2.6.2 Results

The bovine aorta is relatively similar to the ovine aorta in that it has a relatively short ascending aortic portion before giving rise to a single arch vessel the brachiocephalic trunk, as shown in Figure 119 and 120 below:

Figure 119 Bovine aorta with single bracheocephalic trunk

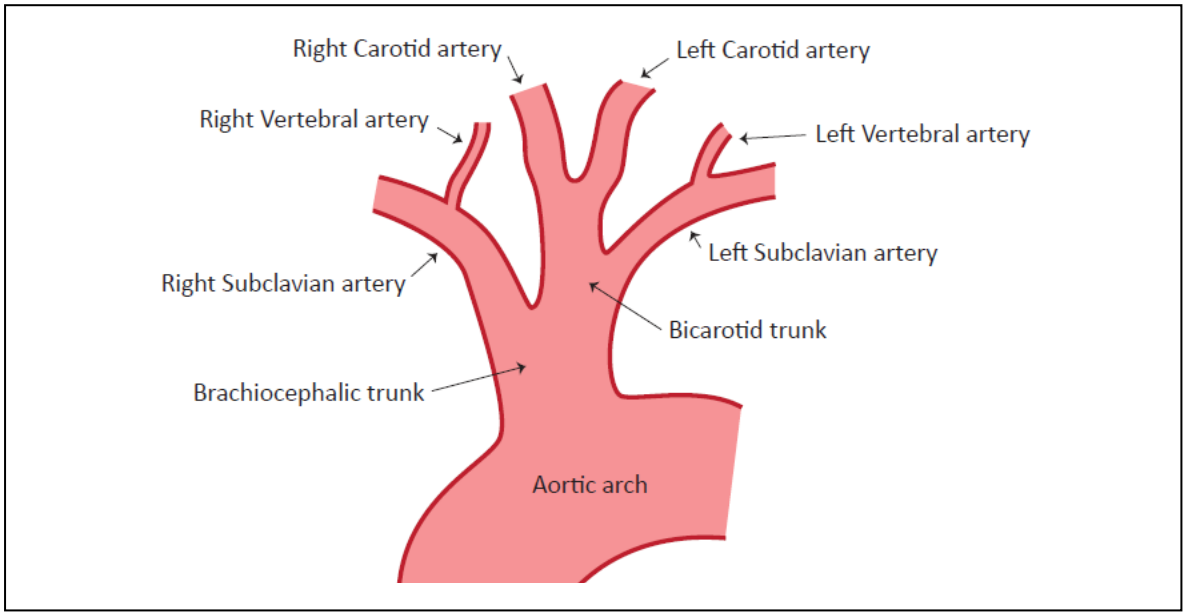

The bovine aorti has a single brachiocephalic trunk, which then further subdivides into the right subclavian artery, a bi-carotid trunk and the LSCA.

Figure 120 Photographs of bovine ascending aorta, single great head and neck vessel and proximal arch

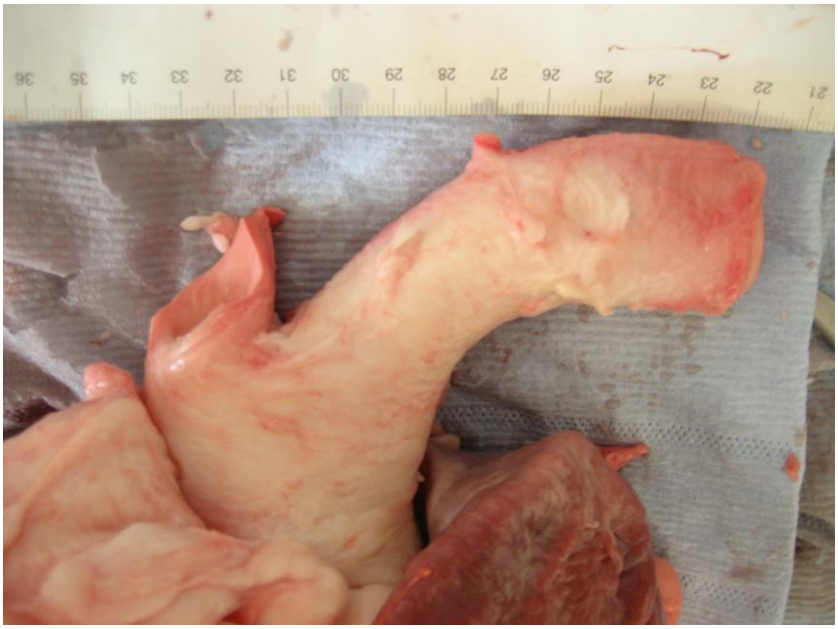

Table 35 Bovine aorta and coronary measurements

Sample	Asc. Aortic diameter (mm)	LMCA diameter (mm)	RCA diameter (mm)	Distance from RCA to 1st branch (mm)	Distance from LMCA to point opposite first branch (mm)	Diameter aortic arch (mm)	Diameter of the 1st aortic branch (mm)
1	32.5	8.4	3.7	29.0	27.7	23.8	20.7
2	32.6	8.3	5.3	31.5	29.1	21.5	16.7
3	32.0	7.8	3.4	30.6	27.0	23.2	19.6
Mean	**32.4**	**8.2**	**4.1**	**30.4**	**27.9**	**22.8**	**19.0**
Standard Deviation	0.3	0.3	1.0	1.3	1.1	1.2	2.1

5.2.2.6.3 Conclusions

The juvenile calf shares a similar aortic size to the human, but has just one common head and neck branch, which divides into three main vessels.

The coronary arteries are LMCA 8.2 mm and RCA 4.1 mm in size, but again the distance from the coronary arteries to the first great head and neck vessel is short at only around 30 mm.

5.2.3 Discussion of potential animal model results

Table 36 below summarises the mean measurements from each animal model:

Table 36 Comparing the mean measurements of each animals vessel sizes

Sample	Asc. Aortic diameter (mm)	LMCA diameter (mm)	RCA diameter (mm)	Distance from RCA to 1st branch	Distance from LMCA to point opposite first branch (mm)	Diameter aortic arch (mm)	Diameter of the 1st aortic branch (mm)
Sheep	19.9	7.1	2.4	18.7	12.5	14.9	10.7
Pig	20.1	7.8	4	35	37.7	17.1	9.7
Calf	32.4	8.2	4.1	30.4	27.9	22.8	19

The first thing to say is that both the ovine and porcine animal cohorts were of adult size, whereas the calves were Juveniles and as compared to the literature search the juvenile aortic diameter is about half of the full grown aortic diameter. The size of the animal at

the time of implantation and the animal's ability for growth are important features for 2 reasons:

I) If we implant a 4 cm diameter ATAG graft into a juvenile calf 3.4 cm aorta, then by the time the animal is fully grown the graft will be massively undersized to the full grown aortic diameter and this will make it a very unreliable *in vivo* model with many confounding factors in long term follow up.

II) The best endovascular graft follow up is achieved by CT or MRI scanning, but this is not technically feasible for full size cows as they are too large and too heavy for the CT scanner at the RVC.

All three animal models have a different aortic arch configuration compared to the human (traditionally with 3 arch vessels). This is itself not a problem, but it is the relative short distance between coronary arteries and first great head and neck vessel that will require a bespoke "shortened ATAG" for *in vivo* testing. We must also factor into the *in vivo* ATAG the fact that the coronary arteries are relatively large compared to the human, and their angle of take off relative to one another may be very different to the human angle of 154 degrees (not possible to accurately measure in these cadaveric samples).

Because of the relative large size, and growth considerations with follow up I think it is unlikely that the bovine model will be a robust survival model.

We are therefore left with both the ovine and porcine model. The aortic diameter is very similar in both (approximately 20 mm), considerably smaller than humans, but the ovine model has an even shorter distance from coronary artery to first great vessel (<20 mm) which I think makes the ovine model impractical. As a result I think the model that is

likely to best approximate that of the human is the porcine. The Pig has a mean aortic diameter of 20.1 mm, and an ascending aortic portion of 37.7 mm. My only concern about the porcine model are the personal communication comments from the Chuter group during their ascending aorta stent graft testing in pigs where they felt the model did not tolerate the procedure very well (presumably coronary ischaemia), but this data is unpublished.

The adult porcine and ovine models are both of sufficient size for device implantation - although as has been discussed both will require ATAG devices specifically designed for their aortic anatomy with smaller aortic diameter, larger coronary sleeves, and a shorter main body portion. Utilising the adult porcine model will also enable CT follow up as they can easily be accommodated within the CT scanner at RVC.

5.2.3.1 Study limitations

The flaccid nature of the vessels meant it was difficult to determine the exact diameter, also the vessels had to be held to make them circular for the measurements to be taken. This investigation was also limited by the difficulty faced, even with the help of a veterinary surgeon in identifying some of the structures.

5.2.3.2 Recommendation ATAG In Vivo testing model

From the information gained from the anatomical study any animal model implantation is going to require a bespoke graft for that species, taking into account the aortic diameter, coronary diameter and distance to first head and neck vessel. The bovine model, while

of good aortic calibre may be useful for a first acute non survival model, but its relative size and growth potential make survival model follow up in the form of CT impossible.

The ovine model while it has a smaller aortic diameter of 20 mm, and will fit easily within a CT scanner for robust survival follow up, it has a very short ascending aorta from coronary arteries to first head and neck vessel (<20 mm). As a result I would propose that for the reasons outlined above the porcine model in the first instance is the best animal model for future 3G ATAG *in vivo* studies although the models ability to tolerate myocardial ischaemia will need to be critically appraised. If the procedural tolerability is an issue a shortened ATAG may be utilised potentially in an ovine model. Further testing is required before these decisions can be taken.

Chapter Six

Health Economics

Chapter Six : Health Economics

6.0 Health economic and cost considerations

A medical device in its early stage of development is difficult to accurately assess the proposed final device cost. The final proposed market price for ATAG will be affected by many factors including the effectiveness of the device, the health care cost of the 'conventional' treatment, the price and performance of potential competitor devices.

I will give some insight into potential ATAG costings by commenting on the current costs associated with 2 related clinical areas:

i) The endovascular treatment of abdominal aortic aneurysm (AAA)
ii) Trans-catheter aortic valve (TAVI) therapies

Endovascular treatment of abdominal aortic aneurysm (AAA) has high success rates and has reduced hospital stay from a mean of 13 days to 6 days (140). There are a number of competing devices on the market and currently in the UK they sell for around £5k, and in the US $12k. This is set against a fully loaded build cost of around £800 for one device manufactured in the UK (verbal communication with Professor Rothman who is a main board director of this company).

Treatment of aortic stenosis in Octogenarians and other high risk groups turned down for conventional aortic valve replacement surgery has been revolutionised in the last 4 years with the development of TAVI with very encouraging mortality, morbidity and quality of life improvements. In the UK and Europe there are 2 commercially available devices; the

Edwards Sapien™ aortic valve, and the Medtronic CoreValve™. Both devices currently sell in the UK for approximately £12,500.

In the UK the Department of Health categorises each surgical procedure performed with an HRG reimbursement code specific to the procedure. There is currently no specific code for "surgical treatment of ascending aortic dissection", or "surgical treatment of ascending aortic aneurysm", but instead :

- Coronary artery bypass
- Cardiac valve procedures
- Other cardio-thoracic procedures with cardio-pulmonary support

Depending on the exact nature of the aortic dissection and aneurysm surgery required different tariffs will be attracted depending on the anatomy and concomitant coronary and valve disease (the tariffs vary between £4.5k – £7.5k). However this tariff does not reflect additional ITU stay, or the cost of renal dialysis where extra costs are incurred and are not reimbursed. Other factors affecting length of stay are co-morbidities and age. Neri *et al* report that operation for AAAD in Octogenarians (a high risk group n=24) had an 83% in-hospital mortality rate. Mean hospital stay was 37 days and mean intensive care stay was 19 days. None of the patients were able to function normally and survival at 6 months was 0% (141).

In our institution (London Chest Hospital, E2) an intensive care bed day costs £2k, HDU bed £800, and CCU bed £300. One can therefore extrapolate from this high risk elderly cohort described that the mean cost would be:

Procedural tariff	= £4.5 – £7.5k
19 ITU bed days * £2k	= £38k
5 HDU bed days * £800	= £4k
13 bed days * £300	= £3.5k

This therefore corresponds to a mean cost in this high risk group of £51.5k with horrendous levels of associated morbidity and mortality.

Depending on the final ATAG clinical performance we believe that a cost similar to that of the percutaneous aortic valve plus potentially an “unmet clinical need premium” would be appropriate. We would hope that in a similar way to endovascular treatment of both the abdominal aorta and aortic valve, ATAG would reduce hospital stay and morbidity and mortality which may result in cost effectiveness – this will be fully analysed as the project progresses.

Thus in summary we expect the health care cost of an admission to be of the order of £50k, against which the ATAG end-user price (if the only solution in the market) would be set at around £20k, with a fully loaded manufacturing cost (when production is stabilised) of around £1000.

Chapter Seven

ATAG Conclusion

Chapter Seven : ATAG Conclusion

7.0 ATAG thesis discussion and Conclusions

There is a huge unmet clinical need for a new, safe and effective minimally invasive treatment for Acute Ascending Aortic Dissection. In 2012 AAAD has a mortality rate of 1-2% per hour within the first 24 hours, and even with contemporary surgical techniques, advanced intensive and post operative care, the mortality from AAAD following surgery in most series remains in the unacceptable range of 10-30% at 30 days (2;3). 28% of patients presenting with AAAD are denied life saving surgery often because of age or co-morbidity - medical therapy alone associated with an in hospital mortality rate in excess of 50% (2;4-6).

The last decade has seen a rapid expansion in percutaneous therapies for cardiovascular disease. The emergence of TAVI is now offering elderly and high risk patients with severe aortic stenosis an alternative to conventional aortic valve surgery, with proven outcome and symptom improvement at 1 year (28;113). Endovascular repair of infra-renal abdominal aortic aneurysm (EVAR) is now a standard of care, and TEVAR has an emerging role in the treatment of complicated Type B aortic dissection and descending thoracic aortic aneurysm (5;6;94).

There are however stark differences in uptake and development of technologies between TAVI and endovascular aortic stenting, and I think this partly explains the lack of development of a suitable ascending aortic graft. Despite Cribier's FIM TAVI (2002) being performed 11 years after Parodi's first endovascular aneurysm repair (EVAR

1991), the TAVI devices have evolved much more rapidly, and have accumulated much more randomised clinical data (112;113;142).

In TAVI, both CE marked devices gained early clinical use with a profile >25 F, and within 2 generations and inside 5 years are now 18 F in diameter, with the Edwards Sapien XT being implanted through an expandable 16 F eSheath^{TM}, as compared to the standard range of TEVAR devices (Medtronic Valiant Captiva) whose delivery sheath diameter remains between 22-25 F. TAVI devices have elegant delivery systems capable of traversing the aortic arch, minimising vascular complication, CVA and maximising accurate deployment, while TAA and AAA endografts continue to be deployed with bulky, inflexible and large diameter delivery systems. Many of the stent frame, stowing and delivery sheath technologies developed with TAVI devices are potentially transferable to a ascending aortic graft, and I think will be necessary if a endovascular solution for AAAD is to be realised.

TAVI has also taught us of the importance of working in multi-disciplinary teams, and of a "heart team" to make collegiate decisions for the patient and perform the interventions together with varied skill sets. In the future with the development of ATAG devices I envisage the heart team growing into a cardiovascular team, with the addition of a radiologist, and endovascular surgeon.

This thesis describes in detail the anatomical, and device design barriers that I believe have prevented the development of a dedicated percutaneous solution for ascending aortic syndromes. These include proximity and involvement of AAAD with aortic valve function, and coronary artery location, and the ability of an endovascular graft to obtain proximal seal so close to these vital structures. The curvature of the ascending aorta,

the pulsatile flow and variability in diastolic and systolic diameters, coupled with the landing zone close to the RBCT adds further layers of complexity (15).

The current thoracic endografts are bulky and inflexible, and covered in rigid materials which are prone to infolding. PET and ePTFE as well as conforming poorly to the arterial wall create an overt inflammatory reaction with a cellular migration and infiltration promoting cell adhesion, thrombosis and poor long term patency in small calibre vessels. The anti-migration mechanisms are often crude with 5 mm barbs to anchor the graft into position, a strategy that is liable to complication so close to the aortic valve and coronary arteries. Not only are the current TAA endografts rudimentary they are deployed using large diameter inflexible delivery systems. It is easy to understand why endovascular stent grafting of the ascending aorta is confined to a handful of case reports using short grafts inserted via various access routes (114).

In my opinion successful treatment of AAAD with a dedicated graft will only occur with significant investment from device companies in state of the art nitinol frame design, novel graft material and developing deployment systems similar to those already available for TAVI.

To bring this thesis to a conclusion I am going to discuss in detail what features an ATAG device, or a family of ATAG devices must have to successfully treat AAAD and potentially ATAA. I do not underestimate the complexity and the amount of work involved in bringing my suggested device specifications to reality.

This thesis has informed me that there are likely to be a family of probably 3 ATAG devices, all sharing core technologies, but having different design specifications to deal

with the specific anatomical challenges that are posed. Core features in all grafts will be a low profile nitinol frame with appropriate radial strength, coupled with a thin non-porous polyurethane covering, housed in a flexible delivery sheath with precise and accurate deployment mechanisms. There are likely to be a number of implantation routes including, femoral, subclavian, direct aortic and possibly carotid. The optimal route for each patient will depend upon pre-procedure CT scanning. Implantation is likely to occur in a hybrid theatre with a cardiovascular multi-disciplinary team.

In the simplest terms the 3 embodiments of ATAG that I envisage are:

1) The “supra-coronary tubular ATAG”, for treating AAAD with an intimal tear in the ascending aorta, no coronary or aortic valve involvement and adequate landing zones above the coronary arteries and before the RBCT.

2) The “inverted t-shirt ATAG” to pro-actively protect coronary artery flow and achieve proximal seal within the sinuses in patients with an intimal tear in close association or involving the coronary arteries.

3) The “valved ATAG” to treat patients who have significant AR, to achieve a proximal seal at the annulus when anatomy suggests it would be difficult to achieve with embodiment 1) or 2), and in those patients who have hugely dilated aortic root, so that the ATAG can seal proximally at a relatively normal annulus size to a distal seal at normal ascending aorta proximal to the RBCT.

Embodiment 1) ATAG Tubular Graft

The IRAD reported in 2007 that of the 682 patients who had surgical repair of AAAD, 58.5% had an isolated supra-coronary aortic replacement (9). Sobocinski in 2011 goes on to suggest that at least one third of all AAAD patients based on CT scans could technically be treated by deploying a “simple” supra-coronary tubular endograft, between coronary arteries and RBCT, excluding the intimal tear, and avoiding interference with the coronary arteries or aortic valve (8).

Successful uncomplicated ATAG tubular graft deployment will require considerable technological advances with regard to grafts and delivery systems when compared to current TEVAR endografts.

The graft must be stowable to a lower profile than currently available with 18 F being desirable. The stent frame must be flexible to allow passage around the aortic arch, yet still retain adequate radial strength. The graft is likely to benefit from the advanced laser-cut nitinol frame, which may have longitudinal tie bars on the inner and outer curve capable of relative expansion on the outer aortic wall and compressing on the inner wall enabling better apposition of graft to aortic wall. A novel PU graft material which is thin, non-porous, and biologically inert might oppose the aortic wall and be capable of withstanding the mechanical stress of aortic pulsatility and the 17% variability in aortic size between systole and diastole (15). The delivery catheter must resemble that of a TAVI device with accurate and precise deployment mechanism, probably with the aid of rapid ventricular pacing.

ATAG graft sizing is an important consideration. Currently the largest commercially available TEVAR graft is 46 mm in diameter. This means with a 20% over-sizing protocol the largest true lumen size that can be treated is 38 mm (which corresponds to a total aortic size of 46 mm). The Parish AAAD dimension data suggests that to be able to treat 85% of aortic diameters an endovascular graft will need to be capable of treating total aortic diameters between 40 – 65 mm (87). The problem with treating larger aortic diameters, is that the stent graft has to be of a greater size which in turn has both stent design and stowing implications. Only with further stent bench testing will it become clear as to the maximal aortic diameter that can be manufactured and stowed to our 18 F goal.

All embodiments of ATAG will need to be stocked in the cardiac centre in a number of diameters and lengths, immediately available given the urgent nature of AAAD intervention. If during the procedure the aortic valve becomes compromised, commercially available TAVI implantation can be considered so long as the annulus size is acceptable.

Embodiment 2 "inverted t- shirt" ATAG

In patients with AAAD who have coronary artery involvement, or whose intimal tear is within 2 cm of a coronary artery, to enable proximal endograft seal and to pro-actively secure coronary artery flow the "inverted t-shirt ATAG" should be developed. Compared to embodiment 1) this is a more complex device.

The proximal "sinus feelers" must oppose the sinus wall, creating a proximal seal, delivering the coronary sleeves to both LMCA and RCA at the same time not interfering

with aortic valve competence. While I have proven that in a normal glass aorta this technique is feasible there are many *in vivo* complexities which will make successful deployment of this device very challenging.

There is the need for 3 wires – one in each coronary and one within the left ventricle. One of the major limitations in the proof of concept testing was the fact that these guidewires were fixed in position - a manoeuvre that cannot be replicated *in vivo*. In the future as the 3G ATAG device and delivery system is iterated and developed simultaneous bench top testing must occur to determine the guidewire forces required to keep position and design wires with appropriate holding specifications. Another complicating factor that may be difficult to resolve *in vivo* is the fact that the coronary wires tend to cross 2 cm above the implantation zone. *In vitro* and under fluoroscopy this is resolved by retracting the LV wire from the LV, turning the delivery catheter through 180 degrees clockwise and then re-advancing the LV wire. This manoeuvre allows the coronary sleeves to re-align towards their respective ostia, and may be more difficult to reproduce *in vivo*.

As we move into the future 3G ATAG *in vitro* testing it will be vital to critically appraise the adequacy of ATAG graft, coronary sleeves and delivery system fluoroscopic markers, and this will be something that must be optimised before moving into the *in vivo* setting. It is also possible that while animal model implantations will be performed using C-arm fluoroscopy, ATAG implantation in humans may be aided in the hybrid catheter lab by 3D realtime CT to help guide graft and coronary sleeve orientation.

At this stage an important unknown is the human's ability to tolerate prolonged global and particularly coronary hypo-perfusion during the rapid ventricular pacing and proximal

ATAG deployment. There is still a question mark over whether bilateral protection of coronary flow with sleeves is technically feasible and physiologically tolerated. In the future, 3G ATAG will be tested most likely in the porcine model and this data will help tell us more as to whether the procedure can be performed. As has already been elucidated if “inverted t-shirt” ATAG is too technically and physiologically challenging we may need to retreat to a position where only one coronary is protected and the other is opposed by a fenestration. The answers to these questions should be addressed in the I4I future work packages which are found in section 8.0 and within the Appendix.

I designed the proximal end of the ATAG “inverted t-shirt” embodiment to mirror the natural sinuses of Valsalva so that the sinus “feelers” enter into the sinuses, with an external flare to gain adequate proximal seal to prevent endoleak, but do not interfere or disrupt the aortic valve integrity. This theory is as yet unproven, and it will be interesting during testing of the 3G ATAG whether these assumptions are substantiated. It is highly likely that further iterations will be required following *in vitro* testing to optimise proximal graft seal and understand the extent of aortic valve interference. In keeping with embodiment 1), if the aortic valve competence is compromised so long as the annulus is of an appropriate size the implantation of a commercially available TAVI can be considered.

Important novel anatomical information was gained from the CT analysis of patients presenting with AAAD, which informed the device specification of this embodiment. My AAAD CT data suggests that the annulus is normal sized, leading into a mildly dilated sinus of 29.1 mm, a dilated STJ of 41.6 mm, an ascending aorta of 43.5 mm. The RCA

would seem to be displaced cranially by about 10 mm (23 mm above annulus), with the LMCA only mildly displaced 3.8 mm compared to normal) (11).

The angle between both coronary arteries in the AP plane is a mean of 162.5 degrees (range 131.6 – 201.8), and has important implications for the design specification of the coronary sleeves for both embodiment 2) and 3). It will decide what angle the sleeves are attached to the graft body, and the material considerations enabling the sleeves to treat a range of coronary angles. During bench testing we must critically appraise the coronary angulations that PU coronary sleeves are able to treat, and whether further sleeve designs are required. Bench testing will also focus on the durability of sleeve / body join (currently glued), and whether with time the "inverted t-shirt" can be electro-spun in a single piece. Given the cell infiltration and poor long term patency rates of small diameter PET and ePTFE grafts I do believe that investigating a novel material for this embodiment is mandated.

Embodiment 3 "The Valved ATAG"

The "valved ATAG" is an endograft that would have its proximal seal at the aortic annulus, leading to a functional aortic valve, then into a coronary portion with two coronary artery sleeves to protect coronary flow, and finally a tubular portion with distal seal before the RBCT. I envisage this being a potential percutaneous solution for the 25-35% of AAAD patients who require aortic valve repair or replacement conventionally during AAAD surgery (9). It might also be a possible endovascular solution for treating ATAA if it can be performed with similarly low complication rates when compared to contemporary surgery.

It will I believe also be the percutaneous solution for patients with significantly dilated sinus segments of aorta with AAAD, in which achieving an adequate proximal seal with either embodiment 1) or 2) will probably be unsuccessful.

It is possible that a valved ATAG might be deployable without coronary sleeves (depending on the dissection anatomy), with a valved portion deployed into the aortic annulus giving aortic valve function, followed by a uncovered region opposing the coronary arteries allowing for unrestricted coronary flow, necessitating a robust and adequate seal at the sino-tubular junction to prevent type 1 endoleak.

Like all other embodiments of ATAG I do not underestimate the design and mechanical engineering challenges that must be overcome to realise this device.

Conclusion

I have demonstrated within this thesis a thorough understanding of the disease processes of AAAD and ATAA, and the current contemporary surgery management. I have identified that the largest current unmet clinical need is AAAD. The current endovascular stent grafts designed for use in the thoracic and abdominal aorta are not capable of being deployed reliably in the ascending aorta.

Within this thesis novel CT and MRI anatomical data in association with a literature search has led to the formulation of a design specification for 3 ATAG embodiments, one of which the “inverted t-shirt” ATAG has been successfully built and delivered within a normal sized glass model. A second generation (2G) ATAG has been manufactured

using a laser-cut nitinol frame and covered in 200 μm PU, being stowed to 28 F. The graft has a similar radial strength to competitor devices.

As co-applicant with Professor Rothman I have written a full 3 year future ATAG development plan that will build and test a 3G ATAG with delivery system both *in vitro* and *in vivo*, with survival animals. At the end of this period of investigation the aim will be to licence out the technology for commercialisation, or spin out a company and seek a large commercial partner to help move us a step closer to providing a percutaneous solution for treating patients with AAAD.

Chapter Eight

Future directions

Chapter Eight : Future directions

8.0 ATAG future directions

I have divided the future directions of the ATAG project into 5 discrete work packages which mirror the project plan from the NIHR funded I4I grant.

These work packages are described briefly below for directional purposes and more detail can be found within the attached NIHR proposal found in Appendix.

8.1 Work package 1

Development of a 3G ATAG prototype, with *in-vitro* flow testing.

Flow models allow detailed investigation of the graft behaviour under anatomical and physiologically realistic situations allowing graft and delivery system optimisation.

8.1.1 Aim

To characterise the behaviour of a 3G ATAG in different anatomical flow models.

3G ATAG stent graft prototypes will be specified and built in close collaboration with our contracted medical engineering partner (Qualimed, Hamburg, Germany). A basic delivery system will be designed and built. The stent graft samples will be mechanically characterised (stowing, radial forces, forces to deliver).

Elastrat (www.elastrat.com) will manufacture 4 silicone ascending aortic models from CT images (normal, proximal AATA, distal AATA, and dilated aorta like that seen in AAAD). A flow rig to simulate physiological conditions (pulsatile pressure and flow at body temperature and blood viscosity) will be assembled and characterised.

The ATAG will be repeatedly implanted under direct vision into the 4 silicone flow models with differing aortic anatomy to see how the graft behaves, documenting the following objective end points:

a) Pressure and flow measurements within the coronary arteries, the excluded aneurysm portion (sac), across the aortic valve and ascending aorta.
b) Interference with aortic valve function
c) Flow pattern analysis using a dye tracer
d) Expansion of the graft body assessed using an endoscope
e) Presence of endoleak
f) Proximal and distal seal assessment
g) Extent of ATAG migration

The results will be fed back and used to design an advanced prototype 4G stent graft for WP2.

8.2 Work package 2

In-vitro graft delivery and deployment study

8.2.1 Aim

Design specification and development of fully functional 2nd generation delivery system for ATAG.

Stent graft prototypes and delivery systems will be manufactured and characterised in bench top set up (tracking forces, forces to deploy and traction on guide wires). A series of samples will be used to study the deployment in detail in the flow-rigs under direct vision.

The study will then be repeated for delivery and deployment of ATAG in the 4 flow models under both direct vision and fluoroscopic guidance.

Focus will be upon measuring the following:

a) Positioning precision

b) Force required to push device and delivery system around aortic arch from femoral artery into implantation position

c) The torque forces of the delivery system

d) Force needed to deploy coronary stents on push rods

There will also be considerable end user feedback with the investigator critically appraising the ability of the device to track around the aortic arch, provide adequate

“pushability” of the coronary arms, and torque to allow the delivery system to transfer subtle movement of the hands to the front of the device in positioning.

WP2 is again likely to lead to further design iterations of both graft and delivery system.

At this time point the new ATAG stent graft samples will also be subject to cyclic load testing to ensure durability of up to 6 months to satisfy the 6 month survival and safety study. Full regulatory cyclic load testing and durability is beyond the scope of this project.

8.3 Work package 3

Acute *In-vivo* study

A 60-90 Kg pig may well provide the best *in-vivo* model for testing graft design and deliverability. The pig has an aortic diameter smaller than that of a human, but it has the longest “ascending aorta” before the first great head and neck vessel compared to both ovine and bovine models. Tolerability of the procedure may be an issue, but this experience will only be gained by an acute *in vivo study.*

All in-vivo studies will be carried out at the Royal Veterinary College with supervision by Professor Dan Brockman, and TOE guidance provided by RVC cardiologist Dr David Connelly. Dr Chris Lamb will provide CT follow up for survival animals and Prof Cheryl Scudamore will provide histopathology analysis post mortem.

8.3.1 Aim

To evaluate acute ATAG deployment in a porcine (non-survival) model

8.3.2 Methods

In 5 adult pigs under GA the ATAG device will be delivered to the aortic root under x-ray guidance and simultaneous TOE.

8.3.3 End Points

- Ability to implant ATAG in correct position without complication
- Stenting and patency of coronary arteries
- Integrity of aortic valve function (measured by TOE)
- Incidence of early migration
- Ability to create proximal and distal seal
- Incidence of early endoleak
- Incidence of heart rhythm disturbance
- Incidence of death as a result of implantation and its likely mechanism

- Histopathology of explanted samples

8.4 Work package 4

In-vivo survival and safety study

It is envisaged that there will be a further device update following on from WP3.

8.4.1 Aim

To evaluate the survival and safety of the ATAG device implanted in a porcine model (under x-ray and TOE guidance).

8.4.2 Methods

In 15 adult pigs under GA deliver the ATAG device and characterise the safety and 1, 3, & 6 month survival. (Identical implant team to WP3)

The first 5 will have a CT scan at 1 month before device is explanted and examined.

The second cohort of 5 will have a CT at 1 and 3 months before explantation and histo-pathological analysis.

The last 5 will have CT scan at 1, 3, and 6 months before explantation and analysis.

8.4.3 End points

- The ability to implant ATAG in correct position without complication
- Stenting and patency of coronary arteries 0, 1, 3 and 6 months (on CT)
- Integrity of aortic valve function (measured by echocardiography at 0, 1, 3 & 6 months)
- Incidence of early migration acutely, 1, 3, & 6 months
- Ability to create proximal and distal seal
- Incidence of endoleak
- Incidence of heart rhythm disturbance
- Implantation leading to death and mechanism
- Histopathology of explanted samples

8.5 Work package 5

Development of IP and business plan

In order to take the device to CE mark (regulatory processes), significant investment will be required. A business plan will be drafted to reflect this financial input and also to highlight potential exit points for investors.

Patentable IP will be collated and decisions will be made on patent filing at monthly meetings with patent team. Non-patentable IP including know how will be protected through a strict non-disclosure policy throughout the project.

Appendix

GRANTS WON / EQUIPMENT SPONSORSHIP

Grant won October 2006

Grant body	NHS Innovations London – PoC funding
Grant holder	Prof Martin T Rothman
Grant amount	£ 50,000

Grant won October 2007

Grant body	NHS Innovations London - 2G development
Grant holder	Prof Martin T Rothman
Grant amount	£ 75,000

Grant won December 2009

Grant body	NIHR i4i stream 2 funding body
Grant holder	Dr Thomas Keeble, Prof Stephen Greenwald, Prof Dan Brockman, Prof Martin T Rothman,
Grant amount	£ 743,000

Grant won December 2010

Company	GE healthcare and diagnostic imaging
Grant holder	Dr Thomas Keeble
Equipment	Delivery, installation and application training of the GE 9800 C-arm and cardiovascular table
Cost	Not disclosed, covered by GE healthcare and diagnostic imaging.

Grant won December 2010

Company	GE healthcare and diagnostic imaging
Grant holder	Dr Thomas Keeble
Equipment	Delivery, and use of 2 TOE probes for *in vivo* ATAG testing
Cost	Not disclosed, covered by GE healthcare and diagnostic imaging.

PRELIMINARY DELIVERY SYSTEM TESTING

Purpose of test

I) To define length of system components

II) To define proposed procedure sequence

III) To demonstrate the positioning of balloon and coronary stent using a twin delivery system.

Methods

Silicone tubing was used to simulate the aorta and artery path. Silicone tube 11mm OD x 7mm ID was taped to a bench top to form a 2D profile which represents entry through the femoral artery, abdominal aorta and descending aorta, into ascending aorta. The total cut length of the tube was 1000mm.

Two 7mm OD x 4mm ID Silicone side tubes represent the left and right coronary artery.

All tubes were lubricated with silicone oil. A tape measure was secured alongside the model to add scaling.

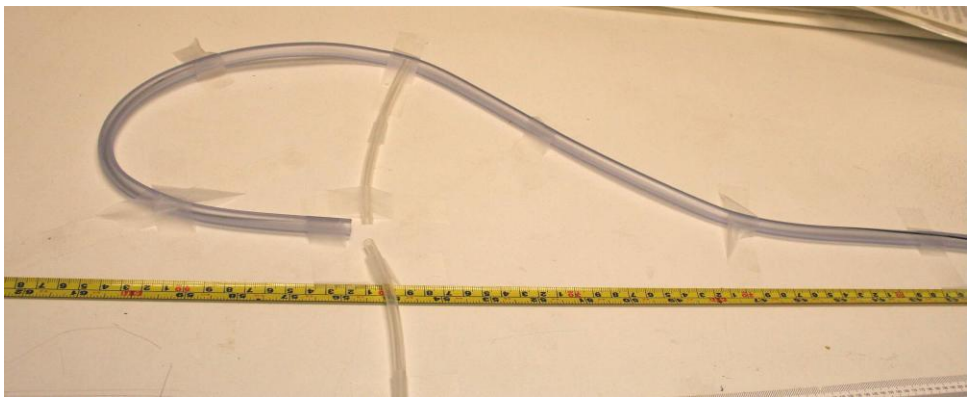

Figure A-1 showing photograph of the first mock aorta and coronary sleeves (before delivery of realistic glass model)

During the measurement of the device lengths, consideration was given to the 2D layout and we accept this is a simplification as we are not taking into account the "depth" of tissues and tortuosity of the arteries in the third dimension. At this time of testing we had not taken receipt of the life size aortic glass model and as such this was the most realistic testing available to us.

Delivery Sequence

Over a standard J tipped 0.038" floppy guide wire 130cm usable length a 6F JR4 standard guide catheter was advanced into the "left ventricular cavity". The floppy wire was then retracted and replaced with a 260cm usable length Superstiff wire into the LV followed by removal of the 6F catheter.

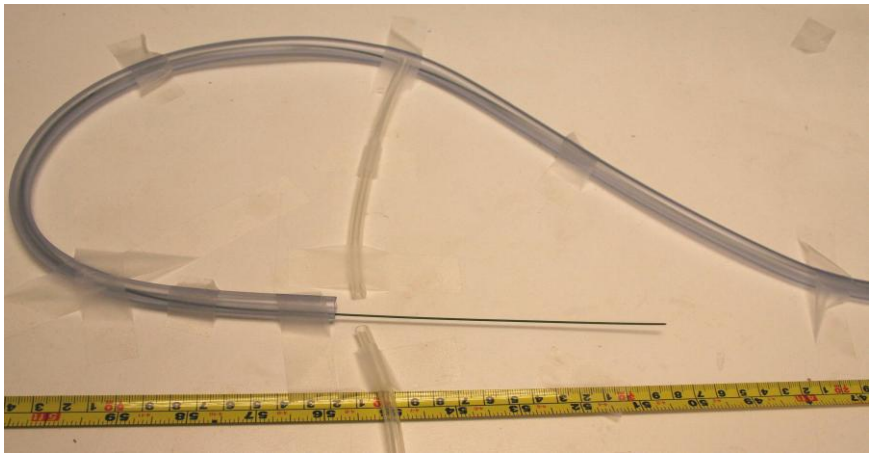

Figure A-2 showing 0.038” Superstiff guide wire in “LV” of the mock silicone aorta

Location of Left Coronary Guide Wire

A 6F JL4 Guide Catheter was located in to the left tube (LMCA) with ease over a standard 0.038 J wire.

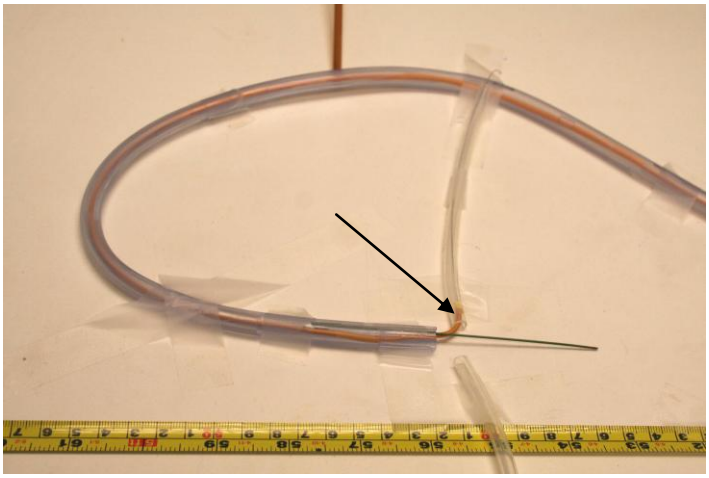

Figure A-3 shows JL4 guide catheter (arrow) in LMCA

A 260cm “floppy tip 0.014” guide wire was inserted in to the left branch, and the JL4 guide catheter removed. The process was then repeated for the RCA, with a 6F JR4

guide catheter advanced to the RCA ostium and a 260cm “floppy tip 0.014” guide inserted into the right coronary branch. Both guide catheters were then removed to leave the 3 guide wires in situ.

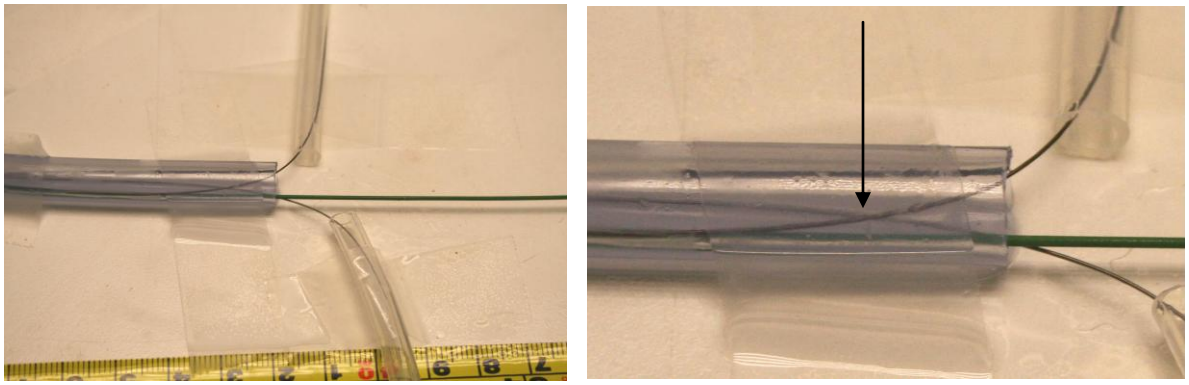

Figure A-4 show that the RCA guide wire has a tendency to hug the inner curve of the ascending aorta, and the LMCA coronary wire has a tendency to curve towards the outer wall of the aorta, leaving a crossing point marked by the arrow.

Success of ATAG delivery will require techniques to allow these wires to straighten and “uncross”.

Insertion of Delivery Catheter

A basic model of the delivery catheter was fabricated using two 7Fr guide catheters. These were inserted in to a 4.5mm polyamide sleeve. This allowed adequate space for the both of the 7Fr catheters and the 0.038” guide wire, whilst remaining within the design limits.

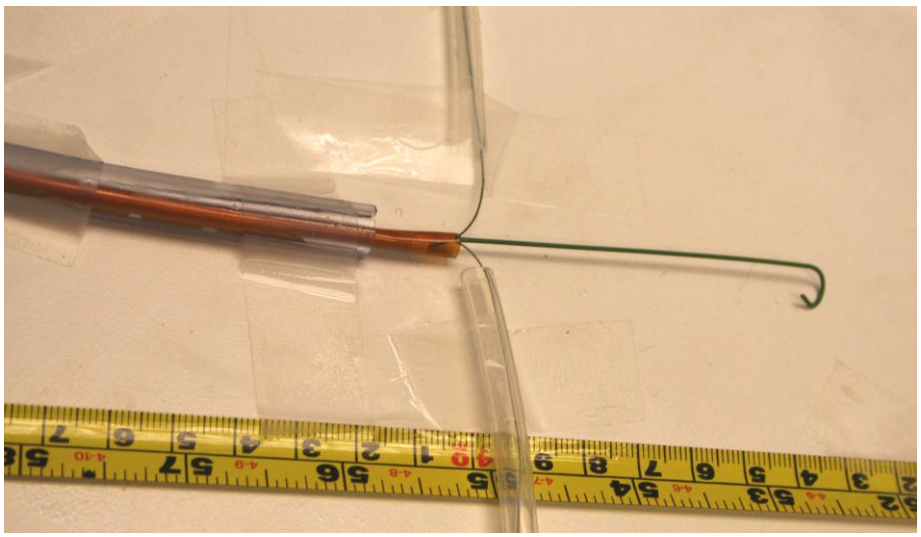

Figure A-5 Delivery catheter was advanced to the guide wire crossing location

During the advancement it was noted that the guide wires find their natural path and no pull back of the wires within the coronary branches was seen. Twisting did not occur.

Insertion of Coronary Stents

Two expired monorail Liberté^{TM} 3.0mm x 20mm coronary stent systems (Boston Scientific, USA) were loaded in to the 7Fr guide catheters over the 0.014" guide wires. They were positioned within the Delivery catheter in the "as loaded" location. The balloon catheters did not affect the tracking of the delivery device.

The balloon catheters have a 26cm flex monorail section and 120cm steel inflation shaft. The balloon catheters tracked through the delivery and into the side arms without any problems.

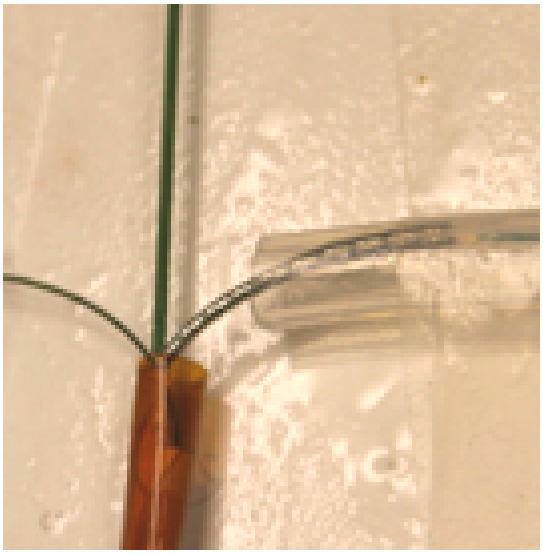

Figure A-6 Tracking of Right Coronary Stent from Delivery Catheter

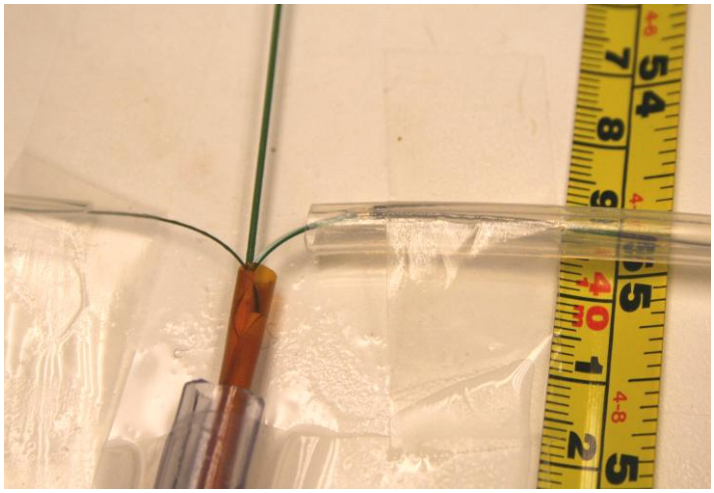

Figure A-7 Advancement of Right Coronary Stent

The process was repeated using the Left Coronary Stent. This process would be used to deploy the side arms of the graft.

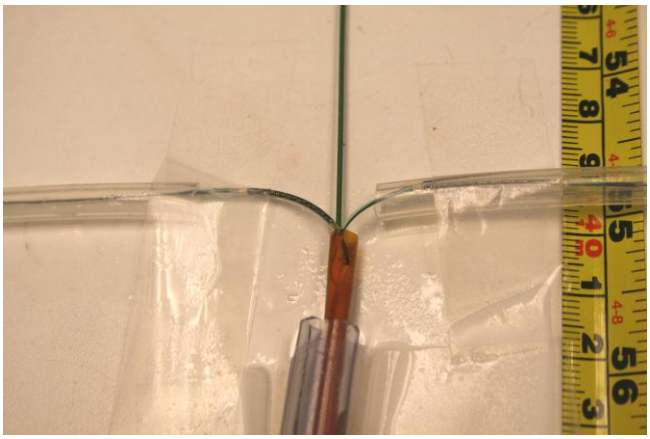

Figure A-8 Left and Right Coronary Stents in position close to “ostium” of LMCA and RCA

Figure A-9 Left and Right stent and balloon catheters (rapid exchange) loaded in Delivery Device 7F Lumens

At this stage the balloons would be inflated delivering the stents and thereby releasing the side arms of graft.

Removal of the Delivery Device

Once the stents are located, it is possible to remove the delivery catheter leaving the wires in place, thereby completing the test.

Conclusions

We have shown in the most simplistic way that a delivery catheter with 3 separate lumens can be advanced over 3 guide wires (2 * 0.014" * 260cm guide wires and 1 * 0.038" * 260cm Superstiff LV wire) around the arch and into the landing zone. Standard over the wire balloons can then tracked and delivered to the implantation zone. The stents can be delivered and the delivery system can be retracted without removal of the guide wires. It also enabled us to calculate all of the usable lengths for each component part.

Study Limitations

This hugely simplified model with component parts was extremely useful for planning the 1st generation proof of concept delivery system. We must however acknowledge that it had a number of limitations:

i) The ID of the silicone tubing was only 7mm as compared to the glass model which will be between 19 and 25mm. This unrealistic internal diameter (ID) was chosen as it was the only silicone tubing that we had available to us.

ii) The simplified model was made of silicone tubing with lubricated silicone oil as compared to a glass model aorta.

iii) There was no tortuosity of either the aortic arch of the peripheral vessels which in the aortic glass model and in real life will add another layer of complexity.

iv) The ATAG device and inverted “T-Shirt” coronary sleeves were not fully functional / loaded in this device testing.

v) Because the guide catheters could move within the 4.5mm delivery sheath the wire crossing was never going to be a significant issue as they were capable of just untangling and the coronary stents then navigating around any bends. This will not be the case with the “real device”, which will require a technique to “uncross” the wires and allow smooth implantation of the coronary sleeves into the respective coronary arteries.

vi) This preliminary test gave us no idea as to the push forces needed to deploy the coronary arms / stents. Further work is required to elucidate the push needed, and whether either rapid exchange type balloons or OTW are capable of delivering the coronary sleeves in vitro.

A DETAILED ASSESSMENT OF 2G ATAG, COREVALVE NITINOL FRAME AND THE MEDTRONIC TALENT STENT GRAFT

ATAG 2ND Generation stent frame body only

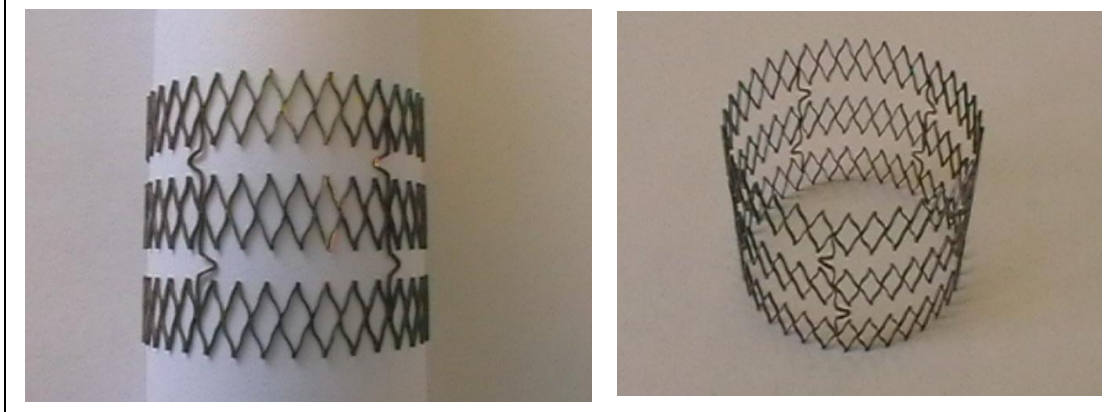

A10 Photographs of 3 ringed ATAG with longitudinal tie bars

Dimension before electro polishing (incoming inspection)

Average material thickness	489 µm
Average strut width	184 µm and 204 µm (at different measuring point)
Average connector width	246 µm

Medtronic talent stent graft

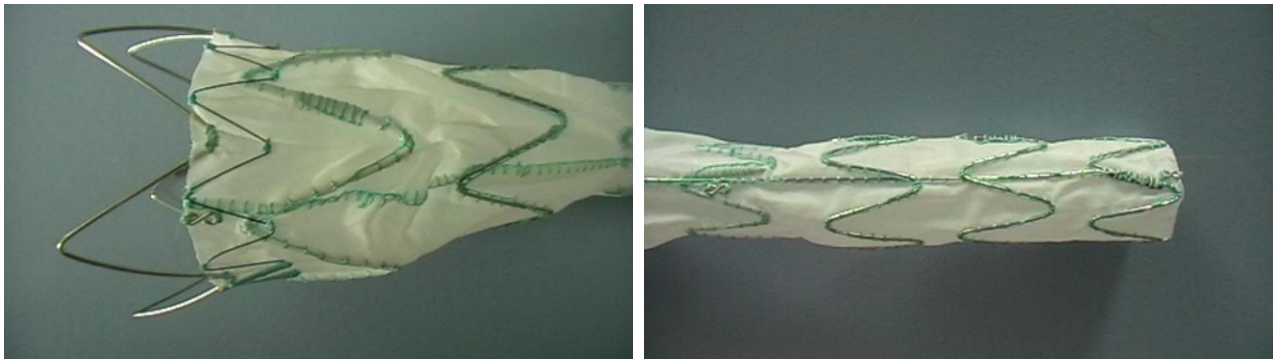

Expanded Stent Graft proximal part Expanded Stent Graft distal part

Figure A-11 macroscopic photographs of graft

Microscope 50x wide angle

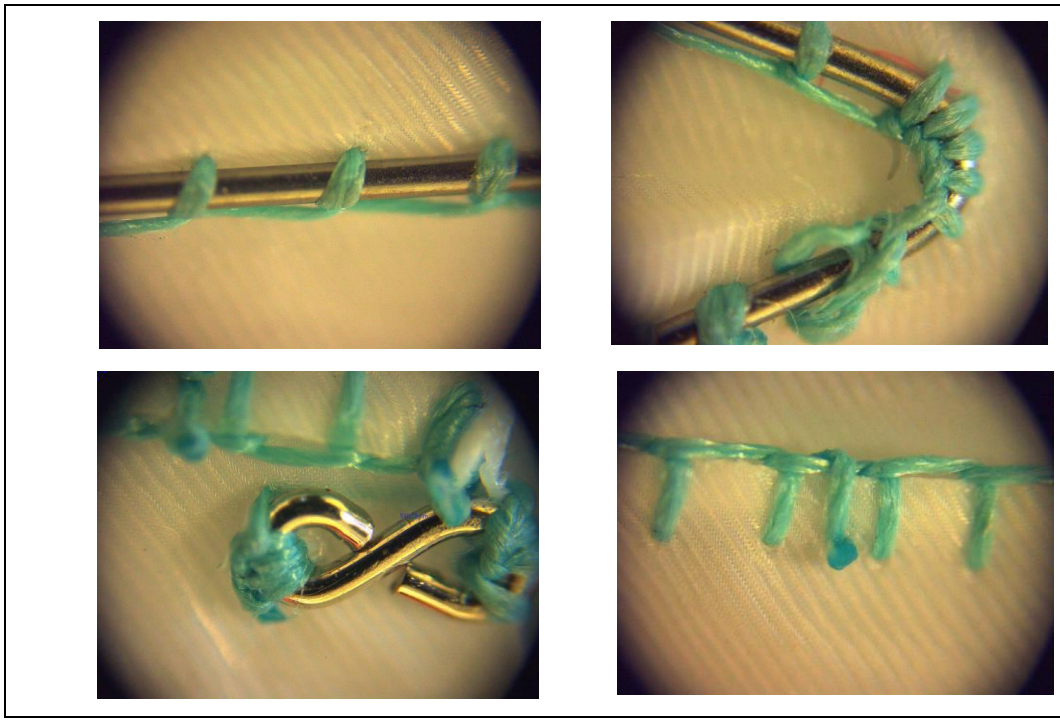

Figure A-12 Microscopic *50 magnification photographs of the Medtronic graft

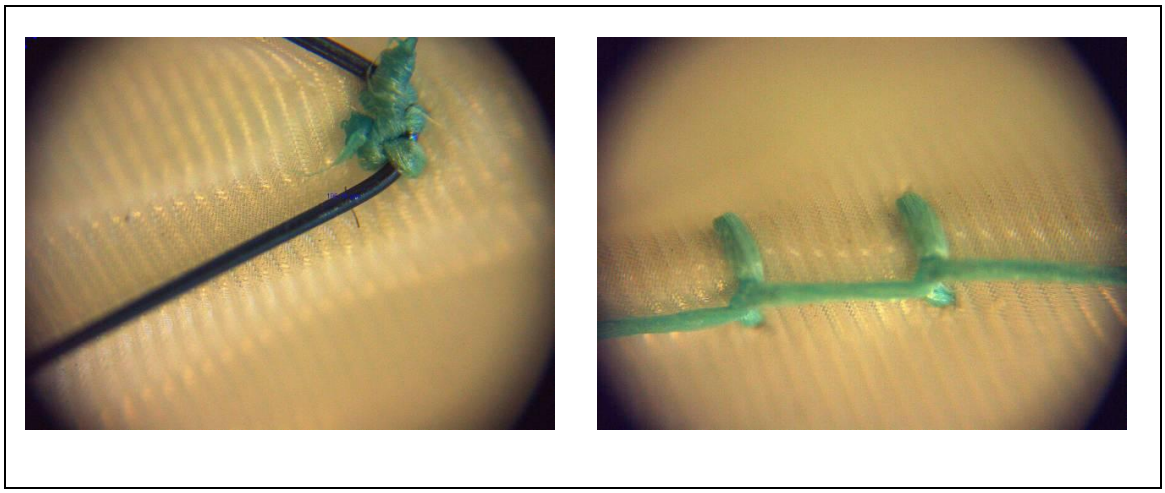

Figure A-13 Microscopic *50 magnification photographs of the Medtronic graft

Wire frame measurement

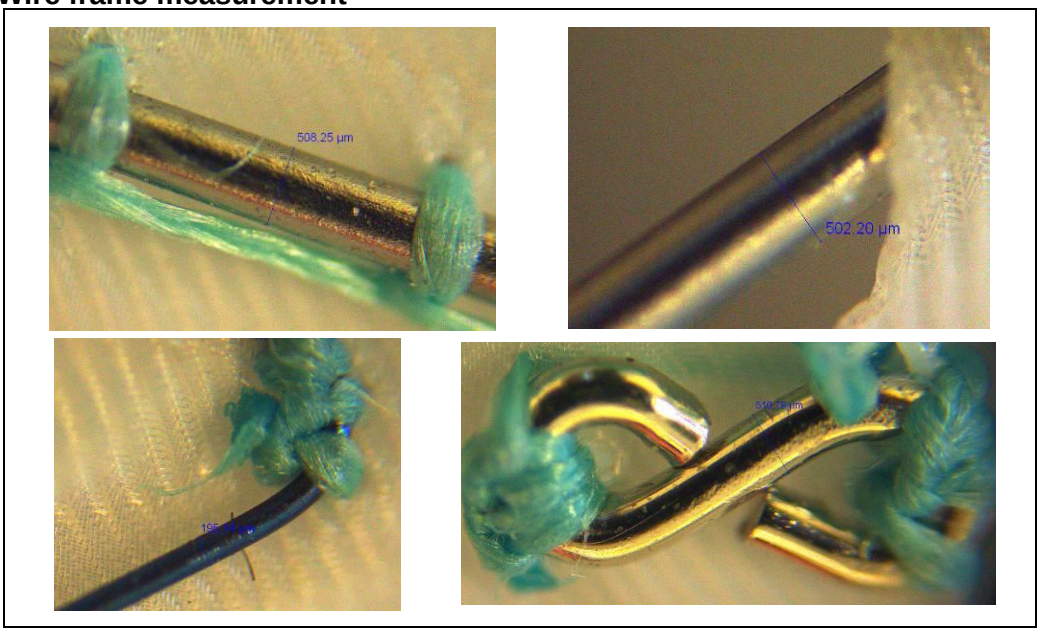

Bracing wire diameter approx 195µm Wire diameter approx 500µm

Figure A-14 microscopic measurement assessment of wire frame of the Medtronic graft

Corevalve re-valving system nitinol frame

Figure A-15 macroscopic photograph of CoreValve frame

Microscope 50x wide angle

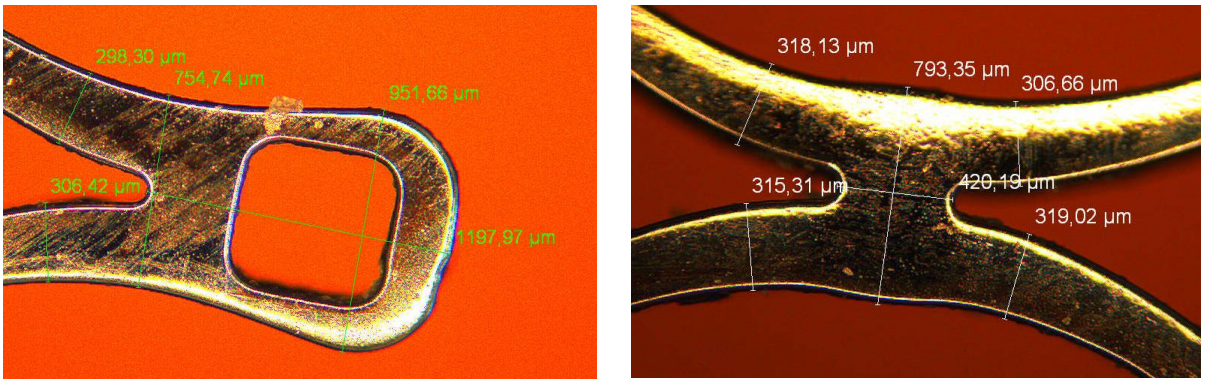

Figure A-16 microscopic frame measurements assessment (*50)

IN VITRO ASSESSMENT OF PLATELET ACTIVATION OF THE NICAST ELECTRO SPUN COVERING VERSUS DACRON AND ePTFE

This platelet activation work was devised and supervised by TK, but performed by Stephanie Parnell within the laboratory of Prof Tim Warner.

Aim

To assess the platelet activation of the 2G ATAG Nicast polyurethane coating, and compare it to Dacron and ePTFE from currently available thoracic aortic stent grafts.

Background

Nicast have produced a polyurethane covering for the 2G ATAG graft in 2 thickness coatings – 200□m and 110□m. The polyurethane that they use already has a vascular device which has CE mark and is in clinical trial (AVflo fistula material).

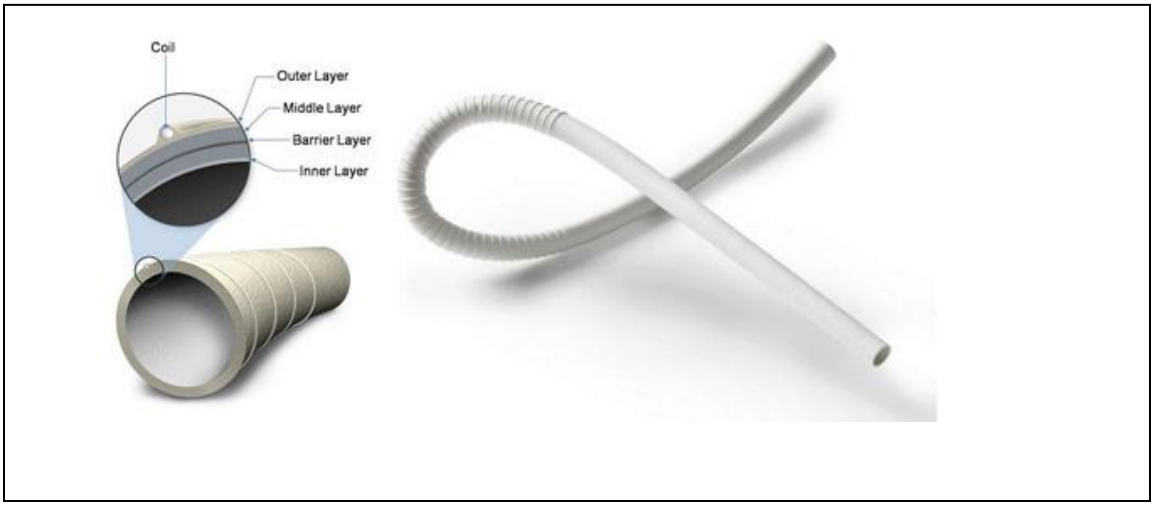

Figure A-17 Nicast AVFlow™ A-V fistula graft

Literature suggests that when prosthetic grafts are placed in arterial vessels a pseudo-intima forms upon the surface of the Dacron and ePTFE, made of fibrin and platelets. Vascular injury caused by insertion of the graft can also result in the exposure of highly thrombogenic substances present in the vessel wall.(143)

In the aorta the relative large diameter means complete occlusion is unlikely unless the material implanted is highly thrombogenic. However, if a platelet clump forms (particularly if close to the sleeves of the coronary ostia) it has a potential risk of embolisation due to the high shear stress caused by the blood flow in the ascending aorta, releasing small platelet rich fragments into the circulation which could occlude coronary vessels leading to myocardial infarction, or intracranial arteries causing a stroke.

Although Dacron and ePTFE have 5 year patency rates in aortic bifurcation grafts of 93% and 91-95% respectively they are not suitable for small diameter grafts (<4mm) with 5 year patency rates for femoro-popliteal bypass grafts reported as 43% and 45% respectively.(144)

My main aim was to assess the Nicast materials ability to activate platelets and ensure that it was non-inferior to that of both currently utilised materials Dacron and ePTFE, as if it were significantly higher it may be a covering which is unlikely to useful in the critical position of the ostium of the LMCA and RCA. I hoped that this would de-risk the use of this novel material as the ATAG system moved into 3rd generation development.

Methods

Platelet adhesion of the 3 graft materials (Dacron, ePTFE, and Nicast PU) was assessed using 96 well plate aggregometry method followed by assessment of platelet adherence. Platelet rich plasma (PRP) and platelet poor plasma (PPP) were obtained from the citrated blood of healthy volunteers.

Material preparation

Materials were prepared and tested in a standardised manner. To achieve this goal a hole punch was utilised to make 5mm round pieces of respective graft material. The thickness of the material was also measured using a micrometer screw gauge, so that surface area could be calculated for each sample as the Nicast material was thicker and as such the result must be standardised for the relative surface area.

The ePTFE (taken from commercially obtained LeMaitre TEVAR graft) and Dacron (taken from commercially available Jotec TEVAR graft) had material thickness measured at 157µm and 79µm respectively compared to the Nicast sample used which had a thickness of 727µm (we were sent this material from Nicast, rather than destroy one of our 2 manufactured grafts).

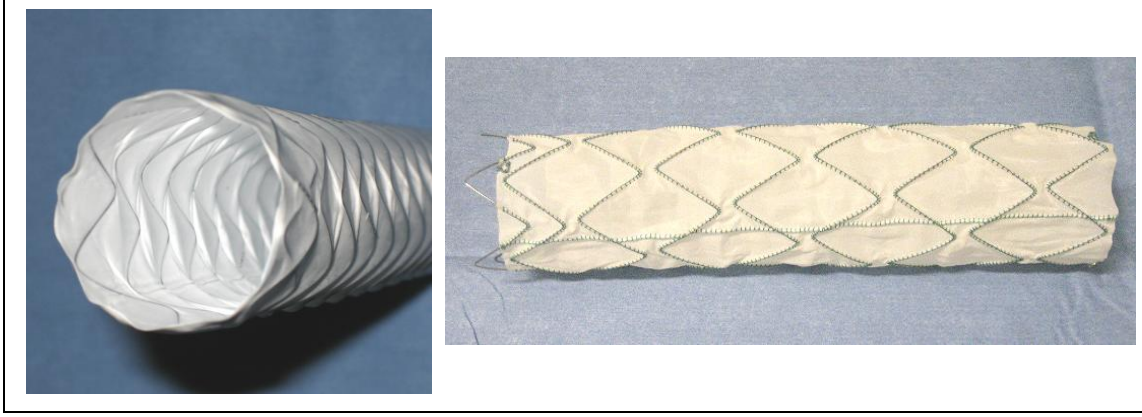

Figure A18 a) ePTFE LeMaitre graft b) Jotec Dacron graft

Platelet adhesion methodology

The PRP was added to the wells of a 96 well plate as shown in the diagram below. PRP was pipetted into 2 half rows of each of the graft materials (standardised 5mm hole punches of each material) and 2 half rows with no material as a control; one row for each of the agonists, collagen and ADP at 6 different concentrations – allowing comparison of the graft materials with different concentrations of the agonists collagen and ADP. The material itself is unlikely to promote platelet activation and as such the agonists ADP and Collagen are required to facilitate the platelet activation / adherence process in a standardised way.

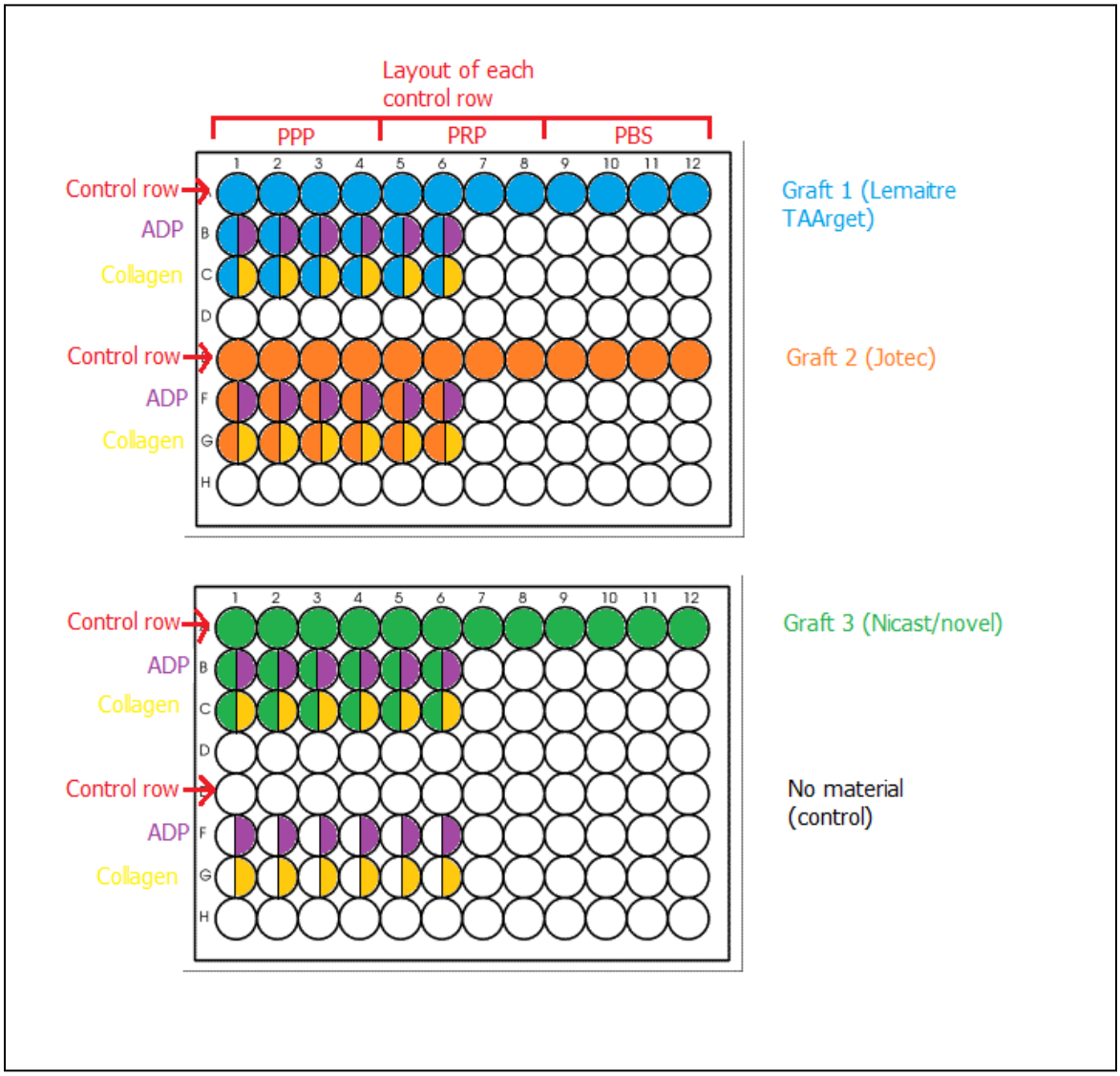

Figure A19 Schematic diagram of plate organisation for Platelet Aggregometry

There was also a control row for each graft material, and 1 with no material, where no agonist was added. These rows contained 4 wells of phosphate buffered saline (PBS), 4 wells of PRP and 4 wells of PPP. The plates were then placed in a plate reader (Sunrise, Tecan Group, Mannedorf, Germany), and the results given by the plate reader were not used as the wells contained pieces of graft material. The plate reader was

used to give reproducible shaking of the wells and heat them to 37^{o}C to encourage platelet activation.

The graft specimens were then removed from the plates and washed twice with 0.9% phosphate-buffered saline, as were the plates themselves to remove the platelets that had not adhered properly to either the plates or the material. The specimens were then returned to clean wells in the other half of the plates and assay buffer was put into all the wells except the wells previously containing PBS where a 100% control was added. This allowed platelet adhesion to the wells and the graft materials to be measured separately, so that any platelets found in the wells when measuring platelet adhesion to the grafts had adhered to the graft material itself and not the plates. The plates were incubated at 37 °C for 30 minutes. The assay buffer contained p-nitrophenyl phosphate at pH4 with detergent. This buffer breaks down the platelets adhered to the material or plate and the acid phosphatase within converts the p-nitrophenyl phosphate to p-nitrophenyl. 2M NaOH was then added to each well which turns the p-nitrophenyl yellow. So that where there is a high concentration of platelets there is strong yellow colour. All specimens were then removed and the plates put in the plate reader again. The concentration of platelets in each well (and therefore the degree of platelet adhesion) was thus assessed colorimetrically by measuring the optical absorption at a wavelength of 405 nm for each well using the wells containing 100% platelets as controls. The results were analysed using GraphPad Prism 5 software.

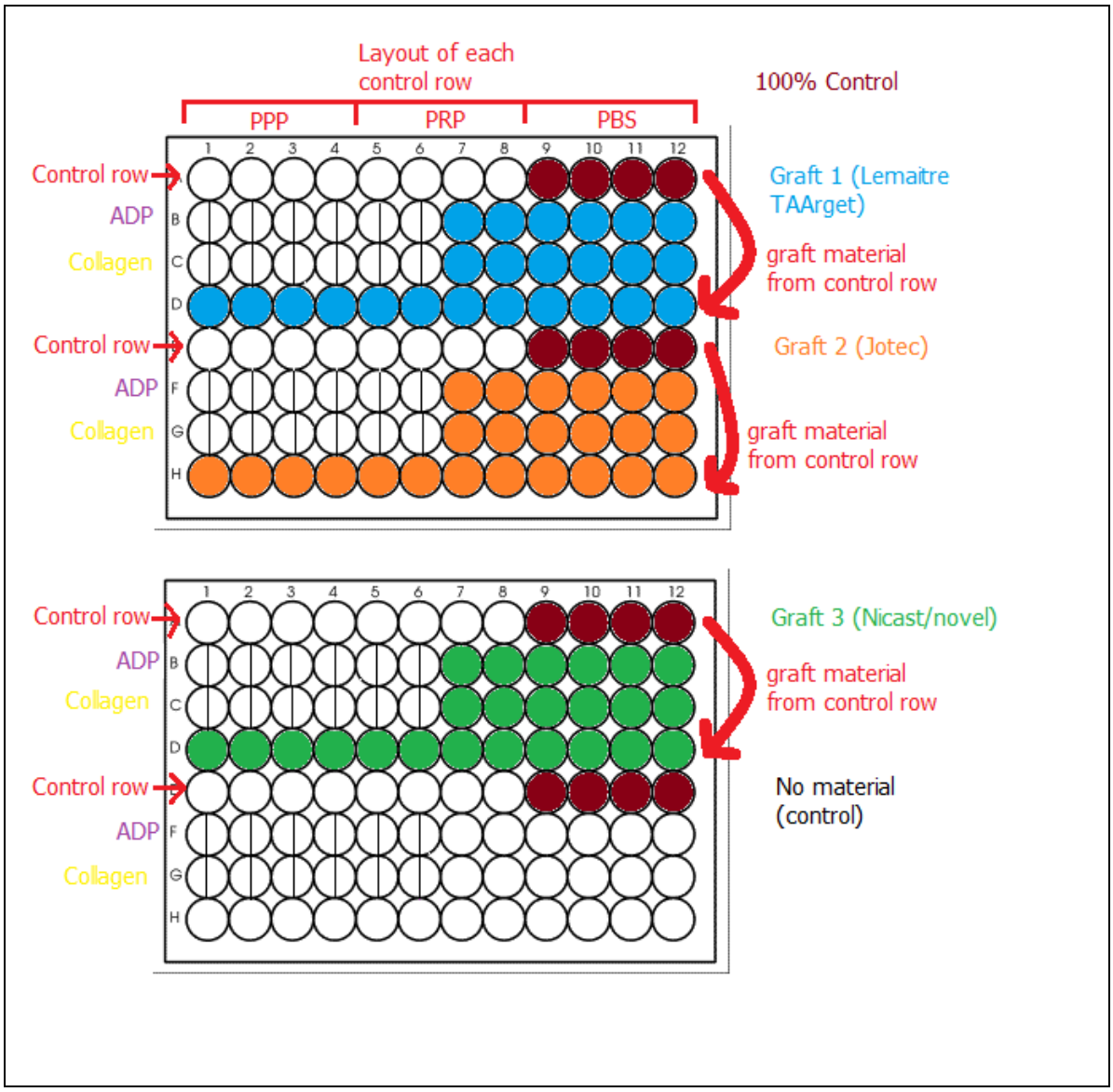

Figure A20 Schematic diagram of organisation of Graft Material for Colourimetric Analysis

Results

Results of experiments comparing the platelet adhesion to 3 graft materials.

Graft 1: **Lemaitre,** *ePTFE material*

Graft 2: **Jotec**, *Dacron material*

Graft 3: **Nicast**, *Polyurethane*

Graft Material Thickness

	Lemaitre Material (ePTFE) (μm)	**Jotec Material (Dacron) (μm)**	**Nicast Sample from AVFlo stent (polyurethane) (μm)**
1	152	76.2	737
2	152	88.9	737
3	152	76.2	711
4	165	76.2	711
5	165	76.2	737
Mean	157.2	78.74	726.6
Surface Area of 5mm Diameter Hole Punch Piece of Each Material (mm^2)	41.7	40.5	50.7

Material thickness measurements using a micrometer screw gauge

Therefore there was 25% and 22% more Nicast material in each experiment than Dacron (Jotec) and ePTFE (Lemaitre) respectively.

Each graph shows the mean results for each graft material +/- the standard error.

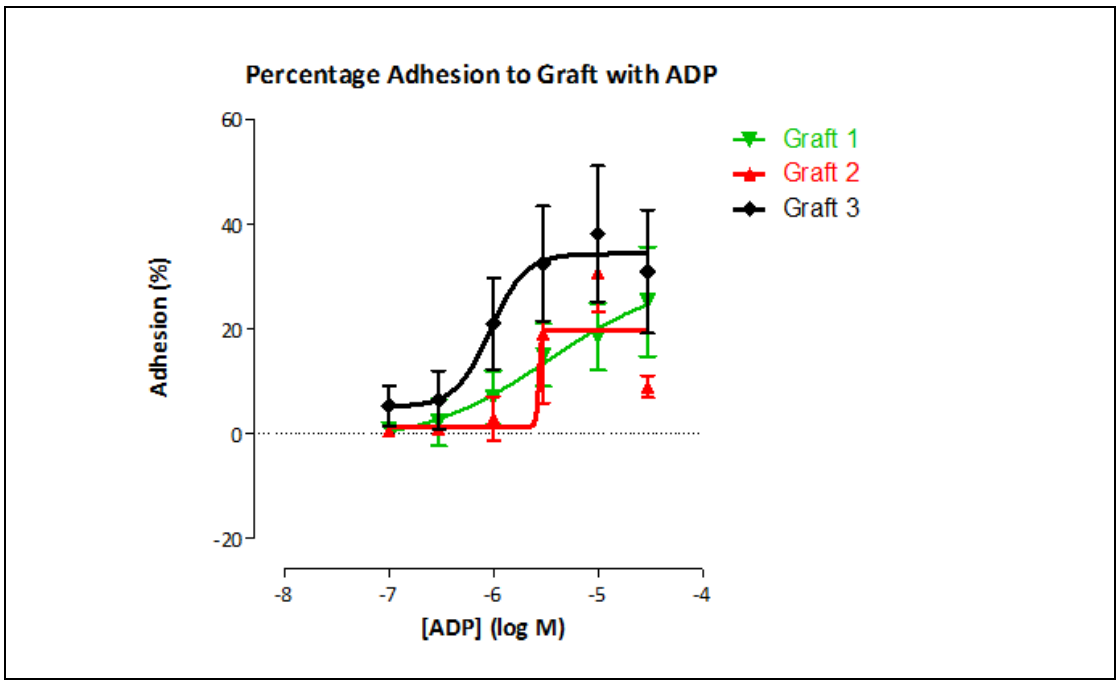

Figure A21 Percentage platelet adhesion to materials with ADP

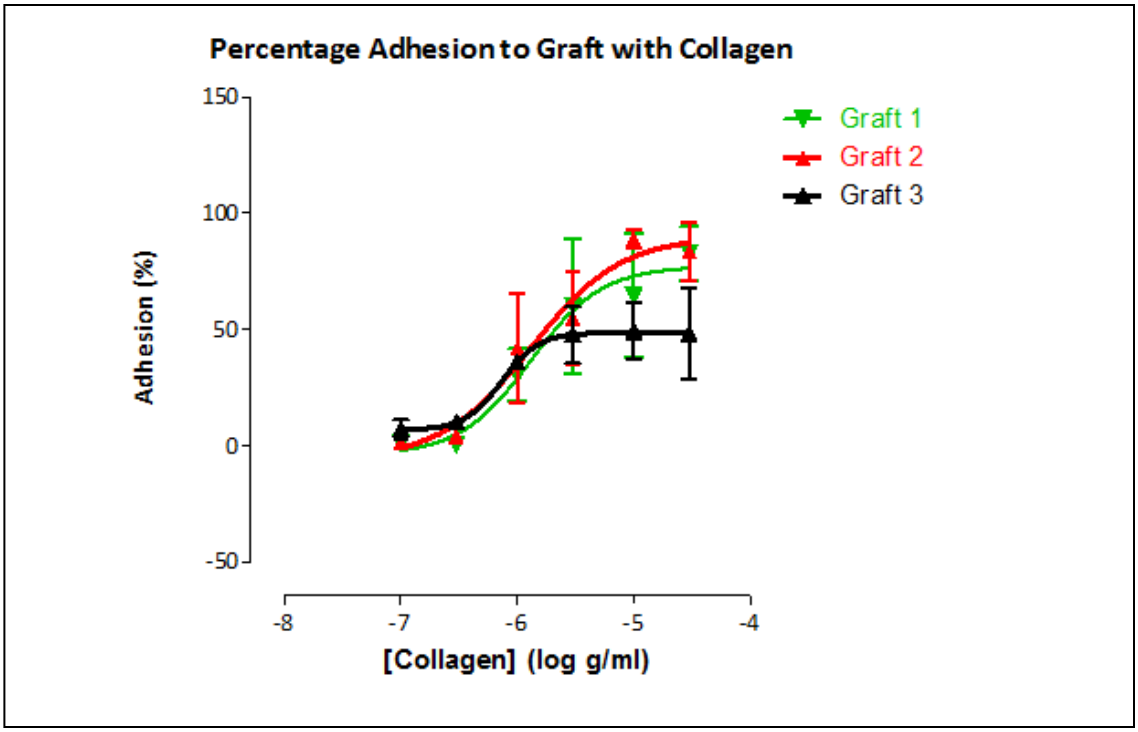

Figure A-22 Percentage platelet adhesion to materials with collagen

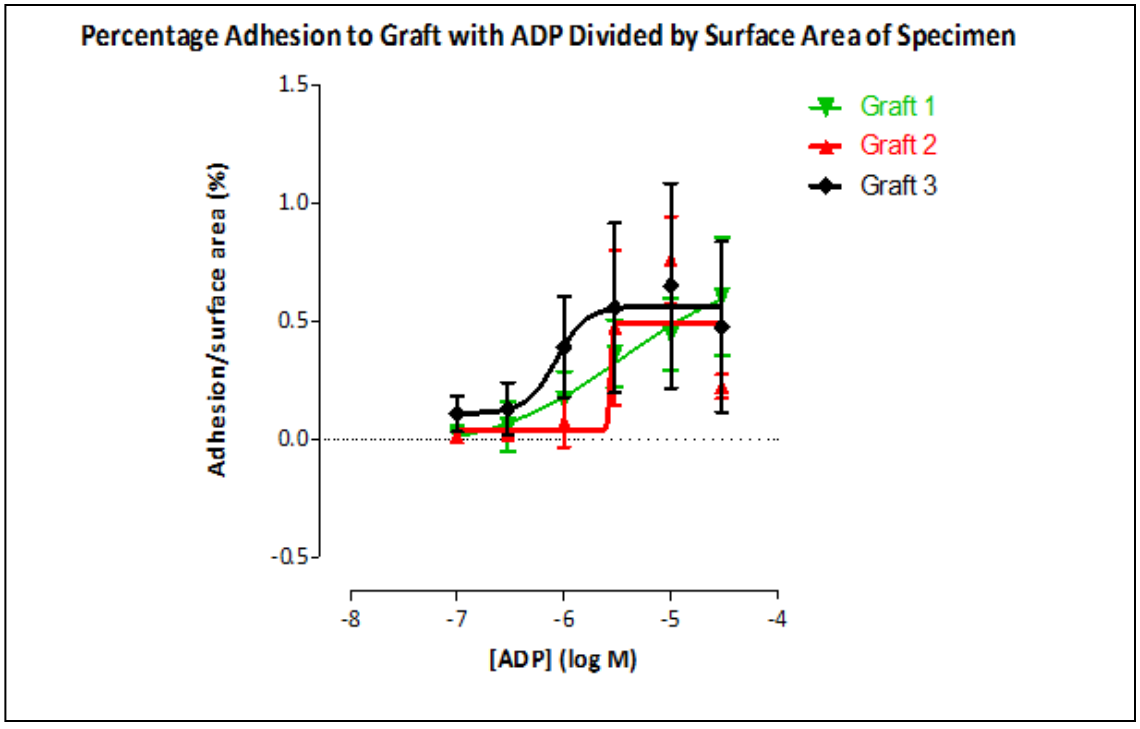

Figure A-23 Percentage adhesion to graft with ADP as agonist / corrected for surface area

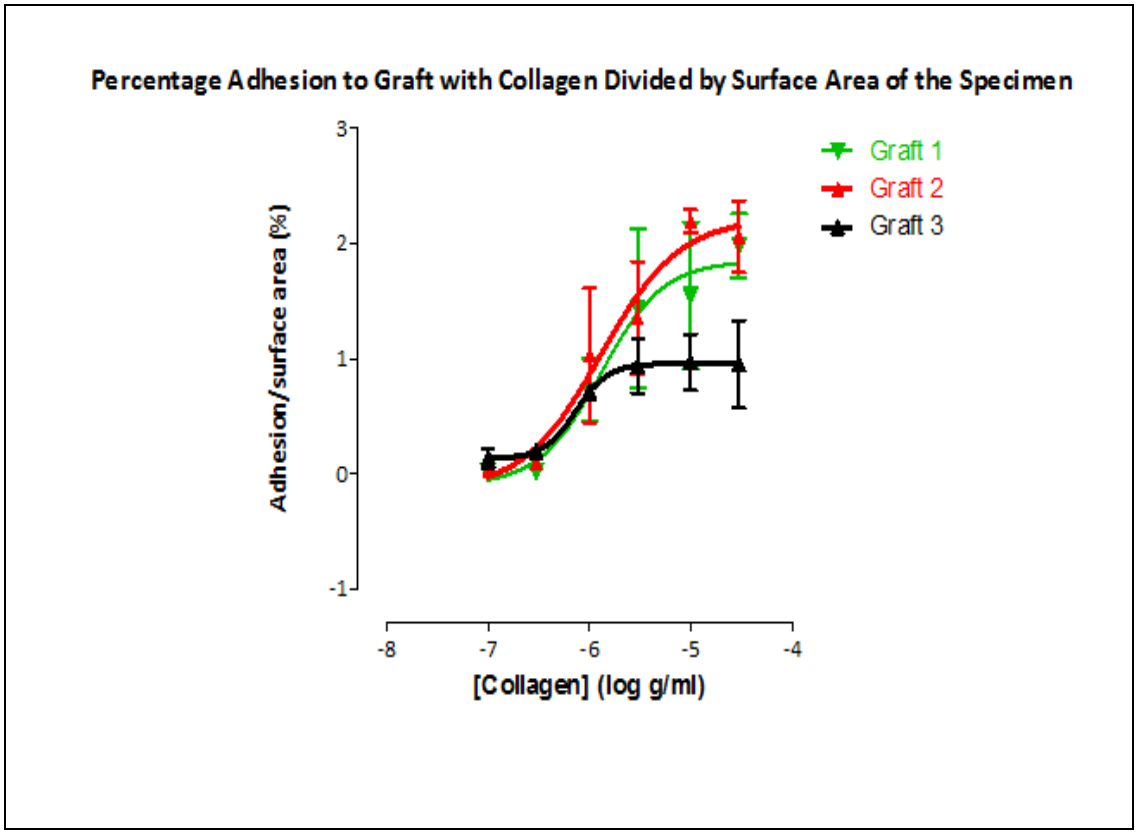

Figure A-24 Percentage adhesion to graft with Collagen as agonist / corrected for surface area

Statistical results

Even before correction for material surface area there is no statistically significant difference between the platelet activation of Nicast PU when compared to both the ePTFE and Dacron with both agonists (ADP and Collagen). Similar non significant differences are also seen when the samples are corrected for surface area. (TTest P>0.05).

Conclusion

The Nicast polyurethane material when tested against both ePTFE and Dacron would appear to have statistically similar platelet activation characteristics when corrected for surface area.

Using Collagen as an agonist Nicast PU is clearly the least activating although it does not reach statistical significance. The raw values for ADP agonist platelet activation would appear to suggest a trend towards more activation for the Nicast PU material as compared to the ePTFE and Dacron, but this does not reach statistical significance, and the trend disappears when proper correction for surface area is factored in.

Platelet adhesion to the wells which contained the specimens of graft material was similar for all the grafts with both the agonists. Therefore, differences in platelet adhesion to the graft specimens were only due to the graft specimens themselves.

Discussion

Dacron and ePTFE in small diameter grafts (<4mm) have poor 5 year patency rates.(144) Our simple first analysis of platelet activation and adherence to graft materials suggests that the Nicast PU material is likely to activate platelets to a similar degree as currently commercially available stent graft materials. With the Nicast PU material there is a trend towards decreased activation when using collagen as an agonist, but a similar degree when ADP is utilised.

ADP binds to receptors on platelets causing platelet activation. $P2Y_{12}$ is one of these receptors which are targeted for antiplatelet therapy. $P2Y_{12}$ ADP receptor antagonists include Clopidogrel and Prasugrel. Clopidogrel with aspirin is given as standard-of-care therapy for all patients undergoing percutaneous coronary intervention (PCI) to reduce the risk of ischaemic events. Prasugrel, which is licensed in the US and Europe for use in Primary PCI and is a more potent platelet inhibitor with a 19% relative risk reduction for ischaemic events compared to clopidogrel and aspirin.(145)

Patients with aortic dissection, for whom this stent is designed are highly likely to have other cardiovascular co morbidities and may already be on antiplatelet therapy. With $P2Y_{12}$ ADP receptor antagonist treatment, ADP induced platelet aggregation can be inhibited and this may allow the use of this material in ascending aortic and coronary sleeves. To further test this theory the experiments should be repeated using commonly used anti-platelet therapies to evaluate their potential effects.

Future animal experiments may also help in establishing the thrombogenic properties of the graft material under in-vivo conditions, although we must accept that animal models of platelet activation and clotting cascade do have differences when compared to the human.

ATAG hazard analysis

Below is a tabulated list of potential ATAG failure modes. It is broken down into 3 specific parts:

- Arterial access / ATAG delivery failure modes
- ATAG deployment failure modes
- Longer term follow up failure modes

Arterial access / percutaneous delivery failure modes

Arterial access / ATAG delivery failure modes

Unable to crimp ATAG onto delivery system / poor coronary alignment
Sheath gains access into the false lumen which extends into the femoral artery
Peripheral artery too small / tortuous / calcified to accept ATAG device/ sheath
Unable to pass device onto the 3 guide wires
Device will not advance smoothly on guide wires
Inadequate guidewire support to allow ATAG to advance
Device will not advance in the descending aorta because of calcification or tortuosity
Clot / aortic debris on proximal end of device / embolises

Sheath or device causes dissection or rupture of the arterial wall
Wrapped wires mean that device cannot advance
Impossible to ascertain exact position of device in 3D therefore unsure as to correct orientation
Unable to elucidate exact position of 3 wires and therefore unable to “unwrap”
Device will not traverse the aortic arch
During arch manipulation causes embolic phenomenon to brain / arms / gut / kidneys / legs
Clot formation on guide wires (What is the optimal desired ACT)

Deployment failure modes

Table ATAG deployment failure modes

Unable to engage coronary ostia with guide catheter and position the guide wires
Coronary guide wires do not possess sufficient “hold” in coronary arteries and pullout upon ATAG device advancement.
Unable to engage correct position of front end of ATAG device
Coronary arms do not align correctly
Coronary arms kink and occlude
Coronary ostia angles / distances are beyond scope of the device
Balloon dilatation in the coronaries causes LMS / RCA dissection / slow flow / occlusion
AV becomes disrupted with torrential AR

Unable to achieve a proximal seal resulting in endoleak and subsequent coronary collapse
Proximal seal causes a proximal dissection with significant false lumen filling compromising true lumen
Distal dissection causes spiral false lumen and occlusive arterial complication (CVA / renals etc – dependent on anatomy)
Device is poorly positioned and is too long and occludes right bracheo-cephalic trunk and / or arch vessels
Over sizing causes constant outward radial force resulting in aneurysm formation / dissection
Undersized device resulting in distal embolisation / migration and risk of coronary occlusion and arterial occlusion depending on site of coverage. Migration by hydrodynamic forces (either shear or inertia)
Thrombus formation in coronary arms (material considerations)
Cover material fracture / degrading promoting endoleak
Stent strut fracture – depending on site could be detrimental to coronary arms, potential to pierce arterial wall
Distal segment of stent does not adhere to wall adequately (because of poor sizing or curvature of the aortic wall) resulting in endoleak
Device expansion could trap a calcified AV leaflet behind graft causing occlusion of the LMS / RCA and severe AR
95% of patients will have LMS and RCA in recognized angulation approx 1% will have anomalous anatomy and potentially device could occlude an anomalous artery
Removal of device delivery system – possible pullback of the device from its optimal position
Aortic or peripheral vessel damage secondary to delivery system removal
Vascular complication related to sheath and hole closure (percutaneous suture based closure device)
Coronary blood flow reduction – slow deployment of coronary branches (LMS and RCA cannot be done simultaneously)
Failure of coronary deployment / incomplete expansion

Kinking of coronary arms
Cardiac arrest during coronary sleeve implantation
Coronary arms of insufficient length for the aortic anatomy
Coronary side branches – pull out under pressure
Kinking of body of stent graft
Coronary stent thrombosis due to lack of endothelialisation (? Optimal duration of anti-platelet agents)
Aortic thrombosis

Longer term follow up events

Table Longer term failure modes

Instent re-stenosis (ISR) of coronary sleeves– how to treat – use of drug eluting coronary stents (DES) / drug eluting balloons (DEB) how will material fare with this. Does the LMS / RCA need to elute drugs in the first instance? Is this possible?
Endoleak (I,II, III or IV)
Aneurysm formation
If too low in the LVOT ? Potential for conduction problems and need for PPM
Constant outward radial force ? Dilatation of the sinus and possible resultant AR
Material degradation (Fatigue under cyclic load)
Stent frame fracture and fatigue
Aortic flow reduction

NHS
National Institute for
Health Research

Invention for Innovation (i4i) Programme
Future Product Development Funding Stream 2: Full Proposal

For office use only

IMPORTANT
Before completing this form, please read the accompanying Guidance Notes.
Note the maximum field sizes shown include both printing and non printing characters such as spaces and carriage returns.
THIS FORM MUST BE RETURNED BY 28 AUGUST 2009, 5 PM.

Reference Number II-AR-0209-10092

Date submitted

1. Application

Short Project Title*:	Ascending Thoracic Aortic Graft (ATAG)		
Project Duration *: (months)	36.0	Total funding requested *: (£'s)	£747,497.00
		Proposed Start Date *:	01 January 2010

2. Lead Applicant's Details

Title*:	Prof
Surname*:	Rothman
Forename*	Martin
Post held*:	Professor of Interventional Cardiology
Department*:	Cardiology
Role in project*:	Principle Investigator / Project Lead

4. Co-applicant details

Co-applicant 1

Title:	Prof
Surname:	Brockman
Forename:	Dan
Post held:	Professor of Surgery
Department:	Small animal surgery
Organisation:	Royal Veterinary College, University of London
Telephone:	01707 666389
Extension:	
e-mail address:	djbrockman@rvc.ac.uk
Role in project:	In-vivo testing programme

Co-applicant 2

Title:	Prof
Surname:	Greenwald
Forename:	Stephen
Post held:	Professor of Cardiovascular Mechanics
Department:	Institute of Cell and Molecular Science
Organisation:	Queen Mary's School of Medicine and Dentistry
Telephone:	0203 2460178
Extension:	
e-mail address:	s.e.greenwald@qmul.ac.uk
Role in project:	In-vitro testing programme

Co-applicant 3

Title:	Dr
Surname:	Keeble
Forename:	Thomas
Post held:	Interventional Research Specialist Registrar
Department:	Cardiology
Organisation:	London Chest Hospital
Telephone:	0208 9832213
Extension:	
e-mail address:	Thomas.Keeble@bartsandthelondon.nhs.uk
Role in project:	ATAG design, specification and testing

5. Scientific Summary*

Background (400-800 characters):
Ascending Thoracic Aneurysm (ATA) and Ascending Aortic Dissection (AAD) are increasingly common. Current gold standard treatment for both conditions is highly invasive open cardiac surgery. Despite refined surgical techniques 30% of patients with AAD die within the first 48 hours, & only 50% survive to discharge. Many patients refuse or are turned down for surgery because of co-morbidity or perceived surgical risk despite the fact that in AAD medical treatment is associated with a doubling of mortality [Circ 2002;105:200].

Endovascular stent treatment of descending aortic aneurysm and dissection is the current treatment of choice, but these devices cannot be used for treatment of the ascending aorta because they are not designed to preserve coronary blood flow and aortic valve integrity.

Aims (400-800 characters):
To develop & test an Ascending Thoracic Aortic Graft (ATAG) - a novel covered stent graft designed specifically to treat both ATA and AAD, protecting coronary blood flow and aortic valve integrity.

1) Design and develop a 2nd generation ATAG prototype for testing (1st generation testing completed – see Annex 4 page 10)
2) Perform in-vitro prototype graft testing programme (glass model/flow rig)
3) In-vitro delivery system design and development programme
4) In-vivo development programme, including acute and in-vivo survival / safety data
5) Development of IP / business plan to take ATAG to market

All device testing will be performed by the investigator team. Design and device manufacture / regulatory approval will be outsourced to Qualimed.

Plan of Investigation (400-800 characters):
A review of aortic size and coronary anatomy in healthy and diseased states has been undertaken and this information was integral to the formulation of the ATAG design specification document. Both documents are found within Annex 4 (WP1 and 2 from original application as requested by FPD2 Committee).

PLAN
1) Design and develop specification for a 2nd generation ATAG prototype ready for in-vitro and in-vivo testing
2) Perform in-vitro prototype graft testing (glass model and flow rig tests)
3) Design, develop and test delivery system using in-vitro flow rig
4) Conduct in-vivo evaluations of ATAG and delivery system in acute and survival animal models in readiness for first in man (FIM) trials
5) Develop IP / business plan to take device to market

Potential Impact (400-800 characters):
The world Authority on aortic dissection - The International Registry of Aortic Dissection (IRAD) Centres report a surgical turn down rate of 21% in patients presenting with AAD. 90% of these patients not treated surgically will be dead at 3 months [Circ 2002;105:200-206]. Surgery for both AAD and ATA is highly invasive, with cardio-pulmonary bypass, deep circulatory arrest, and a prolonged intensive care stay.

Endovascular stent treatment has revolutionized the treatment of aortic dissection and aneurysm in the abdominal and descending thoracic aorta [NEJM 351 (16):1607-18]. The ATAG intends to take this revolution to the ascending aorta allowing more patients access to life saving percutaneous treatment, more quickly with less morbidity and mortality than conventional surgery.

7. Aims of the project*:

Including a description of the **inventive step(s)** and the technical challenges to be addressed and overcome. **(Maximum 3500 characters)**

Our team have already developed the first prototype ATAG device and proved that delivery to the ascending aorta and protecting the coronary arteries is possible in a glass model under x-ray guidance (Annex 4 Page 10-11). We now aim to develop a second generation device capable of a full in-vitro and in-vivo testing programme; following which the device can be considered for a first in man (FIM) trial.

For the ATAG to successfully treat the ascending portion of the aorta it must have the ability to pro-actively protect the coronary artery blood flow, avoid disruption of the aortic valve and have adequate "sealing" of the aortic wall so as to prevent "endoleak" to adequately exclude and de-pressurise the aneurysm or dissection flap. This poses many technical challenges in stent design and delivery:

1) Stent graft design must protect and actively retain coronary artery blood flow
2) Graft covering material must be compressible, flexible, thin and impermeable
3) Graft design must ensure proximal and distal sealing point to prevent endoleak
4) Anatomical design to prevent disruption of aortic valve
5) Ability to cope with the anatomical variations of both aortic size and coronary artery origin angle
6) Delivery system must have adequate pushability and torque but be flexible and of small enough calibre to be delivered via a 6mm (termed 18 French) introducer from the femoral artery

Inventive steps

1) "Inverted T-shirt" endograft design, with a main stent body for aorta (self expanding) attached to 2 balloon expandable coronary stents. Coronary ostia will be pro-actively stented to protect coronary blood flow and enable adequate proximal stent fixation (Annex 4 page 19)

2) To ensure proximal sealing point the graft body may be designed with 3 "semi-lunar" portions to match the natural anatomy of the tri-leaflet aortic valve. Each "semi-lunar" lobe will have a pre-formed outward force flare to optimise proximal sealing

3) The "semi-lunar" proximal graft lobes are short (<10mm) allowing them to sit in the sinuses and minimise disruption to the aortic valve apparatus. The coronary stents are attached at the distal most end of the semi-lunar lobes

4) To enable safe and easy passage of the device around the aortic arch and to facilitate packing to the desired introducer sheath size the graft covering material that we are planning to use is Polycarbonurethane electrospun on a former by a contracted partner Nicast, Israel (www.nicast.com). The material utilised is CE marked and sold in the EU as AVFlo a vascular access graft. It will allow the coronary arms of the "T-shirt" to have anatomical flexibility and kink resistant material design to retain long term patency. This stent covering material provides an impermeable barrier to blood

5) The over the wire balloon expandable stent "push rod" to push the graft sleeves into the coronary ostia and protect them is novel and already patented by our group. This solution will enable pro-active protection of coronary flow and secure proximal fixation

Annex 4 contains a full review of the size of the aorta and proximity of coronary arteries and aortic valve (page 4). It also contains the current ATAG prototype design specification (page 13) including further information about the Nicast Polycarbonurethane material (page 19).

8. Background*:

Referring to Criterion 3, please provide details of other products on the market and the novelty of the proposed project; include details of any other existing IP and its significance to your freedom to operate. **(Maximum 2000 characters).**

The innovative aspect of the ATAG device is it's ability to fit the anatomical variations present in the ascending aorta whilst having branches that protect coronary flow, these having walls thin enough to resist thrombus formation in the coronary arteries. The ATAG ability to ensure coronary & aortic flow whilst preserving valve function is novel.

Current branched aortic stent graft technology cannot be used in the coronary vessels due the thickness of the graft material and potential for thrombosis. They do not have the construct to match the unique anatomy of the ascending thoracic aorta.

There are currently no competing devices on the market. Cook Biomedical are in development of an unbranched ascending aorta graft.

The ATAG device uses delivery techniques & clinical practices currently used in both vascular, and coronary stenting, thus training will be intuitive allowing rapid adoption of the technique.

The investigator team has filed two international patents:

WO2008/025983 covers a branched prosthesis for deployment at the aortic root having coronary arms releasably mounted on pushrods.

PCT/GB2009/000485 describes a branched blood vessel prosthesis having flexible branches on valve sparing lobe projections.

An extensive prior art search has been completed by NHS Innovations London (NHSIL) and a third party organization commissioned through NHSIL. Search reports have been generated for the 2 patents filed and attorney opinions have been sought. No inventive step or novelty issues were cited against a series of claims in the patents which will form the basis for differentiation from the prior art.

A patent attorney opinion states that the prior art documents can be circumnavigated with a minor claim adjustment prior to examination and poses only a low risk to FTO. A full FTO and prior art report is found within Annex 4 (page 24).

We anticipate further IP will be developed during the project. It will be captured by NHSIL as described in Annex 4.

10. Project plan and methodology*:

Please provide a detailed description of specific milestones and deliverables. A Gantt chart must be supplied in Annex 3. In addition (please refer to Criterion 3), an indication of how any IP which might arise during the project would be handled should be provided. **(Maximum 10000 characters)**

There are 5 major work packages:

1) Work package 1 - Second generation ATAG prototypes & in-vitro flow study
2) Work package 2 - In-vitro graft delivery and deployment study
3) Work package 3 - Acute in-vivo ovine study
4) Work package 4 - In-vivo survival and safety study
5) Work package 5 - Development of IP and business plan

WP1 (months 1-7) Second generation ATAG prototypes & in-vitro flow study
Flow models allow detailed investigation of the graft behaviour under anatomical and physiologically realistic situations allowing graft and delivery system optimisation.

All in-vitro flow-rig work will be undertaken by SG, TK and MTR at the QM campus.

Aim:
To characterise the behaviour of the ATAG in different anatomical flow models.

Methods:
Stent graft prototypes will be specified and built in close collaboration with our contracted medical engineering partner (Qualimed - Q). A basic delivery system will be designed and built. The stent graft samples will be mechanically characterised (stowing, radial forces, forces to deliver).

Elastrat (www.elastrat.com) will manufacture 4 silicone ascending aortic models from CT images (normal, proximal ATA, distal ATA, and dilated aorta like that seen in AAD). A flow rig to simulate physiological conditions (pulsatile pressure and flow at body temperature and blood viscosity) will be assembled and characterised (SG / TK).

The ATAG will be repeatedly implanted under direct vision into the 4 silicone flow models with differing aortic anatomy to see how the graft behaves, documenting the following objective end points.

Pressure and flow measurements within the coronary arteries, the excluded aneurysm portion (sac), across the aortic valve and ascending aorta.
Interference with aortic valve function
Flow pattern analysis using a dye tracer
Expansion of the graft body assessed using an endoscope
Presence of endoleak
Proximal and distal seal assessment
Extent of ATAG migration

The results will be fed back and used to design an advanced prototype stent graft for WP2. It can also be decided if a final product will have to be offered in different sizes and what the key sizing criteria will be.

Deliverables:
Specification, design and build of ATAG samples. (Q / BLT)
Specification, design and build of a basic delivery system (Q / BLT)
Report on build and characterisation of a flow rig simulating physiological conditions for different patient aortic anatomies (SG / TK / MTR)
Report of ATAG testing in variant aortic anatomies (TK / SG / MTR)
IP protection of stent graft design (AM)

WP2 (month 8-14) In-vitro graft delivery and deployment study

The ATAG will only function properly if it can be deployed with the required precision and control from a peripheral arterial route (most commonly femoral artery). One of the major considerations with delivery of the ATAG is that it is likely to be 6mm in diameter and up to 9cm long. When inserted from the femoral artery it must track smoothly around the aortic arch which has an internal radius of 3cm and bends over 180 degrees. This poses a particular challenge to the graft, and the delivery system.

Aim:
Design specification and development of 2nd generation delivery system for ATAG.

Methods:
The 4 flow rig set-ups will now be well established. We anticipate some graft design iterations following data collected from WP1.

Stent graft prototypes and delivery systems will be manufactured and characterised in bench top set up (tracking forces, forces to deploy and traction on guide wires). A series of samples will be used to study the deployment in detail in the flow-rigs under direct vision.

The study will then be repeated for delivery and deployment of ATAG in the 4 flow models under x-ray guidance.

End points: Will be objective & subjective

Objective
All end points from WP1 will be repeated. In addition we will measure:
Positioning precision
Force required to push device and delivery system around aortic arch from femoral artery into implantation position
The torque forces of the delivery system
The force needed to deploy ATAG
Force needed to deploy coronary stents on push rods
Force that ATAG exerts on the vessel wall (apposition at proximal and distal ends of graft)
Force required for device migration

Subjective
There will also be considerable end user feedback with TK and MTR critically appraising the ability of the device to track around the aortic arch, provide adequate "pushability" of the coronary arms, and torque to allow the delivery system to transfer subtle movement of the hands to the front of the device in positioning.

WP2 is again likely to lead to further design iterations of both graft and delivery system.

At this time point the new ATAG stent graft samples will also be subject to cyclic load testing to ensure durability of up to 6 months to satisfy the 6 month survival and safety study. Full regulatory cyclic load testing and durability is beyond the scope of this project.

Deliverables and Milestones:

Specification, design and build of ATAG stent graft delivery system. (Q)
Critical appraisal report of the 2nd generation delivery system and stent graft in-vitro testing (SG/TK/MTR)
IP protection of novel delivery system features (AM)

WP3 (month 14-20) Acute In-vivo ovine study

A 60-90Kg sheep provides the best in-vivo model for testing graft design and deliverability. It has an aortic diameter similar to that of the human (see Annex 4 page 12). It also has a left dominant coronary system, and access vessels capable of a 6mm (18 French) sheath insertion for percutaneous delivery. All in-vivo studies will be carried out by DB, TK and MTR at RVC. Trans-oesophageal echo (TOE) will be provided by RVC cardiologist Dr David Connelly (DC), CT by Dr Chris Lamb (CL), & histopathology by Prof Cheryl Scudamore (CS).

Aim
To evaluate acute ATAG deployment in an ovine (non-survival) model

Methods
In 5 adult sheep under general anaesthetic we will deliver the ATAG device to the aortic root under x-ray guidance and simultaneous TOE (DC).

End points
Ability to implant ATAG in correct position without complication
Stenting and patency of coronary arteries
Integrity of aortic valve function (measured by TOE)
Incidence of early migration
Ability to create proximal and distal seal
Incidence of early endoleak
Incidence of heart rhythm disturbance
Incidence of death as a result of implantation and its likely mechanism
Histopathology of explanted samples (CS)

Deliverables
ATAG graft and delivery system updated prototype * 5 for acute in-vivo study (Q)

DB / TK / MTR / CS Report detailing the clinical course of the acute implants, the end points as above and potential design iterations that might improve the device for next development cycle.

WP4 (month 20-32) In-vivo Ovine survival and safety study

It is envisaged that there will be a further device update following on from WP3.

Aim
To evaluate the survival and safety of the ATAG device implanted in an ovine model (under x-ray and TOE guidance).

Methods
In 15 adult sheep under general anaesthetic deliver the ATAG device and characterise the safety and 1, 3, & 6 month survival.(Identical implant team to WP3)

The first 5 will have a CT scan at 1 month before device is explanted and examined
The second cohort of 5 will have a CT at 1 and 3 months before explantation and histopathological analysis
The last 5 will have CT scan at 1, 3, and 6 months before explantation and analysis

End Points
Ability to implant ATAG in correct position without complication
Stenting and patency of coronary arteries 0, 1, 3 and 6 months (on CT by CL)
Integrity of aortic valve function (measured by echocardiography at 0, 1, 3 & 6 months)
Incidence of early migration acutely, 1, 3, & 6 months
Ability to create proximal and distal seal
Incidence of endoleak
Incidence of heart rhythm disturbance
Implantation leading to death and mechanism
Histopathology of explanted samples

Deliverables
Qualified ATAG device update. Supply of 15 devices for survival and safety implantation
DB / TK / MTR / DC / CL / CS Report detailing end points as above and design iterations to potentially improve device for next development cycle.

We anticipate that the device upgrades used in both WP3 and WP4 will go through some pre-clinical in-vitro flow-rig testing prior to commencing the next in-vivo stage.

WP5 (Month 1-36) Development of IP and business plan

The best route to market for the technology developed in the course of the project will be via a new company spin-out. Spin-out will provide the dedicated effort and resources to maximise the value and market penetration that the product requires to bring patient benefit in the short term.

Several outputs at different stages of the project will be critical to the development of a business plan aimed at series A funding from VC sources. In order to take the device to CE mark and FDA approval, significant investment will be required. A business plan will be drafted to reflect this financial input and also to highlight potential exit points for investors. The outputs of the project will provide increasing uplift in value as new IP and design & development data is gathered. This will significantly reduce investment risk and bring the project to a critical value inflection point where favourable equity terms can be sought from investors.

At monthly intervals throughout the development project an IP audit will be carried out by NHSIL(AM). The audit will consist of a thorough analysis of recent project outputs and a forward looking discussion to assess areas of potential IP generation in the future. Patentable IP will be collated and decisions will be made on patent filing at these monthly meetings by NHSIL. Non-patentable IP including Know how will be protected through a strict non-disclosure policy throughout the project. Any published data, presentations or news-flow will be agreed by NHSIL prior to release to ensure against IP leak.

11. Research Team*:

Include an explanation of the specific expertise that each member of the research group will be bringing to the project. **(Maximum 3000 characters)**

Professor Martin Rothman is a vastly experienced cardiovascular interventionalist. He is a serial innovator / inventor taking devices from the "ideas stage", through the development / regulatory cycle and into first in man trials. In particular he has been involved in stent and valve development programmes and this knowledge will be vital in design optimisation of ATAG. Professor Rothman remains a practicing Interventional Cardiologist at the London Chest Hospital where he sees patients presenting with both ascending aortic dissection and aneurysm.

Professor Stephen Greenwald is Professor of Cardiovascular Mechanics and has a lifelong interest in vascular biology / systemic resistance and vessel compliance. He has enormous understanding of flow dynamics and has set up and published on many flow-rig set-ups. He will provide direct supervision to the in-vitro testing programme and also lab space and much of the flow-rig equipment required. He has the ideal credentials to run the in-vitro flow rig testing programme on all prototypes.

Professor Dan Brockman is professor of small animal surgery at Royal Veterinary College (RVC). He has an enormous experience in interventional procedures in animals and runs the only open heart surgery programme for animals in the UK (one of only a handful in the world). During some of the early in-vivo work, while the delivery system is in development Prof Brockman may implant some of the ATAG devices under direct vision from a small aortic incision.

The RVC has an expert Cardiologist (DC) to perform real time trans-oesophageal echocardiography (TOE) examination during ATAG implantation and follow up. TOE allows us to immediately assess ATAG position and degree of aortic valve regurgitation. RVC Radiologist (CL) will perform and interpret CT follow up on all survival animals. Histopathologist (CS) will provide expert histopathological analysis on all explanted material. The BLT / RVC collaboration provides truly world-class facilities and expertise to carry out the rigorous in-vivo testing programme.

Dr Thomas Keeble is a Interventional Cardiology Research Registrar working with Professor Rothman at the London Chest Hospital. He has been involved in the ATAG project for the last 2 years and has undertaken the prototype development and proof of concept models produced so far. He has demonstrated delivery of a proof of concept model is possible under x-ray guidance.

Our dedicated medical engineering partner is Qualimed, who are based in Hamburg, Germany. We have already we have built up a very close working relationship with weekly telephone conferences and monthly visits. The UK team above are integrally involved in the prototype design and the early testing programmes. Hamburg can be visited by day trip from London Heathrow.

Overall project management and Intellectual Property expertise will be sub-contracted to Torsten Struntz (TS) & Andrew McCulloch (AM) of NHSIL.

Reference List

(1) Chuter TA. Endovascular repair in the ascending aorta: stretching the limits of current technology. J Endovasc Ther 2007 December;14(6):799-800.

(2) Hagan PG, Nienaber CA, Isselbacher EM, Bruckman D, Karavite DJ, Russman PL et al. The International Registry of Acute Aortic Dissection (IRAD): new insights into an old disease. JAMA 2000 February 16;283(7):897-903.

(3) Suzuki S, Masuda M. An update on surgery for acute type A aortic dissection: aortic root repair, endovascular stent graft, and genetic research. Surg Today 2009;39(4):281-9.

(4) Pretre R, von Segesser LK. Aortic dissection. Lancet 1997 May 17;349(9063):1461-4.

(5) Lee WA, Carter JW, Upchurch G, Seeger JM, Huber TS. Perioperative outcomes after open and endovascular repair of intact abdominal aortic aneurysms in the United States during 2001. J Vasc Surg 2004 March;39(3):491-6.

(6) Gowda RM, Misra D, Tranbaugh RF, Ohki T, Khan IA. Endovascular stent grafting of descending thoracic aortic aneurysms. Chest 2003 August;124(2):714-9.

(7) Sioris T, David TE, Ivanov J, Armstrong S, Feindel CM. Clinical outcomes after separate and composite replacement of the aortic valve and ascending aorta. J Thorac Cardiovasc Surg 2004 August;128(2):260-5.

(8) Sobocinski J, O'Brien N, Maurel B, Bartoli M, Goueffic Y, Sassard T et al. Endovascular approaches to acute aortic type A dissection: a CT-based feasibility study. Eur J Vasc Endovasc Surg 2011 October;42(4):442-7.

(9) Rampoldi V, Trimarchi S, Eagle KA, Nienaber CA, Oh JK, Bossone E et al. Simple risk models to predict surgical mortality in acute type A aortic

dissection: the International Registry of Acute Aortic Dissection score. Ann Thorac Surg 2007 January;83(1):55-61.

(10) Krohg-Sorensen K, Hafsahl G, Fosse E, Geiran OR. Acceptable short-term results after endovascular repair of diseases of the thoracic aorta in high risk patients. Eur J Cardiothorac Surg 2003 September;24(3):379-87.

(11) Lu TL, Huber CH, Rizzo E, Dehmeshki J, von Segesser LK, Qanadli SD. Ascending aorta measurements as assessed by ECG-gated multi-detector computed tomography: a pilot study to establish normative values for transcatheter therapies. Eur Radiol 2009 March;19(3):664-9.

(12) Palmaz JC, Richter GM, Noldge G, Kauffmann GW, Wenz W. [Intraluminal Palmaz stent implantation. The first clinical case report on a balloon-expanded vascular prosthesis]. Radiologe 1987 December;27(12):560-3.

(13) Aronberg DJ, Glazer HS, Madsen K, Sagel SS. Normal thoracic aortic diameters by computed tomography. J Comput Assist Tomogr 1984 April;8(2):247-50.

(14) Pearce WH, Slaughter MS, LeMaire S, Salyapongse AN, Feinglass J, McCarthy WJ et al. Aortic diameter as a function of age, gender, and body surface area. Surgery 1993 October;114(4):691-7.

(15) van PJ, Vincken KL, Muhs BE, Barwegen GK, Bartels LW, Prokop M et al. Toward endografting of the ascending aorta: insight into dynamics using dynamic cine-CTA. J Endovasc Ther 2007 August;14(4):551-60.

(16) de Heer LM, Budde RP, Mali WP, de Vos AM, van Herwerden LA, Kluin J. Aortic root dimension changes during systole and diastole: evaluation with ECG-gated multidetector row computed tomography. Int J Cardiovasc Imaging 2011 February 27.

(17) Yamanaka O, Hobbs RE. Coronary artery anomalies in 126,595 patients undergoing coronary arteriography. Cathet Cardiovasc Diagn 1990 September;21(1):28-40.

(18) Schmitt R, Froehner S, Brunn J, Wagner M, Brunner H, Cherevatyy O et al. Congenital anomalies of the coronary arteries: imaging with contrast-enhanced, multidetector computed tomography. Eur Radiol 2005 June;15(6):1110-21.

(19) Christensen KN, Harris SR, Froemming AT, Brinjikji W, Araoz P, Asirvatham SJ et al. Anatomic assessment of the bifurcation of the left main coronary artery using multidetector computed tomography. Surg Radiol Anat 2010 December;32(10):903-9.

(20) Reig J, Petit M. Main trunk of the left coronary artery: anatomic study of the parameters of clinical interest. Clin Anat 2004 January;17(1):6-13.

(21) Muriago M, Sheppard MN, Ho SY, Anderson RH. Location of the coronary arterial orifices in the normal heart. Clin Anat 1997;10(5):297-302.

(22) McAlpine WA. Heart and Coronary Arteries: Anatomical Atlas for Clinical Diagnosis, Radiological Investigation, and Surgical Treatment. Berlin: Springer-Verlag, p. 134. 1-1-1975.

(23) Dodge JT, Jr., Brown BG, Bolson EL, Dodge HT. Lumen diameter of normal human coronary arteries. Influence of age, sex, anatomic variation, and left ventricular hypertrophy or dilation. Circulation 1992 July;86(1):232-46.

(24) Dodge JT, Jr., Brown BG, Bolson EL, Dodge HT. Intrathoracic spatial location of specified coronary segments on the normal human heart. Applications in quantitative arteriography, assessment of regional risk and contraction, and anatomic display. Circulation 1988 November;78(5 Pt 1):1167-80.

(25) Dart AM, Kingwell BA, Gatzka CD, Willson K, Liang YL, Berry KL et al. Smaller aortic dimensions do not fully account for the greater pulse pressure in elderly female hypertensives. Hypertension 2008 April;51(4):1129-34.

(26) Wolak A, Gransar H, Thomson LE, Friedman JD, Hachamovitch R, Gutstein A et al. Aortic size assessment by noncontrast cardiac computed tomography: normal limits by age, gender, and body surface area. JACC Cardiovasc Imaging 2008 March;1(2):200-9.

(27) Paivansalo MJ, Merikanto J, Jerkkola T, Savolainen MJ, Rantala AO, Kauma H et al. Effect of hypertension and risk factors on diameters of abdominal aorta and common iliac and femoral arteries in middle-aged hypertensive and control subjects: a cross-sectional systematic study with duplex ultrasound. Atherosclerosis 2000 November;153(1):99-106.

(28) Smith CR, Leon MB, Mack MJ, Miller DC, Moses JW, Svensson LG et al. Transcatheter versus Surgical Aortic-Valve Replacement in High-Risk Patients. N Engl J Med 2011 June 5.

(29) Lin PH, Kougias P, Huynh TT, Huh J, Coselli JS. Endovascular repair of ascending aortic pseudoaneurysm: technical considerations of a common carotid artery approach using the Zenith aortic cuff endograft. J Endovasc Ther 2007 December;14(6):794-8.

(30) Ishimaru S. Endografting of the aortic arch. J Endovasc Ther 2004 December;11 Suppl 2:II62-II71.

(31) Isselbacher EM. Thoracic and abdominal aortic aneurysms. Circulation 2005 February 15;111(6):816-28.

(32) Evangelista A. Diseases of the aorta: aneurysm of the ascending aorta. Heart 2010 June;96(12):979-85.

(33) Hirai S, Hamanaka Y, Mitsui N, Morifuji K, Uegami S. Spontaneous rupture of the ascending thoracic aorta resulting in a mimicking pseudoaneurysm. Ann Thorac Cardiovasc Surg 2006 June;12(3):223-7.

(34) Clouse WD, Hallett JW, Jr., Schaff HV, Gayari MM, Ilstrup DM, Melton LJ, III. Improved prognosis of thoracic aortic aneurysms: a population-based study. JAMA 1998 December 9;280(22):1926-9.

(35) Elefteriades JA. Genetic testing in aortic aneurysm disease: CON. Cardiol Clin 2010 May;28(2):199-204.

(36) Barbour JR, Spinale FG, Ikonomidis JS. Proteinase systems and thoracic aortic aneurysm progression. J Surg Res 2007 May 15;139(2):292-307.

(37) Guo D, Hasham S, Kuang SQ, Vaughan CJ, Boerwinkle E, Chen H et al. Familial thoracic aortic aneurysms and dissections: genetic heterogeneity with a major locus mapping to 5q13-14. Circulation 2001 May 22;103(20):2461-8.

(38) Guo D, Hasham S, Kuang SQ, Vaughan CJ, Boerwinkle E, Chen H et al. Familial thoracic aortic aneurysms and dissections: genetic heterogeneity with a major locus mapping to 5q13-14. Circulation 2001 May 22;103(20):2461-8.

(39) Jones JA, Spinale FG, Ikonomidis JS. Transforming growth factor-beta signaling in thoracic aortic aneurysm development: a paradox in pathogenesis. J Vasc Res 2009;46(2):119-37.

(40) Tadros TM, Klein MD, Shapira OM. Ascending aortic dilatation associated with bicuspid aortic valve: pathophysiology, molecular biology, and clinical implications. Circulation 2009 February 17;119(6):880-90.

(41) Fedak PW, Verma S, David TE, Leask RL, Weisel RD, Butany J. Clinical and pathophysiological implications of a bicuspid aortic valve. Circulation 2002 August 20;106(8):900-4.

(42) Elefteriades JA, Farkas EA. Thoracic aortic aneurysm clinically pertinent controversies and uncertainties. J Am Coll Cardiol 2010 March 2;55(9):841-57.

(43) Brooke BS, Habashi JP, Judge DP, Patel N, Loeys B, Dietz HC, III. Angiotensin II blockade and aortic-root dilation in Marfan's syndrome. N Engl J Med 2008 June 26;358(26):2787-95.

(44) Hiratzka LF, Bakris GL, Beckman JA, Bersin RM, Carr VF, Casey DE, Jr. et al. 2010 ACCF/AHA/AATS/ACR/ASA/SCA/SCAI/SIR/STS/SVM Guidelines for the diagnosis and management of patients with thoracic aortic disease. A Report of the American College of Cardiology Foundation/American Heart Association Task Force on Practice Guidelines, American Association for Thoracic Surgery, American College of Radiology,American Stroke Association, Society of Cardiovascular Anesthesiologists, Society for Cardiovascular Angiography and Interventions, Society of Interventional Radiology, Society of Thoracic Surgeons,and Society for Vascular Medicine. J Am Coll Cardiol 2010 April 6;55(14):e27-e129.

(45) Gersony DR, McClaughlin MA, Jin Z, Gersony WM. The effect of beta-blocker therapy on clinical outcome in patients with Marfan's syndrome: a meta-analysis. Int J Cardiol 2007 January 18;114(3):303-8.

(46) Yetman AT, Bornemeier RA, McCrindle BW. Usefulness of enalapril versus propranolol or atenolol for prevention of aortic dilation in patients with the Marfan syndrome. Am J Cardiol 2005 May 1;95(9):1125-7.

(47) Bentall H, De BA. A technique for complete replacement of the ascending aorta. Thorax 1968 July;23(4):338-9.

(48) David TE, Armstrong S, Maganti M, Colman J, Bradley TJ. Long-term results of aortic valve-sparing operations in patients with Marfan syndrome. J Thorac Cardiovasc Surg 2009 October;138(4):859-64.

(49) Murdoch JL, Walker BA, Halpern BL, Kuzma JW, McKusick VA. Life expectancy and causes of death in the Marfan syndrome. N Engl J Med 1972 April 13;286(15):804-8.

(50) Silverman DI, Burton KJ, Gray J, Bosner MS, Kouchoukos NT, Roman MJ et al. Life expectancy in the Marfan syndrome. Am J Cardiol 1995 January 15;75(2):157-60.

(51) Fleischer KJ, Nousari HC, Anhalt GJ, Stone CD, Laschinger JC. Immunohistochemical abnormalities of fibrillin in cardiovascular tissues in Marfan's syndrome. Ann Thorac Surg 1997 April;63(4):1012-7.

(52) Benedetto U, Melina G, Takkenberg JJ, Roscitano A, Angeloni E, Sinatra R. Surgical management of aortic root disease in Marfan syndrome: a systematic review and meta-analysis. Heart 2011 June;97(12):955-8.

(53) Robicsek F, Thubrikar MJ. Conservative operation in the management of annular dilatation and ascending aortic aneurysm. Ann Thorac Surg 1994 June;57(6):1672-4.

(54) Golesworthy T, Lamperth M, Mohiaddin R, Pepper J, Thornton W, Treasure T. The Tailor of Gloucester: a jacket for the Marfan's aorta. Lancet 2004 October 30;364(9445):1582.

(55) Pepper J, John CK, Gavino J, Golesworthy T, Mohiaddin R, Treasure T. External aortic root support for Marfan syndrome: early clinical results in the first 20 recipients with a bespoke implant. J R Soc Med 2010 September;103(9):370-5.

(56) Pepper J, Golesworthy T, Utley M, Chan J, Ganeshalingam S, Lamperth M et al. Manufacturing and placing a bespoke support for the Marfan aortic root: description of the method and technical results and status at one year for the first ten patients. Interact Cardiovasc Thorac Surg 2010 March;10(3):360-5.

(57) Acierno LJ. The History of Cardiology. 1994.

(58) HIRST AE, Jr., JOHNS VJ, Jr., Kime SW, Jr. Dissecting aneurysm of the aorta: a review of 505 cases. Medicine (Baltimore) 1958 September;37(3):217-79.

(59) Leonard JC. Thomas Bevill Peacock and the early history of dissecting aneurysm. Br Med J 1979 July 28;2(6184):260-2.

(60) Bogaert J, Meyns B, Rademakers FE, Bosmans H, Verschakelen J, Flameng W et al. Follow-up of aortic dissection: contribution of MR angiography for evaluation of the abdominal aorta and its branches. Eur Radiol 1997;7(5):695-702.

(61) DeBakey ME, Beall AC, Jr., Cooley DA, Crawford ES, Morris GC, Jr., Garrett HE et al. Dissecting aneurysms of the aorta. Surg Clin North Am 1966 August;46(4):1045-55.

(62) Meszaros I, Morocz J, Szlavi J, Schmidt J, Tornoci L, Nagy L et al. Epidemiology and clinicopathology of aortic dissection. Chest 2000 May;117(5):1271-8.

(63) Olsson C, Thelin S, Stahle E, Ekbom A, Granath F. Thoracic aortic aneurysm and dissection: increasing prevalence and improved outcomes reported in a nationwide population-based study of more than 14,000 cases from 1987 to 2002. Circulation 2006 December 12;114(24):2611-8.

(64) Nienaber CA, Fattori R, Mehta RH, Richartz BM, Evangelista A, Petzsch M et al. Gender-related differences in acute aortic dissection. Circulation 2004 June 22;109(24):3014-21.

(65) Golledge J, Eagle KA. Acute aortic dissection. Lancet 2008 July 5;372(9632):55-66.

(66) Hasham SN, Willing MC, Guo DC, Muilenburg A, He R, Tran VT et al. Mapping a locus for familial thoracic aortic aneurysms and dissections (TAAD2) to 3p24-25. Circulation 2003 July 1;107(25):3184-90.

(67) Collins JS, Evangelista A, Nienaber CA, Bossone E, Fang J, Cooper JV et al. Differences in clinical presentation, management, and outcomes of acute type a aortic dissection in patients with and without previous cardiac surgery. Circulation 2004 September 14;110(11 Suppl 1):II237-II242.

(68) Shiga T, Wajima Z, Apfel CC, Inoue T, Ohe Y. Diagnostic accuracy of transesophageal echocardiography, helical computed tomography, and magnetic resonance imaging for suspected thoracic aortic dissection: systematic review and meta-analysis. Arch Intern Med 2006 July 10;166(13):1350-6.

(69) Erbel R, Alfonso F, Boileau C, Dirsch O, Eber B, Haverich A et al. Diagnosis and management of aortic dissection. Eur Heart J 2001 September;22(18):1642-81.

(70) Mehta RH, Suzuki T, Hagan PG, Bossone E, Gilon D, Llovet A et al. Predicting death in patients with acute type a aortic dissection. Circulation 2002 January 15;105(2):200-6.

(71) Hiratzka LF, Bakris GL, Beckman JA, Bersin RM, Carr VF, Casey DE, Jr. et al. 2010 ACCF/AHA/AATS/ACR/ASA/SCA/SCAI/SIR/STS/SVM guidelines for the diagnosis and management of patients with Thoracic Aortic Disease: a report of the American College of Cardiology Foundation/American Heart Association Task Force on Practice Guidelines, American Association for Thoracic Surgery, American College of Radiology, American Stroke Association, Society of Cardiovascular Anesthesiologists, Society for Cardiovascular Angiography and Interventions, Society of Interventional Radiology, Society of Thoracic Surgeons, and Society for Vascular Medicine. Circulation 2010 April 6;121(13):e266-e369.

(72) Guilmet D, Bachet J, Goudot B, Laurian C, Gigou F, Bical O et al. Use of biological glue in acute aortic dissection. Preliminary clinical results with a new surgical technique. J Thorac Cardiovasc Surg 1979 April;77(4):516-21.

(73) Bachet J, Guilmet D. The use of biological glue in aortic surgery. Cardiol Clin 1999 November;17(4):779-x.

(74) Bingley JA, Gardner MA, Stafford EG, Mau TK, Pohlner PG, Tam RK et al. Late complications of tissue glues in aortic surgery. Ann Thorac Surg 2000 June;69(6):1764-8.

(75) Kazui T, Washiyama N, Bashar AH, Terada H, Suzuki K, Yamashita K et al. Role of biologic glue repair of proximal aortic dissection in the development of early and midterm redissection of the aortic root. Ann Thorac Surg 2001 August;72(2):509-14.

(76) Raanani E, Georghiou GP, Kogan A, Wandwi B, Shapira Y, Vidne BA. 'BioGlue' for the repair of aortic insufficiency in acute aortic dissection. J Heart Valve Dis 2004 September;13(5):734-7.

(77) Seguin JR, Picard E, Frapier JM, Chaptal PA. Aortic valve repair with fibrin glue for type A acute aortic dissection. Ann Thorac Surg 1994 August;58(2):304-6.

(78) Nakajima T, Kawazoe K, Kataoka T, Kin H, Kazui T, Okabayashi H et al. Midterm results of aortic repair using a fabric neomedia and fibrin glue for type A acute aortic dissection. Ann Thorac Surg 2007 May;83(5):1615-20.

(79) Floten HS, Ravichandran PS, Furnary AP, Gately HL, Starr A. Adventitial inversion technique in repair of aortic dissection. Ann Thorac Surg 1995 March;59(3):771-2.

(80) Tanaka K, Morioka K, Li W, Yamada N, Takamori A, Handa M et al. Adventitial inversion technique without the aid of biologic glue or Teflon buttress for acute type A aortic dissection. Eur J Cardiothorac Surg 2005 December;28(6):864-9.

(81) Ergin MA, McCullough J, Galla JD, Lansman SL, Griepp RB. Radical replacement of the aortic root in acute type A dissection: indications and outcome. Eur J Cardiothorac Surg 1996;10(10):840-4.

(82) Gott VL, Gillinov AM, Pyeritz RE, Cameron DE, Reitz BA, Greene PS et al. Aortic root replacement. Risk factor analysis of a seventeen-year experience with 270 patients. J Thorac Cardiovasc Surg 1995 March;109(3):536-44.

(83) Leyh RG, Fischer S, Kallenbach K, Kofidis T, Pethig K, Harringer W et al. High failure rate after valve-sparing aortic root replacement using the "remodeling technique" in acute type A aortic dissection. Circulation 2002 September 24;106(12 Suppl 1):I229-I233.

(84) David TE, Ivanov J, Armstrong S, Feindel CM, Webb GD. Aortic valve-sparing operations in patients with aneurysms of the aortic root or ascending aorta. Ann Thorac Surg 2002 November;74(5):S1758-S1761.

(85) Fazel SS, David TE. Aortic valve-sparing operations for aortic root and ascending aortic aneurysms. Curr Opin Cardiol 2007 November;22(6):497-503.

(86) Mestres CA, Fernandez C, Josa M, Mulet J. Hybrid antegrade repair of the arch and descending thoracic aorta with a new integrated stent-Dacron graft in acute type A aortic dissection: a look into the future with new devices. Interact Cardiovasc Thorac Surg 2007 April;6(2):257-9.

(87) Parish LM, Gorman JH, III, Kahn S, Plappert T, St John-Sutton MG, Bavaria JE et al. Aortic size in acute type A dissection: implications for preventive ascending aortic replacement. Eur J Cardiothorac Surg 2009 June;35(6):941-5.

(88) Pape LA, Tsai TT, Isselbacher EM, Oh JK, O'Gara PT, Evangelista A et al. Aortic diameter >or = 5.5 cm is not a good predictor of type A aortic dissection: observations from the International Registry of Acute Aortic Dissection (IRAD). Circulation 2007 September 4;116(10):1120-7.

(89) Neri E, Barabesi L, Buklas D, Vricella LA, Benvenuti A, Tucci E et al. Limited role of aortic size in the genesis of acute type A aortic dissection. Eur J Cardiothorac Surg 2005 December;28(6):857-63.

(90) www.medtronicendo.com/us/system/files/TalentCaptivia_brochure.pdf . 2012.

(91) Kouchoukos NT, Rokkas CK. Regarding "Observations on delayed neurologic deficit after thoracoabdominal aortic aneurysm repair". J Vasc Surg 1998 February;27(2):389-92.

(92) Dake MD, Miller DC, Semba CP, Mitchell RS, Walker PJ, Liddell RP. Transluminal placement of endovascular stent-grafts for the treatment of descending thoracic aortic aneurysms. N Engl J Med 1994 December 29;331(26):1729-34.

(93) Dake MD, Kato N, Mitchell RS, Semba CP, Razavi MK, Shimono T et al. Endovascular stent-graft placement for the treatment of acute aortic dissection. N Engl J Med 1999 May 20;340(20):1546-52.

(94) Jonker FH, Verhagen HJ, Lin PH, Heijmen RH, Trimarchi S, Lee WA et al. Open surgery versus endovascular repair of ruptured thoracic aortic aneurysms. J Vasc Surg 2011 May;53(5):1210-6.

(95) Nienaber CA, Rousseau H, Eggebrecht H, Kische S, Fattori R, Rehders TC et al. Randomized comparison of strategies for type B aortic dissection: the INvestigation of STEnt Grafts in Aortic Dissection (INSTEAD) trial. Circulation 2009 December 22;120(25):2519-28.

(96) Nienaber CA, Kische S, Ince H. Thoracic aortic stent-graft devices: problems, failure modes, and applicability. Semin Vasc Surg 2007 June;20(2):81-9.

(97) Blum U, Voshage G, Lammer J, Beyersdorf F, Tollner D, Kretschmer G et al. Endoluminal stent-grafts for infrarenal abdominal aortic aneurysms. N Engl J Med 1997 January 2;336(1):13-20.

(98) Palmaz JC. Review of polymeric graft materials for endovascular applications. J Vasc Interv Radiol 1998 January;9(1 Pt 1):7-13.

(99) Murphy JG, Schwartz RS, Edwards WD, Camrud AR, Vlietstra RE, Holmes DR, Jr. Percutaneous polymeric stents in porcine coronary arteries. Initial experience with polyethylene terephthalate stents. Circulation 1992 November;86(5):1596-604.

(100) Kalman PG, Rotstein OD, Niven J, Glynn MF, Romaschin AD. Differential stimulation of macrophage procoagulant activity by vascular grafts. J Vasc Surg 1993 March;17(3):531-7.

(101) Mastery of vascular and endovascular surgery. Philadelphia, USA: Lippincott Williams and Wilkins; 2006. 2006.

(102) Marin ML, Veith FJ, Cynamon J, Sanchez LA, Bakal CW, Suggs WD et al. Human transluminally placed endovascular stented grafts: preliminary histopathologic analysis of healing grafts in aortoiliac and femoral artery occlusive disease. J Vasc Surg 1995 April;21(4):595-603.

(103) Shimono T, Kato N, Yasuda F, Suzuki T, Yuasa U, Onoda K et al. Transluminal stent-graft placements for the treatments of acute onset and chronic aortic dissections. Circulation 2002 September 24;106(12 Suppl 1):I241-I247.

(104) Jacobs TS, Won J, Gravereaux EC, Faries PL, Morrissey N, Teodorescu VJ et al. Mechanical failure of prosthetic human implants: a 10-year experience with aortic stent graft devices. J Vasc Surg 2003 January;37(1):16-26.

(105) Eggebrecht H, Nienaber CA, Neuhauser M, Baumgart D, Kische S, Schmermund A et al. Endovascular stent-graft placement in aortic dissection: a meta-analysis. Eur Heart J 2006 February;27(4):489-98.

(106) Brott TG, Hobson RW, Howard G, Roubin GS, Clark WM, Brooks W et al. Stenting versus endarterectomy for treatment of carotid-artery stenosis. N Engl J Med 2010 July 1;363(1):11-23.

(107) Criado FJ, Clark NS, Barnatan MF. Stent graft repair in the aortic arch and descending thoracic aorta: a 4-year experience. J Vasc Surg 2002 December;36(6):1121-8.

(108) Gorich J, Asquan Y, Seifarth H, Kramer S, Kapfer X, Orend KH et al. Initial experience with intentional stent-graft coverage of the subclavian artery during endovascular thoracic aortic repairs. J Endovasc Ther 2002 June;9 Suppl 2:II39-II43.

(109) Inoue K, Hosokawa H, Iwase T, Sato M, Yoshida Y, Ueno K et al. Aortic arch reconstruction by transluminally placed endovascular branched stent graft. Circulation 1999 November 9;100(19 Suppl):II316-II321.

(110) Chuter TA, Buck DG, Schneider DB, Reilly LM, Messina LM. Development of a branched stent-graft for endovascular repair of aortic arch aneurysms. J Endovasc Ther 2003 October;10(5):940-5.

(111) Monahan TS, Schneider DB. Fenestrated and branched stent grafts for repair of complex aortic aneurysms. Semin Vasc Surg 2009 September;22(3):132-9.

(112) Cribier A, Eltchaninoff H, Bash A, Borenstein N, Tron C, Bauer F et al. Percutaneous transcatheter implantation of an aortic valve prosthesis for calcific aortic stenosis: first human case description. Circulation 2002 December 10;106(24):3006-8.

(113) Leon MB, Smith CR, Mack M, Miller DC, Moses JW, Svensson LG et al. Transcatheter aortic-valve implantation for aortic stenosis in patients who cannot undergo surgery. N Engl J Med 2010 October 21;363(17):1597-607.

(114) Senay S, Alhan C, Toraman F, Karabulut H, Dagdelen S, Cagil H. Endovascular stent-graft treatment of type A dissection: case report and review of literature. Eur J Vasc Endovasc Surg 2007 October;34(4):457-60.

(115) Zhang H, Li M, Jin W, Wang Z. Endoluminal and surgical treatment for the management of Stanford Type A aortic dissection. Eur J Cardiothorac Surg 2004 October;26(4):857-9.

(116) Ihnken K, Sze D, Dake MD, Fleischmann D, Van der Starre P, Robbins R. Successful treatment of a Stanford type A dissection by percutaneous placement of a covered stent graft in the ascending aorta. J Thorac Cardiovasc Surg 2004 June;127(6):1808-10.

(117) Szeto WY, Fairman RM, Acker MA, Skelly CL, Augoustides JG, McGarvey M et al. Emergency endovascular deployment of stent graft in the ascending aorta for contained rupture of innominate artery pseudoaneurysm in a pediatric patient. Ann Thorac Surg 2006 May;81(5):1872-5.

(118) Ruchat P, Chassot PG, Rizzo E. Endoprosthetic exclusion of type A aortic dissection through carotid artery. J Thorac Cardiovasc Surg 2009 October;138(4):1035-7.

(119) Zimpfer D, Czerny M, Kettenbach J, Schoder M, Wolner E, Lammer J et al. Treatment of acute type a dissection by percutaneous endovascular stent-graft placement. Ann Thorac Surg 2006 August;82(2):747-9.

(120) Szeto WY, Moser WG, Desai ND, Milewski RK, Cheung AT, Pochettino A et al. Transapical deployment of endovascular thoracic aortic stent graft for an ascending aortic pseudoaneurysm. Ann Thorac Surg 2010 February;89(2):616-8.

(121) Chavan A, Karck M, Hagl C, Winterhalter M, Baus S, Galanski M et al. Hybrid endograft for one-step treatment of multisegment disease of the thoracic aorta. J Vasc Interv Radiol 2005 June;16(6):823-9.

(122) Lansman SL, McCullough JN, Nguyen KH, Spielvogel D, Klein JJ, Galla JD et al. Subtypes of acute aortic dissection. Ann Thorac Surg 1999 June;67(6):1975-8.

(123) Bonhoeffer P, Boudjemline Y, Saliba Z, Merckx J, Aggoun Y, Bonnet D et al. Percutaneous replacement of pulmonary valve in a right-ventricle to pulmonary-artery prosthetic conduit with valve dysfunction. Lancet 2000 October 21;356(9239):1403-5.

(124) Ong SH, Mueller R, Gerckens U. Iatrogenic dissection of the ascending aorta during TAVI sealed with the corevalve revalving prosthesis. Catheter Cardiovasc Interv 2011 March 21.

(125) Khawaja MZ, Rajani R, Cook A, Khavandi A, Moynagh A, Chowdhary S et al. Permanent pacemaker insertion after CoreValve transcatheter aortic valve implantation: incidence and contributing factors (the UK CoreValve Collaborative). Circulation 2011 March 8;123(9):951-60.

(126) O'Neill S, Greenberg RK, Resch T, Bathurst S, Fleming D, Kashyap V et al. An evaluation of centerline of flow measurement techniques to assess migration after thoracic endovascular aneurysm repair. J Vasc Surg 2006 June;43(6):1103-10.

(127) Tsai TT, Trimarchi S, Nienaber CA. Acute aortic dissection: perspectives from the International Registry of Acute Aortic Dissection (IRAD). Eur J Vasc Endovasc Surg 2009 February;37(2):149-59.

(128) Trimarchi S, Eagle KA, Nienaber CA, Rampoldi V, Jonker FH, De VC et al. Role of age in acute type A aortic dissection outcome: report from the International Registry of Acute Aortic Dissection (IRAD). J Thorac Cardiovasc Surg 2010 October;140(4):784-9.

(129) Roman MJ, Devereux RB, Kramer-Fox R, O'Loughlin J. Two-dimensional echocardiographic aortic root dimensions in normal children and adults. Am J Cardiol 1989 September 1;64(8):507-12.

(130) Kallenbach K, Baraki H, Khaladj N, Kamiya H, Hagl C, Haverich A et al. Aortic valve-sparing operation in Marfan syndrome: what do we know after a decade? Ann Thorac Surg 2007 February;83(2):S764-S768.

(131) Riepe G, Heilberger P, Umscheid T, Chakfe N, Raithel D, Stelter W et al. Frame dislocation of body middle rings in endovascular stent tube grafts. Eur J Vasc Endovasc Surg 1999 January;17(1):28-34.

(132) Duerig TW, Pelton AR, Stockel D. The utility of superelasticity in medicine. Biomed Mater Eng 1996;6(4):255-66.

(133) Salacinski H, Tiwari A, Hamilton G, Seifalian AM. Performance of a polyurethane vascular prosthesis carrying a dipyridamole (Persantin) coating on its lumenal surface. J Biomed Mater Res 2002 August;61(2):337-8.

(134) Salacinski HJ, Hamilton G, Seifalian AM. Surface functionalization and grafting of heparin and/or RGD by an aqueous-based process to a poly(carbonate-urea)urethane cardiovascular graft for cellular engineering applications. J Biomed Mater Res A 2003 September 1;66(3):688-97.

(135) Guyton AC. Textbook of medical physiology. 1996.

(136) Moses BL, Ross JN, Jr. M-mode echocardiographic values in sheep. Am J Vet Res 1987 September;48(9):1313-8.

(137) Pipers FS, Muir WW, III, Hamlin RL. Echocardiography in swine. Am J Vet Res 1978 April;39(4):707-10.

(138) Gwathmey JK, Nakao S, Come PC, Abelmann WH. Echocardiographic assessment of cardiac chamber size and functional performance in swine. Am J Vet Res 1989 February;50(2):192-7.

(139) Amory H, Jakovljevic S, Lekeux P. Quantitative M-mode and two-dimensional echocardiography in calves. Vet Rec 1991 January 12;128(2):25-31.

(140) Prinssen M, Verhoeven EL, Buth J, Cuypers PW, van Sambeek MR, Balm R et al. A randomized trial comparing conventional and endovascular repair of abdominal aortic aneurysms. N Engl J Med 2004 October 14;351(16):1607-18.

(141) Neri E, Massetti M. Acute type A dissection and advanced age. Ann Thorac Surg 2005 July;80(1):384-5.

(142) Parodi JC, Palmaz JC, Barone HD. Transfemoral intraluminal graft implantation for abdominal aortic aneurysms. Ann Vasc Surg 1991 November;5(6):491-9.

(143) Rubin BG, Toursarkissian B, Petrinec D, Yang LY, Eisenberg PR, Abendschein DR. Preincubation of Dacron grafts with recombinant tissue factor pathway inhibitor decreases their thrombogenicity in vivo. J Vasc Surg 1996 November;24(5):865-70.

(144) Xue L, Greisler HP. Biomaterials in the development and future of vascular grafts. J Vasc Surg 2003 February;37(2):472-80.

(145) Angiolillo DJ, Ueno M, Goto S. Basic principles of platelet biology and clinical implications. Circ J 2010 April;74(4):597-607.

Declaration

I declare that this thesis has been composed by myself and that the work of which it is a record has been done by myself. Any results which were generated in collaboration with others is fully acknowledged. It has not been previously presented to any institution for a higher degree.

Dr Thomas Roger Keeble

27th July 2013